**UNIVERSIDADE FEDERAL DE PELOTAS**
**Centro de Ciências Químicas, Farmacêuticas e de Alimentos - CCQFA**
**Programa de Pós-Graduação em Bioquímica e Bioprospecção**

**Tese**

# Fungo endofítico isolado de *Achyrocline satureioides*: identificação molecular, caracterização química e investigação do efeito antitumoral de metabólitos bioativos

**Nathalia Stark Pedra**

Pelotas, 2022

**Nathalia Stark Pedra**

# Fungo endofítico isolado de *Achyrocline satureioides*: identificação molecular, caracterização química e investigação do efeito antitumoral de metabólitos bioativos

Tese apresentada ao Programa de Pós-Graduação em Bioquímica e Bioprospecção do Centro de Ciências Químicas, Farmacêuticas e de Alimentos da Universidade Federal de Pelotas, como requisito parcial à obtenção do título de Doutora em Ciências (Bioquímica e Bioprospecção).

Orientadora: Profª Dra. Roselia Maria Spanevello

Co-orientadora: Profª Dra. Elizandra Braganhol

Pelotas, 2022

Universidade Federal de Pelotas / Sistema de BibliotecasCatalogação na Publicação

P371f Pedra, Nathalia Stark

Fungo endofítico isolado de *Achyrocline satureioides* : identificação molecular, caracterização química e investigação do efeito antitumoral de metabólitos bioativos / Nathalia Stark Pedra ; Roselia Maria Spanevello, orientadora ; Elizandra Braganhol, coorientadora. — Pelotas, 2022.

212 f. : il.

Tese (Doutorado) — Bioquímica e Bioprospecção, Centro de Ciências Químicas, Farmacêuticas e de Alimentos, Universidade Federal de Pelotas, 2022.

1. *Achyrocline satureioides*. 2. Fungo endofítico. 3. *Biscogniauxia* sp.. 4. Ácido gálico. 5. Glioma. I. Spanevello,Roselia Maria, orient. II. Braganhol, Elizandra, coorient. III. Título.

CDD : 589.204634

Elaborada por Ubirajara Buddin Cruz CRB: 10/901

**Nathalia Stark Pedra**

**Fungo endofítico isolado de *Achyrocline satureioides*: identificação molecular, caracterização química e investigação do efeito antitumoral de metabólitos bioativos**

Tese aprovada, como requisito parcial, para a obtenção do grau de Doutora em Ciências (Bioquímica e Bioprospecção), Programa de Pós-Graduação em Bioquímica e Bioprospecção, Centro de Ciências Químicas, Farmacêuticas e de Alimentos, Universidade Federal de Pelotas.

Data da defesa: 21/09/2022

Banca examinadora:

.....

Profª. Dra. Roselia Maria Spanevello (Orientadora) – Doutora em Ciências Biológicas (Bioquímica) pela Universidade Federal do Rio Grande do Sul.

Documento assinado digitalmente
Alfeu Zanotto Filho
Data: 31/10/2022 21:00:12-0300
CPF: ***.553.300-**
Verifique as assinaturas em https://v.ufsc.br

.....

Prof. Dr. Alfeu Zanotto Filho – Doutor em Ciências Biológicas (Bioquímica) pela Universidade Federal do Rio Grande do Sul.

.....

Profª. Dra. Elessandra da Rosa Zavareze – Doutora em Engenharia e Ciência de Alimentos pela Universidade Federal do Rio Grande.

.....

Profª. Dra. Karine Rech Begnini – Doutora em Ciências (Biotecnologia) pela Universidade Federal de Pelotas.

Dedico este trabalho aos professores que contribuíram para a minha formação, em especial a Rose e a Eliz. Aos meus pais, à minha irmã e ao meu noivo.

## Agradecimentos

Primeiramente agradeço a Deus por ter me dado força e determinação para chegar até aqui.

Aos meus pais, Luiz Mar e Ilani, por serem tão especiais e amorosos. Pelo incentivo e apoio incondicional em todos os momentos, pelas constantes palavras de coragem e carinho. Por sempre me ensinar o valor do trabalho e da dedicação! Por serem exemplos de caráter, honestidade e amor. Vocês são a minha maior inspiração!

A minha irmã e melhor amiga, Sabrina, que é tudo para mim! Obrigada por todo amor e carinho, pela força e ajuda, pelo apoio e motivação. Por saber que eu sempre posso contar contigo. Obrigada por ser a melhor irmã do mundo! Sou muito, mas muito mais feliz por te ter na minha vida. Obrigada por tanto!

Ao meu noivo e melhor amigo Giovano, pelo apoio, carinho, compreensão e motivação. Obrigada por me auxiliar tanto durante a pandemia, por ser escudo e amparo, por ser luz nos momentos difíceis. Obrigada por ser meu motorista e "iniciação científica' nos finais de semana, nos feriados e no auge da pandemia.

Aos meus familiares que mesmo à distância, sempre me apoiaram. Obrigada pelas palavras de carinho e incentivo!

As minhas incríveis orientadoras, Roselia e Elizandra, por toda sabedoria, incentivo e oportunidade. Pelo entusiasmo, carisma e profissionalismo com que conduziram a minha formação. Agradeço o carinho, a dedicação, a confiança e a torcida. Sou extremamente grata pela liberdade de ideias e disposição em desafiar... 'abraçar' o novo. Vocês são exemplos de profissionais e pessoas. Obrigada por serem tão fantásticas, vocês me inspiram todos os dias! Agradeço por tudo de coração!

A Profª Francieli por todo conhecimento e aprendizado desde a graduação. Por ser tão acolhedora e atenciosa!

A Mayara pelo apoio e colaboração. És uma pessoa iluminada e exemplo de liderança! Agradeço por todo carinho, amizade e preocupação. Agradeço também à Luiza pelo apoio, ternura e amizade. Com certeza és um dos muitos presentes que o PPGBBio me proporcionou!

A Nati Bona, um super agradecimento. Pelo apoio, disposição e contribuição incondicionais. Obrigada pelo convívio diário, amizade e

companheirismo. Por ser, desde o mestrado, o meu ‘braço direito’ no laboratório. Esse espaço é, com certeza, pequeno demais para expressar todo o meu carinho e agradecimento.

As queridas Francieli e Juliane por todo auxílio, comprometimento, dedicação e apoio no cultivo celular. Vocês são as melhores ICs! Sou muito grata a vocês por toda ajuda! Ao Fernando, pelo apoio e contribuição. Obrigada por tornar o ambiente de trabalho alegre!

A todos os colegas e amigos que passaram pelo Neurocan e Biomarcadores, assim como aos que fazem parte do nosso grupo atualmente! Vocês foram essenciais nessa jornada! Agradeço profundamente a colaboração, as discussões científicas, o carinho e o apoio. Vocês são demais!

Ao Kirley Canuto e à equipe da Embrapa Agroindústria Tropical pela disponibilidade e colaboração no desenvolvimento deste trabalho. Vocês foram fundamentais no desenvolvimento dessa tese.

A Priscila de Souza por toda ajuda experimental. Te agradeço imensamente pela disponibilidade, parceria e colaboração.

A equipe do Laboratório de Genômica Funcional da Biotecnologia, em especial ao Willian e ao Prof° Vinícius que nos auxiliaram muito na etapa final do Doutorado. Agradeço a colaboração na realização de experimentos que foram fundamentais para a finalização desta tese.

A todas as instituições e grupos de pesquisa que colaboraram para o desenvolvimento deste trabalho. Ao Biotério Central, em especial à Anelize, por toda a colaboração e risadas ao longo dos experimentos do grupo.

Aos professores e funcionários do PPGBBio que muito contribuíram para a realização deste trabalho e para a minha formação.

Aos professores da banca por aceitarem o convite para avaliação do trabalho.

A UFPel pela formação acadêmica desde a Graduação até o Doutorado.

A CAPES pelo apoio financeiro.

A todos que direta ou indiretamente fizeram parte da minha formação, o meu muito obrigado!

*“Por vezes, sentimos que aquilo que fazemos não é, senão, uma gota de água no mar.*
*Mas o mar seria menor se lhe faltasse uma gota.”*

(Madre Tereza de Calcutá)

## Resumo

PEDRA, Nathalia Stark. **Fungo endofítico isolado de *Achyrocline satureioides*: identificação molecular, caracterização química e investigação do efeito antitumoral de metabólitos bioativos**. 2022. 212 f. Tese (Doutorado) - Programa de Pós-Graduação em Bioquímica e Bioprospecção. Universidade Federal de Pelotas, Pelotas, 2022.

O câncer é a principal causa de morte prematura na maioria dos países. A urgência por alternativas terapêuticas tem encorajado a busca por novos agentes anticâncer a partir de produtos naturais. Evidências sugerem que plantas medicinais são colonizadas por fungos endofíticos, os quais consistem em uma importante fonte de estruturas químicas únicas geradas pelas relações coevolutivas com a planta hospedeira. Conhecida como 'marcela', a *Achyrocline satureioides* é uma planta medicinal cujos efeitos antitumorais do extrato vegetal têm sido atribuídos à presença de polifenóis. Recentemente, descrevemos o isolamento e o efeito antiglioma de um fungo endofítico de *A. satureioides*. Assim, este estudo teve como objetivo principal elucidar a taxonomia do fungo isolado, caracterizar os metabólitos presentes na fração purificada ($F_{DCM}$) e avaliar o seu efeito antimelanoma e antiglioma. Diante das propriedades antitumorais de polifenóis associados à *A. satureioides*, este estudo também investigou o impacto antiglioma do ácido gálico (AG) comercial através de testes *in vitro* e *in vivo*. Através da análise molecular da região ITS, o fungo endofítico foi identificado como *Biscogniauxia* sp. (Xylariaceae). A caracterização química de $F_{DCM}$ por cromatografia líquida de ultra-eficiência acoplada ao espectrômetro de massas, demonstrou pela primeira vez a capacidade deste fungo em produzir compostos da classe das isocumarinas, terpenoides, e outros derivados de policetídeos. Sendo este, o primeiro estudo a relatar a biossíntese da lactona Sch-642305 pela família Xylariaceae. De acordo com as análises citotóxicas, o $F_{DCM}$ (1 a 20 µg/mL) reduziu a proliferação das células de melanoma humano (A375) e glioma de rato (C6), induzindo morte e alterações no ciclo celular após 72 h de tratamento. Para compreender a atividade antiglioma no microambiente tumoral, astrócitos corticais de ratos neonatos e células C6 foram cocultivadas e expostas ao $F_{DCM}$ por 72 h. Assim como na C6, em condições de cocultivo o $F_{DCM}$ também reduziu a atividade metabólica, regulou o catabolismo de nucleotídeos extracelulares de adenina e reduziu o estresse oxidativo. Além disso, o $F_{DCM}$ reduziu a resposta inflamatória nos modelos de glioma, além de modular a expressão de genes envolvidos na progressão tumoral como *ERK*, *COX-2*, *Casp-1* e *IL-1β*. Nenhuma alteração foi observada em astrócitos saudáveis. Já o AG (50 a 400 µM) reduziu o crescimento celular de C6 após 48 h, modulando a resposta purinérgica e oxidativa. Por fim, a administração intragástrica de AG (50 e 100 mg/kg/dia) por 15 dias reduziu o volume tumoral, regulou a sinalização purinérgica e preveniu os danos oxidativos no cérebro, soro, plaquetas e/ou linfócitos de ratos submetidos à injeção intracerebroventricular de C6. Nossos dados destacam o elevado potencial dos produtos naturais na modulação de vias relacionadas à progressão neoplásica, ressaltando a importância dos fungos endofíticos como exímios produtores de compostos de interesse farmacológico.



**Palavras-chave**: *Achyrocline satureioides*; fungo endofítico; *Biscogniauxia* sp.; melanoma; glioma; ácido gálico; ATP; adenosina; estresse oxidativo.

## Abstract

PEDRA, Nathalia Stark. **Endophytic fungus isolated from *Achyrocline satureioides*: molecular identification, chemical characterization and investigation of the antitumor effect of bioactive metabolites**. 2022. 212 f. Thesis (Doctorate) - Programa de Pós-Graduação em Bioquímica e Bioprospecção. Universidade Federal de Pelotas, Pelotas, 2022.

Cancer is the leading cause of premature death in most countries. The urgency for therapeutic alternatives has encouraged the search for new anticancer agents from natural products. Evidence suggests that medicinal plants are colonized by endophytic fungi, which are an important source of unique chemical structures generated by coevolutionary relationships with the host plant. Known as 'marcela', *Achyrocline satureioides* is a medicinal plant whose antitumor effects of the plant extract have been attributed to the presence of polyphenols. We recently described the isolation and antiglioma effect of an endophytic fungus of *A. satureioides*. Thus, the main objective of this study was to elucidate the taxonomy of the isolated fungus, to characterize the metabolites present in the purified fraction ($F_{DCM}$) and to evaluate its antimelanoma and antiglioma effect. Given the antitumor properties of polyphenols associated with *A. satureioides*, this study also investigated the antiglioma impact of commercial gallic acid (GA) through in vitro and in vivo tests. Through molecular analysis of the ITS region, the endophytic fungus was identified as *Biscogniauxia* sp. (Xylariaceae). The chemical characterization of $F_{DCM}$ by ultra-performance liquid chromatography coupled to a mass spectrometer demonstrated for the first time the ability of this fungus to produce compounds of the isocoumarins, terpenoids, and other polyketide derivatives. This is the first study to report the biosynthesis of lactone Sch-642305 by the Xylariaceae family. According to cytotoxic analyses, $F_{DCM}$ (1 to 20 µg/mL) reduced the proliferation of human melanoma (A375) and mouse glioma (C6) cells, inducing death and cell cycle changes after 72 h of treatment. To understand the antiglioma activity in the tumor microenvironment, neonatal rat cortical astrocytes and C6 cells were cocultured and exposed to $F_{DCM}$ for 72 h. As with C6, under coculture conditions $F_{DCM}$ also reduced metabolic activity, regulated the catabolism of extracellular adenine nucleotides and reduced oxidative stress. In addition, $F_{DCM}$ reduced the inflammatory response in glioma models, in addition to modulating the expression of genes involved in tumor progression such as *ERK*, *COX-2*, *Casp-1* and *IL-1β*. No changes were observed in healthy astrocytes. AG (50 to 400 µM) reduced C6 cell growth after 48 h, modulating the purinergic and oxidative response. Finally, the intragastric administration of AG (50 and 100 mg/kg/day) for 15 days reduced the tumor volume, regulated purinergic signaling and prevented oxidative damage in brain, serum, platelets and/or lymphocytes of rats submitted to injection of C6 intra-cerebroventricular. Our data highlight the high potential of natural products in modulating pathways related to neoplastic progression, highlighting the importance of endophytic fungi as excellent producers of compounds of pharmacological interest.



**Keywords**: *Achyrocline satureioides*; endophytic fungi; *Biscogniauxia* sp.; melanoma; glioma; gallic acid; ATP; adenosine; oxidative stress.

## Lista de figuras

**Figura 1 -** Resistência terapêutica à quimioterápicos alquilantes..... 23

**Figura 2 -** População heterogênea de células no GBM..... 25

**Figura 3 -** Ativação de receptores purinérgicos estimula a produção de espécies reativas..... 28

**Figura 4 -** Estresse oxidativo no microambiente tumoral..... 30

**Figura 5 -** Mutualismo entre plantas e endófitos..... 33

## Lista de abreviaturas

AG – Ácido Gálico

ADA – Adenosina Deaminase

ADO – Adenosina

ADP – Difosfato de Adenosina

AMP – Monofosfato de Adenosina

ANVISA – Agência Nacional de Vigilância Sanitária

ATP – Trifosfato de Adenosina

Casp-1 – Caspase 1

CAT – Catalase

COX-1 – Ciclooxigenase 1

COX-2 – Cicloogigenase 2

ERK – Quinase Regulada por Sinal Extracelular

ERO – Espécies Reativas de Oxigênio

FDA – Administração de Alimentos e Medicamentos

$F_{DCM}$ – Fração Purificada a partir de Diclorometano

GBM – Glioblastoma

GLOBOCAN – Observatório Global do Câncer

GPx – Glutationa Peroxidase

GST – Glutationa S-Transferase

$H_2O_2$ – Peróxido de Hidrogênio

$IC_{50}$ – Concentração Inibitória Média

IDH – Isocitrato desidrogenase

IL-1β – Interleucina 1β

IL-6 – Interleucina 6

IL-10 – Interleucina 10

INCA – Instituto Nacional do Câncer

ITS – Espaçador Interno Transcrito

MGMT – $O_6$-metilguanina metiltransferase

NTPDase – Ecto-Nucleosideo Trifosfato Difosfohidrolases

$O_2^{\bullet -}$ – Ânion Superóxido

OMS – Organização Mundial da Saúde

RTK – Receptor Tirosina Quinase

SNC – Sistema Nervoso Central

SOD – Superóxido Dismutase

SUS – Sistema Único de Saúde

TMZ – Temozolomida

UV – Ultravioleta

## Apresentação

Os resultados que fazem parte desta tese estão apresentados em três capítulos que correspondem aos dois manuscritos submetidos a revistas científicas (Capitulos 1 e 2) e ao artigo aceito para publicação (Capítulo 3). As seções materiais e métodos, resultados, discussão e referências encontram-se no próprio artigo e manuscritos e representam a íntegra deste estudo.

Os itens discussão e conclusões que se encontram no final desta tese apresentam interpretações e comentários gerais sobre os resultados contidos nesse trabalho.

A lista de referência no final da tese, são apenas de citações que aparecem nos itens introdução, referencial teórico e discussão integrada da tese.

O artigo e os manuscritos estão estruturados de acordo com as revistas as quais foram publicados ou submetidos.

**SUMÁRIO**

1. Introdução..... 15

2. Objetivos..... 18

2.1 Objetivo geral..... 18

2.2 Objetivos específicos..... 18

3. Referencial teórico..... 20

3.1 Câncer..... 20

3.1.1 Melanoma..... 21

3.1.2 Glioma..... 24

3.2 Sinalização purinérgica na progressão do GBM..... 26

3.3 Estresse oxidativo na progressão do GBM..... 28

3.4 Potencial antitumoral de *Achyrocline satureioides*..... 30

3.5 Papel do ácido gálico como agente anticâncer..... 31

3.6 Fungos endofíticos como fonte de compostos antitumorais..... 33

4. Resultados..... 36

4.1 Capítulo 1..... 36

4.2 Capítulo 2..... 89

4.3 Capítulo 3..... 126

5. Discussão integrada..... 168

6. Conclusões..... 184

7. Referências..... 186

Anexos..... 202

## 1. INTRODUÇÃO

Atualmente, o câncer consiste na causa mais comum de morte prematura na maioria dos países (SOERJOMATARAM; BRAY, 2021). Diversos fatores contribuem para o baixo prognóstico das neoplasias malignas, entretanto, a metástase cerebral representa o principal componente relacionado à mortalidade de 20% dos pacientes com câncer (SACKS; RAHMAN, 2020). A disseminação cerebral acomete mais de 50% dos pacientes diagnosticados com melanoma no estágio mais agressivo da doença (SUNDARAJAN *et al*., 2022). Pesquisas crescentes indicam ainda que indivíduos com propensão genética ao melanoma têm maiores chances de desenvolver glioma, o tumor cerebral primário mais comum do sistema nervoso central (SNC), sugerindo que tais tumores compartilham alterações moleculares que favorecem o desenvolvimento da carcinogênese (SCARBROUGH *et al*., 2014; ENDICOTT; TAYLOR; WALSH, 2016; HOWELL *et al*., 2019; YAUN; WANG; MA, 2022).

De acordo com o sistema de classificação da Organização Mundial da Saúde (OMS), os gliomas de grau 4 são caracterizados por mecanismos complexos de malignidade, constituindo os tumores mais agressivos e letais do SNC (LOUIS *et al*., 2021; STEWARDT *et al*., 2022). Os mecanismos envolvidos na transformação de células gliais sadias em células malignas constituem um processo multifatorial, no qual as interações entre as células de glioma e o microambiente tecidual são essenciais para fornecer suporte fisiológico para o desenvolvimento do tumor (BRAGANHOL *et al*., 2013). Evidências sugerem que a sinalização purinérgica participa na regulação da proliferação, diferenciação, mobilidade e morte celular de diversos tipos de câncer (MORRONE *et al*., 2003; BRAGANHOL *et al*., 2009, 2013; BURNSTOCK; DI VIRGILLIO *et al*., 2013).

De maneira geral, o SNC possui uma elevada atividade metabólica e é particularmente sensível aos danos causados pelos radicais livres. Estudos destacam que a ativação de receptores purinérgicos mediada por nucleotídeos e nucleosídeos extracelulares desencadeia a produção de espécies reativas de oxigênio e de nitrogênio e altera as defesas antioxidantes (SAVIO *et al*., 2021; HUANG; TANG; SPERLAGH, 2022). De fato, o aumento dos danos oxidativos encontrados nos gliomas contribuem para as alterações bioquímicas e

moleculares necessárias para o desenvolvimento e progressão do tumor (RAMÍREZ-EXPÓSITO; MARTÍNEZ-MARTOS, 2019).

No Brasil, tanto o melanoma metastático quanto os gliomas de alto grau são pouco responsivos à terapia convencional disponibilizada pelo Sistema Único de Saúde (SUS). Atualmente, os agentes quimioterápicos dacarbazina e temozolomida (TMZ) são utilizados no tratamento do melanoma e do glioma de alto grau, respectivamente (CONITEC, 2020a, 2020b). Contudo, ambas as neoplasias são marcadas por quimioresistência, tornando o prognóstico dos pacientes extremamente ruim (JIANG *et al*., 2011; FAN *et al*., 2013; SOLAK; KILICKAP; CELIK; 2021), sendo por isso extremamente necessário a busca por novas modalidades terapêuticas.

Desta forma, os produtos naturais, têm desempenhado importante papel no desenvolvimento de fármacos clinicamente úteis (ERICES *et al*., 2018). Popularmente conhecida como “marcela”, a *Achyrocline satureioides* apresenta diversos efeitos farmacológicos, incluindo potencial citotóxico sobre linhagens de glioma (DE SOUZA *et al*., 2018) e melanoma humano (DONEDA *et al*., 2021), cujos efeitos foram relacionados à biossíntese de polifenóis, especialmente flavonóides. Embora os efeitos antitumorais de outros compostos fenólicos produzidos pela *A. satureioides*, como o ácido gálico (AG), sejam bem documentados (HATAMI *et al*., 2012; FERNÁNDEZ-FERNÁNDEZ *et al*., 2021), não há estudos avaliando o seu efeito em modelo pré-clínico de glioma.

Além das plantas, os microrganismos constituem outra fonte promissora para a busca de metabólitos bioativos (JIA *et al*., 2016). Strobel e Long (1998) revelam que microorganismos endofíticos associados às plantas, em especial fungos endofíticos, podem oferecer uma gama superior de compostos químicos com atividade terapêutica do que a própria planta, representando assim, uma fonte promissora de compostos bioativos. Considerando os efeitos farmacológicos exercidos pela *A. satureioides* e a falta de estudos elucidando a composição endofítica desta planta medicinal, nosso grupo de pesquisa tem trabalhado no isolamento de fungos endofíticos a partir de *A. satureioides*.

Recentemente nosso grupo analisou a atividade antitumoral de extratos brutos e purificados do fungo endofítico isolado de *A. satureioides* (PEDRA *et*

*al*., 2018). Neste estudo, foi possível identificar a fração mais efetiva e, a partir dela, isolou-se a lactona Sch-642305, a qual reduziu significativamente a proliferação e migração celular e induziu apoptose exibindo efeito antiglioma seletivo (PEDRA *et al*., 2018). Diante dos resultados alcançados, torna-se importante esclarecer a taxonomia do fungo endofítico isolado e elucidar os efeitos farmacológicos e bioquímicos da fração purificada obtida a partir do extrato de atividade mais promissora.

# 2. OBJETIVOS

## 2.1 Objetivo geral

O objetivo geral desse trabalho foi identificar o fungo endofítico de *Achyrocline satureioides*, caracterizar os componentes químicos e avaliar o efeito citotóxico da fração purificada ($F_{DCM}$) sobre linhagem celular de melanoma cutâneo (A375) e glioma (C6). Além disso, outro objetivo deste estudo foi elucidar o impacto do ácido gálico na terapia antiglioma através de testes *in vitro* e em modelo pré-clínico de glioblastoma.

## 2.2 Objetivos específicos

**Capítulo 1**

- Quanto ao fungo endofítico isolado de *A. satureioides* e seu efeito citotóxico sobre linhagem celular de melanoma humano (A375)*:*

- Identificar a taxonomia;
- Identificar os compostos presentes na fração purificada ($F_{DCM}$);
- Determinar o efeito citotóxico mediante análise da viabilidade, proliferação, ciclo e morte celular.

**Capítulo 2**

- Quanto ao efeito de $F_{DCM}$ sobre linhagem celular de glioma (C6), cultura primária de astrócitos e condições de cocultivo astrócito-glioma:

- Avaliar a viabilidade celular;
- Determinar a atividade das enzimas NTPDases e 5'-nucleotidase;
- Analisar os níveis de espécies reativas de oxigênio, conteúdo tiólico total, e atividade das enzimas antioxidantes superóxido dismutase, catalase e glutationa-S-transferase;
- Determinar os níveis de interleucina 6 e interleucina 10;
- Avaliar a expressão de ciclooxigenase-1, ciclooxigenase-2, caspase-1, interleucina 1-β e quinase regulada por sinal extracelular.

**Capítulo 3**

- Quanto ao efeito do ácido gálico em linhagem celular de glioma (C6):

- Avaliar a viabilidade e proliferação celular sobre linhagem de glioma (C6) e cultura primária de astrócitos;
- Analisar os níveis de espécies reativas de oxigênio, conteúdo tiólico total, e atividade das enzimas antioxidantes superóxido dismutase, catalase e glutationa peroxidase sobre linhagem de glioma (C6);
- Determinar a atividade das enzimas NTPDases e 5'-nucleotidase.

- Quanto ao efeito do ácido gálico em modelo pré-clínico de GBM:

- Quantificar o crescimento do tumor mediante análise histológica;
- Avaliar a atividade locomotora através do teste do campo aberto;
- Quantificar os níveis de glicose, alanina aminotransferase, aspartato aminotransferase, creatinina e ureia em soro;
- Analisar os níveis de espécies reativas de oxigênio, níveis de nitritos, conteúdo tiólico total, peroxidação lipídica e atividade das enzimas antioxidantes superóxido dismutase, catalase e glutationa S-transferase no tecido tumoral;
- Determinar os níveis de espécies reativas de oxigênio, níveis de nitritos, conteúdo tiólico total e atividade das enzimas antioxidantes superóxido dismutase, catalase e glutationa S-transferase em soro e plaquetas;
- Avaliar a atividade das enzimas NTPDases, 5'-nucleotidase e/ou adenosina deaminase em soro, linfócitos e plaquetas.

# 3. REFERENCIAL TEÓRICO

## 3.1 Câncer

O câncer é uma doença heterogênea caracterizada pela desregulação de múltiplas vias envolvidas na manutenção do crescimento, diferenciação, migração e morte celular (KREEGER; LAUFFENBURGER, 2010; PERES-HERRERO; FERNÁNDEZ-MEDARDE, 2015). A transformação maligna é geralmente desencadeada pelo acúmulo de mutações, cujas alterações genômicas promovem traços característicos da oncogênese como proliferação celular sustentada, imortalidade replicativa, ativação de invasão e metástase, reprogramação do metabolismo celular e resistência à morte celular (HANAHAN, 2022).

Além das capacidades adquiridas para evitar supressores de crescimento e a destruição imunológica, quatro novas características facilitadoras têm emergido como importantes componentes na progressão de neoplasias malignas. Neste contexto, (1) o desbloqueio da plasticidade fenotípica permitindo diversas interrupções da diferenciação celular; (2) a reprogramação do genoma não mutacional, cujas alterações podem manifestar-se como mecanismos puramente epigenéticos na evolução do câncer; (3) o potencial do microbioma tecidual em estimular ou inibir vias de sinalização proliferativas ou supressoras de tumor; e (4) o impacto da senescência celular na indução da angiogênese e resistência terapêutica desempenham um papel decisivo no microambiente tumoral (HANAHAN, 2022).

Com base nos dados epidemiológicos da OMS, o câncer é considerado a principal causa de morte prematura em países desenvolvidos, além de representar a segunda principal causa de morte no mundo (WHO, 2020; SUNG *et al*., 2021). A alta taxa de incidência e mortalidade é refletida em parte pelo aumento da idade e crescimento populacional (SUNG *et al*., 2021). Pilleron e colaboradores (2020) estimam que o número de novos casos de câncer deve triplicar em adultos com 80 anos ou mais até 2050. Além disso, mudanças na distribuição socioeconômica contribuem para o aumento da taxa de mortalidade global (SUNG *et al*., 2021). Segundo a Organização Pan-Americana da Saúde

(ORGANIZAÇÃO PAN-AMERICANA DA SAÚDE, 2020), aproximadamente 70% das mortes por câncer ocorrem em países de baixa e média renda, 40% dos casos poderiam ser prevenidos evitando fatores de risco e 30% dos casos poderiam ser curados se houvesse detecção precoce e tratamento adequado. No Brasil, o Instituto Nacional de Câncer (INCA) estima que para cada ano do triênio 2020-2022, ocorrerão 625 mil casos novos de câncer (INCA, 2020).

Entre os diferentes tipos de câncer, o melanoma cutâneo e os gliomas de alto grau, especialmente o glioblastoma, destacam-se no presente estudo. De acordo com Sundararajan e colaboradores (2022), dados epidemiológicos sugerem que o melanoma ocupa a quinta e sexta posição entre os tumores de maior malignidade em homens e mulheres de países desenvolvidos como os Estados Unidos, respectivamente. Mais de 60% dos pacientes com melanoma mestastático desenvolvem metástases cerebrais durante o curso da doença, as quais representam a segunda principal causa de óbitos relacionados a esta patologia (GUO, WANG; LI, 2021; SUNDARAJAN *et al*., 2022). Em relação às estatísticas disponíveis atualmente para neoplasias do SNC, os tumores cerebrais não estão incluídos nos 10 tipos de cânceres mais comuns. Entretanto, a elevada taxa de mortalidade de pacientes diagnosticados com gliomas de alto grau indica um prognóstico extremamente ruim para esse grupo de pacientes (SUNG *et al*., 2021).

### 3.1.1 Melanoma

O melanoma representa a neoplasia cutânea primária mais letal (GUO, WANG; LI, 2021). De acordo com a Agência Internacional de Pesquisa do Câncer (IARC, do inglês *Internacional Agency for Research on Cancer*), a incidência global de melanoma aumentou de forma constante nos últimos 30 anos (ARNOLD *et al*., 2022). Em 2020 foram registrados 325 mil novos casos e 57 mil óbitos por melanoma. Com base nas mudanças populacionais globais, os cientistas estimam que mais de 500 mil novos casos de melanoma por ano e quase 100 mil mortes por melanoma devem ser esperados em todo o mundo até 2040 (ARNOLD *et al*., 2022).

O melanoma origina-se a partir da transformação maligna dos melanócitos, células derivadas da crista neural e responsáveis pela produção de melanina (HIDA *et al*., 2020). Após ser sintetizada a partir da enzima tirosinase, a melanina é empacotada em organelas especializadas, os melanossomos, os quais são transferidos mediante processos dendríticos para os queratinócitos vizinhos (BOHJANEN, 2017). Apesar dos melanócitos representarem uma população minoritária e dividirem-se com pouca frequência, a radiação UV estimula a sua proliferação e consequentemente, a produção de melanina. Neste contexto, apesar da melanina atuar como um sistema de defesa protegendo os queratinócitos epidérmicos contra danos ao DNA, a exposição excessiva à radiação UV promove uma elevada carga mutacional cujo acúmulo sequencial de alterações genéticas favorecem o desenvolvimento do melanomagênese (JACKETT; SCOLYER, 2019).

Embora a exposição à radiação UV represente um dos principais fatores de risco para o desenvolvimento do melanoma, o fototipo da pele, a presença de nevos pigmentados, condições imunossupressoras, fatores genéticos e hereditários também compreendem componentes importantes relacionados à iniciação e progressão do tumor (STRASHILOV; YORDANOV, 2021). De acordo com o sistema de classificação da OMS, o melanoma cutâneo pode ser classificado de acordo com suas características histológicas, clínicas, epidemiológicas e genéticas (ELDER *et al*., 2018). O estadiamento do melanoma pode ser dividido em 5 fases (0 a 4), sendo os estágios 3 e 4 caracterizados por metástases cutâneas e linfáticas respectivamente, disseminando-se para outras regiões do corpo. Embora outros órgãos também possam ser afetados, as metástases mais relevantes envolvem órgãos importantes como cérebro, pulmão e fígado (PAPP *et al*., 2021).

O tratamento utilizado em pacientes diagnosticados com melanoma em estágios iniciais é a cirurgia. Entretanto, neoplasias cutâneas avançadas podem contar com outras estratégias terapêuticas como quimioterapia, imunoterapia ou terapias-alvo. Enquanto a quimioterapia ataca células cancerosas e saudáveis provocando efeitos adversos e quimioresistência, as terapias-alvo atuam apenas em células que apresentam mutações no gene *BRAF*, o qual está mutado em

cerca de 50% dos casos de melanoma maligno e é responsável pela desregulação do ciclo celular e crescimento descontrolado das células tumorais (HUBER *et al*., 2016). No Brasil, o quimioterápico dacarbazina é a única opção terapêutica disponível no Sistema Único de Saúde (SUS) para pacientes com melanoma metastático (CONITEC, 2020a).

A dacarbazina é um agente alquilante que provoca danos ao DNA, induzindo parada no crescimento e morte celular (JIANG *et al*., 2011). Apesar de ser o único quimioterápico aprovado pelo *Food and Drug Administration* (FDA) para terapia antimelanoma, a dacarbazina promove uma taxa de resposta de 8 a 20% e uma sobrevida média de apenas 4 a 6 meses (SOLAK *et al*., 2021). Um dos principais mecanismos de resistência envolvendo da dacarbazina é a atividade aumentada da enzima de reparo do DNA, $O^6$-metilguanina-DNA-metiltransferase (MGMT) (**Figura 1**). O MGMT repara as lesões de DNA induzidas pelo quimioterápico transferindo o grupo alquilo da guanina para um resíduo de cisteína, desta forma, a metilação da região promotora de MGMT contribui para a resistência à dacarbazina em pacientes com melanoma metastático (TAWBI *et al*., 2011; WU *et al*., 2021). Diante do exposto, a busca por novas estratégias terapêuticas torna-se essencial a fim de melhorar o prognóstico dos pacientes com melanoma mestastático.

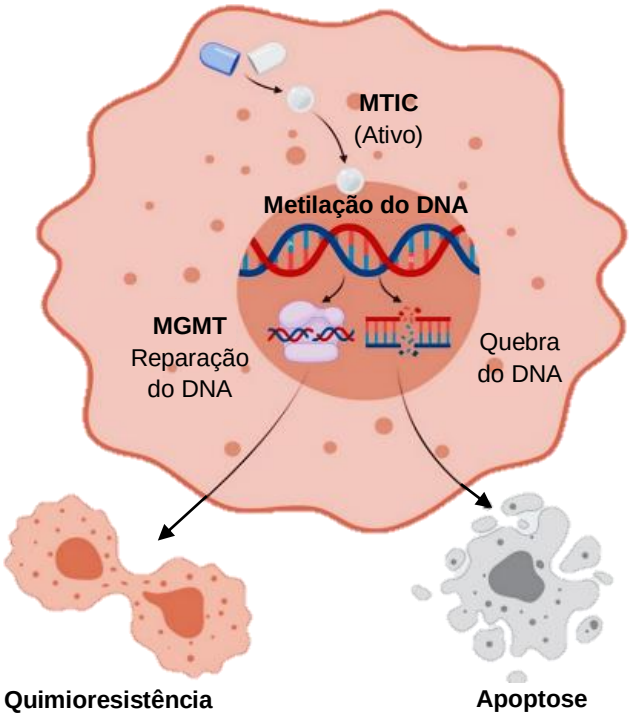


**Figura 1 –** Resistência terapêutica à quimioterápicos alquilantes. Fonte: LUCIFERO; LUZZI, 2021, com modificações.

### 3.1.2 Glioma

Entre as neoplasias cerebrais do SNC, os gliomas difusos consistem na forma mais comum de tumor intracraniano primário (YUAN; WANG; MA, 2022). A incidência dos gliomas varia de acordo com a idade, sexo, raça e região geográfica. No geral, esta neoplasia representa aproximadamente 30% de todos os tumores cerebrais primários e mais de 80% de todos os tumores agressivos em adultos (PELLERINO *et al*., 2022), com uma incidência anual de 6 casos a cada 100 mil pessoas dependendo do país (OSTROM *et al*., 2018). No Brasil, a taxa de incidência de tumores do SNC estimada para o triênio 2020-2022, segundo o INCA, é de 5,87 novos casos a cada 100 mil homens e 5,23 casos novos para cada 100 mil mulheres por ano (INCA, 2020).

Os gliomas podem apresentar características fenotípicas e moleculares similares às células gliais, como astrócitos, oligodendrócitos e células ependimárias. Historicamente, a classificação dos gliomas era baseada nas alterações morfológicas do tumor, cujas características histopatológicas eram presumidas conforme a origem celular. Conceitualmente, os astrócitos representavam as células progenitoras dos astrocitomas (grau I a III) e dos glioblastomas (GBMs) (grau IV). Contudo avanços recentes permitiram o refinamento da classificação tumoral com base em alterações moleculares (WHITFIELD; HUSE, 2022). De acordo com a 4ª edição da classificação da OMS de tumores cerebrais do SNC publicada em 2016, pacientes com GBM poderiam apresentar mutação na enzima isocitrato desidrogenase (IDH mutante) ou não (IDH-tipo selvagem) (LOUIS *et al*., 2016).

Atualmente, a 5ª edição do sistema de classificação da OMS distingue os gliomas de acordo com o padrão de crescimento (em difuso ou circunscrito), a faixa etária (em glioma difuso tipo-adulto ou tipo-pediátrico) e o grau de malignidade (em números arábicos de 1 a 4) conforme as alterações genéticas apresentadas pelo paciente (LOUIS *et al*., 2021). Nesta nova classificação, a OMS formaliza o *status* mutacional da enzima IDH como característica definidora de astrocitomas do tipo-adulto, reservando o termo “glioblastoma” especificamente para tumores IDH-tipo selvagem (LOUIS *et al*., 2021; WHITFIELD; HUSE, 2022). Neste contexto, os gliomas difusos tipo-adulto de

maior malignidade podem ser de dois tipos: astrocitoma de grau 4 (IDH-mutante) e GBM (neoplasia de grau 4 que exibe IDH-tipo selvagem) (LOUIS *et al*., 2021).

Stewardt e colaboradores (2022) revelam que pacientes diagnosticados com astrocitoma de grau 4 possuem uma sobrevida global e livre de progressão tumoral superior, comparado à pacientes com GBM. Uma possível justificativa para esse achado pode estar relacionada ao fato dos astrocitomas IDH-mutantes apresentarem um menor número de alterações moleculares, enquanto os GBMs normalmente abrigam diversas anormalidades genéticas espalhadas por redes oncológicas clássicas, incluindo a p53 e genes do receptor tirosina quinase (RTK, do inglês *Receptor Tyrosine Kinase*) (WHITFIELD; HUSE, 2022).

Além de ser caracterizado por múltiplas mutações, o microambiente do GBM é composto por uma população heterogênea de células (**Figura 2**) (SCHIFFER *et al*., 2019). A modulação de componentes da matriz extracelular por diferentes vias de sinalização favorece significativamente a migração e invasão das células tumorais no parênquima cerebral, tornando as áreas de necrose, as quais correspondem regiões de hipóxia circundadas por células altamente infiltrativas, características marcantes do GBM (MANINI *et al*., 2018). Tais características presentes no microambiente tumoral tornam esta neoplasia maligna altamente agressiva, conferindo aos pacientes acometidos pelo GBM, uma sobrevida média de um ano (OSTROM *et al*., 2016).

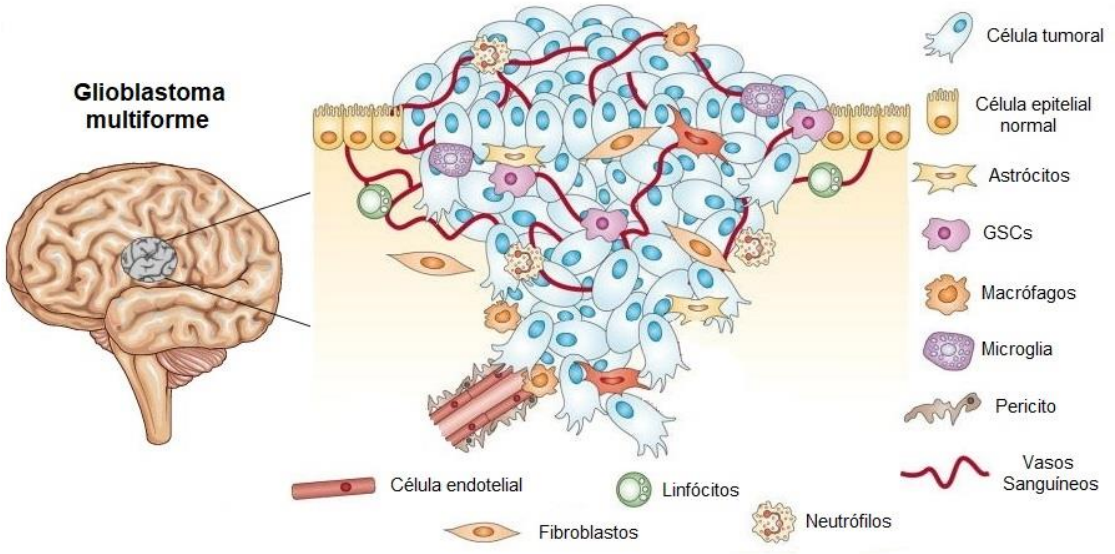


**Figura 2** – População heterogênea de células no GBM.
Fonte: SCHIFFER *et al*., 2019, com modificações.

Atualmente, o tratamento para os gliomas consiste em uma terapia multimodal envolvendo ressecção cirúrgica, radioterapia e/ou quimioterapia (SCHIFFER *et al*., 2019). O quimioterápico atualmente utilizado para o tratamento do GBM, a temolozomida (TMZ), consiste em um agente alquilante que ultrapassa a barreira hematoencefálica provocando danos ao DNA e apoptose celular (LEE, 2016). Entretanto, a atividade aumentada da MGMT induzida pelo TMZ consiste em um dos principais mecanismos de resistência dos pacientes com GBM (FAN *et al*., 2013).

Neste contexto, além das alterações em vias que controlam a proliferação, morte e diferenciação das células tumorais tem sido demonstrado que a presença de um microambiente favorável é elemento essencial para a progressão do câncer (HANAHAN; WEINBERG, 2011). Entre as características patológicas que conferem potencial invasivo às células de GBM, a sinalização purinérgica e o estresse oxidativo têm emergido como importantes componentes favorecendo o crescimento tumoral (SALAZAR-RAMIRO *et al*., 2016; BRAGANHOL *et al*., 2020).

### 3.2 Sinalização purinérgica na progressão do GBM

O conceito de sinalização purinérgica utilizando nucleotídeos e nucleosídeos de purinas e de pirimidinas como mensageiros extracelulares, foi inicialmente proposto na década de 1970 por Geoffrey Burnstock (BURNSTOCK, 2006). Os nucleotídeos de adenina - adenosina trifosfato (ATP), adenosina difosfato (ADP) e adenosina monofosfato (AMP) - e o nucleosídeo adenosina (ADO), constituem importantes moléculas sinalizadoras que atuam neste sistema de comunicação (BURNSTOCK, 2006; GIULIANI; SARTI; DI VIRGILLIO, 2018).

O ATP e os seus produtos de degradação têm sido caracterizados como moléculas sinalizadoras em diversos processos celulares (GIULIANI; SARTI; DI VIRGILLIO, 2018). No SNC, os neurônios e as células gliais atuam como importantes fontes de purinas extracelulares (WELSH; KUCENAS, 2018). Sob condições fisiológicas, o ATP pode ser armazenado em vesículas e liberado no meio extracelular por exocitose juntamente com outros neurotransmissores

(FRANKE *et al*., 2012). Já no microambiente tumoral, o ATP pode ser liberado para o espaço extracelular a partir de áreas de necrose, hemorragia, excitotoxicidade e/ou lesões desencadeadas pela ressecção cirúrgica do tumor (GEHRING *et al*., 2015).

Uma vez liberados no espaço extracelular, os nucleotídeos interagem com receptores transmembrana e finalmente são hidrolisados por ectoenzimas até os seus respectivos nucleosídeos (ZIMMERMANN, 2006; GIULIANI; SARTI; DI VIRGILLIO, 2018). As ações biológicas do ATP e da ADO extracelular dependem da ativação de receptores purinérgicos, os quais são amplamente expressos no SNC. Esses receptores são divididos em duas classes principais: os receptores P1 e P2. Os receptores P1 (A1, A2a, A2b e A3) são acoplados à proteína G e ativados pela ADO, enquanto os receptores P2 têm preferência por nucleosídeos di- e trifosfatados e são classificados de acordo com o subtipo: P2X (ionotrópicos) ou P2Y (metabotrópicos). Até o momento, são conhecidos sete subtipos de receptores $P2X_{1-7}$ e oito subtipos de receptores $P2Y_{1,2,4,6,11-14}$ (WELSH; KUCENAS, 2018).

A família das NTPDases é constituída por 8 membros (NTPDase1-8) as quais diferem quanto à especificidade pelo substrato, distribuição tecidual e localização celular. Tais enzimas atuam hidrolisando nucleosídeos tri- e difosfatados (ATP e ADP, respectivamente), produzindo nucleosídeos monofosfatados (AMP) como produto final (GIULIANI; SARTI; DI VIRGILLIO, 2018). Já a enzima CD73 hidrolisa com alta afinidade o AMP extracelular, produzindo assim, ADO, sendo considerada enzima chave no controle da concentração de ADO extracelular (GIULIANI; SARTI; DI VIRGILLIO, 2018). Posteriormente, a ADO é desaminada à inosina pela ação da adenosina deaminase (ADA) (VIJAYAN; SMYTH; TENG, 2018).

Evidências relatam o envolvimento de enzimas e receptores purinérgicos na malignidade do GBM. Tem sido demonstrada a expressão das enzimas NTPDase2, NTPDase3 e CD73, bem como dos receptores P1, $P2Y_{1, 2, 4, 12-14}$ e P2X4 e 7 tanto em linhagens de glioma quanto em células presentes na massa tumoral de pacientes acometidos pelo GBM, entretanto os mecanismos exatos

ainda não estão completamente elucidados (BRAGANHOL *et al*., 2009; XU *et al*., 2013; WANG *et al*., 2016; JI *et al*., 2018).

Por ativar receptores específicos em linhagens tumorais, o ATP e a ADO extracelular têm sido associados a eventos relacionados à proliferação, diferenciação, migração, invasão, angiogênese e morte celular (WHITE; BURNSTOCK, 2006; VIJAYAN; SMYTH; TENG, 2018; AZAMBUJA *et al*., 2019). Além disso, estudos apontam que a ativação de receptores purinérgicos favorecem a produção de espécies reativas de oxigênio e redução defesas antioxidante enzimáticas, acelerando a progressão tumoral (**Figura 3**) (SAVIO *et al*., 2021; HUANG; TANG; SPERLAGH, 2022).

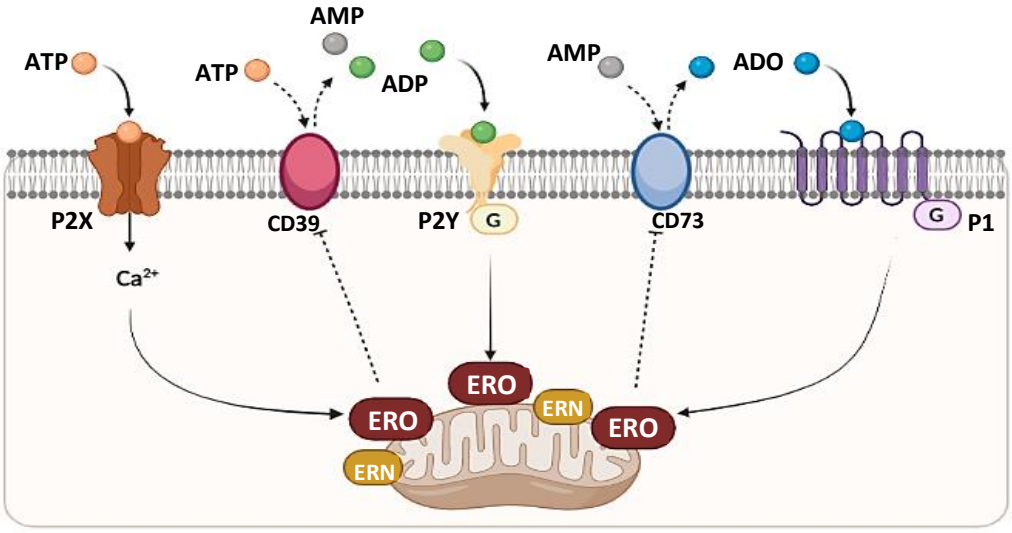


**Figura 3 -** Ativação de receptores purinérgicos estimula a produção de espécies reativas.
Fonte: O autor (2022).

### 3.3 Estresse oxidativo na progressão do GBM

De maneira geral, os compostos oxidantes são formados continuamente em condições fisiológicas como produtos de reações metabólicas, enquanto os antioxidantes atuam como um mecanismo de adaptação utilizando sinais necessários para a produção de radicais livres, além de prevenir a formação ou reação excessiva desses compostos (IGHODARO; AKINLOYE, 2018; DI MEO; VINDITTI, 2020). Quando esse equilíbrio é interrompido os compostos oxidantes

promovem peroxidação lipídica das membranas celulares, oxidação de proteínas e DNA, além de desencadear alterações cromossômicas e mutações genéticas, favorecendo a formação e/ou progressão de diversas patologias humanas, incluindo o câncer (RAMÍREZ-EXPÓSITO; MARTÍNEZ-MARTOS, 2019; KLAUNING, 2018). O desequilíbrio entre os níveis de oxidantes (espécies reativas ou radicais livres) e o sistema de defesa antioxidante é denominado estresse oxidativo (KLAUNING, 2018).

Os radicais livres derivam principalmente a partir de: a) espécies reativas de oxigênio (ERO) como oxigênio singleto, ânion superóxido ($O_2^{\bullet -}$), peróxido de hidrogênio ($H_2O_2$), radical hidroxil, radical peroxil e ácido hipocloroso; b) espécies reativas de nitrogênio como óxido nítrico, dióxido nítrico, nitroxil e peroxinitrito e c) espécies reativas de enxofre como sulfeto de hidrogênio, persulfetos e óxido de enxofre (RAMÍREZ-EXPÓSITO; MATÍNEZ-MARTOS, 2019). Entretanto, evidências têm focado no importante papel de ERO na progressão do GBM devido ao seu papel na proliferação, diferenciação e morte celular (SALAZAR-RAMIRO *et al*., 2016; RAMÍREZ-EXPÓSITO; MATÍNEZ-MARTOS, 2019).

A produção de ERO é inibida por antioxidantes endógenos como as enzimas superóxido dismutase (SOD), catalase (CAT) e glutationa peroxidase (GPx), as quais atuam como a primeira linha de defesa antioxidante (IGHODARO; AKINLOYE, 2018). A SOD catalisa a dismutação de $O_2^{\bullet -}$ em $H_2O_2$, enquanto as enzimas CAT e GPx são responsáveis pela desintegração de $H_2O_2$, impedindo assim a formação do radical hidroxil (IGHODARO; AKINLOYE, 2018; RAMÍREZ-EXPÓSITO; MATÍNEZ-MARTOS, 2019). Nos tumores cerebrais, os genes responsáveis pelo controle da atividade dessas enzimas podem ser alterados pelos radicais livres. Dessa forma, o desenvolvimento dos gliomas não envolve apenas a produção excessiva de ERO, mas também a resposta reduzida do sistema de defesa antioxidante (**Figura 4**) (ILLÁN-CABEZA *et al*., 2013).

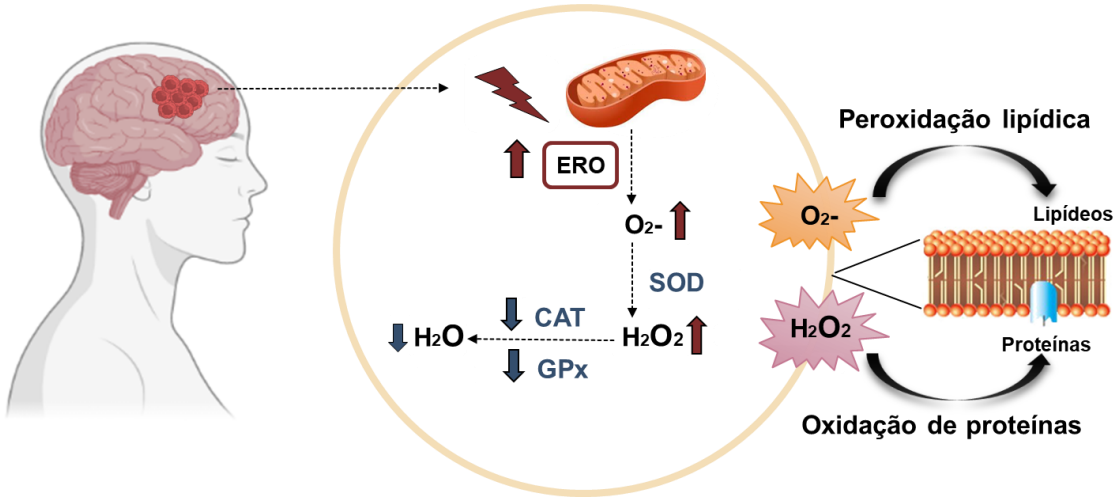


**Figura 4 –** Estresse oxidativo no microambiente tumoral.
Fonte: O autor (2022).

### 3.4 Potencial antitumoral de *Achyrocline satureioides*

Os produtos naturais têm sido utilizados por séculos para o tratamento de diversas doenças, incluindo o câncer. A importância desses compostos naturais reside na possibilidade de descobrir novos compostos para a terapia antineoplásica (ERICES *et al*., 2018).

O gênero *Achyrocline* compreende espécies de plantas pertencentes à família Asteraceae. Há cerca de 40 espécies de *Achyrocline* spp. distribuídas em regiões tropicais e subtropicais das Américas Central e Sul (RETTA *et al*., 2012). Popularmente conhecida como “macela ou marcela”, a *A. satureioides* está inserida na lista de espécies medicinais da Agência Nacional de Vigilância Sanitária (ANVISA) e no Formulário de Fitoterápicos da Farmacopeia Brasileira (RETTA *et al*., 2012; GONÇALVEZ; FERREIRA; MING, 2018).

Dados da literatura têm demonstrado o potencial antitumoral de *A. satureioides*. Ruffa e colaboradores (2002) revelaram atividade citotóxica de extratos de *A. satureioides* sobre o carcinoma hepatocelular humano (Hep-G2). Além disso, extratos provenientes de *A. satureioides* exibem importantes efeitos antineoplásicos sobre linhagens de câncer de mama humano BT-474 (WALKER, 2013) e MDA-MB-231 (BIANCHI *et al*., 2020). De acordo com Bianchi e colaboradores (2020), compostos provenientes de *A. satureioides* induzem apoptose mediante ativação das caspases 3/7. Ainda segundo os autores, o

efeito antitumoral promovido pela planta medicinal foi seletivo, não exibindo citotoxicidade sobre células epiteliais humana não tumorigênicas.

De Souza e colaboradores (2018) demonstraram, ainda, os mecanismos envolvidos com a atividade anticâncer de *A. satureioides* em linhagens de GBM (U87MG, U251 e C6). De acordo com os autores, os extratos de *A. satureioides* reduziram a proliferação e a sobrevivência clonogênica, induzindo apoptose nas células de glioma e reduzindo a ativação de ERK e JNK envolvidas com a progressão do GBM. Além disso, os compostos produzidos pela planta potencializaram o efeito citotóxico e indução de apoptose pelo quimioterápico TMZ (DE SOUZA *et al*., 2018).

A atividade citotóxica de *A. satureioides* também tem sido evidenciada em linhagem de melanoma humano A375 (DONEDA *et al*., 2021). Neste estudo, o potencial antimelanoma do metabólito bioativo foi associado à sua capacidade de alterar o ciclo celular. Os efeitos antiproliferativos também foram atribuídos à indução de apoptose em concentrações menores e apoptose tardia/necrose de maneira dependente da concentração (DONEDA *et al*., 2021).

De maneira geral, o potencial antitumoral de *A. satureioides* tem sido atribuído principalmente à biossíntese de achyrobichalcona, 3-O-metilquercetina, quercetina e luteolina (DE SOUZA *et al*., 2018; BIANCHI *et al*., 2020; DONEDA *et al*., 2021). Além dos flavonóides, outros compostos fenólicos também têm sido identificados em extratos de *A. satureioides* como ácido clorogênico, ácido cafeico e ácido gálico (HATAMI *et al*., 2012; FERNÁNDEZ-FERNÁNDEZ *et al*., 2021). Diante dos efeitos antineoplásicos dos polifenóis e seus derivados (KUO *et al*., 2006; KUDUGUNTI *et al*., 2009; SUBRAMANIAN *et al*., 2014; YE *et al*., 2020; ZHAN *et al*., 2020), os compostos fenólicos têm emergido como interessantes agentes antitumorais estimulando pesquisas no campo.

### 3.5 Papel do ácido gálico como agente anticâncer

O ácido gálico (AG) (3,4,5-ácido trihidroxibenzóico) é um potente antioxidante amplamente encontrado em produtos naturais e tem sido extensivamente estudado como agente anti-inflamatório e antitumoral (HSU *et*

*al*., 2016; KAHKESHANI *et al*., 2019). Evidências sugerem que o AG exerce os seus efeitos antineoplásicos através da modulação de vias envolvidas na migração, parada do ciclo celular, metástase, apoptose, angiogênese e expressão de oncogenes (VERMA; SINGH; MISHRA, 2013; JIANG *et al*., 2021).

Na linhagem de carcinoma de células não pequenas de pulmão humano (NCI-H460), o AG reduziu o percentual de células viáveis mediante a indução de apoptose através da via mitocondrial dependente de caspase e parada do ciclo celular em G2/M (JI *et al*., 2009). Além de estimular a produção de $Ca^{+2}$ intracelular e perda do potencial de membrana mitocondrial sobre a linhagem celular tumoral, o AG inibiu o crescimento das células NCI-H460 em modelos animais de xenoenxerto *in vivo* (JI *et al*., 2009).

Os efeitos antimelanoma do AG também têm sido reportados. O AG induz apoptose em linhagem de melanoma humano (A375) através de mecanismos dependentes e independentes de caspases (LO *et al*., 2010), além de suprimir a migração e invasão destas células mediante alteração da via de sinalização *Ras* resultando na inibição da metaloproteinase de matriz 2 (LO *et al*., 2011). Pesquisadores destacam ainda o potencial do AG na inibição da iniciação e progressão do melanoma. De acordo com Su e colaboradores (2013), o AG inibe a síntese de melanina e atividade da enzima tirosinase de maneira tempo e concentração dependente, reduzindo a expressão de proteínas relacionadas ao melanomagênese. Já em modelo experimental *in vivo*, a aplicação tópica de AG suprime significativamente as fases de iniciação e progressão da carcinogênese cutânea através da modulação da atividade de enzimas antioxidantes e metaloproteinases (SUBRAMANIAN *et al*., 2014).

Estudos crescentes têm avaliado a atividade citotóxica do AG em células de glioma. Lu e colaboradores (2010) observaram uma redução expressiva da proliferação, angiogênese e invasão celular em linhagens de GBM humano (U87 e U251) expostas ao AG. Em células de glioma humano DBTRG-05MG, o AG também ativou vias mitocondriais de apoptose associadas ao $Ca^{2+}$ intracelular, desencadeando a produção de ERO (HSU *et al*., 2016). Recentemente, Yang e colaboradores (2022) revelaram que a associação do AG ao TMZ potencializou os efeitos citotóxicos e nível apoptótico do quimioterápico em linhagem de GBM

U87. Ainda segundo os autores, este efeito antiproliferativo correlacionou-se com a diminuição da expressão da proteína anti-apoptótica Bcl-2 e regulação da via de transdução de sinal *Akt*, a qual regula a sobrevivência e apoptose celular em resposta a sinais extracelulares. Além disso, o AG atua impedindo a produção ERO induzida pelo TMZ (YANG *et al*., 2022).

Apesar de pesquisas crescentes destacarem o potencial antiglioma do AG, não há estudos investigando a atividade antitumoral deste composto fenólico em modelos experimentais *in vivo* de glioma.

### 3.6 Fungos endofíticos como fonte de compostos antitumorais

Os produtos naturais podem ser amplamente definidos como qualquer composto derivado de uma fonte viva, incluindo plantas, organismos marinhos, bactérias e fungos (CHAMBERLIN *et al*., 2019). Strobel e Long (1998) revelam que microrganismos associados às plantas podem oferecer mais compostos com efeitos terapêuticos do que a própria planta. Os endófitos ou fungos endofíticos vivem no interior de tecidos saudáveis dos vegetais e são importantes componentes do micro-ecossistema da planta (**Figura 5**).

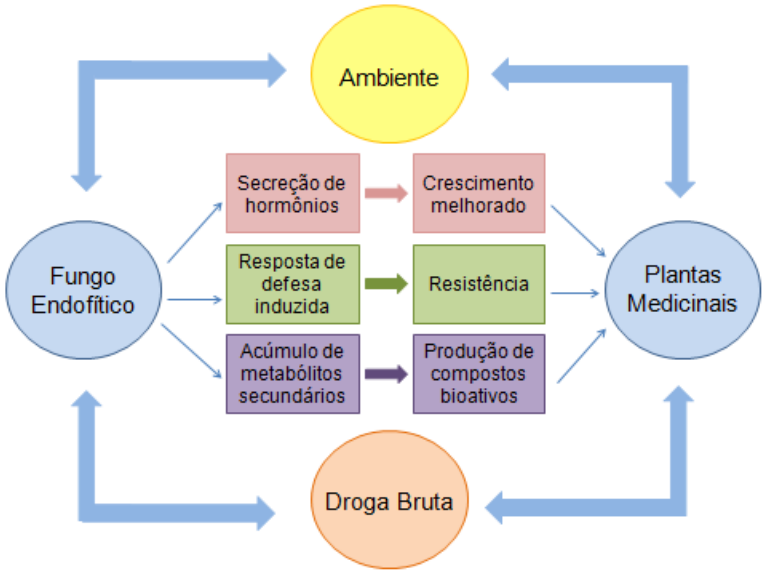


**Figura 5 –** Mutualismo entre plantas e endófitos. Relações benéficas estabelecidas entre endófito e planta, incluindo melhoramento no crescimento e resistência a estresses bióticos e abióticos de suas plantas hospedeiras, bem como promovendo o acúmulo de metabólitos secundários.

Fonte: JIA *et al*., 2016 com modificações.

Ao longo da evolução, endófitos e suas plantas hospedeiras têm estabelecido uma relação mutualística, a qual pode ter influenciado significativamente a formação de produtos metabólicos, afetando a qualidade e a quantidade de compostos derivados a partir de plantas medicinais (JIA *et al*., 2016). Neste sentido, os micro-organismos diferenciam-se dos fitopatógenos, que são prejudiciais e causadores de doenças, e dos epífitos, que habitam a superfície vegetal (AZEVEDO, 1998; STROBEL; DAISY, 2003). Tais micro-organismos são encontrados em todos os tipos de plantas, como vegetais superiores, gramíneas, algas e plantas herbáceas (NISA *et al*., 2015).

Um amplo espectro de atividades biológicas tem sido atribuído aos fungos endofíticos (JIA *et al*., 2016, NISA *et al*., 2015). Além disso, tais microrganismos têm sido reconhecidos como um importante recurso de bioativos naturais, especialmente na terapia anticâncer (CHEN *et al*., 2016). Stierle, Strobel e Stierle (1993) descreveram a produção do diterpenoide “Taxol” (ou Paclitaxel), um importante fármaco quimioterápico, pelo fungo endofítico *Taxomyces andreanae*, o qual foi isolado das entrecascas da planta *Taxus brevifolia*, apenas adequando-se as condições de cultivo. Tal descoberta motivou diversos estudos para a busca de outros microrganismos capazes de sintetizar o Paclitaxel. Além do taxol, a produção de outros bioativos naturais de interesse farmacêutico tem sido caracterizada por fungos endofíticos obtidos a partir de diversas espécies vegetais (WANG *et al*., 2014).

Em relação aos tumores cerebrais, nosso grupo de pesquisa tem demonstrado o potencial citotóxico de microrganismos endofíticos sobre linhagens de GBM (GALDINO, 2016; PEDRA *et al*., 2018). Extratos provenientes de fungo endofítico a partir da planta medicinal *Mikania hastato-cordata* reduziram significativamente a viabilidade de células de glioma C6, mas não de astrócitos demonstrando citotoxicidade seletiva (GALDINO, 2016). Além disso, Pedra e colaboradores (2018) demonstraram o potencial antiglioma da lactona macrocíclica Sch-642305 produzida por fungo endofítico isolado a partir da planta medicinal *A. satureioides*. Neste estudo, a lactona reduziu a sobrevivência clonogênica, proliferação e migração celular de linhagens de GBM, induzindo apoptose e modulando o estado redox (PEDRA *et al*., 2018).

Diante do exposto e conforme evidenciado por Lacava, Andreote e Azevedo (2008), devido ao potencial biotecnológico dos fungos endofíticos, muitas pesquisas têm focado na busca por novas espécies, bem como novos produtos, como resultado do metabolismo secundário destes microrganismos. Os autores revelam ainda, que “a busca por novos metabólitos deve concentrar-se em organismos que habitam novos ecossistemas, ou ainda nichos pouco explorados”. Assim, os microrganismos endofíticos atuam como uma fonte renovável, reprodutível e inesgotável de novas estruturas com elevado potencial farmacêutico.

Neste contexto, considerando o arsenal terapêutico limitado para o tratamento de neoplasias malignas como o melanoma metastático e o GBM, o potencial antiglioma da espécie *A. satureioides*, bem como do fungo endofítico isolado desta planta, a busca por novos compostos naturais e potentes metabólitos antitumorais a partir de fontes inexploradas como os microrganismos endofíticos encorajam pesquisas neste campo.

# 4. RESULTADOS

## 4.1 Capítulo 1

Endophytic fungus of *Achyrocline satureioides*: molecular identification, chemical characterization and cytotoxic evaluation of its metabolites on human melanoma cell line

Nathalia Stark Pedra, Kirley Marques Canuto, Ana Sheila de Queiroz Souza, Paulo Riceli Vasconcelos Ribeiro, Natália Pontes Bona, Roberto Ramos Sobrinho, Priscila Oliveira de Souza, Roselia Maria Spanevello, Elizandra Braganhol

**Status:** Submetido no periódico *Applied Biochemistry and Biotecnhology*

# Endophytic fungus of *Achyrocline satureioides*: molecular identification, chemical characterization and cytotoxic evaluation of its metabolites on human melanoma cell line

Nathalia Stark Pedra[1], Kirley Marques Canuto[2], Ana Sheila de Queiroz Souza[2], Paulo Riceli Vasconcelos Ribeiro[2], Natália Pontes Bona[3], Roberto Ramos Sobrinho[4], Priscila Oliveira de Souza[5], Roselia Maria Spanevello[1], Elizandra Braganhol[5]

[1] Programa de Pós-Graduação em Bioquímica e Bioprospecção - Laboratório de Neuroquímica, Inflamação e Câncer, Universidade Federal de Pelotas, Pelotas, RS, Brazil

[2] Embrapa Agroindústria Tropical, Fortaleza, CE, Brazil

[3] Programa de Pós-Graduação em Bioquímica e Bioprospecção - Laboratório de Biomarcadores, Universidade Federal de Pelotas, Pelotas, RS, Brazil

[4] Centro de Ciências Agrárias/Fitossanidade, Universidade Federal de Alagoas, Rio Largo, Alagoas, Brazil

[5] Programa de Pós-Graduação em Biociências – Universidade Federal de Ciências da Saúde de Porto Alegre, Porto Alegre, RS, Brazil

**Correspondence –** Roselia Maria Spanevello (rspanevello@gmail.com) or Nathalia Stark Pedra (nathaliastark@hotmail.com) Centro de Ciências Químicas, Farmacêuticas e de Alimentos, Universidade Federal de Pelotas, Campus Capão do Leão, s/n, CEP 9601090 - Pelotas, RS, Brazil Phone: +55 53 327573

**Abstract**

The lack of evidence reporting the endophytic composition of *Achyrocline satureioides*, a medicinal plant native to South America, has stimulated research in this field. In the present study, the endophytic fungus isolated from *A. satureioides* was identified as *Biscogniauxia* sp. by analysis of the ITS region (ITS1-ITS4), whose metabolites from the purified fractionated extract of this microorganism ($F_{DCM}$), were elucidated by UPLC-ESI-QTOF-MSE analysis. This is the first report of the ability of *Biscogniauxia* sp. in producing the isocoumarin orthosporin (**7**); the terpenoids nigriterpene A (**8**) and 10-xylariterpenoid (**12**); and the polyketide derivatives daldinin C (**4**), 7'dechloro-5'-hydroxygriseofulvin (**6**), daldinone D (**17**) and Sch-642305 (**22**), curtachalasin A (**23**), cytochalasin E (**25**), and the epoxycytochalasins Z8, Z8 isomer, and Z17 (**26-28**). Furthermore, the biosynthesis of **22** by a Xylariaceae fungus is unprecedented. $F_{DCM}$ significantly reduces the viability and cell proliferation of human melanoma cells (A375), exhibiting $IC_{50}$ values of 10.34 µg/mL and 6.89 µg/mL, respectively, and induced late apoptosis/necrosis and cell cycle arrest in S-G2/M phases after 72 h of treatment. Given the ability to produce unique metabolites with promising cytotoxic effects, the present study highlights the potential of *Biscogniauxia* sp. from *A. satureioides* as a reservoir of compounds with important therapeutic applications.

**Keywords:** *Biscogniauxia* sp., *Achyrocline satureioides*, Sch-642305, melanoma

## Introduction

Cancer is one of the main causes of mortality in the world [1]. Among the different types of cancer, melanoma is the most aggressive skin malignancy in terms of metastases and mortality, whose incidence rates have progressively increased worldwide [2]. This malignant neoplasm originates in melanocytes, whose prolonged exposure to ultraviolet light or radiation results in DNA damage triggering mutations, uncontrolled cell proliferation and tumorigenesis [3]. When diagnosed in the early stages, surgical removal is curative in most cases. However, in advanced stages, standard chemotherapy with dacarbazine presents a low therapeutic efficacy, exhibiting a response rate limited to 10-14% and a lifespan of 9-11 months [3, 4].

The main difficulty in cancer treatment has been the increased occurrence of chemoresistant tumors [1,2]. Considering the aggressiveness of metastatic melanoma and the resistance acquired by patients to conventional therapy [4], the search for therapeutic alternatives becomes essential. Natural products have emerged as the major source of anticancer agents, acting in the regulation of key signaling pathways in tumor pathogenesis and progression [1]. Increasing evidence has shown that medicinal plants possesses a microbial repository of immense potential for the discovery of new structural classes of pharmacological interest [5, 6]. These microorganisms known as endophytic fungi or endophytes inhabit the internal tissues of medicinal plants and can be influenced by the micro-ecosystem and genetic background of their host plant [5].

Endophytic fungi have been widely recognized for their ability to produce several bioactive secondary metabolites [6]. In addition, to producing compounds that help in the defense of your host plant, these microorganisms are capable of generating structural classes with unique pharmacologic effects [5, 6]. Among medicinal plants, Asteraceae

species host a variety of endophytic microorganisms capable of producing antitumor compounds [7, 8]. Native to South America and belonging to the Asteraceae family, *Achyrocline satureioides* is one of the medicinal plants included in the list of medicinal species of the Agência Nacional de Vigilância Sanitária of Brazil (ANVISA) and widely used in folk medicine due to its pharmacological properties [7].

Given the lack of studies evaluating the endophytic composition of *Achyrocline satureioides*, a medicinal plant belonging to the Asteraceae family, we described for the first time the isolation of an endophytic fungus from this plant [9]. Previous findings have shown that the secondary metabolism of the isolated microorganism exhibits selective cytotoxic effects on a panel of glioblastoma cell lines, being able to reduce the oxidative damage characteristic of the tumor microenvironment [9]. Considering the promising effects of bioactive compounds from the endophyte of *A. satureioides*, it is important to clarify the taxonomy and chemical characterization of the secondary metabolites produced by this endophytic fungus. Thus, this study aimed to identify the isolated endophytic microorganism, characterize and evaluate the effect of its bioactive compounds on the proliferation of human melanoma cells.

## Materials and methods

### Isolation of endophytic fungus from *Achyrocline satureioides*

The endophytic fungus used in this study was obtained from healthy stems of the plant *Achyrocline satureioides* (Lam.) D.C. The collection of plant samples (Rodovia Transbrasiliana, Rio Grande do Sul, Brazil; geographic coordinates: 31◦44′34.7″S and 54◦09′19.2″W) and it was identified by Dra. Raquel Ludke from the Botany Department (Biology Institute, UFPel) (PEL N◦ 21079). The isolation of the endophytic fungus was performed as previously described by Pedra et al. [9]. Briefly, stem samples of *A.*

*satureioides* were cut into small segments (6-10 mm in size) with the aid of a sterile blade, placed in agar-potato-dextrose (BDA) and incubated in an oven at 25 ± 2 °C (Thelga; Dom Bosco, MG, BR). After seven days, the fungal mycelia that emerged from the cut surface of the segments were periodically transferred to fresh BDA medium for purification and maintained at 25 ± 2°C under controlled light conditions.

**Molecular identification of the endophytic fungus**

*DNA extraction*

Hyphal-tip culture was initially obtained to ensure the genetic purity of the isolate, then, it was grown in potato-dextrose (PD) liquid media at 25 ± 2 °C for three days. The mycelial growth was collected using a sterile filter paper and washed with autoclaved distilled water. Total DNA was extracted from 50 mg of fresh mycelium according to Doyle and Doyle [10], and the DNA quality was evaluated through 1% agarose gel electrophoresis, stained with GelRed (Biotium®) and visualized under UV light. Total DNA was stored at -20°C until use.

*Amplification and Sequencing*

Total DNA was used as a template for amplification via polymerase chain reaction (PCR), of the Internal Transcribed Spacer (ITS) genomic region using the primer pair ITS1-5'-TCCGTAGGTGAACCTGCGG-3'/ ITS4-5'-TCCTCCGCTTATTGATATGC-3'. The PCR reactions were performed as follows: 1X MyTaqMasterMix (Bioline®), 0.2 μM of each forward and reverse primers, 1μL of total DNA (template), and nuclease-free water to a final volume of 25 μL. The cycling conditions were: 2 min at 95ºC as initial denaturation, followed by 35 cycles of denaturation at 95ºC for 20 s, annealing at 58ºC for 30 s, extension at 72ºC for 1 min, with a final extension step at 72ºC for 5 min. The

expected size fragments were purified using the Illustra GFX PCR and DNA Gel Band Purification kit (GE Healthcare Life Sciences), following the manufacturer's protocol, and sequenced bidirectionally at Macrogen Inc., (South Korea). Finally, the nucleotide sequences were identified in the GenBank database using the NCBI BLAST research program.

**Preparation and fractionation of the endophytic fungus extract**

Agar plugs (8 mm) with the mycelium of the isolated endophytic fungus were transferred to Erlenmeyers containing potato dextrose broth (PDB, 1.7%) medium and incubated at 25 ± 2°C (1 plug per 100 mL of PDB 1.7%). After 25 days the culture medium was filtered and the compounds produced by the endophytic fungus were extracted with the dichloromethane solvent (culture medium:dichloromethane, 2/1). The organic phases were separated and evaporated to dryness using a rotary evaporator under reduced pressure at 60°C (Rota-evaporador MA120-Marconi). Subsequently, solid phase extraction was performed as described by Pedra et al. [9]. Briefly, the obtained extract (20 mg) was dissolved in methanol (MeOH) (200 µL), applied on a Supelclean reverse phase cartridge (C18, 500 mg, Supelco, Bellefonte, PA, USA) and eluted with 50% MeOH (5 mL). This procedure was repeated twice and the fraction obtained was dried in a SpeedVac vacuum centrifuge for 24 h at 40°C and named $F_{DCM}$ (Thermo-Fischer).

**Chemical characterization of compounds produced by the endophytic fungus**

The chemical characterization was performed on an Acquity UPLC system (Waters, Milford, MA, USA) coupled to quadrupole and time-of-flight (QTOF) mass spectrometers (Waters, Milford, MA, USA) in accordance with adereplication method described by our group earlier [11]. The separation was achieved on an Acquity BEH C18

column (1.7 µm, 2.1 × 150 mm, Waters, Milford, MA, USA) maintained at 40°C, injecting 5 µL of sample. The mobile phase was a combination of A (0.1% formic acid in water) and B (0.1% formic acid in acetonitrile) at a flow rate of 0.4 mL/min. The elution gradient varied linearly from 5% to 95% of B (v/v) over 15 min, and then the column was washed for 2 min and conditioned for 2 min. The mass spectra were recorded in both positive and negative modes in a mass range between 110–1180 Da. The source temperature was set at 120°C, desolvation temperature of 350°C, desolvation gas flow rate of 500 L/h and capillary voltage of 3.2 kV. Leucine enkephalin was used as the lock mass. The spectrometer operated in $MS^E$ centroid mode, using a tension ramp from 20 to 40 V. The instrument was controlled by the Masslynx 4.1 software (Waters Corporation). The compounds were tentatively characterized through molecular formula provided by MassLynx 4.1 software from their accurate masses (error < 5 ppm), isotopic patterns (i-fit) and MS fragmentation pattern as well as chemotaxonomic surveyon the occurrence of secondary metabolites in the Xylariaceae family using Scifinder database. Additionally, compounds were identified by comparison with reference standards when available.

**Cell culture**

The human melanoma cell line (A375) was purchased from American Type Culture Collection (ATCC; Rockville, Maryland, USA). The cells were cultured in Dulbecco's modified Eagle's medium (DMEM), containing penicillin/streptomycin (100 U/L), fungizone (0.1%) and supplemented with 10% (v/v) fetal bovine serum (FBS) (pH 7.4). Cells were kept in a humidified incubator with 5% $CO_2$.

**Cell treatment**

$F_{DCM}$ was firstly dissolved in dimethylsulphoxide (DMSO) at the concentration of 10 mM (stock solution) and further diluted in DMEM supplemented with 10% FBS (pH 7.4) to obtain 1, 2.5, 5, 7.5, 10, 15 and 20 µg/mL. For the cytotoxicity assays, the human melanoma cell line A375 was seeded in 96-well plates at $5x10^3$ cells/well and treated with $F_{DCM}$ concentrations for 24, 48 and 72 h. For cell cycle and death analysis, human melanoma cells were seeded at a density of $50x10^4$ cells/well in 12-well plates and treated with $F_{DCM}$ for 72 h. Cells exposed to DMSO (0.05% final concentration) were considered control.

**Cytotoxicity assays**

*Cell viability assay*

Cell viability was measured by 3-[4,5-dimethylthiazole-2-yl]-2,5-diphenyltetrazolium bromide (MTT) test according to Mosmann [12]. This assay evaluates the ability of mitochondria to reduce MTT to blue formazan crystals. Briefly, cells were washed with CMF, MTT solution (0.5 mg/mL) was added and incubated for 90 min at 37 °C in a humidified 5% $CO_2$ atmosphere. The MTT was removed and the precipitate dissolved with DMSO. The optical density (OD) was measured at 492 nm through a microplate reader (SpectraMax 190, Molecular Devices, San Jose, CA, USA). The results were analyzed using Prism 5.0 software (Prism GraphPad Software, San Diego, USA) according to the following formula: cell viability rate (%) = ($OD_{492}$ of cells exposed to $F_{DCM}$/$OD_{492}$ control) × 100%.

*Cell proliferation assay*

Cell proliferation was analyzed by the sulphorodamine B (SRB) assay, which assesses the dye's ability to bind to cellular proteins. Initially, cells were fixed in 50%

trichloroacetic acid for 45 min at 4 °C and then washed with distilled water. Subsequently, 0.4% SRB was added and incubated in the dark at room temperature for 30 min. Afterwards, cells were washed with 1% acetic acid for complete removal of non-protein-complexed dye and SRB was eluted with 10 mM Tris [9]. OD was determined at 530 nm using a microplate reader (SpectraMax190) and the results obtained were calculated using Prism 5.0 software (Prism GraphPad Software, San Diego, USA) according to the following formula: cell proliferation rate (%) = ($OD_{530}$ of exposed cells to $F_{DCM}$/$OD_{530}$ of control) × 100%.

**Cell cycle analysis**

For cell cycle analysis, the medium and cells were harvested and centrifuged at 1200 rpm for 6 min. Subsequently, the supernatant was discarded, cells were washed with PBS (10 mM), centrifuged, and suspended in lysis buffer [trisodium citrate 3.5 mM; Tris-HCl 0.5 mM (pH 7.6); Nonidet-P40 0.1%; RNAse 100 µg/mL and propidium iodide (PI) 50 µg/mL]. After 15 min, data were collected using a flow cytometer (BD FACS Calibur flow cytometer, BD Biosciences, CA, USA). FACS analyses were performed in the FLOWJO® software and results were expressed as percentage of control.

**Cell death analysis**

For cell death analysis, the apoptotic or necrotic cells were quantified using an annexin V-FITC-PI double staining kit. The medium and the cells were centrifuged at 12000 rpm for 6 min. Subsequently, the supernatant was discarded, cells were washed with PBS (10 mM), centrifuged, and suspended in a binding buffer containing FITC-conjugated annexin V and PI. The samples were incubated for 15 min in the dark prior to analysis by flow cytometry. Quantification of apoptotic or necrotic cells was assessed by

dual-color flow cytometry (BD FACS Calibur flow cytometer, BD Biosciences, CA, USA) and the data were analyzed with FLOWJO® software. Cells were classified as follows: live (Annexin-/ PI-), early apoptotic (Annexin+/ PI-) or late apoptotic/necrotic (Annexin+/ PI+). Results were expressed as percentage of control.

**Statistical analysis**

Data were analyzed by one-way analysis of variance (ANOVA) followed by the Tukey post-hoc test using GraphPad Prism version 5.0 Program (Intuitive Software for Science, San Diego, CA). The results were expressed as mean ± standard error of the mean (SEM) and considered statistically significant when $P<0.05$.

**Results**

**Molecular Identification of Endophytic Fungus from *A. satureioides***

The strain of endophytic fungi isolated from stem of *A. satureioides* was characterized by colonies 70-75 mm diameter after 7 days of culture in PDA medium at 25 °C. The filamentous colonies had a white color with a cotton surface and a reddish-brown reverse color, while the hyaline and septate hyphae branched into cylindrical phialides with unicellular conidia at the ends of the branches as described previously by our research group [9] (**Fig. 1**).

Due to the difficulty in characterizing the reproductive structures, the endophytic fungus could not be identified based on its morphological aspects. Thus, in order to identify the taxonomy in the endophytic fungus isolated from *A. satureioides*, the ITS region was amplified and the obtained sequences were compared with existing ITS sequences in GenBank repository. Based on the molecular data obtained, the endophytic fungus of *A. satureioides* exhibited 99% similarity (90-95% query coverage) with

*Biscogniauxia* sp. of the family Xylariaceae, order Xylariales (MZ570840.1; KP306931.1). Thus, this fungal strain was identified as *Biscogniauxia* sp. and nucleotide sequence data were submitted and deposited to Genbank (accession number ON257911).

**Chemical elucidation of the compounds of the secondary metabolism of the endophytic fungus *Biscogniauxia***

Seventeen out of twenty-eight compounds were putatively identified in the fractionated $F_{DCM}$ extract obtained from the endophytic fungus *Biscogniauxia* isolated from the *A. satureioides* plant using UPLC-ESI-QTOF-$MS^E$ (**Fig. 2**): nine polyketides derivatives, five terpenoids and three isocoumarins. The compounds were annotated on the basis of levels, namely: level 1 - authentic analytical standard (**22**); level 2 - exact mass, MS/MS fragmentation patterns and occurrence in Xylariaceae (**4**, **8**, **13**, **14**, **18**, **25-28**); level 3 - molecular formulas, exact mass and occurrence in Xylariaceae (**6**, **7**, **10**, **12**, **15**, **17** and **23**); and level 4 - unknown compound (**1-3**, **5**, **9**, **11**, **16**, **19-21** and **24**) (**Table 1**). The spectra and proposed MS/MS fragmentation mechanisms of compounds **4, 8, 13, 14, 18, 22, 25, 26,** and **28** are available as Supporting Information (**Fig. S1-S9**).

Peak **4** (RT=4.59 min) presented a protonated molecular ion $[M+H]^+$ at *m/z* 267.1583 ($C_{15}H_{22}O_4$), being characterized as the azafilone-type polyketide daldinin C [13]. Peak **6** (RT=4.72 min) showed precursor ions $[M-H]^-$ at *m/z* 333.0984 ($C_{17}H_{18}O_7$), therefore it was annotated as the heptaketide 7'dechloro-5'-hydroxigriseofulvin [14]. Peak **7** (RT=4.87 min) had a precursor ion $[M-H]^-$ at *m/z* 235.0576 ($C_{12}H_{12}O_5$) and therefore was annotated as the isocoumarin orthosporin [15].

The peaks **8** (RT=5.31 min), **12** (RT=5.66 min) and **13** (RT=5.75 min) showed precursor ions $[M+H]^+$ at *m/z* 249.1492 ($C_{15}H_{20}O_3$), $[M-H]^-$ at *m/z* 251.1631 ($C_{15}H_{24}O_3$) and $[M+H]^+$ at *m/z* 221.0812 ($C_{12}H_{12}O_4$), respectively. Thus, such compounds were

annotated as the sesquiterpenes nigriterpene A [16], 10-xylariterpenoid [17], besides the meroterpenoid biscogniacid A [18], respectively.

Peaks **10** (RT=5.47 min) provided precursor ion $[M-H]^-$ at *m/z* 221.0444 ($C_{11}H_{10}O_5$), while peak **15** (RT=6.04 min) gave a protonated molecular ion $[M+H]^+$ at *m/z* 213.1124 ($C_{11}H_{16}O_4$). Based on Raja et al. [19], they were found to be compatible with the meroterpenoids biscognin B and biscognin A, respectively. Peaks **14** (RT=5.83 min) and **18** (RT= 6.60 min) exhibited molecular protonated ions $[M+H]^+$ at *m/z* 207.1024 ($C_{12}H_{14}O_3$) and *m/z* 237.0759 ($C_{12}H_{12}O_5$). Thus, such isocoumarins were identified as 8-methoxy-5-methylmellein (**14**) and 5-Methoxycarbonylmellein (**18**) [20, 21]. Peak **17** (RT=6.41 min) had a precursor ion $[M-H]^-$ at *m/z* 351.1255 ($C_{21}H_{20}O_5$) and was characterized as the benzo-fluoroanthene type polyketide daldinone D [22].

Peaks **23** (RT=7.69 min) and **25** (RT=8.27 min) were proposed to be the polyketides curtachalasin A [23] and cytochalasin E [24] due to the precursor ions $[M-H]^-$ at *m/z* 498.2474 ($C_{28}H_{37}NO_7$) and *m/z* 494.2193 ($C_{28}H_{33}NO_7$), respectively. Additionally, peaks **26** (RT=8.35 min); **27** (RT=8.87 min) and **28** (RT=10.23 min) exhibited precursor ions consistent with the molecular formulas $C_{28}H_{35}NO_6$ ($[M+H]^+$ at *m/z* 482.2542 and $[M-H]^-$ at *m/z* 480.2380), $C_{28}H_{35}NO_6$ ($[M+H]^+$ at *m/z* 482.2541e $[M-H]^-$ at *m/z* 480.2395) and $C_{28}H_{33}NO_6$ ($[M+H]^+$ at *m/z* 480.2383 and $[M-H]^-$ at *m/z* 478.2222), respectively. Thus, such cytochalasin-type polyketides were characterized as epoxycytochalasin Z8 (**26**), epoxycytochalasin Z8 isomer (**27**) and epoxycytochalasin Z17 (**28**) [25].

Interestingly, the peak **22** (RT= 7.66 min) was identified as the macrolide type polyketide Sch-642305 ($C_{14}H_{20}O_4$) by comparison with an authentic analytical standard [9]. This macrocyclic lactone presented molecular ion $[M+H]^+$ at *m/z*253.1438 and [M-

H]$^-$ at *m/z* 251.1279 (**Figure S6**). In the present study, 11 of the 28 compounds (Unknown A–J), could not be identified, as their chromatographic or spectral data did not match those in the literature. Among the annotated metabolites, only meleins (**14** and **18**), the isoprenylbenzoic acid meroterpenoid (**13**) and biscognins A (**15**) and B (**10**) were previously described as compounds produced by *Biscogniauxia* genus fungi. Furthermore, although most of the compounds characterized are produced by microorganisms of the Xylariaceae family, our study reveals for the first time the ability of an endophytic fungus of this family to produce the macrocyclic lactone Sch-642305 (**22**).

**$F_{DCM}$ exhibits antiproliferative effects, alters cell cycle and induces late apoptosis/necrosis in human melanoma cells**

Compounds from the secondary metabolism of *Biscogniauxia* sp. reduced the viability of human melanoma cells following 24, 48 and 72 h of exposure by about 30%, 35% and 80%, respectively (**Fig. 3a**). Additionally, the cytotoxic effect of $F_{DCM}$ was also evidenced by the SRB assay. As shown in **Fig. 3b**, the fractionated extract decreased cell proliferation after 48 and 72 h of treatment by up to 30% and 80%, respectively, compared to control cells. Notably, $F_{DCM}$ promoted an interesting time- and concentration-dependent antitumor activity on the human melanoma cell line, whose concentration capable of inhibiting 50% of cell viability and proliferation ($IC_{50}$) was 10.34 µg/mL and 6.89 µg/mL following 72 h of treatment, respectively.

To determine whether $F_{DCM}$-induced cell growth inhibition involved cell cycle changes, we examined the distribution of cells in cell cycle phases by flow cytometry (**Fig. 4**). Treatment of melanoma cells with $F_{DCM}$ led to accumulation of cells in the sub-

G1 fraction, suggestive of cell death. Exposure to $F_{DCM}$ (10 and 15 µg/mL) for 72 h led to cell accumulation in S and G2/M cell cycle phases compared to control cells. Concurrent with these increases in cell population, a decrease in cell population was observed in the G1 phase. This result implies that $F_{DCM}$ induced an arrest of A375 melanoma cells in the S-G2/M phase.

Finally, to investigate the effect of bioactive compounds of *Biscogniauxia* sp. on cell death, we performed Annexin V/PI staining after $F_{DCM}$ treatment at 72 h (**Fig. 5**). The results indicated a significant increase in late apoptosis/necrosis compared to control cells. This increase was accompanied by a reduction in the percentage of cells in early apoptosis. The percentages of late apoptotic/necrotic cells induced by $F_{DCM}$ (5, 10 and 15 µg/mL) were 27.6%, 25.6% and 25.2%, respectively.

**Discussion**

Increasing studies highlight the occurrence of a diversity of endophytic microorganisms in all ecosystems in the world, where each plant species can host one or more species of endophytic fungi of pharmacological interest [5, 8]. Among medicinal plants, the Asteraceae family represents about 10% of the world vascular flora, whose therapeutic effects have been associated with endophytic microorganisms that coexist with these plants, especially species of *Colletotrichum* sp., *Alternaria* sp., *Penicillium* sp., *Diaporthe*sp. (anamorph of *Phomopsis* sp.), *Fusarium* sp., *Nigrospora* sp., and *Xylaria* sp. [7,8].

Despite presenting several biological activities, there are no studies describing the taxonomy of endophytic fungi of *Achyrocline satureioides,* a medicinal plant of Asteraceae family. Recently, we demonstrated the promising antiglioma effects of the bioactive metabolites of an endophytic fungus (initially named as MF31b11) obtained

from *A. satureioides*, however, the morphological characterization of the conidia and phialides has hindered the taxonomic identification of the isolated microorganism [9]. Thus, in this study we aimed to identify and characterize the secondary metabolites of the endophytic fungus MF31b11 isolated from the medicinal plant *A. satureioides*.

Upon analysis of the nucleotide sequences, the endophytic fungus isolated from *A. satureioides* was identified molecularly as *Biscogniauxia* sp. *Biscogniauxia* genus comprises ascomycete fungi belonging to the Xylariaceae family (Xylariales order), whose occurrence has been reported in medicinal plants of the genus *Cinnamomum* sp., and *Echinacea* sp. [26, 27]. This study describes for the first time (1) the taxonomic identification of an endophytic microorganism from a medicinal plant belonging to the genus *Achyrocline* sp., and (2) the occurrence of *Biscogniauxia* sp. as an endophytic fungus for *A. satureioides* species.

The compounds of endophytic fungi isolated from medicinal plants are characterized by diverse and unique structural groups [8]. Indeed, Xylariaceae represents one of the most prolific families of secondary metabolites in the order Xylariales [28]. According to the chemical characterization performed in this study, only meroterpenoids (compounds **10**, **13** and **15**) and melleins (compounds **14** and **18**) had been previously reported as metabolites produced by strains of *Biscogniauxia* sp. In this context, the biosynthesis of twelve (**4, 6-8, 12, 17, 23** and **25-28)** of the seventeen identified compounds is described for the first time as secondary metabolites produced by an endophytic fungus of the genus *Biscogniauxia* sp.

Among these compounds, daldinin C (**4**) and daldinone D (**17**) are characteristics of some endophytic species of *Daldinia* sp. and *Hypoxylon* sp. (Hypoxylaceae family) [13,22], while orthosporin (**7**) and 10-xylariterpenoid (**12**) were first isolated from

*Graphostroma* sp. (Graphostromataceae family) [15,17]. Chemotaxonomic characteristics indicate that fungi of the genus *Hypoxylon* sp. evolved from species of *Biscogniauxia* sp., suggesting that *Biscogniauxia* could be an intermediate lineage between Hypoxylaceae and Xylariaceae [29]. Furthermore, evidence also shows a close phylogenetic and morphological relationship between *Biscogniauxia* and *Graphostroma* [29]. In this context, the biosynthesis of similar metabolites between species of *Graphostroma* sp., *Hypoxylon* sp. and *Biscogniauxia* sp. could be related to the evolutionary capacity of these microorganisms from a common ancestor.

In general, the compounds generated by a single endophytic fungus can be influenced both by interactions between these microorganisms and by the chemical components of the host plant [6]. Among the endophytes widely found in medicinal plants of the Astereaceae family, the *Xylaria* genus represents 50% of the species belonging to the Xylariaceae family, suggesting that most bioactive metabolites related to the Xylariaceae family are derived from endophytic *Xylaria* species [28]. Indeed, compounds **6**, **8**, **23**, **25**, **26**, and **28** produced by the endophytic fungus *Biscogniauxia* sp. isolated from *A. satureioides* are described as metabolites originated from strains of *Xylaria* sp. [14, 16, 23, 24, 25].

In the present study, we verified the biosynthesis of the 10-membered macrolide Sch-642305 (**22**) by *Biscogniauxia* sp. isolated from *A. satureioides*. Sch-642305 has been isolated from cultures of *Penicillium verrucosum* [30], and *Phomopsis* sp. [31]. Although these microorganisms do not belong to the Xylariaceae family, the genera *Penicillium* and *Phomopsis* (anamorphs of *Diaporthe* sp.) comprise the most abundant fungal strains in plant species of the Asteraceae family [8]. Thus, as far as we know, this

is the first report demonstrating the ability of an endophytic fungus of the Xylariaceae family to produce the macrocyclic lactone Sch-642305 (**22**).

The secondary metabolism of *Biscogniauxia* sp. isolated from *A. satureioides* showed interesting effects against the human melanoma cell line, exhibiting $IC_{50}$ values between 6.89-10.34 µg/mL after 72 h of treatment. According to Laux et al. [32], the $IC_{50}$ value of A375 cells exposed to dacarbazine, a chemotherapy drug used in the therapy of metastatic melanoma, is 29.27 ug/mL after 72 h of treatment.

Xu and MacArthur [33] point out that cell cycle dysregulation is an important hallmark related to the initiation and progression of melanoma. The authors also point out that compounds targeting the G2/M checkpoints show promising activity in preclinical studies of melanoma. In the present study, $F_{DCM}$ (15 µg/mL) promoted an accumulation of cells in the S and G2/M phases of the cell cycle and induced cell death by late apoptosis/necrosis. While early apoptosis is characterized by cytoplasmic condensation and DNA fragmentation without loss of plasma membrane permeability, in late apoptosis/necrosis there is permeabilization of cell membranes and loss of fragmented DNA [34]. Currently, several anticancer agents can also induce cell death by necrosis [35]. According to Zhang and colleagues [36], necrosis favors the death of tumor cells due to the release of cellular debris, thus stimulating the patient's immunogenic and inflammatory response.

Among the metabolites produced by *Biscogniauxia* sp. and described for the first time in this study, compounds **4**, **7**, **12**, **17**, **22**, and **25** exhibit interesting antineoplastic effects described in the literature. Daldinin C (**4**) [37] and daldinone D (**17**) [22] exhibit potent cytotoxic activity against human breast cancer cells, and human colorectal cancer, respectively. On the other hand, orthosporin (**7**) [26] and 10-xylariterpenoid A (**12**) inhibit

the proliferation of human leukemia cells [38]. In addition to exhibiting important cytotoxic effects on human colorectal carcinoma tumor line [31], Sch-642305 showed selective antitumor activity on glioblastoma cell lines [9]. These antiglioma effects were attributed to its ability to induce early/late apoptosis, arrest the cell cycle in G2/M, inhibit cell migration, and reduce the oxidative stress characteristic of gliomas [9].

Cytochalasin E (**25**) is also described as a potent antiangiogenic agent, whose effects have been attributed to the presence of an epoxide ring in its structure [39]. Udagawa et al. [40] demonstrated the *in vivo* effect of this cytochalasin, which reduced more than 70% of tumor growth in a model of lung carcinoma. Furthermore, the cytotoxic effects of compound **25** have already been evaluated in several tumor lines such as human lung adenocarcinoma, cervical cancer, hepatocellular carcinoma, and colorectal adenocarcinoma [39]. Although there are no studies evaluating the cytotoxic effects of epoxycytochalasin Z8 (**26**), epoxycytochalasin Z8 isomer (**27**), and epoxycytochalasin Z17 (**28**), experimental evidence highlights that molecules containing epoxide in their structure have a high therapeutic value, especially as anticancer agents, whose mechanisms mainly involve enzymatic inhibition, induction of apoptosis, and arrest in the cell cycle [39, 40].

## Conclusion

Endophytic fungi represent an inexhaustible source of compounds of pharmacological interest. The ability of these microorganisms to produce unique metabolites, especially anticancer agents, associated with the therapeutic difficulty of malignant neoplasms due to side effects and chemoresistance, has stimulated research in this field. Although most of the annotated compounds present cytotoxic effects described in the literature, the synergism of these bioactive metabolites in the $F_{DCM}$ favored a

significant reduction in the viability and proliferation of human melanoma cells, inducing death and cell cycle arrest. These results suggest *Biscogniauxia* sp. as a prominent reservoir of cytotoxic agents, encouraging the analysis of the mechanisms involved with its anticancer effect, which could be used in therapeutic applications.

**Supporting Information**

The spectra and proposed MS/MS fragmentation mechanisms of compounds **4, 8, 13, 14, 18, 22, 25, 26,** and **28** are available as Supporting Information.

## Statements & Declarations

### Funding

This work was supported by the Conselho Nacional de Desenvolvimento Científico e Tecnológico (CNPq) and Fundação de Amparo à Pesquisa do Estado do Rio Grande do Sul (FAPERGS). This study was financed in part by Coordenação de Aperfeiçoamento de Pessoal de Nível Superior- Brasil (CAPES) - Finance code 001. R.M.S is recipient of CNPq fellowship (310472/2021-0).

### Competing Interest

The authors have no relevant financial or non-financial interest to disclose.

### Author Contributions

All authors contributed to the study conception and design. Material preparation, data collection and fungus analysis were performed Nathalia Pedra, Kirley Canuto, Ana Souza and Paulo Ribeiro. Material preparation, data collection and cells analysis were performed Nathalia Pedra, Natália Bona, Priscila Souza, Roselia Spanevello and Elizandra Braganhol. The first draft of the manuscript was written by Nathalia Pedra and all authors commented on previous versions of the manuscript. All authors read and approved the final manuscript.

### Ethics Approval

This study did not require ethics approval.

**References**

[1] Tyagi, G., Kapoor, N., Chandra, G. and Gambhir, L. (2021) Cure lies in nature: medicinal plants and endophytic fungi in curbing cancer. 3 Biotech 11, 1-24.

[2] Carr, S., Smith, C. and Wernberg, J. (2019) Epidemiology and Risk Factors of Melanoma. Surgical Clinics of North America. Surg. Clin. 100, 1-12.

[3] Patel, M., Eckburg, A., Gantiwala, S., Hart, Z., Dein, J., Lam, K., and Puri, N. (2021) Resistance to Molecularly Targeted Therapies in Melanoma. Cancers 13,1115-1140.

[4] Gupta, A., Gomes, F., Lorigan, P. (2017) The role for chemotherapy in the modern management of melanoma. Melanoma Manag. 4, 125–136.

[5] Jia, M., Chen, L., Xin, H., Zheng, C., Rahman, K., Han, T. and Qin, L. (2016) A friendly relationship between endophytic fungi and medicinal plants: a systematic review. Front. Microbiol. 7, 906-920.

[6] Uzma, F., Mohan, C.D., Hashem, A., Konappa, N.M., Rangappa, S., Kamath, P.V., Singh, B.P., Mudili, V., Gupta, V.K., Siddaiah, C.N., Chowdappa, S., Alqarawi, A. and Allah, E. (2018) Endophytic fungi—alternative sources of cytotoxic compounds: a review. Front. Pharmacol. 9,309-346

[7] Gonçalves, G., Ferreira, M.I., Ming, L.C. (2018) *Achyrocline satureioides* (Lam.) DC. first ed., Dordrecht: Springer.

[8] Caruso, G., Abdelhamid, M.T., Kalisz, A. and Sekara, A. (2020) Linking endophytic fungi to medicinal plants therapeutic activity. A case study on Asteraceae. Agriculture 10,286-309.

[9] Pedra, N.S., Galdino, K., Da Silva, D., Ramos, P., Bona, N., Soares, M., Azambuja, J., Canuto, K., De Brito, E., Ribeiro, P., Souza, A., Cunico, W., Stefanello, F.M., Spanevello, R.M., Braganhol, E. (2018) Endophytic Fungus Isolated From *Achyrocline*

*satureioides* Exhibits Selective Antiglioma Activity—The Role of Sch-642305. Front. Oncol. 8, 476-496.

[10] Doyle, J.J. and Doyle, J.L. (1990) Isolation of plant DNA from fresh tissue. Focus 12, 39-40.

[11] Sobreira, A.C., Pinto, F., Florêncio, K., Wilke, D., Staats, C.C., Streit, R., Freire, F., Pessoa, O., Silva, A. and Canuto, K. (2018) Endophytic fungus *Pseudofusicoccum stromaticum* produces cyclopeptides and plant-related bioactive rotenoids. RSC Adv. 8, 35575-35586.

[12] Mosmann, T. (1983) Rapid colorimetric assay for cellular growth and survival: application to proliferation and cytotoxicity assays. J. Immunol. Methods 65, 55-63.

[13] Shao, H., Qin, X., Dong, Z., Zhang, H. and Liu, J. (2008) Induced daldinin A, B, C with a new skeleton from cultures of the ascomycete *Daldinia concentrica*. J. Antibiot. 61,115-119.

[14] Paguigan, N., Al-Huniti, M., Raja, H., Czarnecki, A., Burdette, J., González-Medina M., Medina-Franco, J., Polyak, S., Pearce, C., Croatt, M. and Oberlies, N. (2017) Chemoselective fluorination and chemoinformatic analysis of griseofulvin: Natural vs fluorinated fungal metabolites. Bioorg. Med. Chem. 25, 5238-5246.

[15] Niu, S., Liu, Q., Xia, J.M., Xie, C.L., Luo, Z., Shao, Z., Liu, G. and Yang, X.W. (2018) Polyketides from the deep-sea-derived fungus *Graphostroma* sp. MCCC 3A00421 showed potent antifood allergic activities. J. Agric. Food Chem. 66, 1369-1376.

[16] Chang, J., Hsiao, G., Lin, R., Kuo, Y., Ju, Y. and Lee, T. (2017) Bioactive constituents from the termite nest-derived medicinal fungus *Xylaria nigripes*. J. Nat. Prod. 80, 38-44.

[17] Niu, S., Xie, C. L., Zhong, T., Xu, W., Luo, Z.H., Shao, Z. and Yang, X. (2017) Sesquiterpenes from a deep-sea-derived fungus *Graphostroma* sp. MCCC 3A00421. Tetrahedron 73, 7267-7273.

[18] Zhao, H., Chen, G.D., Zou, J., He, R.R., Qin, S.Y., Hu, D., Li, G.Q., Guo, L. D. and Yao, X. (2017) Dimericbiscognienyne A: A Meroterpenoid Dimer from *Biscogniauxia* sp. with New Skeleton and Its Activity. Org. Lett. 19, 38-41.

[19] Raja, H., Kaur, A., El-Elimat, T., Figueroa, M., Kumar, R., Deep, G., Faeth, S.H., Cech, N.B. and Oberlies, N.H. (2015) Phylogenetic and chemical diversity of fungal endophytes isolated from *Silybum marianum* (L) Gaertn.(milk thistle). Mycology 6, 8-27.

[20] Amand, S., Langenfeld, A., Blond, A., Dupont, J., Nay, B. and Prado, S. (2012) Guaiane sesquiterpenes from *Biscogniauxia nummularia* featuring potent antigerminative activity. J. Nat. Prod. 75,798-801.

[21] Rubalcaba, M.L.M. and Fernández, R.E.S. (2017) Secondary metabolites of endophytic *Xylaria* species with potential applications in medicine and agriculture. World J. Microbiol. Biotechnol. 33, 1-22.

[22] Gu, W., Ge, H.M., Song, Y.C., Ding, H., Zhu, H., Zhao, X.A. and Tan, R.X. (2007) Cytotoxic benzo [j] fluoranthene metabolites from Hypoxylontruncatum IFB-18, an endophyte of *Artemisia annua*. J. Nat. Prod. 70, 114-117.

[23] Wang, W.X., Li, Z.H., Feng, T., Li, J., Sun, H., Huang, R. and Liu, J.K. (2018) Curtachalasins A and B, two cytochalasans with a tetracyclic skeleton from the endophytic fungus *Xylaria curta* E10. Org. Lett. 20, 7758-7761.

[24] Zhang, Q., Xiao, J., Sun, Q.Q., Qin, J.C., Pescitelli, G. and Gao, J.M. (2014) Characterization of cytochalasins from the endophytic *Xylaria* sp. and their biological functions. J. Agric. Food Chem. 62, 10962-10969.

[25] Han, W.B., Zhai, Y.J., Gao, Y., Zhou, H.Y., Xiao, J., Pescitelli, G., and Gao, J.M. (2019) Cytochalasins and an abietane-type diterpenoid with allelopathic activities from the endophytic fungus *Xylaria* species. J. Agricul. Food Chem. 67, 3643-3650.

[26] Cheng, M., Wu, M., Yanai, H., Su, Y.S., Chen, I., Yuan, G., Hsieh, S.Y. and Chen, J.J. (2012) Secondary metabolites from the endophytic fungus *Biscogniauxia formosana* and their antimycobacterial activity. Phytochem. Lett 5, 467-472.

[27] Carvalho, C.R., Wedge, D.E., Cantrell, C.L., Silva-Hughes, A.F., Pan, Z., Moraes, R.M., Maddox, V.L. and Rosa, L.H. (2016) Molecular phylogeny, diversity, and bioprospecting of endophytic fungi associated with wild ethnomedicinal North American plant *Echinacea purpurea* (Asteraceae). Chem. Biodiver. 13, 918-930.

[28] Becker, K. and Stadler, M. (2021) Recent progress in biodiversity research on the Xylariales and their secondary metabolism. J. Antibiot. 74, 1–23.

[29] Daranagama, D.A., Hyde, K.D., Sir, E.B., Thambugala, K.M., Tian, Q., Samarakoon, M.C., McKenzie, E., Jayasiri, S.C., Tibpromma, S., Bhat, J.D., Liu, X., and Stadler, M. (2018) Towards a natural classification and backbone tree for Graphostromataceae, Hypoxylaceae, Lopadostomataceae and Xylariaceae. Fungal Divers 88, 1-165.

[30] Chu, M., Mierzwa, R., Xu, L., He, L., Terracciano, J., Patel, M., Gullo, V., Black, T., Zhao, W., Chan, T. and McPhail, A. (2003) Isolation and Structure Elucidation of Sch 642305, a Novel Bacterial DNA Primase Inhibitor Produced by *Penicillium verrucosum*. J. Nat. Prod. 66, 1527-1530.

[31] Adelin, E., Servy, C., Cortial, S., Lévaique, H., Martin, M.T., Retailleau, P., and Le, G., Bussaban, B., Lumyong, S. and Ouazzani, J. (2011) Isolation, structure

elucidation and biological activity of metabolites from Sch-642305-producing endophytic fungus *Phomopsis* sp. CMU-LMA. Phytochem. 7, 2406-2412.

[32] Laux, A., Hamman, J., Svitina, H., Wrzesinski, K. and Gouws, C. (2022) In vitro evaluation of the anti-melanoma effects (A375 cell line) of the gel and whole leaf extracts from selected aloe species. J. Herb. Med. 31,100539.

[33] Xu, W. and McArthur, G. (2016) Cell Cycle Regulation and Melanoma. Curr. Oncol. Rep. 18,34.

[34] Poon, I., Hulett, M. and Parish, C. (2010) Molecular mechanisms of late apoptotic/necrotic cell clearance. Cell Death Differ. 17, 381–397.

[35] Sergey, Y. and Vladimir, L.G. (2010) Mechanisms of Tumor Cell Necrosis. Curr. Pharm. Des. 16:56-68.

[36] Zhang, J., Lou, X., Jin, L., Zhou, R., Liu, S., Xu, N. and Liao, D.J. (2014). Necrosis, and then stress induced necrosis-like cell death, but not apoptosis, should be the preferred cell death mode for chemotherapy: clearance of a few misconceptions. Oncoscience 1, 407.

[37] Li, W., Ding, L., Wang, N., Xu, J., Zhang, W., Zhang, B., He, S., Wu, B., Jin, H (2019) Isolation and characterization of two new metabolites from the sponge-derived fungus *Aspergillus* sp. LS34 by OSMAC approach. Mar Drugs 17, 283-292.

[38] Wu, B., Wiese, J., Schmaljohann, R., Imhoff, J.F. (2016) Biscogniauxone, a new isopyrrolonaphthoquinone compound from the fungus *Biscogniauxia mediterranea* isolated from deep-sea sediments. Mar Drugs 14, 204-213.

[39] Delebassée, S., Mambu, L., Pinault, E., Champavier, Y., Liagre, B. and Millot, M. (2017) Cytochalasin E in the lichen *Pleurosticta acetabulum*. Anti-proliferative activity

against human HT-29 colorectal cancer cells and quantitative variability. Fitoterapia 121,146-151.

[40] Udagawa, T., Yuan, J., Panigrahy, D., Chang, Y.H., Shah, J. and D'Amato, R.J. (2000) Cytochalasin E, an epoxide containing *Aspergillus*-derived fungal metabolite, inhibits angiogenesis and tumor growth. J. Pharmacol. Exp. Ther. 294, 421-427.

**Table 1.** Compounds putatively identified in $F_{DCM}$ fraction obtained of endophytic fungus *Biscogniauxia* sp. from *Achyrocline satureioides* by UPLC-ESI-QTOF-MSE in positive and negative ionization mode.

| Peak | Rt (Min) | Positive ion mode | | | Negative ion mode | | | $MS^2$ ions ($[M+H]^{+a}$ or $[M-H]^{-b}$) | Molecular Formula | Putative Name | ID level[c] | Ref. |
|---|---|---|---|---|---|---|---|---|---|---|---|---|
| | | $[M+H]^+$ Observed | $[M+H]^+$ Calculated | Error (ppm) | $[M-H]^-$ Observed | $[M-H]^-$ Calculated | Error (ppm) | | | | | |
| **1** | 3.91 | - | - | - | 609.1436 | 609.1456 | - 3.3 | 301.0352, 300.0251, 281.1013, 271.1594, 209.1044, 166.0192, 123.0163, 108.0201[b] | $C_{27}H_{30}O_{16}$ | Unknown A | 4 | - |
| **2** | 4.25 | - | - | - | 451.1741 | 451.1757 | - 3.5 | 433.1524, 369.0946, 345.1656, 333.1213, 285.1711, 253.0341, 220.0344, 209.0334, 195.0272, 178.0241, 166.0241, 137.0231, 124.0163[b] | $C_{26}H_{28}O_7$ | Unknown B | 4 | - |
| **3** | 4.41 | - | - | - | 301.1283 | 301.1287 | - 1.3 | 269.1513, 237.0379, 222.0147, 207.0294, 177.0178, 149.0210[b] | $C_{14}H_{22}O_7$ | Unknown C | 4 | - |

| | | | | | | | | | | | | |
|---|---|---|---|---|---|---|---|---|---|---|---|---|
| **4** | 4.59 | 267.1583 | 267.1596 | - 4.9 | - | - | - | 249.1470, 231.1386, 213.11386, 185.1301, 157.0991[a] | $C_{15}H_{22}O_4$ | DaldininC | 2 | 15 |
| **5** | 4.62 | - | - | - | 455.1351 | 455.1342 | 2.0 | 285.1364, 239.1216, 205.0519, 191.0314, 162.0297, 123.0430[b] | $C_{24}H_{24}O_9$ | Unknown D | 4 | - |
| **6** | 4.72 | - | - | - | 333.0984 | 333.0974 | 3.0 | 277.0716, 219.0282, 191.0332, 147.0424, 123.0429, 80.9670[b] | $C_{17}H_{18}O_7$ | 7-Dechloro-5'-hydroxygriseofulvin | 3 | 16 |
| **7** | 4.87 | - | - | - | 235.0576 | 235.0606 | - 12.8 | 191.0279, 146.0343, 123.0439, 118.0410, 81.0347[b] | $C_{12}H_{12}O_5$ | Orthosporin | 3 | 17 |
| **8** | 5.31 | 249.1492 | 249.1491 | 0.4 | - | - | - | 231.1384, 213.1264, 185.1307, 171.1123, 159.1167, 157.1002[a] | $C_{15}H_{20}O_3$ | Nigriterpene A | 2 | 18 |
| **9** | 5.39 | 277.1434 | 277.1440 | - 2.2 | - | - | - | 261.1600, 219.1384, 185.1334, 173.1308, 159.1148, 131.0829, 117.0682, 105.0681, 91.0537[a] | $C_{16}H_{20}O_4$ | Unknown E | 4 | - |

| | | | | | | | | | | | |
|---|---|---|---|---|---|---|---|---|---|---|---|
| **10** | 5.47 | - | - | - | 221.0444 | 221.0450 | - 2.7 | 177.0504, 148.0152, 133.0609, 120.0203, 92.0264[b] | $C_{11}H_{10}O_5$ | Biscognin B | 3 | 21 |
| **11** | 5.61 | 522.3102 | 522.3126 | - 4.6 | - | - | - | 504.2967, 486.2923, 346.1634, 252.1598, 235.1295, 189.1270, 129.0679, 105.0672, 91.0553[a] | $C_{21}H_{47}NO_{13}$ | Unknown F | 4 | - |
| **12** | 5.66 | - | - | - | 251.1631 | 251.1647 | - 6.4 | 235.0597,191.0304, 149.0212, 123.0448, 81.0348[b] | $C_{15}H_{24}O_3$ | 10-Xylariterpenoid A | 3 | 19 |
| **13** | 5.75 | 221.0812 | 221.0814 | - 0.9 | - | - | - | 203.0675, 177.0510, 135.0407, 91.0530[a] | $C_{12}H_{12}O_4$ | Biscogniacid A | 2 | 20 |
| **14** | 5.83 | 207.1024 | 207.1021 | 1.4 | - | - | - | 189.0843, 161.0887, 131.0492, 105.0679[a] | $C_{12}H_{14}O_3$ | 8-methoxy-5-methylmellein | 2 | 22 |
| **15** | 6.04 | 213.1124 | 213.1127 | 1.4 | - | - | - | 189.0942, 174.0667, 161.0933, 146.0697, 131.0481, 105.0668, 91.0520[a] | $C_{11}H_{16}O_4$ | Biscognin A | 3 | 21 |

| | | | | | | | | | | | |
|---|---|---|---|---|---|---|---|---|---|---|---|
| **16** | 6.30 | - | - | - | 325.1795 | 325.1804 | - 2.8 | 279.1197, 249.1183, 235.0573, 217.1220, 205.1221, 183.0080, 162.0294, 136.0505, 106.0420[b] | $C_{21}H_{26}O_3$ | Unknown G | 4 | - |
| **17** | 6.41 | - | - | - | 351.1255 | 351.1232 | 6.6 | 325.1831, 251.1330, 235.1330, 217.1199, 183.0106, 120.9954[b] | $C_{21}H_{20}O_5$ | Daldinone D | 3 | 24 |
| **18** | 6.60 | 237.0759 | 237.0763 | - 1.7 | - | - | - | 221.0451, 193.0493, 175.0383, 131.0493[a] | $C_{12}H_{12}O_5$ | 5-Methoxycarbonylmellein | 2 | 23 |
| **19** | 6.67 | - | - | - | 500.2577 | 500.2590 | - 2.6 | 275.1378, 248.1225[b] | $C_{35}H_{35}NO_2$ | Unknown H | 4 | - |
| **20** | 6.94 | 502.2792 | 502.2805 | - 2.6 | - | - | - | 484.2643, 466.2565, 344.1473, 250.1410, 235.1324, 147.1154[a] | $C_{28}H_{39}NO_7$ | Unknown I | 4 | - |
| **21** | 7.28 | 502.2875 | 502.2864 | 2.2 | - | - | - | 484.2853, 438.0791, 344.1478, 262.1448, 250.1465, 235.1336, 189.1270, 131.0485, 119.0863, 105.0691, 91.0535[a] | $C_{21}H_{43}NO_{12}$ | Unknown J | 4 | - |

| | | | | | | | | | | | |
|---|---|---|---|---|---|---|---|---|---|---|---|
| **22** | 7.66 | 253.1438 | 253.1440 | - 0.8 | 251.1279 | 251.1283 | - 1.6 | 235.1334, 189.1253, 147.1163, 119.0858[a] | $C_{14}H_{20}O_4$ | Sch-642305 | 1 | 9 |
| **23** | 7.69 | - | - | - | 498.2474 | 498.2492 | - 3.6 | 480.2375, 469.2167, 454.2568, 438.2257, 394.2281, 339.2028, 325.1846, 274.1433, 248.1286, 230.1164, 209.1144, 183.0124, 116.9303[b] | $C_{28}H_{37}NO_7$ | Curtachalasin A | 3 | 25 |
| **24** | 7.82 | 502.2785 | 502.2805 | - 4.0 | - | - | - | 484.2701, 466.2595, 344.1481, 250.1442, 235.1311, 189.1250, 147.1142, 105.0698[a] | $C_{28}H_{39}NO_7$ | Unknown K | 4 | - |
| **25** | 8.27 | 496.2312 | 496.2335 | - 4.6 | 494.2193 | 494.2179 | 2.8 | 450.2248, 432.2160, 404.2285, 336.1612[a] | $C_{28}H_{33}NO_7$ | Cytochalasin E | 2 | 26 |
| **26** | 8.35 | 482.2542 | 482.2543 | - 0.2 | 480.2380 | 480.2386 | - 1.2 | 500.2653, 450.2260, 422.2414, 302.1365[a] | $C_{28}H_{35}NO_6$ | Epoxycytochalasin $Z_8$ | 2 | 27 |
| **27** | 8.87 | 482.2541 | 482.2543 | - 0.4 | 480.2395 | 480.2386 | 1.9 | 500.2639, 422.2258, 302.1372[a] | $C_{28}H_{35}NO_6$ | Epoxycytochalasin $Z_8$ isomer | 2 | - |
| **28** | 10.23 | 480.2383 | 480.2386 | - 0.6 | 478.2222 | 478.2230 | - 1.7 | 462.2281, 452.2400, 434.2285, 336.1605[a] | $C_{28}H_{33}NO_6$ | Epoxycytochalasin $Z_{17}$ | 2 | 27 |

[a]Fragmentation in positive and [b]negative ionization mode; [c]Identification level: 1. Authentic analytical standard; 2. Exact mass, MS/MS fragments and occurrence in Xylariaceae; 3. Exact mass and occurrence; 4. Unknown compound.

**Figure legends**

**Fig. 1** Endophytic fungus of *Achyrocline satureioides*. Front and reverse (**a**) of colony growth in PDA medium at 8 days of culture. (**b**) Light microscopy image of isolated endophytic fungus (40x magnification).

**Fig. 2** The UPLC-ESI-QTOF-$MS^E$ chromatograms of compounds identified in $F_{DCM}$ fraction obtained of endophytic fungus *Biscogniauxia* sp. from *Achyrocline satureioides* in positive (**a**) and negative (**b**) ionization mode. The numbers on the peaks are referenced in Table 1.

**Fig. 3** Analysis of the cytotoxic effect of $F_{DCM}$ of *Biscogniauxia* sp. on A375 human melanoma cell line after 24, 48 and 72 h of treatment. Cell viability (**a**) and proliferation (**b**) were determined by MTT and SRB assays, respectively. Untreated cells were used as a control. The values represent the mean ± SEM from at least three independent experiments performed in triplicate. Data were analyzed by ANOVA followed by post-hoc comparisons (Tukey test). $^{a,b,c}$Significantly different from the control cells after 24, 48 and 72 h of treatment, respectively ($P < 0.001$).

**Fig. 4** Effect of secondary metabolism of *Biscogniauxia* sp. in the distribution of human melanoma cells in different phases of the cell cycle. A375 cells were treated with 5, 10 and 15 µg/ml $F_{DCM}$ for 72 h. (**a**) Representative flow cytometry charts of melanoma cells exposed to $F_{DCM}$. (**b**) The effect of $F_{DCM}$ on the percentages of A375 cells in the Sub-G1, G1, S, and G2/M phases. $^{*,**,***,****}$Significantly different from the control cells ($P < 0.05$; $P < 0.01$; $P < 0.001$; $P < 0.0001$, respectively).

**Fig. 5** Effect of secondary metabolism of *Biscogniauxia* sp. in the cell death of human melanoma cells. A375 cells were treated with 5, 10 and 15 µg/ml $F_{DCM}$ for 72 h. (**a**) Representative microphotographs (10× magnification) and (**b**) representative flow cytometry charts of melanoma cells exposed to $F_{DCM}$. (**c**) The effect of $F_{DCM}$ on the

percentages of live cells, early apoptotic cells and late apoptotic/necrotic cells. **,***Significantly different from the control cells ($P < 0.01$; $P < 0.001$, respectively).

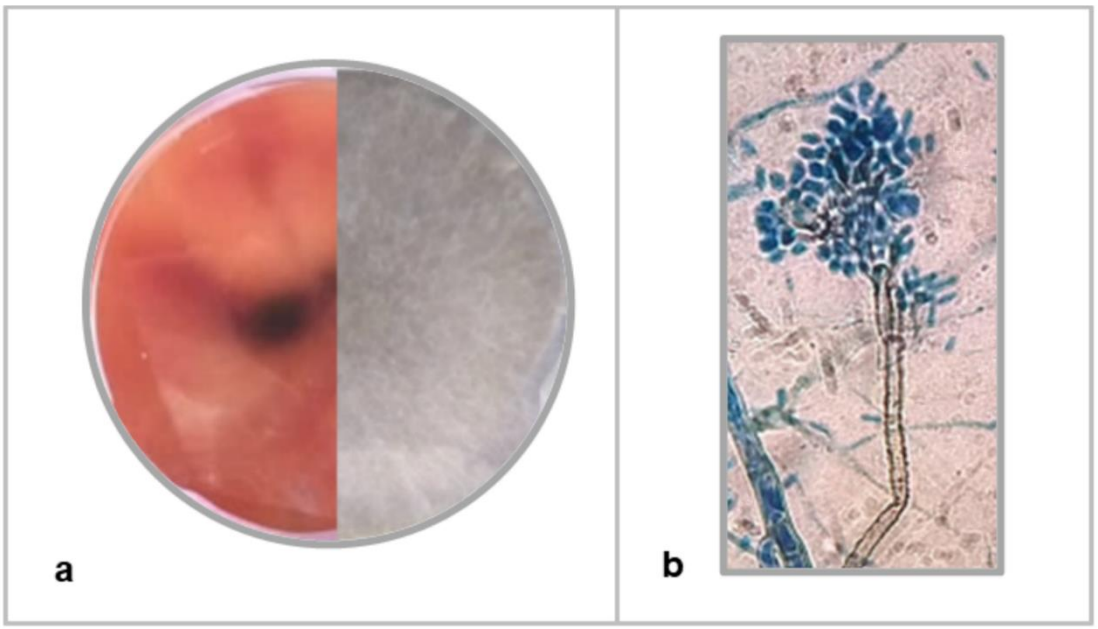


**Figure 1**

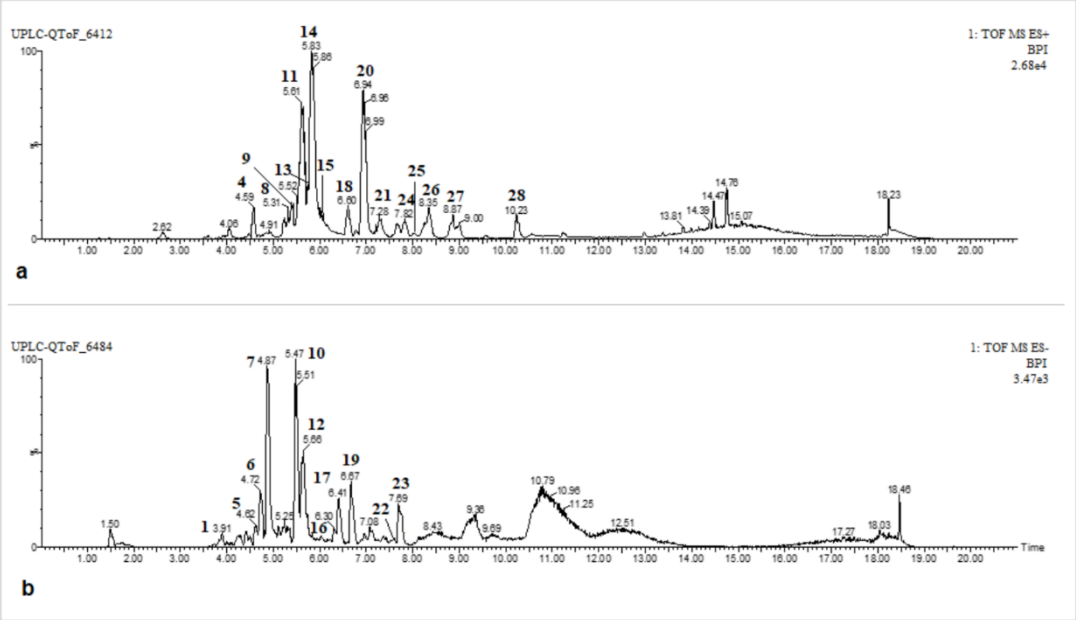
UPLC-QToF_6412
1: TOF MS ES+
BPI
2.68e4
a
UPLC-QToF_6484
1: TOF MS ES-
BPI
3.47e3
b
Time

**Figure 2**

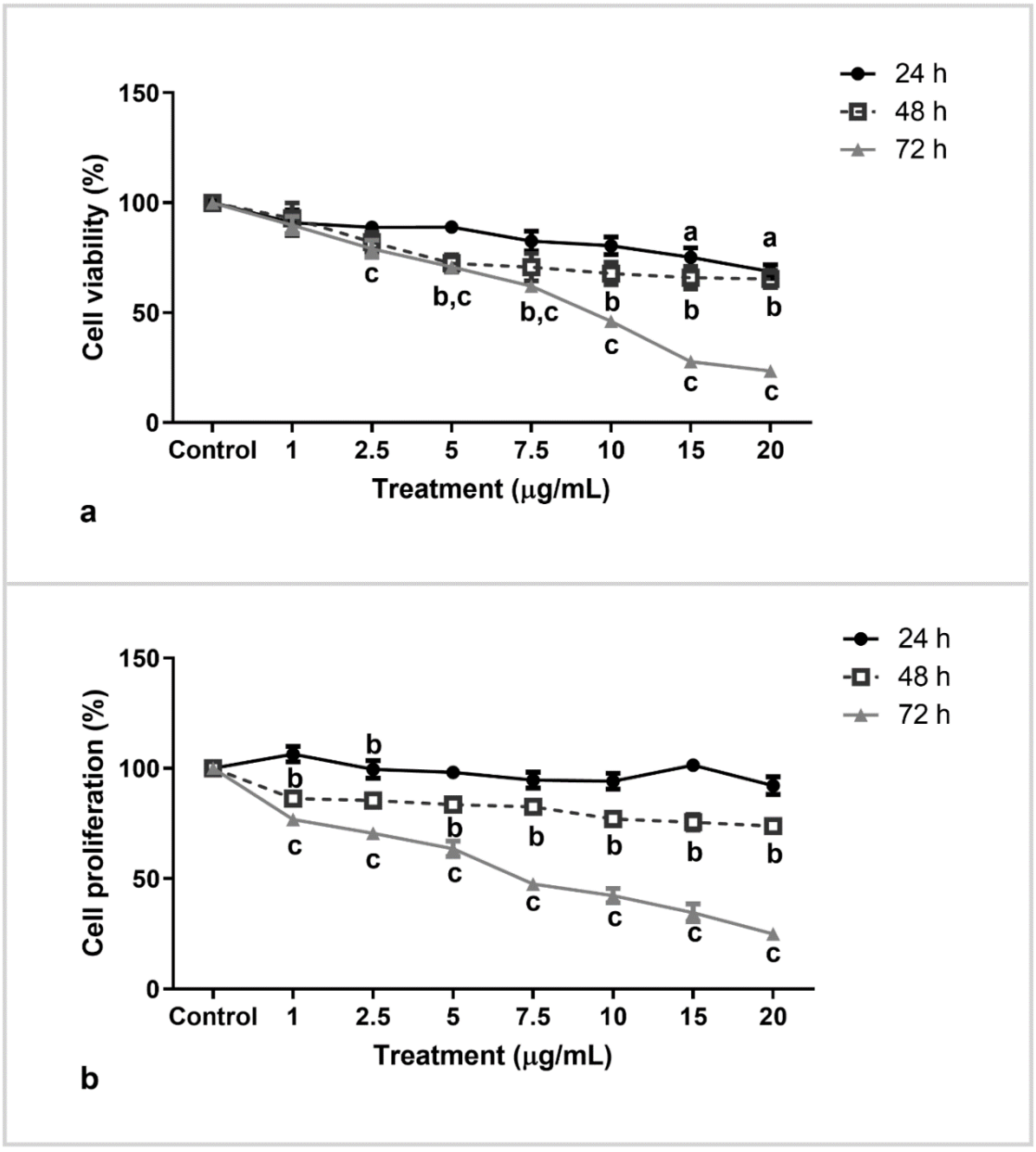
24 h
48 h
72 h
Cell viability (%)
150
100
50
0
Control
1
2.5
5
7.5
10
15
20
Treatment (μg/mL)
a
a
a
c
b,c
b,c
b
b
b
c
c
c
a
Cell proliferation (%)
150
100
50
0
Control
1
2.5
5
7.5
10
15
20
Treatment (μg/mL)
b
b
b
c
c
c
b
b
b
b
b
c
c
c
c
b

**Figure 3**

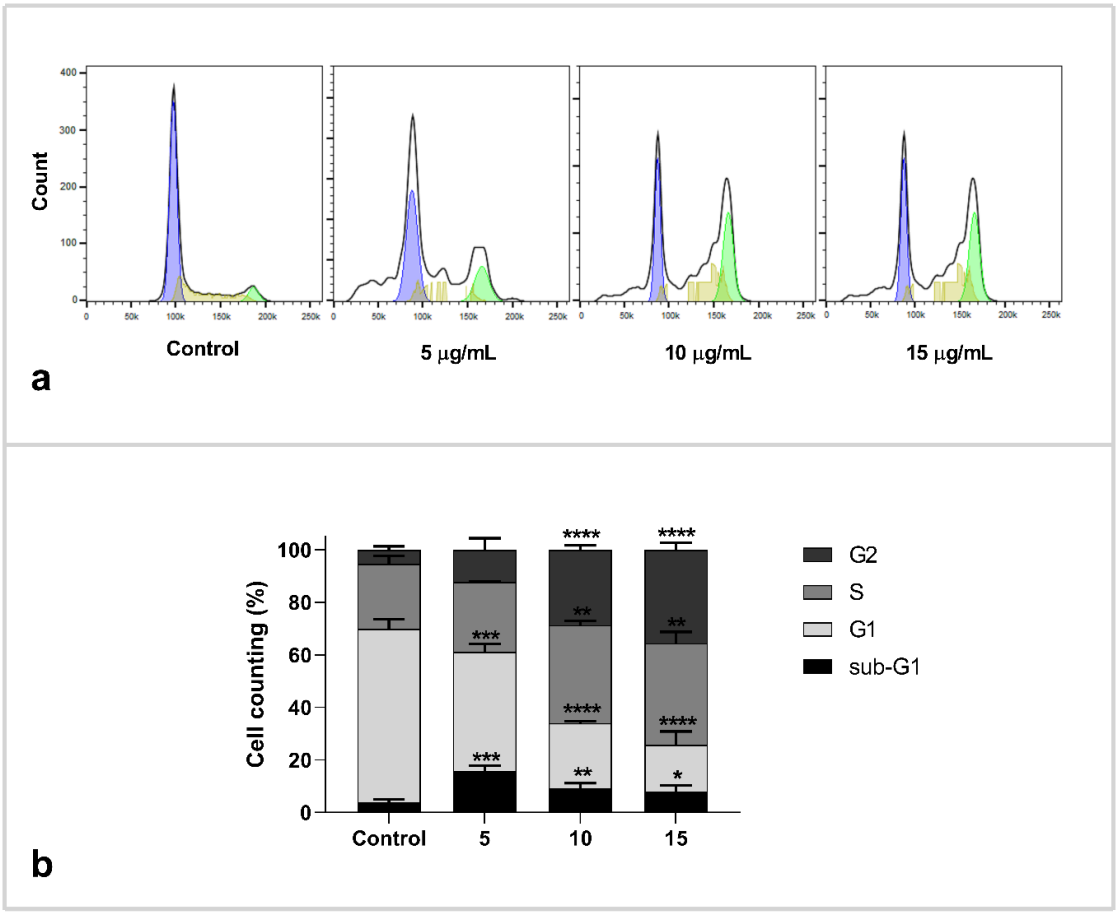
Count
Control
5 μg/mL
10 μg/mL
15 μg/mL
a
Cell counting (%)
Control
5
10
15
G2
S
G1
sub-G1
b

**Figure 4**

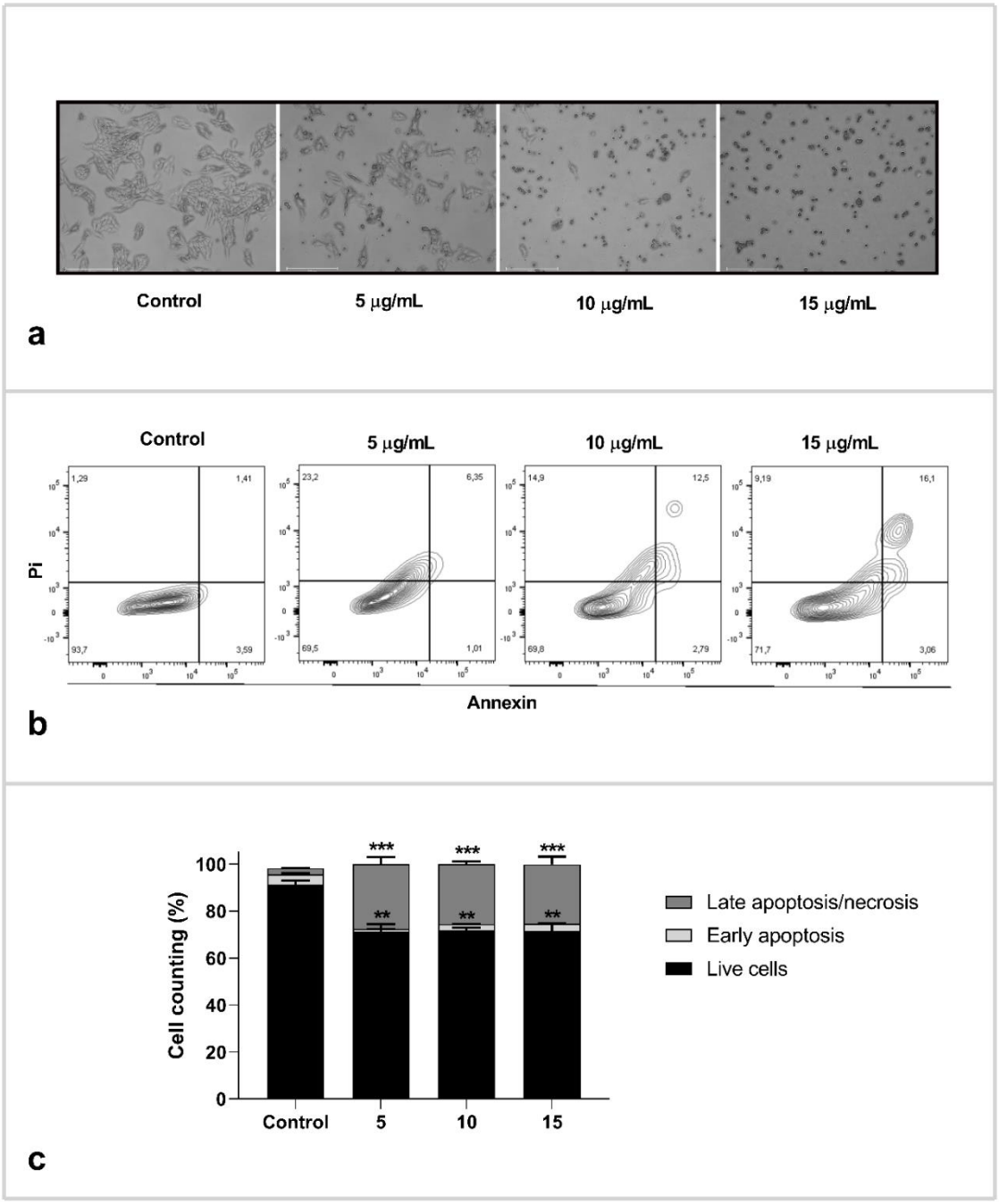
Control
5 μg/mL
10 μg/mL
15 μg/mL
a
Control
5 μg/mL
10 μg/mL
15 μg/mL
Pi
1,29
1,41
93,7
3,59
23,2
6,35
69,5
1,01
14,9
12,5
69,8
2,79
9,19
16,1
71,7
3,06
Annexin
b
Cell counting (%)
100
80
60
40
20
0
***
**
Control
5
10
15
Late apoptosis/necrosis
Early apoptosis
Live cells
c

**Figure 5**

## Graphical abstract

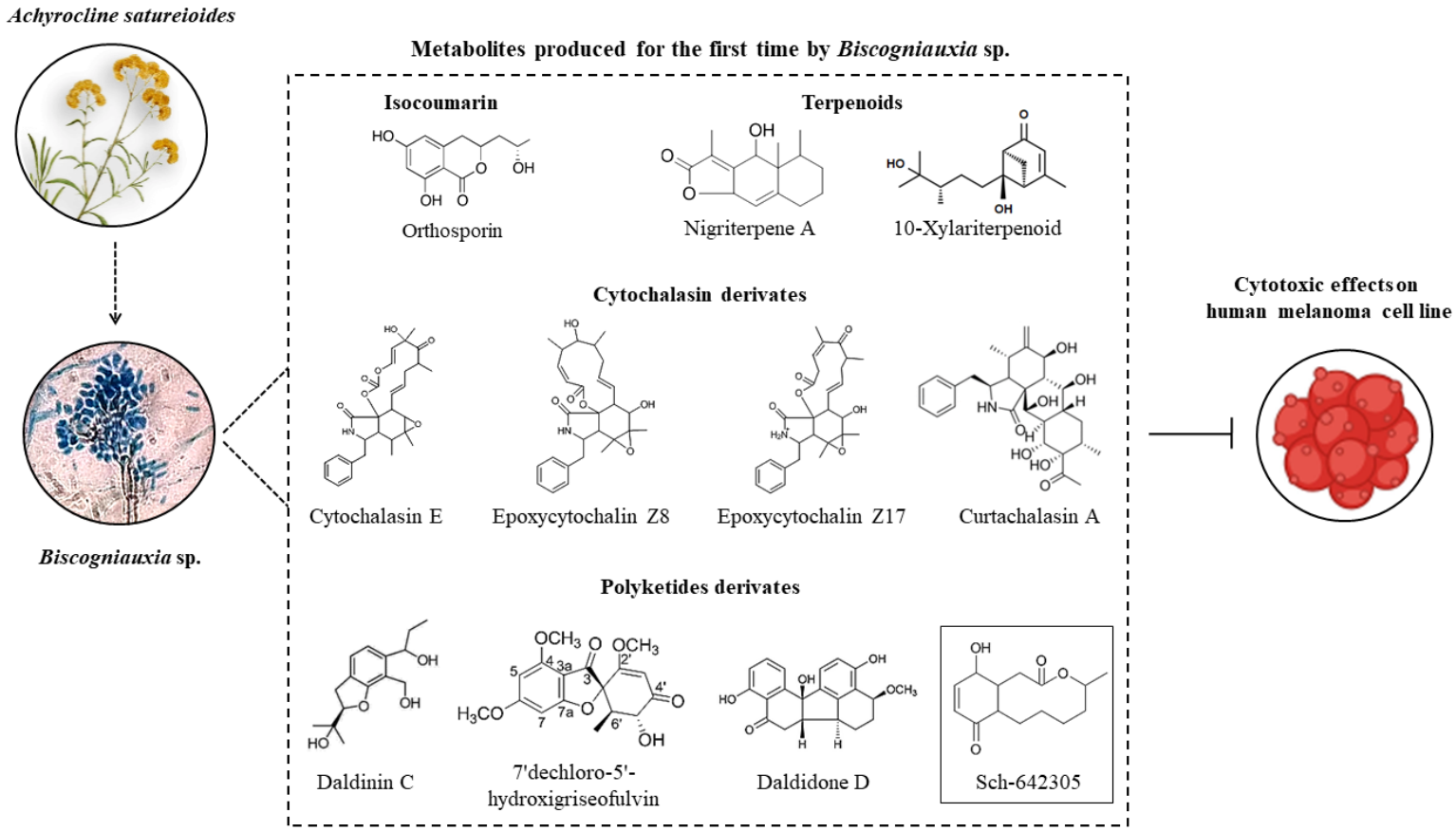

# Supporting Information

**Endophytic fungus of *Achyrocline satureioides*: molecular identification, chemical characterization and cytotoxic evaluation of its metabolites on human melanoma cell line**

**Nathalia Stark Pedra[1], Kirley Marques Canuto[2], Ana Sheila de Queiroz Souza[2], Paulo Riceli Vasconcelos Ribeiro[2], Natália Pontes Bona[3], Roberto Ramos Sobrinho[4], Priscila Oliveira de Souza[5], Roselia Maria Spanevello[1], Elizandra Braganhol[5]**

**Affiliation**

[1] Centro de Ciências Químicas, Farmacêuticas e de Alimentos, Programa de Pós-Graduação em Bioquímica e Bioprospecção - Laboratório de Neuroquímica, Inflamação e Câncer, Universidade Federal de Pelotas, Pelotas, RS, Brazil

[2] Embrapa Agroindústria Tropical, Fortaleza, CE, Brazil

[3] Centro de Ciências Químicas, Farmacêuticas e de Alimentos, Programa de Pós-Graduação em Bioquímica e Bioprospecção - Laboratório de Biomarcadores, Universidade Federal de Pelotas, Pelotas, RS, Brazil

[4] Centro de Ciências Agrárias/Fitossanidade, Universidade Federal de Alagoas, Rio Largo, AL, Brazil

[5] Departamento de Ciências Básicas da Saúde, Programa de Pós-Graduação em Biociências – Universidade Federal de Ciências da Saúde de Porto Alegre (UFCSPA), Porto Alegre, RS, Brazil

**Correspondence**

***Nathalia Stark Pedra***

Centro de Ciências Químicas, Farmacêuticas e de Alimentos, Universidade Federal de Pelotas

Campus Capão do Leão, s/n, CEP 9601090 - Pelotas, RS, Brazil

Phone: +55 53 32757355

nstarkpedra@gmail.com

## Contents

**Fig. 1S** UPLC-ESI-QTOF-MS$^E$ spectra (**a**) and fragmentation mechanism proposed (**b**) for daldinin C (**4**).

**Fig. 2S** UPLC-ESI-QTOF-MS$^E$ spectra (**a**) and fragmentation mechanism proposed (**b**) for nigriterpeneA (**8**).

**Fig. 3S** UPLC-ESI-QTOF-MS$^E$ spectra (**a**) and fragmentation mechanism proposed (**b**) for biscogniacidA (**13**).

**Fig. 4S** UPLC-ESI-QTOF-MS$^E$ spectra (**a**) and fragmentation mechanism proposed (**b**) for 8-methoxy-5-methylmellein (**14**).

**Fig. 5S** UPLC-ESI-QTOF-MS$^E$ spectra (**a**) and fragmentation mechanism proposed (**b**) for 5-methoxycarbonylmellein (**18**).

**Fig. 6S** UPLC-ESI-QTOF-MS$^E$ spectra (**a**) and fragmentation mechanism proposed (**b**) for Sch-642305 (**22**).

**Fig. 7S** UPLC-ESI-QTOF-MS$^E$ spectra (**a**) and fragmentation mechanism proposed (**b**) for cytochalasin E (**25**).

**Fig. 8S** UPLC-ESI-QTOF-MS$^E$ spectra (**a**) and fragmentation mechanism proposed (**b**) for epoxycytochalasin Z8 (**26**).

**Fig. 9S** UPLC-ESI-QTOF-MS$^E$ spectra (**a**) and fragmentation mechanism proposed (**b**) for epoxycytochalasin Z17 (**28**).

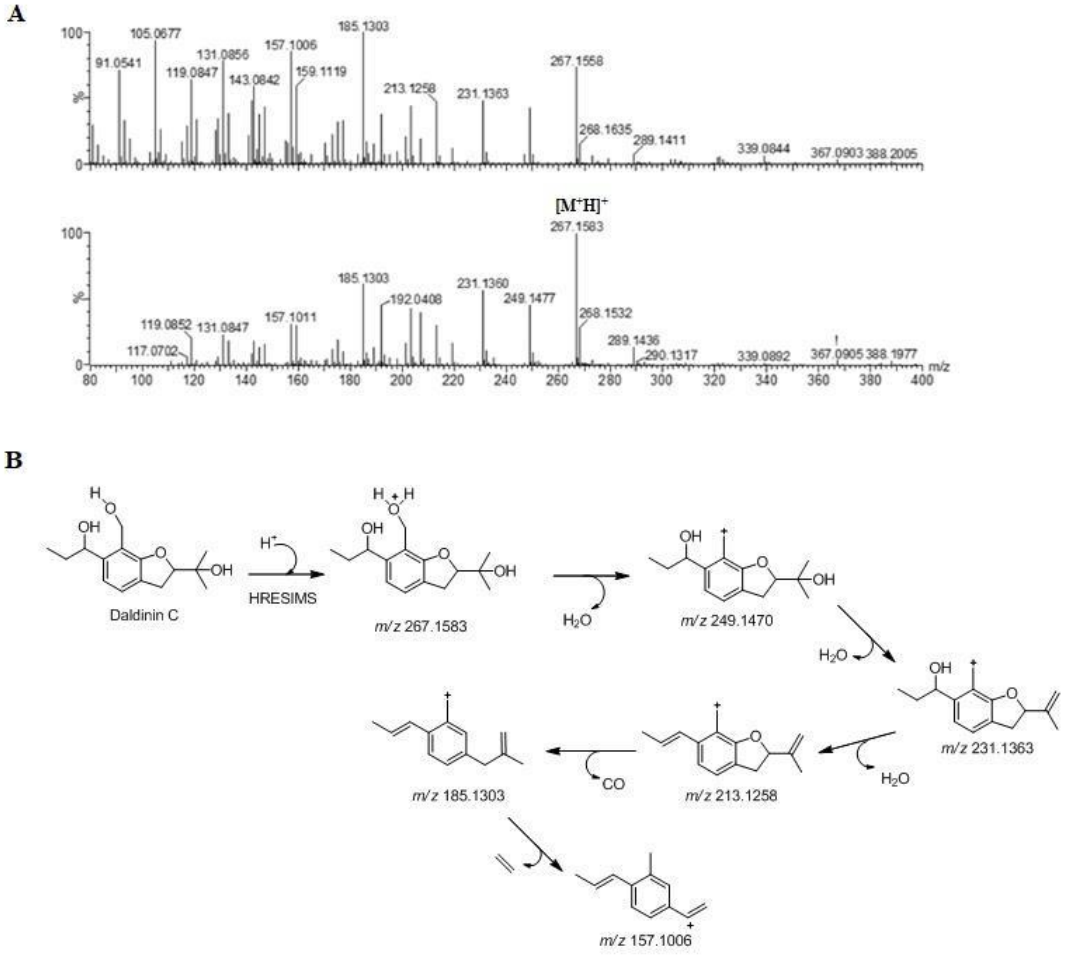


**Fig. S1** UPLC-ESI-QTOF-MS$^E$ spectra (**a**) and fragmentation mechanism proposed (**b**) for daldinin C (**4**)

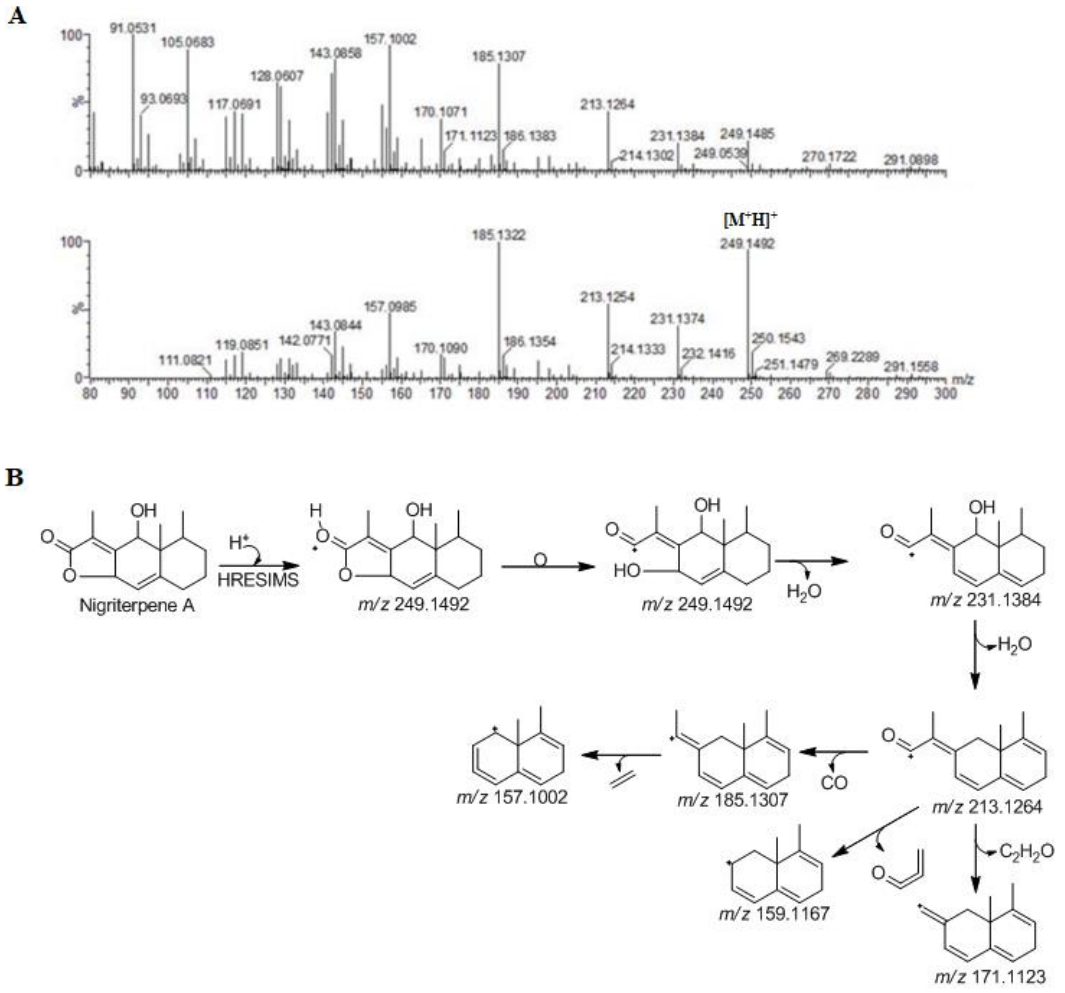


**Fig. 2S** UPLC-ESI-QTOF-MS$^{E}$ spectra (**a**) and fragmentation mechanism proposed (**b**) for nigriterpeneA (**8**)

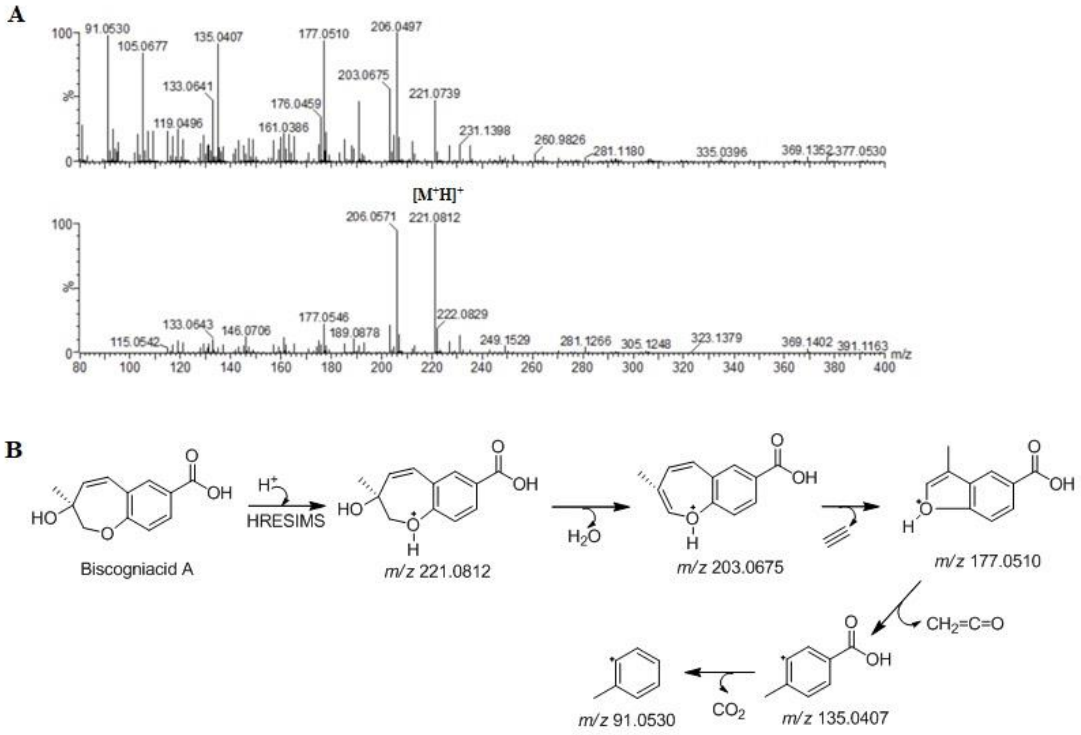


**Fig. 3S** UPLC-ESI-QTOF-MS$^{E}$ spectra (**a**) and fragmentation mechanism proposed (**b**) for biscogniacidA (**13**)

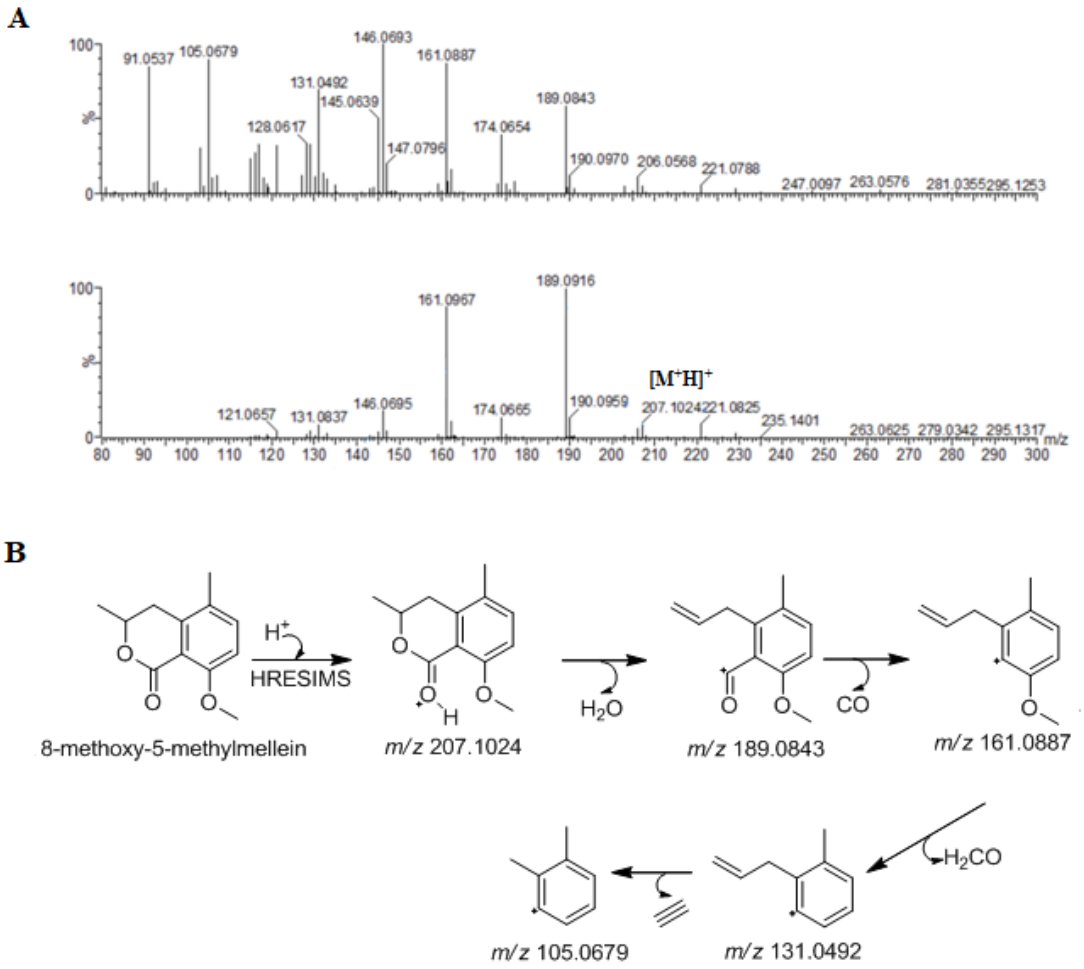


**Fig. 4S** UPLC-ESI-QTOF-MS$^{E}$ spectra (**a**) and fragmentation mechanism proposed (**b**) for 8-methoxy-5-methylmellein (**14**)

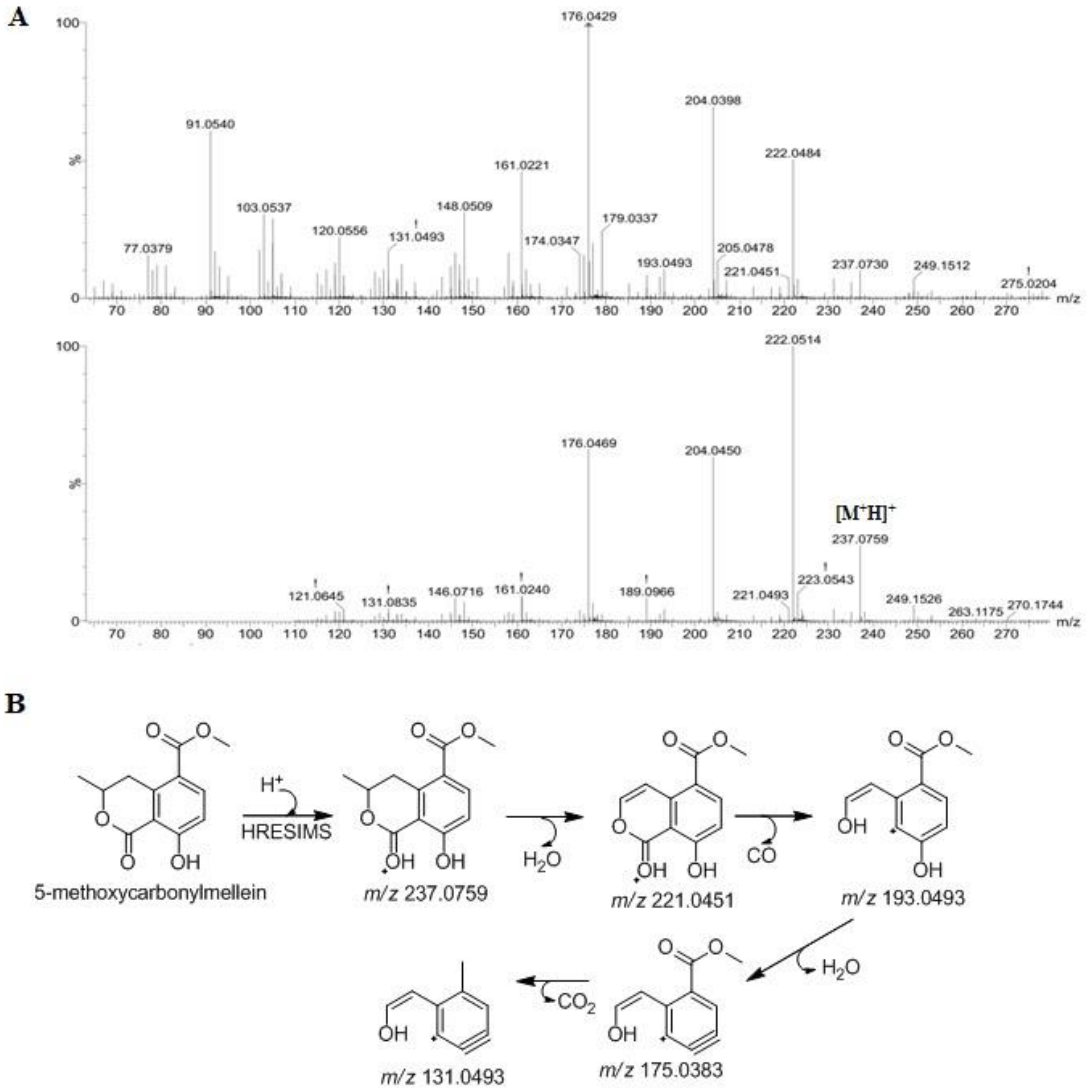


**Fig. 5S** UPLC-ESI-QTOF-MS$^{E}$ spectra (**a**) and fragmentation mechanism proposed (**b**) for 5-methoxycarbonylmellein (**18**)

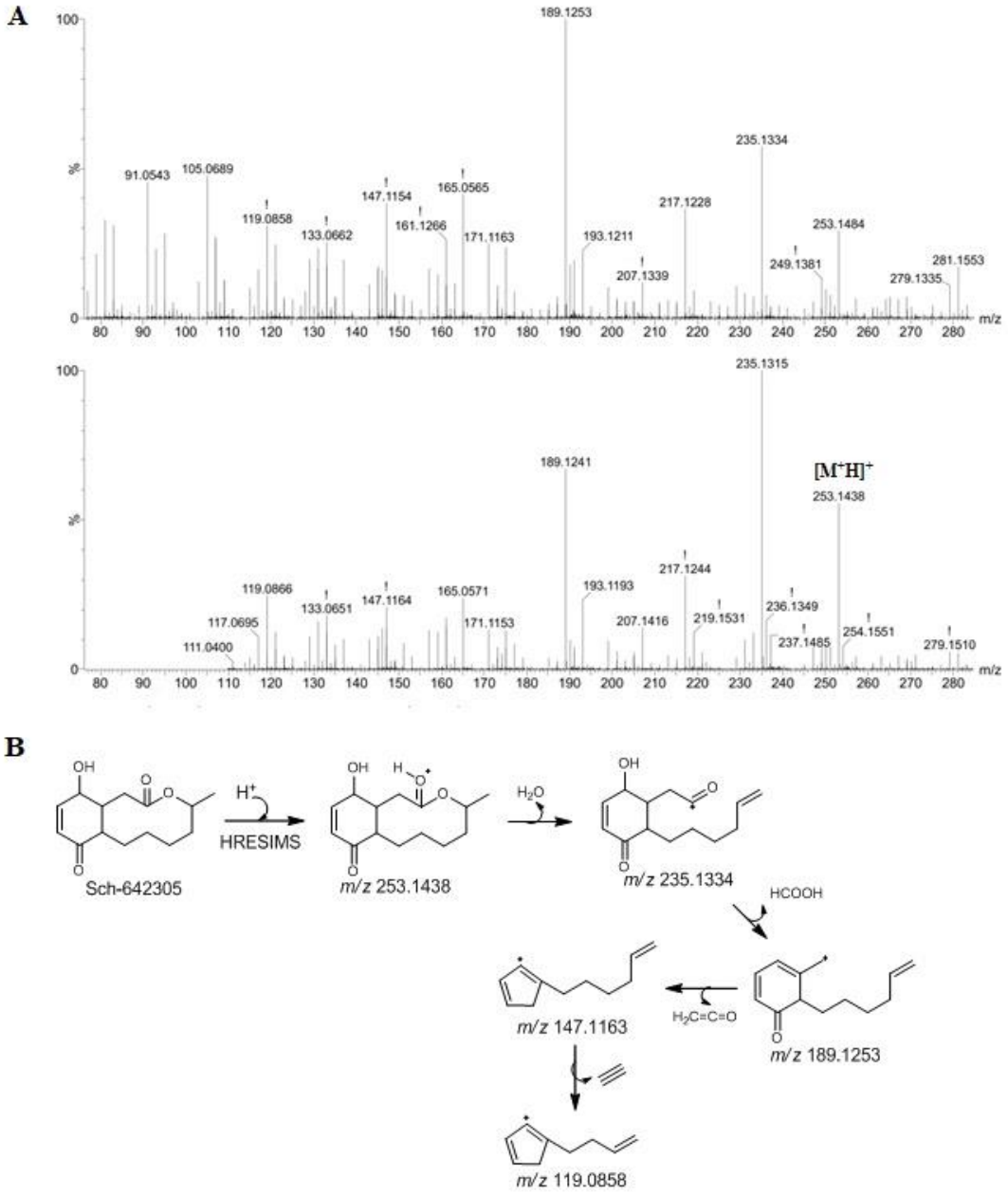


**Fig. 6S** UPLC-ESI-QTOF-MS$^{E}$ spectra (**a**) and fragmentation mechanism proposed (**b**) for Sch-642305 (**22**)

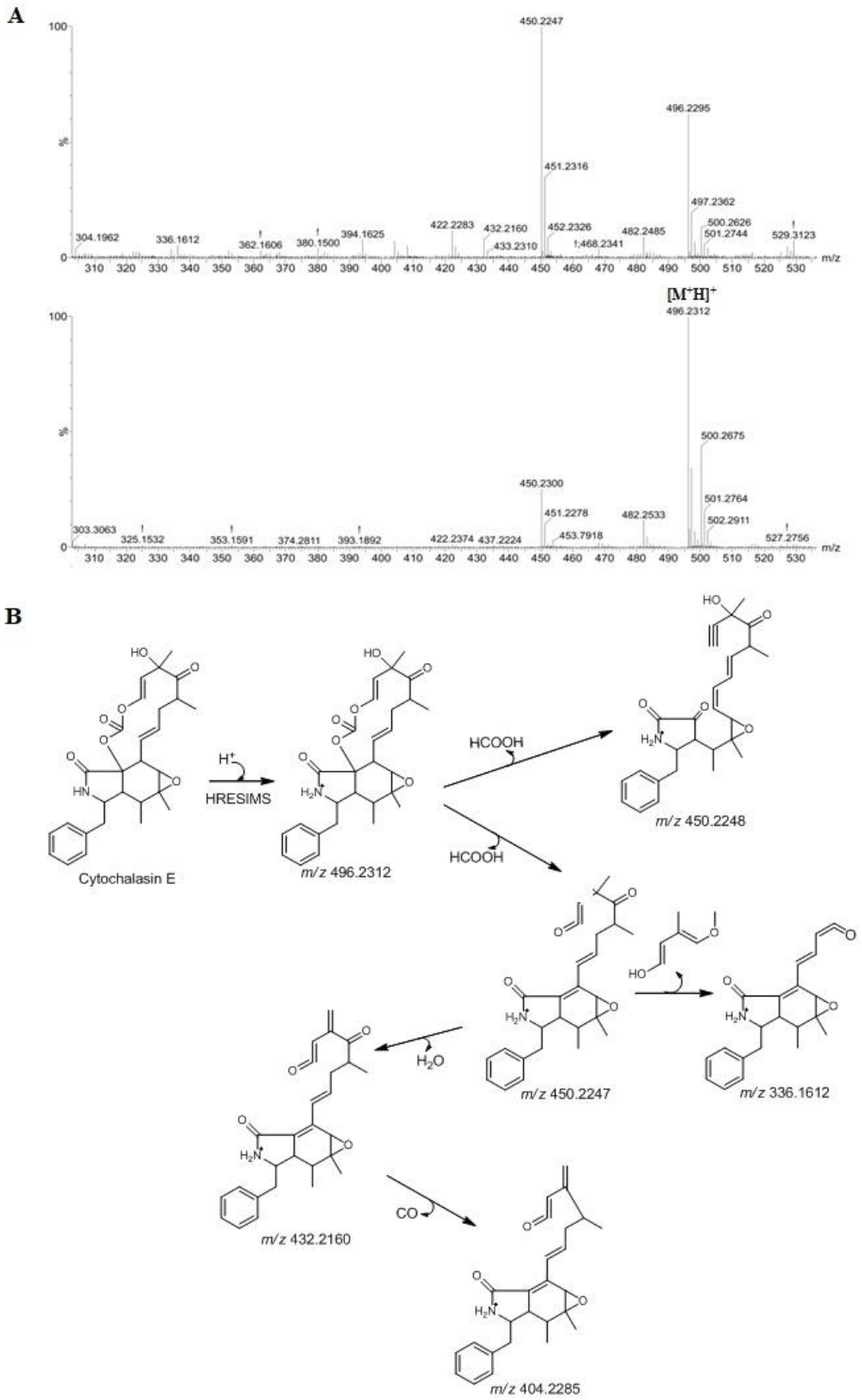


**Fig. 7S** UPLC-ESI-QTOF-MS$^{E}$ spectra (**a**) and fragmentation mechanism proposed (**b**) for cytochalasin E (**25**)

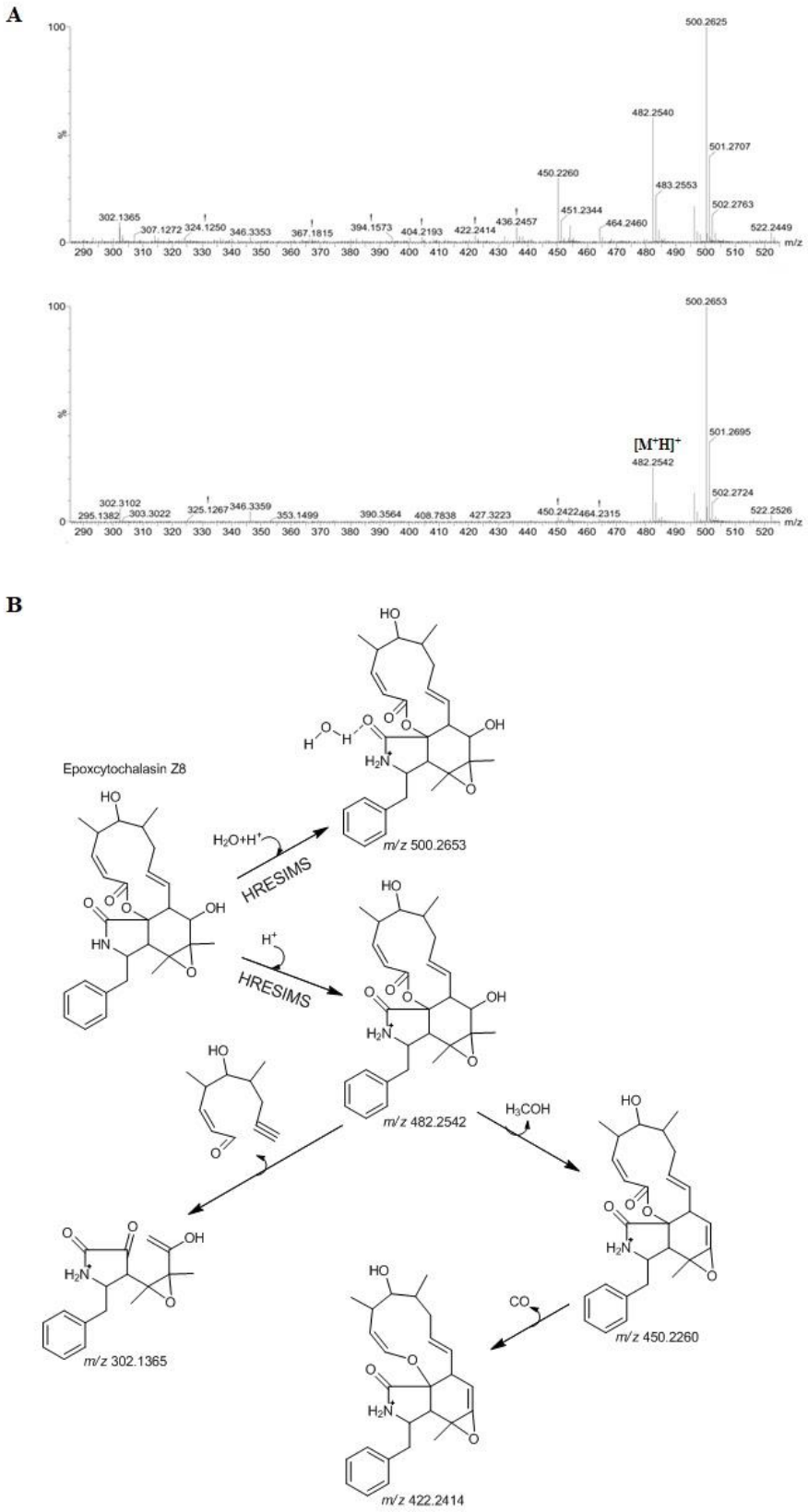


**Fig. 8S** UPLC-ESI-QTOF-MS$^{E}$ spectra (**a**) and fragmentation mechanism proposed (**b**) for epoxycytochalasin Z8 (**26**)

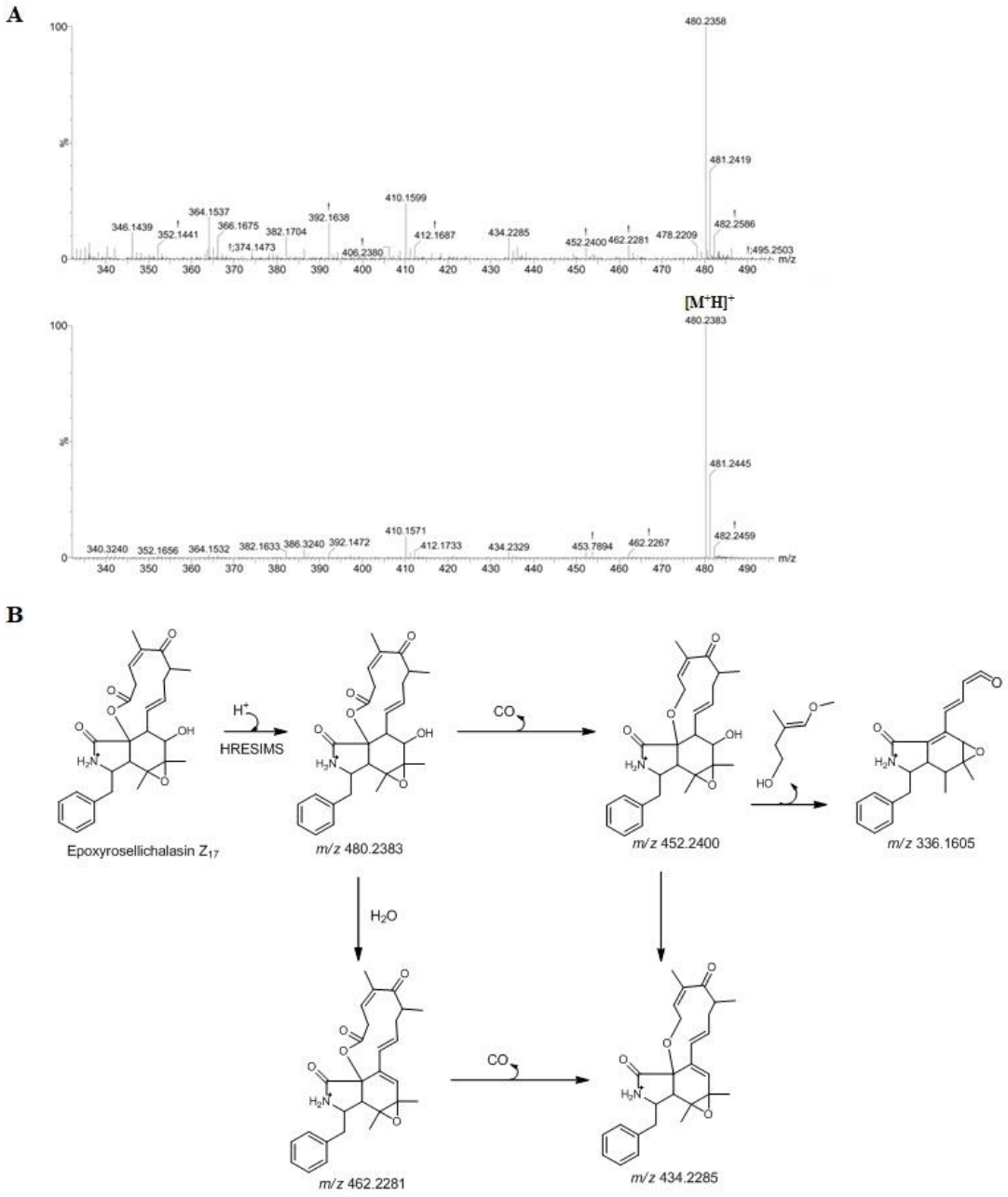


**Fig. 9S** UPLC-ESI-QTOF-MS$^{E}$ spectra (**a**) and fragmentation mechanism proposed (**b**) for epoxycytochalasin Z17 (**28**)

## 4.2 Capítulo 2

Astrocyte-glioma crosstalk: the impact of secondary metabolism of the endophytic fungus *Biscogniauxia* sp. on purinergic modulation, redox regulation and inflammatory response

Nathalia Stark Pedra*[1], Natália Pontes Bona[1], Mayara Sandrielly Pereira Soares[1], Luiza Spohr[1], Fernando Lopez Alvez[1], Francieli da Silva Santos[1], Juliane Torchelsen Saraiva[1], Bernardo de Moraes Meine[1], William Borges Domingues[2], Vinicius Farias Campos[2], Roselia Maria Spanevello*[1], Elizandra Braganhol*[3]

**Status:** A ser submetido.

# Astrocyte-glioma crosstalk: the impact of secondary metabolism of the endophytic fungus *Biscogniauxia* sp. on purinergic modulation, redox regulation, and inflammatory response

Nathalia Stark Pedra*[1], Natália Pontes Bona[1], Mayara Sandrielly Soares de Aguiar[1], Luiza Spohr[1], Fernando Lopez Alvez[1], Francieli da Silva Santos[1], Juliane Torchelsen Saraiva[1], Bernardo de Moraes Meine[1], William Borges Domingues[2], Vinicius Farias Campos[2], Kirley Marques Canuto[3], Roselia Maria Spanevello*[1], Elizandra Braganhol*[4]

[1] Programa de Pós-Graduação em Bioquímica e Bioprospecção, Centro de Ciências Químicas, Farmacêuticas e de Alimentos (CCQFA), Universidade Federal de Pelotas (UFPel), Pelotas, RS, Brazil.

[2] Laboratório de Genômica Estrututal, Programa de Pós-Graduação em Biotecnologia, Universidade Federal de Pelotas (UFPel), Pelotas, RS, Brazil.

[3] Empresa Brasileira de Pesquisa Agropecuária - Embrapa Agroindústria Tropical, Fortaleza, CE, Brazil.

[4] Departamento de Ciências Básicas da Saúde, Universidade Federal de Ciências da Saúde de Porto Alegre (UFCSPA), Porto Alegre, RS, Brazil.

***Corresponding Authors**
Elizandra Braganhol (ebraganhol@ufcspa.edu.br)
Departamento de Ciências Básicas da Saúde (DCBS) - UFCSPA
Rua Sarmento Leite, 245 - Anexo I - sala 304
CEP: 90.050-170, Porto Alegre, RS, Brazil

Roselia Maria Spanevello (roselia.spanevello@ufpel.edu.br) and Nathalia Stark Pedra (Nathalia.pedra@ufpel.edu.br)
Centro de Ciências Químicas, Farmacêuticas e de Alimentos (CCQFA) - UFPel
Campus Universitário s/n - Capão do Leão
CEP: 96010-900, Pelotas, RS, Brazil.

**Acknowledgments**

This research was supported by the Conselho Nacional de Desenvolvimento Científico e Tecnológico (CNPq) and the Fundação de Amparo à Pesquisa do Estado do Rio Grande do Sul (FAPERGS). This study was partially funded by the Coordenação de Aperfeiçoamento de Pessoal de Nível Superior, Brasil (CAPES), Finance code 001.

**Abstract**

Gliomas originate primarily from astrocytes and are the most aggressive primary brain tumors. Therefore, tumor-associated astrocytes provide physiological support for glioma progression. The purinergic system and oxidative stress induce chronic inflammation within the tumor microenvironment. Endophytic fungi reside in healthy plant tissues and represent a source of anti-tumor compounds. Previous studies have reported that the endophytic fungus *Biscogniauxia* sp., isolated from the medicinal plant *Achyrocline satureioides*, possesses antitumor activity. This study aimed to investigate the effect of fractionated extract of *Biscogniauxia* sp. ($F_{DCM}$) (1, 5, and 10 µg/mL) on adenine nucleotide catabolism, modulation of redox homeostasis, inflammatory response in a C6 glioma cell line, primary astrocyte culture, and astrocyte-glioma co-culture. $F_{DCM}$ promoted adenine nucleotide hydrolysis in C6 glioma cells and co-culture after 72 h of treatment. In addition, $F_{DCM}$ suppressed the levels of reactive oxygen species (ROS) and improved the antioxidant defense of C6 cells and co-culture. Finally, $F_{DCM}$ reduced interleukin (IL)-6 levels, increased IL-10 levels, and altered the relative expression of inflammatory genes in C6 cells and co-culture. $F_{DCM}$ suppressed the expression of cyclooxygenase-2 and IL-1β genes, while upregulating extracellular signal-regulated kinases 1/2 (ERK1/2) and caspase-1 genes in C6 glioma cells. However, it downregulated the relative gene expression of IL-1β under co-culture conditions. No changes were observed in primary cultures of healthy astrocytes exposed to $F_{DCM}$. We conclude that the cytotoxic profile of active compounds from *Biscogniauxia* sp. arises due to its ability to modulate pathways related to glioma progression, making this endophytic microorganism a promising source of metabolites of pharmacological interest.

**Keywords:** *Biscogniauxia* sp., Glioma, Astrocyte, Purinergic system, Oxidative stress, Cytokines

## 1. Introduction

Gliomas represent more than 80% of central nervous system (CNS) brain tumors [1]. Currently, molecular changes dictate the classification of these neoplasms into diffuse or circumscribed gliomas, while the integration of histopathological and molecular characteristics determines the grade of these tumors (1 to 4) [1,2]. Although standard therapy consists of maximum safe surgical resection, followed by the concomitant use of radiotherapy and chemotherapy, patients with high-grade gliomas as glioblastoma (GBM) (grade 4) exhibit an average survival of only 18 months [2].

One of the reasons for poor prognosis is the complex infiltrative nature of gliomas, in which the surrounding microenvironment favors their invasiveness [3]. The mechanisms involved in the heterogeneity and pathophysiology of glioma are driven by intercellular interactions present in the tumor microenvironment, inducing the transformation of healthy glial cells into malignant cells [4]. Since astrocytes are the most abundant glial cell in the adult brain, direct contact of tumor-associated astrocyte populations with glioma cells facilitates tumor migration, invasion, proliferation, and consequently, tumor malignancy [3].

Studies have shown that the glioma microenvironment exhibits high concentrations of adenosine triphosphate (ATP) and adenosine (ADO), which act as important purinergic signaling molecules [4-6]. These nucleotides and nucleosides play a fundamental role in cell-cell communication, in physiological processes such as astrocyte survival and proliferation [7, 8], as well as in pathological processes which favor the aggressive nature of gliomas, such as GBM growth, invasion into surrounding brain parenchyma, and angiogenesis [4, 9]. These events are controlled by the metabolism of ATP to ADO (the final product of ATP hydrolysis) via ectonucleotidase enzyme (nucleoside triphosphate diphosphohydrolases and 5'nucleotidase) activity and activation of specific membrane receptors, known as purinergic receptors [9, 10].

Furthermore, studies have indicated that purinergic receptor activation and the decrease in purinergic enzyme activity trigger the production and release of reactive oxygen species (ROS) and reduce glial antioxidant defenses, culminating in oxidative stress [11, 12]. Repeated exposure to ROS accelerates a cascade of intracellular events causing mitochondrial dysfunction and neuroinflammation as well as potential damage to DNA, lipids, and proteins [12, 13]. The mechanism of tumor growth triggered by high-grade gliomas is associated with poor prognosis, necessitating the need to search for new oncological therapies.

Interestingly, therapies based on natural compounds and their derivatives have gained popularity as effective anticancer alternatives [14, 15]. With increasing knowledge of the use of natural metabolites from medicinal plants, endophytic fungi are being increasingly explored as sources of pharmacologically active compounds for antiglioma therapy [16-18]. In recent years, our research group has focused on isolating bioactive secondary metabolites of endophytic fungus from *Achyrocline satureioides* (also known as marcela), a plant characterized by several pharmacological attributes in traditional Brazilian medicine [16]. The isolated microorganism, whose secondary metabolites exhibit important antiproliferative effects on human GBM strains [16], was recently identified as *Biscogniauxia* sp. These studies identified bioactive metabolites of the most promising fraction ($F_{DCM}$), including melleins, terpenoids, isocoumarins, cytochalasins, macrocyclic lactones, and other polyketide derivatives. Although these compounds show dose-dependent cytotoxic effects, they also exhibit high anti-glioma potential [16].

A possible explanation for GBM patients exhibiting refractory responses to currently available pharmacotherapies is that microenvironmental regulation in tumor progression is not considered in standard chemotherapy. Therefore, the heterogeneous microenvironment should be considered when assessing the impact of *Biscogniauxia* sp. secondary metabolites on the tumor site. Since co-culture systems provide the ability to assess cellular communication processes [19], this study aimed to evaluate the effect of the fraction $F_{DCM}$ on the regulation of purinergic signaling and redox modulation under co-culture conditions between glioma and astrocytes, as well as glioma cells and astrocytes separately.

## 2. Materials and Methods

### 2.1 Fungal material

The endophytic fungus *Biscogniauxia* sp. was isolated from healthy stems of *A. satureioides,* which were collected from the Transbrasiliana Highway (Rio Grande do Sul, Brazil; geographic coordinates: 31 °44′34,7″S and 54◦09′19,2″W) in April 2018 [16]. The endophytic fungus was identified by analyzing internal transcribed spacer (ITS) sequence data (GenBank accession no. ON257911).

### 2.2 Fermentation and extraction of metabolites from *Biscogniauxia* sp.

Fermentation of *Biscogniauxia* sp. was carried out in an Erlenmeyers flask containing 100 mL potato dextrose broth (PDB) medium at 25 ± 2 ℃ for 25 days [16]. Compounds produced by the fungi were extracted with dichloromethane (DCM) following incubation. The resulting extract was concentrated using a rotary evaporator (Rota-evaporador MA120-Marconi), dried, and kept at -20 °C. Finally, the DCM extract was subjected to solid phase extraction using Supelclean reversed-phase cartridges (C18, 500 mg), eluted in 50% methanol, and dried for 24 h at 40 ℃ in a SpeedVac centrifuge (Thermo-Fischer) as described by Aguiar-Galvão et al. [20]. The resulting purified fraction was named $F_{DCM}$.

### 2.3 General cell culture procedures

#### 2.3.1 C6 glioma cell line cultures

The C6 rat glioma cell line was obtained from the *American Type Cell Collection* (ATCC; Rockville, Maryland, USA). Cells were cultured in Dulbecco's Modified Eagle Medium (DMEM) (1% DMEM, 8.4 mM HEPES, 23.8 mM $NaHCO_3$, 0.1% fungizone, and penicillin/streptomycin 0.5 U/mL; pH 7.4) supplemented with 10% (v/v) fetal bovine serum (FBS) containing 5% $CO_2$ and maintained at 37 °C. To perform oxidative stress analysis, adenine nucleotide hydrolysis, and cell viability, and determine interleukin (IL)-6 and IL-10 levels, C6 glioma cells were seeded in 6-well, 24-well, and 96-well plates at a density of $3 \times 10^5$, $2 \times 10^4$, and $5 \times 10^3$ cells/well, respectively, after reaching 90% confluence.

#### 2.3.2 Primary astrocyte culture and co-culture with glioma cells

Primary astrocyte cultures were prepared as previously described [21]. Briefly, the cerebral cortices of newborn *Wistar* rats (1-2 days old) were removed and mechanically dissociated at pH 7.4 with calcium and magnesium-free balanced salt solution (137 mM NaCl, 5.36 mM KCl, 0.27 mM $Na_2HPO_4$, 1.1 mM $KH_2PO_4$, and 6.1 mM glucose) (CMF). The resulting cell suspension was centrifuged at 1000 *g* for 10 min and resuspended in DMEM supplemented with 10% FBS (pH 7.6). Then, $8 \times 10^5$, $2 \times 10^5$, and $5 \times 10^4$ cells were seeded in poly-L-lysine-coated 6-, 24-, and 96-multiwell plates respectively, and maintained in a $CO_2$ incubator at 37 °C. The cultures were allowed to grow to confluence for 20 days, and the medium was replaced every four days. Following astrocyte maturation, $8 \times 10^4$, $2 \times 10^4$, and $5 \times 10^3$ C6 glioma cells were seeded onto

astrocyte monolayers in 6-, 24-, and 96-multiwell plates, respectively, and co-cultures were maintained in DMEM supplemented with 10% FBS for 48 h. C6 glioma cells or astrocytes cultured under the same conditions were used as control. All procedures used in this study followed the "principles of Laboratory Animal Care" of the National Institutes of Health and were approved by the Ethical Committee of UFPel (CEEA 31292).

### 2.3.3 Cell culture treatment

$F_{DCM}$ was dissolved in dimethylsulfoxide (DMSO) at a stock concentration of 10 mg/mL and diluted in DMEM with 10% FBS to obtain solutions of 1, 5, and 10 µg/mL. To assess the cytotoxicity, glioma cells, astrocyte cultures, and co-culture were treated with $F_{DCM}$ for 24, 48, and 72 h. For oxidative stress and ectonucleotidase activity analysis, as well as quantifying gene expression and levels of IL-6 and IL-10, cultures were exposed to $F_{DCM}$ for 72 h. In addition, C6 glioma cells were exposed to ADO (product of 5'nucleotidase enzyme activity; 1 µM) and caffeine (non-selective P1 receptor antagonist; 10 µM) for 24 h, as described by Azambuja et al. [22]. In experiments performed in the presence of the ADO receptor antagonist, caffeine was added to the culture medium 30 min before ADO or $F_{DCM}$ treatment to analyze the role of endophytic fungus extract on P1 receptor blockage, cell viability, and glioma colony formation. Controls containing 0.01% DMSO (vehicle) were used.

## 2.4 Cytotoxicity

Cell viability was quantified using the 3-(4.5-dimethylthiazol-2-yl)-2.5-diphenyltetrazolium bromide (MTT) method, which is based on the ability of cells to reduce the salt of MTT into formazan crystals by the action of dehydrogenase enzymes [23]. Following completion of the different treatments described above, the cultures were incubated with MTT solution (0.5 mg/mL per well) at 37 °C in a humidified 5% $CO_2$ atmosphere. After 90 min, the medium was removed, and formazan crystals were diluted in DMSO. Finally, optical density (OD) was measured at 492 nm using a microplate reader (SpectraMAX 190). Results were calculated using GraphPad Prism 8.0 software (Prism GraphPad Software, San Diego, USA) and expressed as the percentage of control using the following formula:

Cell viability rate (%) = (OD of treated cells/OD of control) x 100%

### 2.5 Activity of ectonucleotidases

ATP and adenosine diphosphate (ADP) were used as substrates to determine the activity of nucleoside triphosphate diphosphohydrolases (NTPDases), while adenosine monophosphate (AMP) was used as a substrate for 5'-nucleotidase. Initially, cultures were washed with a phosphate-free incubation medium. The reaction was initiated by adding incubation medium containing 2 mM $CaCl_2$ (2 mM $MgCl_2$ for AMPase assay), 120 mM NaCl, 5 mM KCl, 10 mM glucose, 20 mM HEPES (pH 7.4), and 2 mM of the substrates (ATP, ADP, or AMP). To stop the reaction, 10% trichloroacetic acid (TCA) was added after 10 min of incubation at 37 °C. The released inorganic phosphate (Pi) was quantified using the malachite green method described by Chan et al. [24], using $KH_2PO_4$ as the standard. Protein content was determined by the Coomassie blue method using serum albumin as the standard [25]. Ectonucleotidase activity is reported as nmol Pi/min per milligram of protein.

### 2.6 Clonogenic assay

The clonogenic assay was used to determine the effectiveness of compounds with cytotoxic potential through the ability of tumor cells to form colonies [26]. For this assay, the C6 glioma cells were exposed to $F_{DCM}$ or ADO in the presence or absence of caffeine. After 24 h, the treatment medium was removed. Cells were harvested, seeded at a density of $3 \times 10^2$ cells/well in a 6-well plate, and incubated in a $CO_2$ incubator at 37 °C for 10 days. The colonies were then fixed with 100% methanol and stained with 1% crystal violet. The number of colonies was counted with a microscope using a 40x objective lens and the length of the colonies was measured using ImageJ 1.51j8 software (National Institutes of Health, USA).

### 2.7 Oxidative stress analysis

#### 2.7.1 Quantification of ROS

ROS generation was determined as previously described by Dos Santos [27]. In this method, 2'-7'-dichlorodihydrofluorescein diacetate (DCFH-DA) reacts with intracellular ROS to form an intermediate that emits fluorescence. In brief, the cellular cultures were incubated for 30 min at 37 °C with 1 µM DCFH-DA, and fluorescence was measured at 485/520 nm. ROS production was expressed as µmol DCF/mg protein.

### 2.7.2 Total sulfhydryl (SH) content

The sulfhydryl (SH) content was determined using the 5,5'-dithio-bis-(2-nitrobenzoic acid) (DTNB) method [28]. This assay is based on the reduction of DTNB by thiols, resulting in a yellow derivative 5'-thio-2-nitrobenzoic acid whose absorbance was measured at 412 nm and correlated to the SH content. The results are expressed as nmol TNB/mg of protein.

### 2.7.3 Superoxide dismutase (SOD) activity

Superoxide dismutase (SOD) activity was evaluated according to Misra and Fridovich [29], which is based on the inhibition of superoxide-dependent adrenaline auto-oxidation. In this reaction, SOD scavenges superoxide anions. The OD was measured at 480 nm using a microplate reader (SpectraMax 190), and the results were expressed as units/mg of protein.

### 2.7.4 Catalase (CAT) activity

The Catalase (CAT) activity assay was based on the decomposition of hydrogen peroxide ($H_2O_2$) in potassium phosphate buffer (pH 7.0) [30]. The reaction was monitored using a microplate reader at the absorbance of 240 nm at 37 °C. CAT activity is reported as units/mg of protein.

### 2.7.5 Glutathione-S-transferase (GST) activity

Glutathione-S-transferase (GST) activity was determined as previously described by Habig et al. [31] using 1-chloro-2,4-dinitrobenzene (CDNB) as a substrate. The assay mixture contained 1 mM CDNB diluted in ethanol, 10 mM glutathione (GSH), 20 mM potassium phosphate buffer (pH 6.5), and 20 µl cell lysate. GST activity was expressed as µmol GS-DNB min/mg of protein.

### 2.7.6 Protein determination

Protein determination was performed according to Lowry et al. [32] for oxidative stress parameters. Bovine serum albumin was used as a standard.

## 2.8 Determination of IL-6 and IL-10 levels

IL-6 and IL-10 levels were quantified using an enzyme-linked immunosorbent assay (ELISA) kit (Sigma-Aldrich, St. Louis, MO, USA) according to the manufacturer's instructions. The results are expressed as pg/mg of protein.

### 2.9 RNA extraction, complementary DNA (cDNA) synthesis and real-time quantitative polymerase chain reaction (qPCR)

To investigate the impact of $F_{DCM}$ on the relative mRNA expression levels of extracellular signal-regulated kinases (ERKs), cyclooxygenases (COX) 1 and 2 (COX-1 and COX-2), Caspase-1 (Casp-1), IL-1β, and total RNA was extracted from 1 mL of C6 rat glioma cell line, primary astrocyte cultures, and co-culture of astrocytes and C6 glioma cells (n = 5 for each experimental group) using TRI Reagent® (Sigma-Aldrich, St. Louis, MO, USA). The total RNA isolated was quantified, and purity (260/280 and 260/230 ratios) was examined using a NanoVue spectrophotometer (GE, Fairfield, CT, USA).

cDNA synthesis was performed using a High Capacity cDNA Reverse Transcription kit (Applied Biosystems, UK) following the manufacturer's protocol. For reverse transcription, 500 ng total RNA was used in a reaction volume of 20 µl. Amplification was performed with GoTaq® qPCR Master Mix (Promega, Madison, WI) using the CFX96 Touch Real-Time PCR Detection System (Bio-Rad Laboratories Inc., CA, USA), and the sequences of the primers used are indicated in **Table 1**. The qPCR conditions were as follows: 10 min at 95 °C to activate the hot-start Taq polymerase, followed by 35 cycles of denaturation for 15 s at 95 °C, primer annealing for 60 s at 60 °C, and extension for 30 s at 72 °C. Fluorescence was detected at the end of each cycle. Baseline and threshold values were automatically set using Bio-Rad CFX Manager software.

The number of PCR cycles required to reach the fluorescence threshold for each sample was defined as the Ct value. The $2^{-\Delta\Delta CT}$ method was used to normalize the fold-change in gene expression [33], using *actb* as a housekeeping gene.

### 2.10 Statistical Analysis

Statistical analysis was performed using two-way ANOVA followed by Tukey's post-hoc test when appropriate. The results are expressed as the mean ± SEM. Differences were considered significant at $P < 0.05$ using GraphPad Prism 5.0 software (Prism GraphPad Software, San Diego, USA).

## 3. Results

### 3.1 Metabolites of *Biscogniauxia* sp. reduce viability of glioma cells and co-culture but not astrocytes

To evaluate cytotoxic effects of compounds produced by the endophytic fungus *Biscogniauxia* sp. C6 glioma cells, primary astrocyte culture, and co-culture of astrocytes and C6 were exposed to increasing concentrations of $F_{DCM}$ for 24 h**,** 48 h and 72 h (**Figure 1a-c**). $F_{DCM}$ exhibited time- and concentration-dependent effects, significantly reducing the viability of glioma cells after 48 and 72 h of treatment by approximately 60% and 70%, respectively, when compared to control cells. When exposed to co-culture, $F_{DCM}$ (at a concentration of 10 µg/mL) decreased cell viability by 50% at 48 h, and 60% at 72 h of treatment. However, no significant changes were observed in cell culture viability following 24 h exposure to $F_{DCM}$. Furthermore, metabolites produced by the endophytic fungus did not induce any cytotoxic effects in the primary astrocyte cell culture.

### 3.2 $F_{DCM}$ alters the hydrolysis profile of adenine nucleotides of glioma cells and co-culture but not astrocytes

The activity of NTPDases and 5'-nucleotidase enzymes in astrocytes, C6 glioma cells, and astrocyte-glioma co-culture, as well as the effect of $F_{DCM}$ on purinergic modulation, are shown in **Figure 2**. Initially, differences in nucleotide hydrolysis were observed in control cells. Control C6 glioma cells exhibited a reduction in the hydrolysis of ATP (5.2 ± 0.2 µmol Pi/min/mg of protein) (**Figure 2a**), and ADP (5.7 ± 0.6 µmol Pi/min/mg of protein) (**Figure 2b**) nucleotides when compared to astrocytes (35.6 ± 4.4 µmol Pi/min/mg of protein for ATP, and 12.5 ± 0.6 µmol Pi/min/mg of protein for ADP), and co-culture controls (21.6 ± 2.0 µmol Pi/min/mg of protein for ATP, and 14.9 ± 1.2 µmol Pi/min/mg of protein for ADP). There were no statistical differences in ADP hydrolysis between astrocytes and co-culture. However, ATPase activity was 40% lower in astrocyte-glioma co-culture than in astrocytes alone.

In contrast, C6 glioma cells have higher AMPase activity (17.5 ± 0.8 µmol Pi/min/mg of protein) than astrocytes (8.8 ± 1.1 µmol Pi/min/mg of protein), whereas healthy cells exhibited reduced AMP hydrolysis (ca.40%) compared to co-culture conditions (12.1 ± 2.2 µmol Pi/min/mg of protein) (**Figure 2c**).

When the experimental cultures were exposed to a $F_{DCM}$ for 72 h, fractionated extract promoted a significant increase in the hydrolysis of adenine nucleotides when compared to the respective control cells. In C6 glioma cells, $F_{DCM}$ (10 µg/mL) increased

hydrolysis of ATP, ADP, and AMP by approximately 120%. Under conditions of co-cultivation, $F_{DCM}$ induced an increase of up to 80%, 145%, and 90% in ATP, ADP, and AMP hydrolysis, respectively, when compared to control cells in the co-culture. No changes in nucleotide catabolism were observed in astrocytes exposed to $F_{DCM}$.

### 3.3 $F_{DCM}$ reduces P1 receptor-independent glioma cell survival

In the purinergic signaling cascade, AMP generated from ATP hydrolysis is converted to ADO by the enzyme 5'-nucleotidase [10]. To better understand the effects of bioactive metabolites produced by the endophytic fungus *Biscogniauxia* sp on the adenosynergic pathway, C6 glioma cells were exposed to caffeine, a non-selective antagonist of the ADO receptor, 30 min before treatment with $F_{DCM}$. After 24 h, colony formation was assessed (**Figure 3a**). Consistent with previous studies, cells exposed to ADO exhibited a significant increase in the formation and length of glioma colonies (ca.35% and ca.50%, respectively) (**Figure 3b-c**), whereas pretreatment with caffeine prevented this proliferative effect of ADO. The fractionated *Biscogniauxia* sp. extract (10 µg/mL) reduced the number and colony length of the glioma cell line by approximately 85% and 65%, respectively. However, no significant differences were observed in survival rates of glioma cells exposed to $F_{DCM}$ in the absence or presence of caffeine, suggesting that secondary metabolism of *Biscogniauxia* sp. induced P1 receptor-independent cytotoxic effects.

### 3.4 $F_{DCM}$ reduces oxidative damage and improves antioxidant defense systems in glioma cells and astrocyte-glioma co-culture

The impact of $F_{DCM}$ on the modulation of redox biology was investigated in cell cultures. We observed a significant difference between control cells in the experimental models. Control glioma and co-culture cells exhibited an increase in ROS levels (173.8 ± 15.3 and 174.8 ± 16.7 µmol DCF/mg of protein, respectively) compared to control cells from the primary astrocyte culture (38.5 ± 1.3 µmol DCF/mg of protein) (**Figure 4a**). Furthermore, C6 glioma cells alone and glioma cells co-cultured with astrocytes showed a reduction in total thiol content (35.7 ± 2.8 and 27.6 ± 3.4 nmol TNB/mg of protein, respectively) compared to healthy cells (77.3 ± 10.8 nmol TNB/mg protein) (**Figure 4b**). However, $F_{DCM}$ treatment reduced oxidative damage in a concentration-dependent manner, decreasing ROS production by more than 80% and promoting an increase in total

SH levels by up to 70% in C6 glioma cells and astrocyte-glioma co-culture at a concentration of 10 µg/mL.

Changes in the antioxidant defense system were also observed (**Figure 5**). Healthy cells showed increased enzyme activity (933.4 ± 108.1 units/mg of protein for SOD, 48.5 ± 5.8 units/mg of protein for CAT, and 547.1 ± 99.6 µmol GS-DNB/mg of protein for GST) compared to control glioma cells (180.2 ± 11.6 units/mg of protein for SOD, 5.0 ± 0.4 units/mg of protein for CAT, and 99.2 ± 11.3 µmol GS-DNB/mg of protein) and astrocyte-glioma co-cultures (261.0 ± 8.6 units/mg of protein for SOD, 12.2 ± 0.8 units/mg of protein for CAT, and 92.7 ± 4.7 µmol GS-DNB/mg of protein). According to the data obtained, glioma cells co-cultured with astrocytes exhibited an increase of approximately 30% and 60% in SOD and CAT activities, respectively, when compared to control C6 glioma cells alone.

However, exposure of the C6 glioma cell line to $F_{DCM}$ (10 µg/mL) for 72 h increased SOD, CAT, and GST enzyme activity by approximately 55%, 255%, and 120%, respectively, when compared to untreated glioma cells. Similarly, the secondary metabolites of *Biscogniauxia* sp. increased the enzymatic activity of CAT (ca.160%) and GST (ca.70%) under astrocyte-glioma co-culture conditions, but SOD activity remained unaltered compared to untreated cultures. The purified fraction did not induce changes in redox homeostasis in the primary astrocyte culture.

### 3.5 $F_{DCM}$ reduces IL-6 levels and increases IL-10 release in C6 glioma cells and astrocyte-glioma co-culture

Glioma-astrocyte co-culture had an increase in IL-6 release (580.7 ± 18.2 pg/mL) when compared to C6 glioma cells alone (421.2 ± 21.5 pg/mL) and primary astrocyte culture (352.8 ± 26.6 pg/mL) (**Figure 6a**). Furthermore, the glioma cell line had IL-6 levels 30% lower than those from co-culture conditions. In contrast, $F_{DCM}$ reduced pro-inflammatory cytokine release from glioma cells under co-culture conditions by approximately 30%, but not in primary astrocyte culture.

No significant changes were observed in IL-10 levels between the experimental protocols used in this study (1390.0 ± 75.4 pg/mL for astrocytes, 1058.0 ± 28.4 pg/mL for C6 glioma cells, and 1473.0 ± 217.4 pg/mL for co-culture astrocyte-glioma) (**Figure 6b**). However, the bioactive metabolites present in the purified fraction induced a significant increase in the release of anti-inflammatory cytokines in the C6 glioma cell

line and in co-culture conditions by 60% and 50%, respectively, when compared to untreated cells. No changes were observed in primary astrocyte cultures.

### 3.6 Effect of $F_{DCM}$ on COX, Casp-1, IL-1b, and ERK1/2 gene expression in glioma cells, astrocytes and astrocyte-glioma co-culture

To investigate the role of *Biscogniauxia* sp. secondary metabolites on proliferation and inflammation-related pathways in gliomagenesis, the relative mRNA expression levels of COX-1, COX-2, Casp-1, IL-1β, and ERK1/2 were evaluated in cultures exposed to $F_{DCM}$ for 72 h. Corroborating the previous results, $F_{DCM}$ did not significantly alter the expression levels of any of the analyzed genes in astrocyte cultures (**Figure 7a**). The relative mRNA expression of Casp-1 and ERK1/2 genes was increased in C6 glioma cells exposed to 10 µg/mL $F_{DCM}$ (3.2- and 0.6-fold, respectively) compared to untreated cells. However, COX-2 and IL-1β gene expression was downregulated by up to 0.6-fold in a concentration-dependent manner (**Figure 7b**). Under astrocyte-glioma co-culture conditions, $F_{DCM}$ altered IL-1β gene expression levels, where the relative expression level of mRNA was 0.6-fold downregulated at both concentrations (**Figure 7c**).

## Discussion

GBM usually arises from malignant astrocytic transformations, which play an important role within the tumor microenvironment [38]. Glial cells favor cell proliferation through the secretion of various growth factors and inflammatory mediators [3]. Since glioma-astrocyte interactions play an important role in chemotherapeutic resistance, the use of co-culture techniques allows for the understanding of cell-cell communication and helps in the search for new antiglioma therapeutic approaches [19].

In the present study, we demonstrated the selective anti-glioma effect of the fractionated extract of *Biscogniauxia* sp. ($F_{DCM}$), which did not alter the viability of primary astrocyte cultures. Furthermore, under co-cultivation conditions, astrocytes did not alter the cytotoxic effects induced by $F_{DCM}$ on glioma cells, indicating the therapeutic relevance of the secondary metabolites of the isolated endophytic fungus. According to Yang et al. [39], astrocytes attenuate the cytotoxic effects of temozolomide (TMZ) and doxorubicin chemotherapeutics on glioma cells, thus favoring the development of chemoresistance which subsequently worsens the prognosis for patients with high-grade gliomas. Chen et al. [40] highlighted the role of astrocytes in reducing apoptosis of glioma

cells induced by TMZ and vincristine. According to the authors, the protection provided by astrocytes depends on direct contact between the astrocytes and glioma, which is mediated by gap junction communication.

The inflammatory microenvironment of gliomas involves the participation of nucleotides and nucleosides, which activate pathways related to proliferation, angiogenesis, migration, invasion, and cell death [9]. In this study, we describe the effects of $F_{DCM}$ obtained from *Biscogniauxia* sp. on the hydrolysis of extracellular nucleotides in C6 glioma cells, primary astrocyte cultures, and astrocyte-glioma crosstalk. The C6 glioma cell line consists of chemically transformed astrocytes and is widely used in experimental studies on GBM growth and invasion [9, 22]. It is well established that glioma cells present changes in the catabolism of adenine nucleotides, exhibiting a low hydrolysis rate of di- and triphosphate nucleotides and a high hydrolysis rate of monophosphate nucleotides when compared to primary astrocyte cultivation [41]. We observed that C6 glioma cells hydrolyzed less ATP (approximately 6.8-fold) and ADP (approximately 2.2-fold) than astrocytes, whereas AMP hydrolysis was 2.0-fold greater in C6 cells. The rat glioma cell line has low expression of enzymes involved in the degradation of extracellular ATP (NTPDase1, NTPDase2, and NTPDase3) when compared to primary astrocyte culture [42]. Thus, the increase in ATP and ADP hydrolysis under co-culture conditions when compared to C6 cells alone may be due to astrocyte-glioma crosstalk.

The low ATPase activity of glioma cells promotes the accumulation of extracellular ATP, favoring the progression of brain tumors [41, 42]. In this study, $F_{DCM}$ induced an increase in nucleotide catabolism in C6 glioma cells and astrocyte-glioma co-culture but did not alter the hydrolysis of adenine nucleotides in the primary culture of astrocytes. This suggests that the cytotoxic effect of $F_{DCM}$ selectively modulates purinergic signaling in glioma. The high rate of ATP hydrolysis suggests increased release of this nucleotide into the extracellular space. Under pathological conditions, astrocytes are transformed into reactive astrocytes, releasing more ATP into the tumor microenvironment and favoring the proliferation and aberrant migration of glioma cells [43]. The increased activity of NTPDases induced by $F_{DCM}$ under co-culture conditions could be a compensatory mechanism to reduce the levels of extracellular nucleotides.

While the hydrolysis of ATP and ADP to AMP is mediated by NTPDases, AMP is hydrolyzed to ADO by 5´nucleotidase [5]. In this study, the increased hydrolysis of adenine nucleotides suggests an increase in ADO levels. Under physiological conditions,

glial cells can regulate extracellular ADO levels through the hydrolysis of nucleoside to inosine by the enzyme adenosine deaminase (ADA) [5] or through the uptake of ADO into the cell by extracellular nucleoside transporters (ENTs) [44]. However, the GBM microenvironment is characterized by changes in the extra- and intracellular metabolism of purines, whose imbalance plays an important role in tumor aggressiveness and recurrence [45]. Scientific reports have shown that cells in the tumor microenvironment have reduced ENT-1 activity resulting in the accumulation of extracellular ADO, which stimulates the progression of gliomas via P1 receptor sensitization [22, 46, 47]. Despite promoting an increase in AMPase activity, the metabolites of *Biscogniauxia* sp. significantly reduced the viability of C6 cell line and astrocyte-glioma co-culture. In addition, $F_{DCM}$-induced anti-glioma effects were not altered by inhibition of the ADO receptor, suggesting that the compounds of *Biscogniauxia* sp. do not act via P1 receptor sensitization. However, the effects of $F_{DCM}$ on the hydrolysis and uptake of ADO remain unclear.

Physiologically, the brain requires a large amount of ATP to maintain its neuronal activity. Thus, the high metabolic rate required to maintain the CNS leads to the production of large amounts of free radicals, making the brain highly susceptible to oxidative damage [48, 49]. Growing evidence suggests that changes in brain homeostasis triggered by extracellular ATP and ADO stimulate the production and release of reactive species resulting in oxidative stress [11, 44]. We found that C6 glioma cells alone or in co-culture conditions had a significant increase in ROS production when compared to primary astrocyte culture. However, the secondary metabolites of *Biscogniauxia* sp. effectively reduced the production of these reactive species in C6 glioma cell line and astrocyte-glioma co-culture. Although gliomagenesis favors the neurotoxic phenotype of astrocytes, it has been shown that even after intense oxidative stress, cortical astrocytes do not lose their neuroprotective function and continue to eliminate excess toxic molecules, providing trophic and metabolic support to neighboring cells [50]. This finding may agree with the antiglioma effect exhibited by $F_{DCM}$, whose bioactive metabolites allowed the reduction of ROS in both tumor cultures, reaching levels similar to those exhibited by control astrocytes.

Healthy astrocytes exert their neuroprotective role in redox modulation through endogenous antioxidants such as SOD, CAT, and GSH. We recently demonstrated that brain tumor tissues from rats subjected to intracerebroventricular injection of C6 glioma cells have reduced SOD and CAT activity and reduced total thiol content compared to

healthy tissues [51]. Corroborating previous findings, both the C6 glioma cell line and co-culture exhibited a significant reduction in antioxidant enzyme activity compared to the primary astrocyte culture. However, the astrocyte-glioma interaction induced an improvement in SOD and CAT activity, but a reduction in total thiol content and GST activity, compared to C6 glioma cells alone. Overall, astrocytes contain one of the highest cytosolic concentrations of GSH among CNS cells [52]. GSH is the most abundant thiol-containing small molecule in healthy cells, and its sulfhydryl residues are responsible for maintaining intracellular redox homeostasis. Thus, tumor-associated astrocytic activation compromises the antioxidant capacity of glial cells, making the brain microenvironment susceptible to oxidative lesions that favor tumor progression [53, 54].

In this study, $F_{DCM}$-induced reductions in ROS levels may be related to its potential to increase the activity of antioxidant enzymes and levels of total SH in glioma cells. These results are in agreement with previous findings that highlight the antioxidant potential of metabolites produced by the endophytic fungus *A. satureioides* [16]. Among the metabolites produced by *Biscogniauxia* sp. isolated from *A. satureioides* (data not shown), the macrocyclic lactone Sch-642305 reduces oxidative stress in glioma cells, inducing a significant increase in the activities of the antioxidant enzymes SOD, CAT, and glutathione peroxidase [16]. No alteration in redox homeostasis was observed in the primary culture of astrocytes exposed to $F_{DCM}$, suggesting that bioactive compounds from *Biscogniauxia* sp. selectively alter oxidative parameters in gliomagenesis.

Although the secondary metabolites of *Biscogniauxia* sp. Increased the total thiol levels and activity of CAT and GST enzymes, no changes were observed in SOD activity under co-culture conditions. SOD is the first line of antioxidant defense against oxidative stress and catalyzes superoxide anion dismutation [55]. Some studies indicate a close relationship between SOD and ERK activation in the antineoplastic activity of certain anticancer agents [56-58]. ROS, especially the superoxide anion, modulates the activity of proteins important in signal transduction and carcinogenesis, including the activity of mitogen-activated protein kinases, especially ERK [59]. Although the constitutive activation of ERK is largely related to the induction of cell growth and inhibition of apoptosis, $F_{DCM}$ reduced proliferation and induced apoptosis in C6 glioma cells (data not shown).

Several studies have shown that sustained ERK activation is also involved in apoptotic processes and phosphorylation of nuclear factor erythroid 2-related factor 2, a key regulator of the cellular response against oxidative damage, through the synthesis of

antioxidant enzymes such as SOD and GST [59, 60]. Furthermore, the ERK signaling pathway is considered a key component in the regulation of COX-2 expression. Thus, ERK activation can reduce the expression of this proinflammatory enzyme [61]. In brain tumors, increased COX-2 expression has been correlated with glioma aggressiveness and progression [62, 63]. $F_{DCM}$ significantly increased SOD activity and relative mRNA expression levels of ERK1/2, but reduced COX-2 gene expression in C6 glioma cells. In contrast, such changes were not observed in astrocyte-glioma co-cultures exposed to the fractionated extract. Thus, the antioxidant activity exerted by *Biscogniauxia* sp. in the C6 glioma cell line may be related to the ability of bioactive metabolites to modulate ERK/COX-2 signaling pathways. On the other hand, astrocyte-glioma communication seems to impair the modulation of this pathway by $F_{DCM}$ under co-culture conditions.

It is well established that alterations in redox and purinergic homeostasis contribute to chronic inflammation in the tumor microenvironment [9, 13]. Evidence indicates that ROS accumulation can activate the astrocytic inflammatory cascade by promoting the activation of Casp-1, a key component in regulating the activation, production, and secretion of pro-inflammatory cytokines, especially IL-1β [48]. Under pathological conditions, IL-1β is constantly released in response to chronic inflammation and is the main pro-inflammatory cytokine involved in reactive astrogliosis processes [64, 65]. $F_{DCM}$ significantly downregulated the expression of IL-1β in both the C6 glioma cell line and astrocyte-glioma co-culture. In contrast, the fractionated extract increased the relative expression of Casp-1 mRNA in C6 glioma cells, but not under co-culture conditions. In general, IL-1β is produced by Casp-1 in the inactive pro-form (pro-IL-1β), whose synthesis and subsequent expression of the active form (IL-1β) depends on the recognition receptor pattern [66], suggesting that chemical components of *Biscogniauxia* sp. alter pathways related to IL-1β maturation in glioma cells.

High levels of IL-1β have been associated with increased COX-2 and IL-6 gene expression in GBM cells, favoring cell proliferation, migration, and invasion [67, 68]. In this study, we observed a significant increase in IL-6 levels in the astrocyte-glioma co-culture model compared with C6 glioma cells and healthy astrocytes alone. In line with previous studies, we demonstrated that tumor-associated astrocytes secrete high amounts of IL-6, creating a favorable microenvironment for GBM progression and angiogenesis [69, 70]. However, bioactive compounds from *Biscogniauxia* sp. significantly reduced IL-6 levels and promoted an increase in the release of anti-inflammatory cytokine IL-10. Importantly, no changes were observed in the expression of inflammatory biomarkers in

healthy cortical astrocytes exposed to $F_{DCM}$, suggesting that the antiglioma potential of *Biscogniauxia* sp. is related to its ability to selectively modulate the pathways involved in tumorigenesis.

Few studies have explored the mechanisms underlying the antitumor activity of the genus *Biscogniauxia*. We recently verified that *Biscogniauxia* sp. isolated from *A. satureioides* produces compounds of the terpene class, including isocoumarins, macrocyclic lactone, cytochalasins, and other polyketide derivatives (data not shown). Among these metabolites, studies have highlighted the antitumor potential of macrocyclic lactone Sch-642305 and cytochalasin E. In addition to regulating the redox status of glioma cells, Sch-642305 inhibits cell migration, promotes cell cycle arrest in the G2/M phase, and induces apoptosis in C6 glioma cells [16]. In contrast, the cytochalasin class acts by inhibiting cell proliferation via regulation of the autophagic markers LC3-II and p62 in human lung adenocarcinoma cell line (A549) [71]. In addition, studies have emphasized the impact of cytochalasins on the inflammatory response mediated by Toll-like receptor 4 in macrophages, which acts by suppressing the expression of inflammatory mediators such as COX-2, tumor necrosis factor-α, and inducible nitric oxide [72, 73]. Therefore, the synergistic action of bioactive metabolites of *Biscogniauxia* sp. may have contributed to its antineoplastic effect in multiple pathways related to the progression of gliomas.

**Conclusion**

Given the importance of the tumor microenvironment in the regulation of gliomagenesis and the role of tumor-associated astrocytes in GBM proliferation and treatment resistance, the present study demonstrated for the first time the mechanisms underlying the antiglioma effect of the secondary metabolites of isolated endophytic fungus *Biscogniauxia* sp. of *A. satureioides* using an astrocyte-glioma co-culture model. The fractionated extract of *Biscogniauxia* sp. was capable of reducing cell growth and modulated the hydrolysis of adenine nucleotides both in C6 glioma cells and in astrocyte-glioma co-culture. In addition, $F_{DCM}$ regulates redox homeostasis by efficiently reducing ROS levels through increasing antioxidant enzyme activity, even under co-culture conditions. Additionally, bioactive compounds from endophytic fungus significantly reduced the expression and secretion of inflammatory markers in C6 cells alone and when co-cultured with astrocytes. In contrast, $F_{DCM}$ did not induce any significant changes in cell viability or in the components involved in the inflammatory response of cortical

astrocytes, suggesting an important selective antiglioma effect. Our results encourage further studies in the field to mechanistically explore the antineoplastic potential of the endophytic fungus *Biscogniauxia* sp., whose bioactive metabolites have shown to be promising candidates for antiglioma therapy.

**References**

[1] Louis DN, Perry A, Wesseling P, Brat DJ, Cree IA, Figarella-Branger D, Hawkins C, Ng HK, Pfister SM, Reifenberger G, Soffietti R, Von Deimling A, Ellison DW (2021) The 2021 WHO classification of tumors of the central nervous system: a summary. Neuro-oncology 23:1231-1251. https://doi.org/10.1093/neuonc/noab106

[2] Ostrom QT, Cioffi G, Waite K, Kruchko C, Barnholtz-Sloan JS (2021) CBTRUS statistical report: primary brain and other central nervous system tumors diagnosed in the United States in 2014–2018. Neuro-oncology, 23:iii1-iii105.
https://doi.org/10.1093/neuonc/noab200

[3] Tamai S, Ichinose T, Tsutsui T, Tanaka S, Garaeva F, Sabit H, Nakada M (2022) Tumor Microenvironment in Glioma Invasion. Brain Sci 12:505.
https://doi.org/10.3390/brainsci12040505

[4] Pietrobono D, Giacomelli C, Marchetti L, Martini C, Trincavelli ML (2020) High adenosine extracellular levels induce glioblastoma aggressive traits modulating the mesenchymal stromal cell secretome. Int J Mol Sci 21:7706.
https://doi.org/10.3390/ijms21207706

[5] Campos-Contreras ADR, Díaz-Muñoz M, Vázquez-Cuevas FG (2020) Purinergic signaling in the hallmarks of cancer. Cells 9:1612. https://doi.org/10.3390/cells9071612

[6] Huang R, Li G, Wang Z, Hu H, Zeng F, Zhang K, Wang K, Wu F (2020) Identification of an ATP metabolism-related signature associated with prognosis and immune microenvironment in gliomas. Cancer Sci 111:2325-2335.
https://doi.org/10.1111/cas.14484

[7] Burnstock G (2020) Introduction to purinergic signalling in the brain. Glioma Signal 1-12. https://doi.org/10.1007/978-3-030-30651-9_1

[8] Ceruti S, Abbracchio MP (2013) Adenosine signaling in glioma cells. Glioma Signal 13-30. https://doi.org/10.1007/978-94-007-4719-7_2

[9] Braganhol E, Wink MR, Lenz G, Battastini AMO (2020) Purinergic signaling in glioma progression. Glioma Signal 87-108. https://doi.org/10.1007/978-3-030-30651-9_5

[10] Burnstock G, Di Virgilio F (2013) Purinergic signalling and cancer. Purinerg Signal 9:491-540. https://doi.org/10.1007/s11302-013-9372-5

[11] Savio LEB, Leite-Aguiar R, Alves VS, Coutinho-Silva R, Wyse AT (2021) Purinergic signaling in the modulation of redox biology. Redox Biol 47:102137. https://doi.org/10.1016/j.redox.2021.102137

[12] Huang L, Tang Y, Sperlagh B (2022) Glial Purinergic Signaling-Mediated Oxidative Stress (GPOS) in Neuropsychiatric Disorders. Oxid Med Cell Longev 2022. https://doi.org/10.1155/2022/1075440

[13] Ostrowski RP, Pucko EB (2022) Harnessing oxidative stress for anti-glioma therapy. Neurochem Int 105281. https://doi.org/10.1016/j.neuint.2022.105281

[14] Vengoji R, Macha MA, Batra SK, Shonka NA (2018) Natural products: A hope for glioblastoma patients. Oncotarget 9:22194. https://doi.org/10.18632/oncotarget.25175

[15] Tiwari P, Bae H (2022) Endophytic Fungi: Key Insights, Emerging Prospects, and Challenges in Natural Product Drug Discovery. Microorganisms 10:360. https://doi.org/10.3390/microorganisms10020360

[16] Pedra NS, Galdino KDCA, Da Silva DS, Ramos PT, Bona NP, Soares MSP, Azambuja JH, Canuto KM, De Brito ES, Ribeiro PRV, Souza ASQ, Cunico W, Stefanello FM, Spanevello RM, Braganhol E (2018) Endophytic fungus isolated from *Achyrocline satureioides* exhibits selective Antiglioma activity—the role of Sch-642305. Front Oncol 8:476. https://doi.org/10.3389/fonc.2018.00476

[17] Tapfuma KI, Uche-Okereafor N, Sebola TE, Hussan R, Mekuto L, Makatini MM, Green E, Mavumengwana V (2019) Cytotoxic activity of crude extracts from *Datura stramonium*'s fungal endophytes against A549 lung carcinoma and UMG87 glioblastoma cell lines and LC-QTOF-MS/MS based metabolite profiling. BMC Complement Alter Med 19:1-12. https://doi.org/10.1186/s12906-019-2752-9

[18] Yong K, Kaleem S, Wu B, Zhang Z (2021) New antiproliferative compounds against glioma cells from the marine-sourced fungus *Penicillium* sp. ZZ1750. Mar Drugs 19:483. https://doi.org/10.3390/md19090483

[19] Chekhonin IV, Chistiakov DA, Grinenko NF, Gurina OI (2018) Glioma Cell and Astrocyte Co-cultures As a Model to Study Tumor–Tissue Interactions: A Review of Methods. Cel Mol Neurobiol 38:1179-1195. https://doi.org/10.1007/s10571-018-0588-3

[20] Galvão WA, Braz Filho R, Canuto KM, Ribeiro PRV, Campos AR, Moreira ACOM, Silva SO, Mesquita Filho FA, Santos SAAR, Melo Junior JMA, Gonçalves NGG, Fonseca SGC, Bandeira MAM (2018) Gastroprotective and anti-inflammatory activities

integrated to chemical composition of *Myracrodruon urundeuva* Allemão-A conservationist proposal for the species. J Ethnopharmacol 222:177-189. https://doi.org/10.1016/j.jep.2018.04.024

[21] Da Frota MLC, Braganhol E, Canedo AD, Klamt F, Apel MA, Mothes B, Lerner C, Battastini AMO, Heneiques AT, Moreira JCF (2009) Brazilian marine sponge *Polymastia janeirensis* induces apoptotic cell death in human U138MG glioma cell line, but not in a normal cell culture. Invest New Drugs 27:13-20. https://doi.org/10.1007/s10637-008-9134-3

[22] Azambuja JH, Gelsleichter NE, Beckenkamp LR, Iser IC, Fernandes MC, Figueiró F, Battastini AMO, Scholl JN, De Oliveira FH, Spanevello, RM, Sévigny J, Wink MR, Stefani MA, Teixeira HF, Braganhol E (2019) CD73 downregulation decreases *in vitro* and *in vivo* glioblastoma growth. Mol Neurobiol 56:3260-3279. https://doi.org/10.1007/s12035-018-1240-4

[23] Mosmann T (1983) Rapid colorimetric assay for cellular growth and survival: application to proliferation and cytotoxicity assays. J Immunol Methods 65:55-63. https://doi.org/10.1016/0022-1759(83)90303-4

[24] Chan KM, Delfert D, Junger KD (1986) A direct colorimetric assay for Ca2+-stimulated ATPase activity. Anal Biochem 157:375-380. https://doi.org/10.1016/0003-2697(86)90640-8

[25] Bradford MM (1976) A rapid and sensitive method for the quantitation of microgram quantities of protein utilizing the principle of protein-dye binding. Anal Biochem 72:248-254. https://doi.org/10.1016/0003-2697(76)90527-3

[26] Franken NA, Rodermond HM, Stap J, Haveman J, Van Bree C (2006) Clonogenic assay of cells *in vitro*. Nat Protoc 1:2315-2319. https://doi.org/10.1038/nprot.2006.339

[27] Dos Santos LM, Da Silva TM, Azambuja JH, Ramos PT, Oliveira PS, Da Silveira EF, Pedra NS, Galdino KCA, Do Couto CAT, Soares MSP, Tavares RG, Spanevello RM, Stefanello FM, Braganhol E (2017) Methionine and methionine sulfoxide treatment induces M1/classical macrophage polarization and modulates oxidative stress and purinergic signaling parameters. Mol Cell Biochem 424:69-78. https://doi.org/10.1007/s11010-016-2843-6

[28] Aksenov MY, Markesbery WR (2001) Changes in thiol content and expression of glutathione redox system genes in the hippocampus and cerebellum in Alzheimer's disease. Neurosci Lett 302:141-145. https://doi.org/10.1016/S0304-3940(01)01636-6

[29] Misra HP, Fridovich I (1972) The role of superoxide anion in the autoxidation of epinephrine and a simple assay for superoxide dismutase. J Biol Chem 247:3170-3175. https://doi.org/10.1016/S0021-9258(19)45228-9

[30] Aebi H (1984) Catalase in vitro. Methods Enzymol 105:121-126. https://doi.org/10.1016/S0076-6879(84)05016-3

[31] Habig WH, Pabst MJ, Jakoby WB (1974) Glutathione S-transferases: the first enzymatic step in mercapturic acid formation. J Biol Chem 249:7130-7139. https://doi.org/10.1016/S0021-9258(19)42083-8

[32] Lowry O, Rosebrough N, Farr A, Randall R (1951) Protein measurement with the Folin phenol reagent. J Biol Chem 193:265-75.

[33] Livak KJ, Schmittgen TD (2001) Analysis of relative gene expression data using real-time quantitative PCR and the 2− ΔΔCT method. Methods 25:402-408. https://doi.org/10.1006/meth.2001.1262

[34] Qiao LN, Wang JY, Yang YS, Chen SP, Gao YH, Zhang JL, Liu JL (2013) Effect of electroacupuncture intervention on expression of CGRP, SP, COX-1, and PGE2 of dorsal portion of the cervical spinal cord in rats with neck-incision pain. Evid Based Complement Alter Med, 2013. https://doi.org/10.1155/2013/294091

[35] Font-Nieves M, Sans-Fons MG, Gorina R, Bonfill-Teixidor E, Salas-Pérdomo A, Márquez-Kisinousky L, Santalucia T, Planas AM (2012) Induction of COX-2 enzyme and down-regulation of COX-1 expression by lipopolysaccharide (LPS) control prostaglandin E2 production in astrocytes. J Biol Chem 287:6454-6468. https://doi.org/10.1074/jbc.M111.327874

[36] Jiang L, Tang Z (2018) Expression and regulation of the ERK1/2 and p38 MAPK signaling pathways in periodontal tissue remodeling of orthodontic tooth movement. Mol Med Rep 17:1499-1506. https://doi.org/10.3892/mmr.2017.8021

[37] Dupuis J, Sirois MG, Rhéaume E, Nguyen QT, Clavet-Lanthier MÉ, Brand G, Mihalache-Avram T, Théberge-Julien G, Charperntier D, Rhainds D, Neagoe PE, Tardif JC (2020) Colchicine reduces lung injury in experimental acute respiratory distress syndrome. PLoS One 15:e0242318. https://doi.org/10.1371/journal.pone.0242318

[38] Stanke KM, Kidambi S (2022) Direct-Contact Co-culture of Astrocytes and Glioblastoma Cells Patterned using Polyelectrolyte Multilayer Templates. J Vis Exp: Jove 184. https://doi.org/10.3791/63420

[39] Yang N, Yan T, Zhu H, Liang X, Leiss L, Sakariassen PØ, Skaftnesmo KO, Huang B, Costea DA, Enger PØ, Li X, Wang J (2014) A co-culture model with brain tumor-

specific bioluminescence demonstrates astrocyte-induced drug resistance in glioblastoma. J Trans Med 12:1-9. https://doi.org/10.1186/s12967-014-0278-y

[40] Chen W, Wang D, Du X, He Y, Chen S, Shao Q, Ma C, Huang B, Chen A, Zhao P, Qu X, Li X (2015) Glioma cells escaped from cytotoxicity of temozolomide and vincristine by communicating with human astrocytes. Med Oncol 32:1-13. https://doi.org/10.1007/s12032-015-0487-0

[41] Wink MR, Lenz G, Braganhol E, Tamajusuku AS, Schwartsmann G, Sarkis JJ, Battastini AM (2003) Altered extracellular ATP, ADP and AMP catabolism in glioma cell lines. Cancer Lett 198:211-218. https://doi.org/10.1016/S0304-3835(03)00308-2

[42] Braganhol E, Huppes D, Bernardi A, Wink MR, Lenz G, Battastini AMO (2009) A comparative study of ectonucleotidase and P2 receptor mRNA profiles in C6 cell line cultures and C6 ex vivo glioma model. Cell Tissue Res 335:331-340. https://doi.org/10.1007/s00441-008-0723-4

[43] Guan X, Hasan MN, Maniar S, Jia W, Sun D (2018) Reactive astrocytes in glioblastoma multiforme. Mol Neurobiol 55:6927-6938.
https://doi.org/10.1007/s12035-018-0880-8

[44] Huang L, Tang Y, Sperlagh B (2022) Glial Purinergic Signaling-Mediated Oxidative Stress (GPOS) in Neuropsychiatric Disorders. Oxid Med Cell Long, 2022. https://doi.org/10.1155/2022/1075440

[45] Giuliani P, Carluccio M, Ciccarelli R (2021) Role of Purinome, A Complex Signaling System, In Glioblastoma Aggressiveness. Front Pharmacol 12:632622. https://doi.org/10.3389/fphar.2021.632622

[46] Ohkubo S, Nagata K, Nakahata N (2007) Adenosine uptake-dependent C6 cell growth inhibition. Eur J Pharmacol 577:35-43.
https://doi.org/10.1016/j.ejphar.2007.08.025

[47] Alarcón S, Toro MDLÁ, Villarreal C, Melo R, Fernández R, Ayuso Sacido A, Uribe D, Martín RS, Quezada C (2020) Decreased equilibrative nucleoside transporter 1 (ENT1) activity contributes to the high extracellular adenosine levels in mesenchymal glioblastoma stem-like cells. Cells 9:1914. https://doi.org/10.3390/cells9081914

[48] Chen Y, Qin C, Huang J, Tang X, Liu C, Huang K, Xu J, Guo G, Tong A, Zhou L (2020) The role of astrocytes in oxidative stress of central nervous system: A mixed blessing. Cell Prolif 53:e12781. https://doi.org/10.1111/cpr.12781

[49] Lee KH, Cha M, Lee BH (2021) Crosstalk between Neuron and Glial Cells in Oxidative Injury and Neuroprotection. Int J Mol Sci 22:13315.

https://doi.org/10.3390/ijms222413315

[50] Bhatia TN, Pant DB, Eckhoff EA, Gongaware RN, Do T, Hutchison DF, Gleixner AM, Leak RL (2019) Astrocytes do not forfeit their neuroprotective roles after surviving intense oxidative stress. Front Mol Neurosci 12:87.
https://doi.org/10.3389/fnmol.2019.00087

[51] Pedra NS, Bona NP, De Aguiar MSS, Spohr L, Alves FL, Dos Santos FS, Saraiva JT, Stefanello FM, Braganhol E, Spanevello RM (2022) Impact of gallic acid on tumor supression: Modulation of redox homeostasis and purinergic response in in vitro and a preclinical model. J Nutr Biochem 110:109156.
https://doi.org/10.1016/j.jnutbio.2022.109156

[52] McBean GJ (2017) Cysteine, glutathione, and thiol redox balance in astrocytes. Antioxidants 6:62. https://doi.org/10.3390/antiox6030062

[53] Narayanankutty A, Job JT, Narayanankutty V (2019) Glutathione, an antioxidant tripeptide: Dual roles in Carcinogenesis and Chemoprevention. Curr Protein Pept Sci 20:907-917. https://doi.org/10.2174/1389203720666190206130003

[54] Aoyama K (2021) Glutathione in the Brain. Int J Mol Sci 22:5010. https://doi.org/10.3390/ijms22095010

[55] Ighodaro OM, Akinloye OA (2018) First line defence antioxidants-superoxide dismutase (SOD), catalase (CAT) and glutathione peroxidase (GPX): Their fundamental role in the entire antioxidant defence grid. Alexandria J Med 54:287-293. https://doi.org/10.1016/j.ajme.2017.09.001

[56] Navarro R, Busnadiego I, Ruiz-Larea MB, Ruiz-Sanz JI (2006) Superoxide anions are involved in doxorubicin-induced ERK activation in hepatocyte cultures. Ann N Y Acad Sci 1090:419-428. https://doi.org/10.1196/annals.1378.045

[57] Gomez–Sarosi LA, Strasberg–Rieber M, Rieber M (2009) ERK activation increases nitroprusside induced apoptosis in human melanoma cells irrespective of p53 status: role of superoxide dismutases. Cancer Biol Ther 8:1173-1182.
https://doi.org/10.4161/cbt.8.12.8561

[58] Zhao W, Rao Z, Liu C (2018) Role of ERK signaling pathway in dexmedetomidine against mouse neuroblastoma N2a cell injury induced by oxidative stress. J Clin Anesth 493-496.

[59] Farina F, Milani C, Botto L, Lonati E, Bulbarelli A, Palestini P (2016) Involvement of MEK-ERK1-2 pathway in the anti-oxidant response in C6 glioma cells after diesel exhaust particles exposure. Toxicol Lett 250:57-65.

https://doi.org/10.1016/j.toxlet.2016.04.008

[60] Botto L, Bulbarelli A, Lonati E, Cazzaniga E, Tassotti M, Mena P, Palestini P (2021) Study of the Antioxidant Effects of Coffee Phenolic Metabolites on C6 Glioma Cells Exposed to Diesel Exhaust Particles. Antioxidants 10:1169. https://doi.org/10.3390/antiox10081169

[61] Zhao Y, Xia S, Cao C, Du X (2019) Effect of TGF-β1 on apoptosis of colon cancer cells via the ERK signaling pathway. J Buon 24:449-455.

[62] Onguru O, Gamsizkan M, Ulutin C, Gunhan O (2008) Cyclooxygenase-2 (Cox-2) expression and angiogenesis in glioblastoma. Neuropathol 28:29-34. https://doi.org/10.1111/j.1440-1789.2007.00828.x

[63] Lombardi F, Augello FR, Artone S, Gugu MK, Cifone MG, Cinque B, Palumbo P (2022) Up-regulation of cyclooxygenase-2 (COX-2) expression by temozolomide (TMZ) in human glioblastoma (GBM) cell lines. Int J Mol Sci 23:1545. https://doi.org/10.3390/ijms23031545

[64] Bryan L, Paugh BS, Kapitonov D, Wilczynska KM, Alvarez SM, Singh SK, Milstien S, Spiegel S, Kordula T (2008) Sphingosine-1-phosphate and interleukin-1 independently regulate plasminogen activator inhibitor-1 and urokinase-type plasminogen activator receptor expression in glioblastoma cells: implications for invasiveness. Mol Cancer Res 6:1469-1477. https://doi.org/10.1158/1541-7786.MCR-08-0082

[65] Meini A, Sticozzi C, Massai L, Palmi M (2008) A nitric oxide/Ca2+/calmodulin/ERK1/2 mitogen-activated protein kinase pathway is involved in the mitogenic effect of IL-1β in human astrocytoma cells. Br J Pharmacol 153:1706-1717. https://doi.org/10.1038/bjp.2008.40

[66] Petrasek J, Bala S, Csak T, Lippai D, Kodys K, Menashy V, Barrieau M, Min SY, Kurt-Jones EA, Szabo G (2012) IL-1 receptor antagonist ameliorates inflammasome-dependent alcoholic steatohepatitis in mice. J Clin Invest 122:3476-3489. https://doi.org/10.1172/JCI60777

[67] Taniura S, Kamitani H, Watanabe T, Eling TE (2008) Induction of cyclooxygenase-2 expression by interleukin-1β in human glioma cell line, U87MG. Neurol Med Chir 48:500-505. https://doi.org/10.2176/nmc.48.500

[68] Fathima Hurmath K, Ramaswamy P, Nandakumar DN (2014) IL-1β microenvironment promotes proliferation, migration, and invasion of human glioma cells. Cell Biol Int 38:1415-1422. https://doi.org/10.1002/cbin.10353

[69] Li R, Li G, Deng L, Liu Q, Dai J, Shen J, Zhang J (2010) IL-6 augments the invasiveness of U87MG human glioblastoma multiforme cells via up-regulation of MMP-2 and fascin-1. Oncol Rep 23:1553-1559. https://doi.org/10.3892/or_00000795

[70] Chen W, Xia T, Wang D, Huang B, Zhao P, Wang J, Qu X, Li X (2016) Human astrocytes secrete IL-6 to promote glioma migration and invasion through upregulation of cytomembrane MMP14. Oncotarget 7:62425.
https://doi.org/10.18632/oncotarget.11515

[71] Takanezawa Y, Nakamura R, Kojima Y, Sone Y, Uraguchi S, Kiyono M (2018) Cytochalasin E increased the sensitivity of human lung cancer a549 cells to bortezomib via inhibition of autophagy. Biochem Biophys Res Commun 498:603-608. https://doi.org/10.1016/j.bbrc.2018.03.029

[72] Kim MY, Kim JH, Cho JY (2014) Cytochalasin B modulates macrophage-mediated inflammatory responses. Biomol Ther 22:295.
https://doi.org/10.4062/biomolther.2014.055

[73] Liu Y, Ruan Q, Jiang S, Qu Y, Chen J, Zhao M, Cui H (2019) Cytochalasins and polyketides from the fungus *Diaporthe* sp. GZU-1021 and their anti-inflammatory activity. Fitoterapia 137:104187. https://doi.org/10.1016/j.fitote.2019.104187

## Statements and Declarations

### Funding

This research was supported by the Conselho Nacional de Desenvolvimento Científico e Tecnológico (CNPq) and the Fundação de Amparo à Pesquisa do Estado do Rio Grande do Sul (FAPERGS). This study was partially funded by the Coordenação de Aperfeiçoamento de Pessoal de Nível Superior, Brasil (CAPES), Finance code 001.

### Competing Interests

The authors have no relevant financial or non-financial interests to disclose

### Author Contributions

All authors contributed to the study conception and design. All authors performed material preparation, data collection, and analysis. The first draft of the manuscript was written by Nathalia Stark Pedra and all authors commented on previous versions of the manuscript. All authors read and approved the final manuscript.

### Data Availability

The datasets generated during and/or analyzed during the current study are available from the corresponding author on reasonable request.

### Ethics approval

All procedures used in this study followed the principles of Laboratory Animal Care of the National Institutes of Health and were approved by the Ethical Committee of UFPel (CEEA 31292).

**Table 1.** Primers used for quantitative real-time polymerase chain reaction. Listed are the forward and reverse primer sequences used to amplify each target gene as well as the *actb* endogenous control.

| Primer Name | Sequence | Reference |
|---|---|---|
| Cox1 Forward | 5' TCCTACATGGGATGACGAGC 3' | [34] |
| Cox1 Reverse | 5' GGTTGCGATACTGGAACTGG 3' | |
| Cox2 Forward | 5' GATTGACAGCCCACCAACTT 3' | [35] |
| Cox2 Reverse | 5'CGGGATGAACTCTCTCCTCA 3' | |
| Erk1/2 Forward | 5' TCAAGCCTTCCAACCTC 3' | [36] |
| Erk1/2 Reverse | 5' GCAGCCCACAGACCAAA 3' | |
| IL-1β Forward | 5' GACAGAACATAAGCCAACA 3' | [37] |
| IL-1β Reverse | 5' ACACAGGACAGGTATAGATT 3' | |
| Casp-1 Forward | 5' CGAGACCTGTGCGATCAT 3' | [37] |
| Casp-1 Reverse | 5'GCTGATGGACCTGACTGAA 3' | |
| Actb Forward | 5' CCCTAAGGCCAACCGTGAA 3' | [37] |
| Actb Reverse | 5' GAGGCATACAGGGACAACACAG 3' | |

Abbreviations: COX, cyclooxygenase; ERK, extracellular signal-regulated kinase; IL-1β, interleukin 1β; Casp-1, caspase-1.

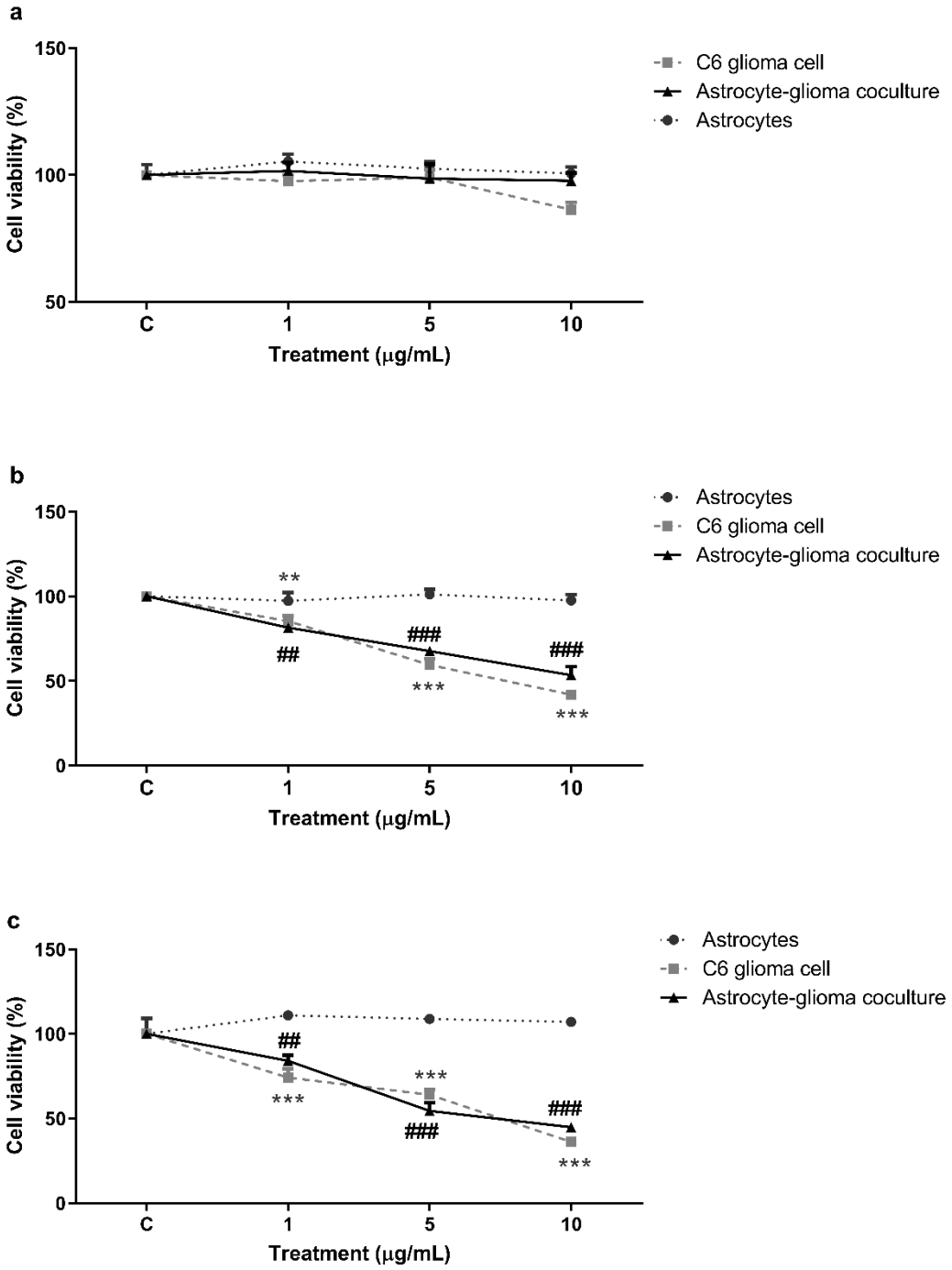


**Fig 1** Evaluation of the cytotoxic effect of $F_{DCM}$ obtained from endophytic fungus *Biscogniauxia* sp. primary rat astrocytes; C6 glioma cells; culture and coculture astrocyte-glioma. The cell viability of the cultures was evaluated after treatment with $F_{DCM}$ for 24 h (**A**), 48 h (**B**), and 72 h (**C**). Results were expressed as percentage of control. One-way ANOVA and post-hoc Tukey's were performed. $^{**,***}$Significantly different from C6 glioma cell control ($P<0.001$, and $P<0.0001$, respectively). $^{\#\#,\#\#\#}$Significantly different from astrocyte-glioma coculture control ($P<0.001$, and $P<0.0001$, respectively)

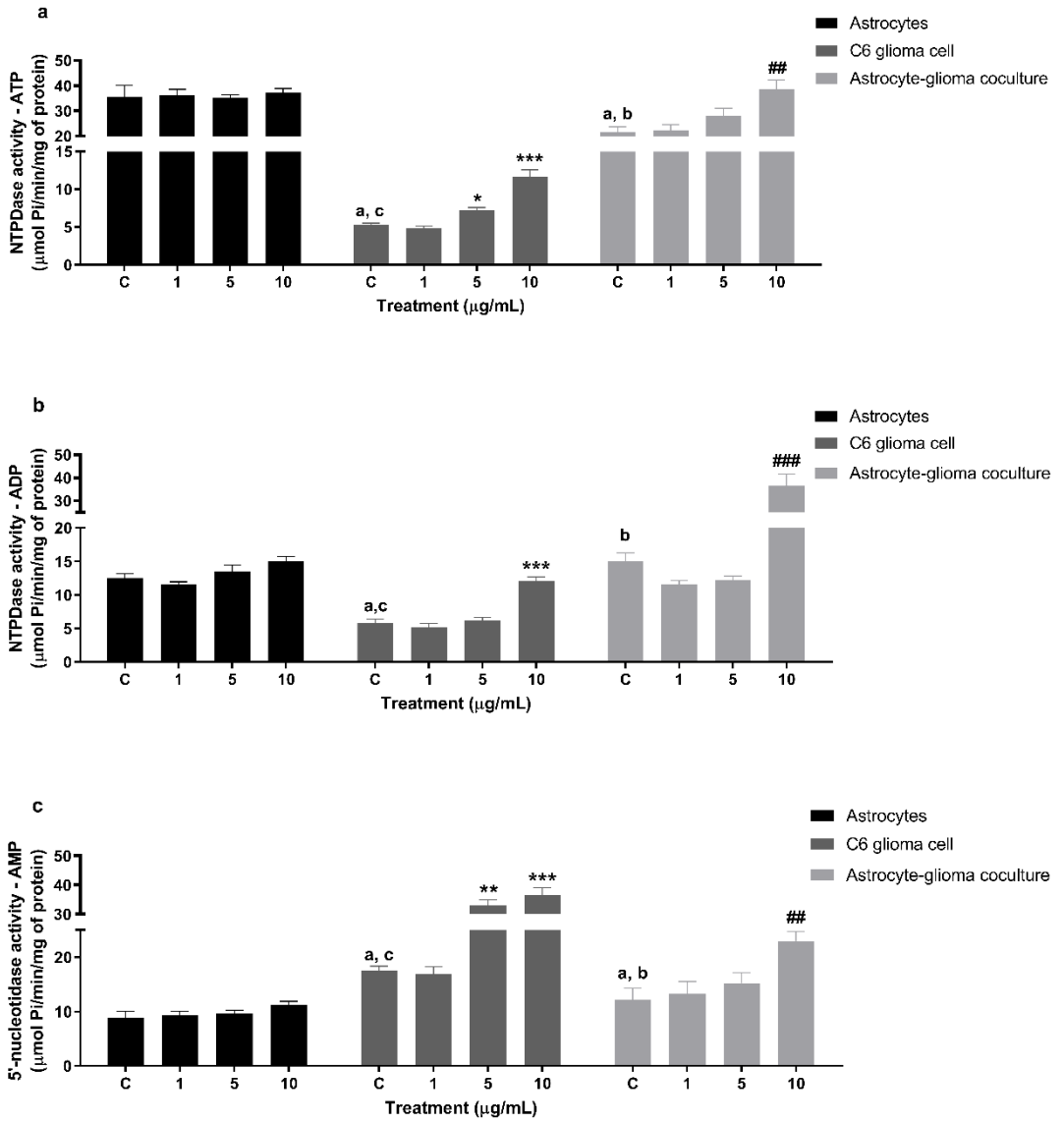


**Fig 2** Nucleotide hydrolysis in primary rat astrocyte culture, C6 glioma cells, and astrocyte-glioma coculture exposed for 72 h to $F_{DCM}$ obtained from *Biscogniauxia* sp. (**A**) ATP, (**B**) ADP and (**C**) AMP. Results were expressed as µmol Pi/mg of protein. Two-way ANOVA and post-hoc Tukey were performed. $^{*,**,***}$Significantly different from C6 glioma cell control ($P<0.05$, $P<0.001$, and $P<0.0001$, respectively). $^{\#,\#\#}$Significantly different from astrocyte-glioma coculture control ($P<0.05$, and $P<0.001$, respectively). $^{a,\ b,\ c}$Significantly different from astrocyte, C6 glioma cells, and coculture astrocyte-glioma, respectively ($P<0.001$)

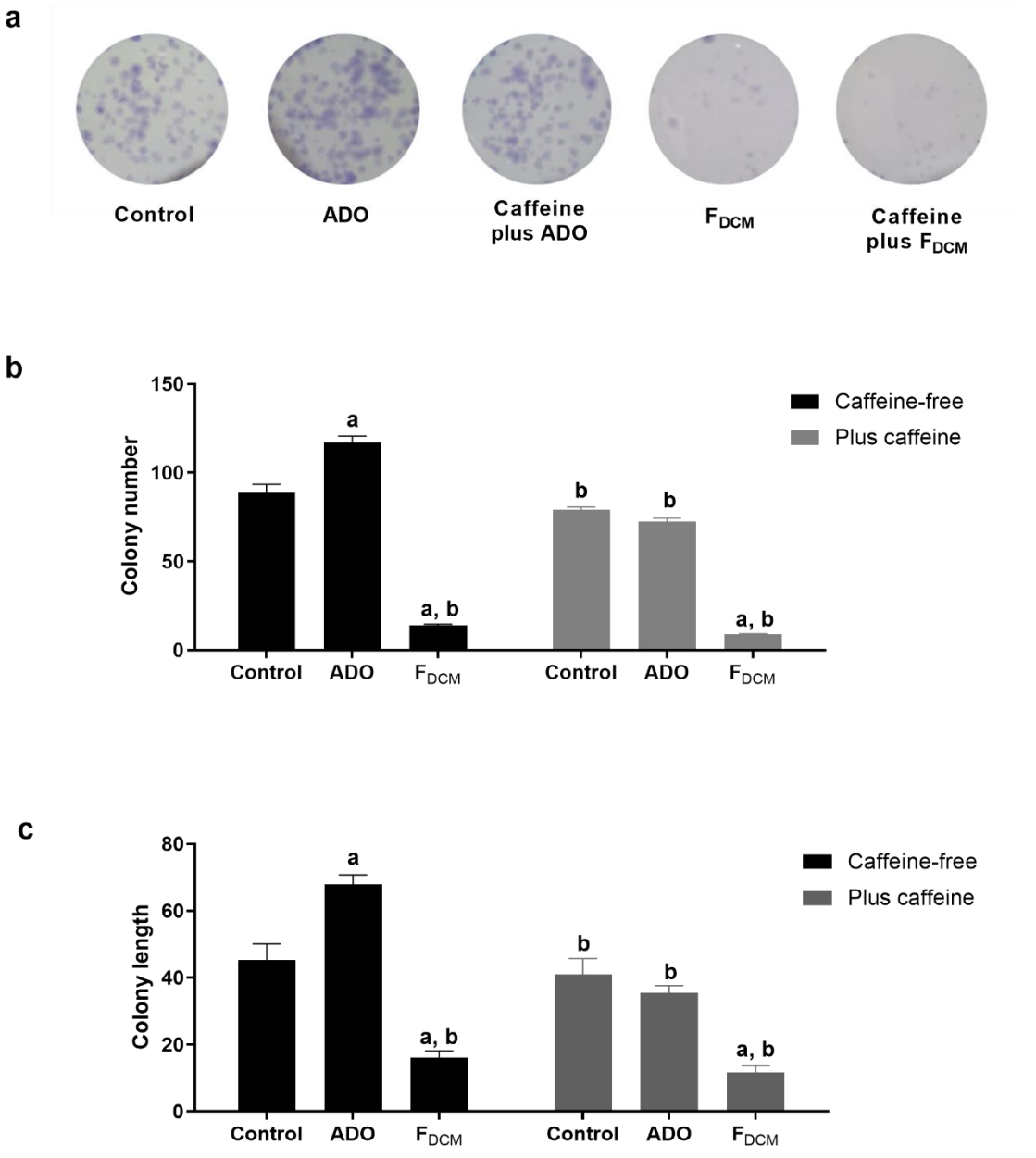


**Fig 3.** Analysis of the effect of $F_{DCM}$ on *in vitro* survival of C6 glioma cells after ADO receptor blockade. (**A**) Cultures were treated with 10 µM caffeine 30 min before exposure to ADO (1 µM) or $F_{DCM}$ (10 µg/mL). (**B**) Colony formation after 24 h of treatment. (**C**) Colony length after 24 hours of treatment. Two-way ANOVA and post-hoc Tukey were performed. [a] Significantly different from control ($P<0.001$). [b]Significantly different from ADO ($P<0.001$)

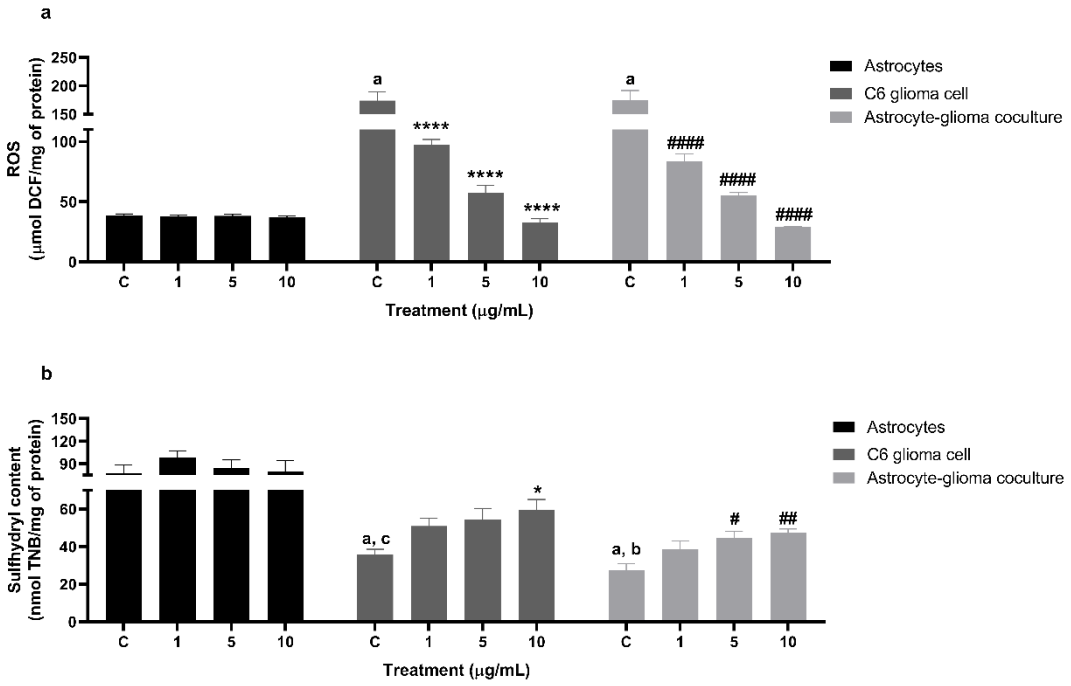


**Fig 4** Determination of ROS (**a)** and sulfhydryl content (**b**) levels in C6 glioma cells, primary rat astrocyte culture, and astrocyte-glioma coculture exposed for 72 h to $F_{DCM}$ obtained from *Biscogniauxia* sp. ROS levels are expressed as µmol DCF/mg of protein, and thiol content as nmol TNB/mg of protein. Two-way ANOVA and post-hoc Tukey were performed. $^{*,***}$Significantly different from C6 glioma cell control ($P<0.05$, and $P<0.0001$, respectively). $^{\#,\#\#,\#\#\#\#}$Significantly different from astrocyte-glioma co-culture control ($P<0.05$, $P<0.001$, and $P<0.0001$ respectively). $^{a,b,c}$Significantly different from astrocyte, coculture astrocyte-glioma and C6 glioma cells, respectively ($P<0.001$).

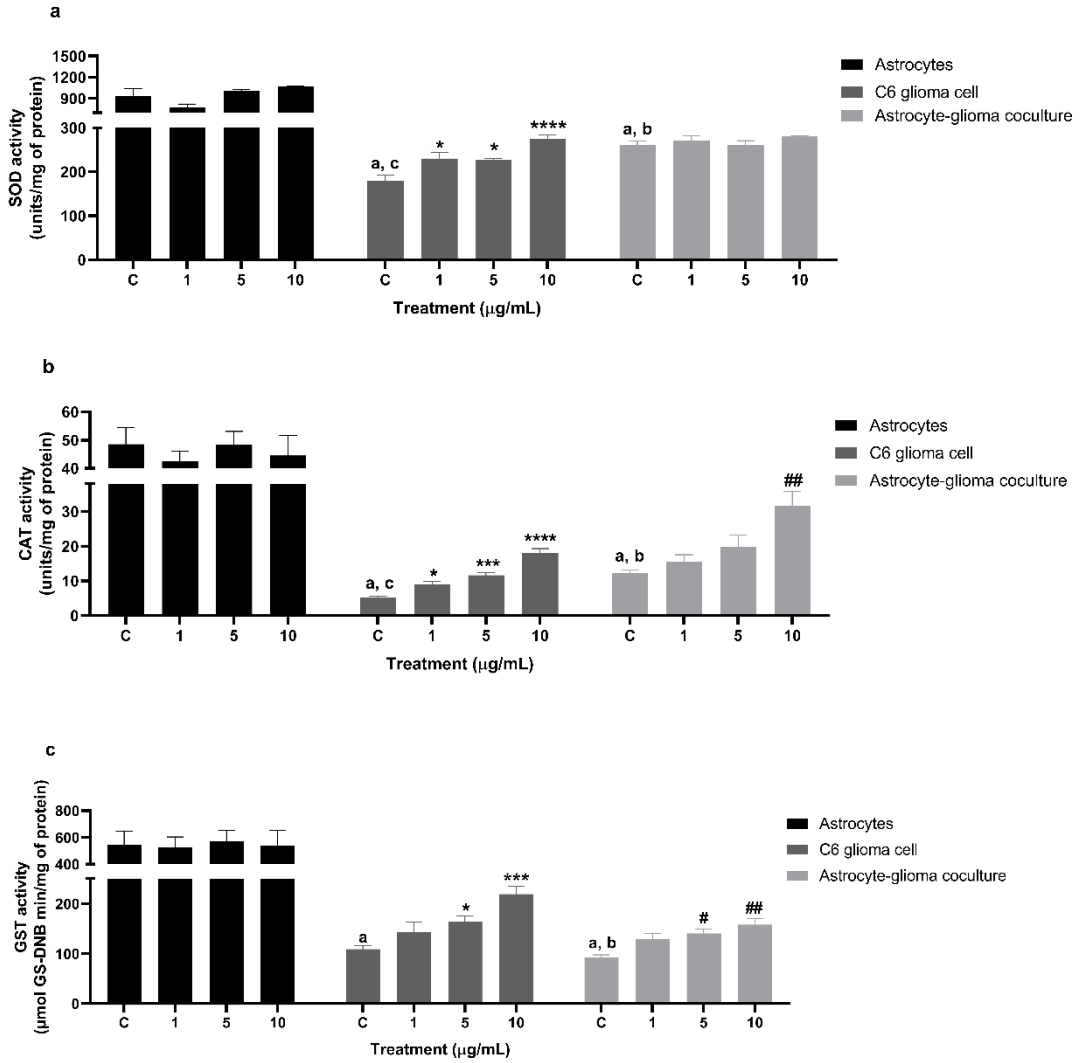


**Fig 5** Analysis of the activity of the antioxidant enzymes SOD (**a)**, CAT (**b**), and GST (**c**) in C6 glioma cells, primary rat astrocyte culture, and astrocyte-glioma coculture exposed for 72 h to $F_{DCM}$ obtained from *Biscogniauxia* sp. SOD and CAT activities are expressed as units/mg of protein, and GST activity as µmol GS-DNB min/mg of protein. Two-way ANOVA and post-hoc Tukey were performed. $^{*,***,***}$Significantly different from C6 glioma cell control ($P<0.05$, $P<0.001$, and $P<0.0001$, respectively). $^{\#,\#\#}$Significantly different from astrocyte-glioma coculture control ($P<0.05$, and $P<0.001$, respectively). $^{a,\ b,\ c}$Significantly different from astrocyte, coculture astrocyte-glioma, and C6 glioma cells, respectively ($P<0.001$)

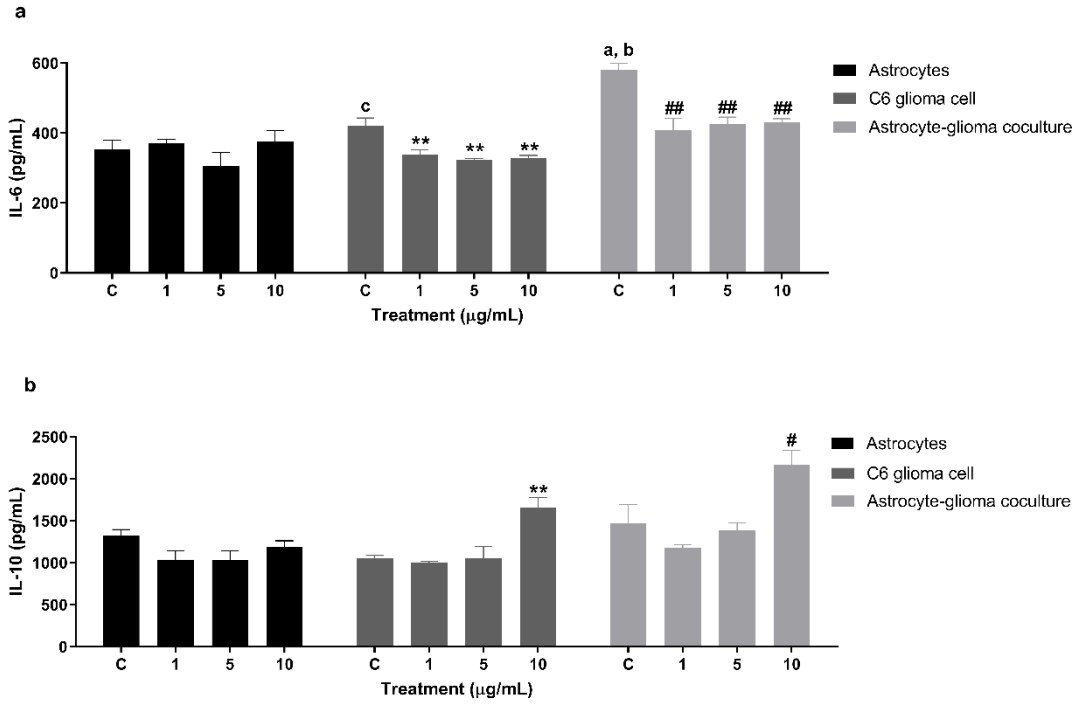


**Fig 6** Determination of IL-6 (**a)**, and IL-10 (**b**) levels in C6 glioma cells, primary rat astrocyte culture, and astrocyte-glioma coculture exposed for 72 h to $F_{DCM}$ obtained from *Biscogniauxia* sp. Interleukin levels are expressed as pg/mL. Two-way ANOVA and post-hoc Tukey were performed. $^{**}$Significantly different from C6 glioma cell control ($P<0.001$). $^{\#,\#\#}$Significantly different from astrocyte-glioma coculture control ($P<0.05$, and $P<0.001$, respectively). $^{a,b,c}$Significantly different from astrocyte, coculture astrocyte-glioma and C6 glioma cells, respectively ($P<0.001$)

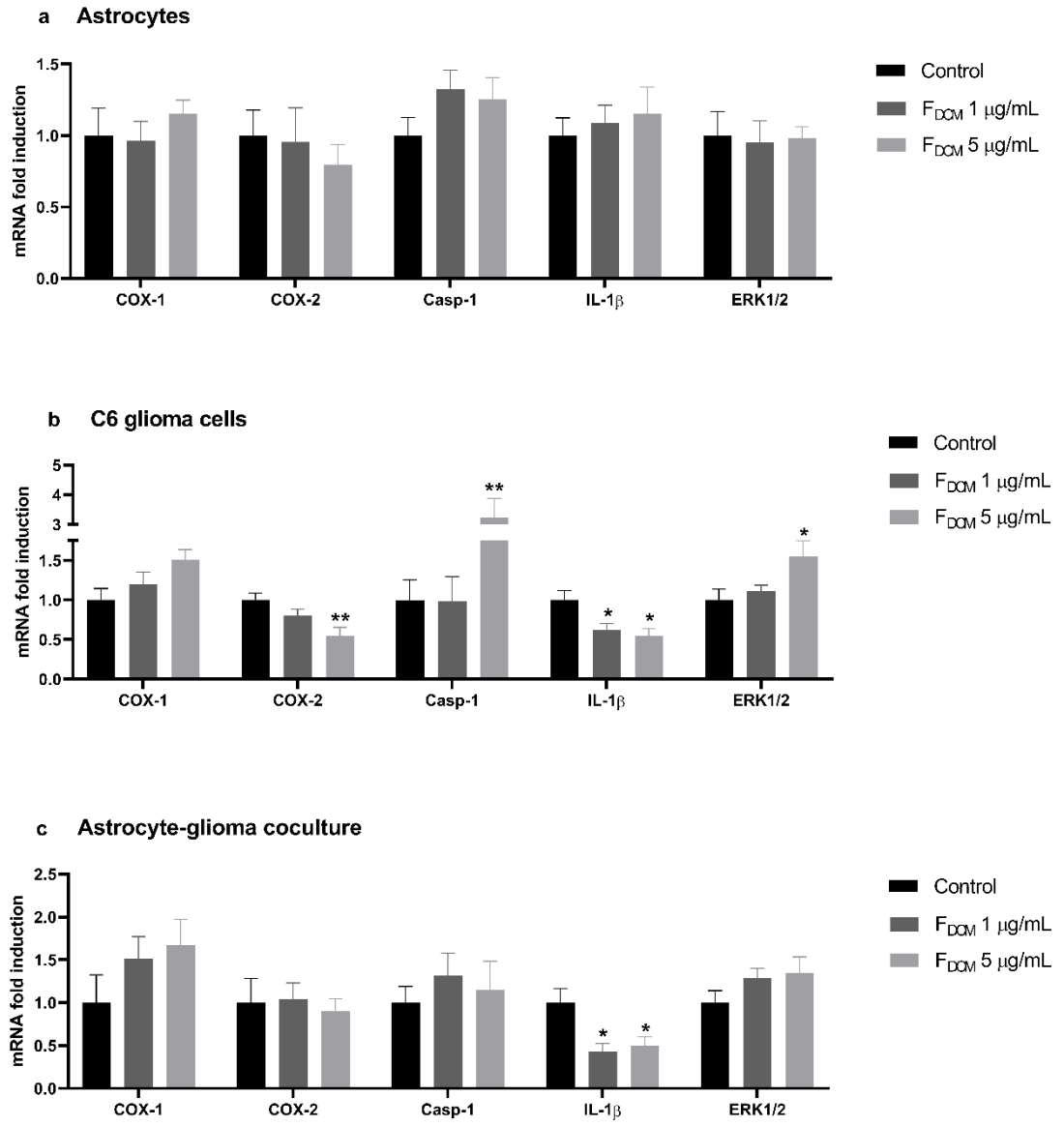


**Fig 7** Effect of $F_{DCM}$ on the expression of protumor inflammatory mediators on primary astrocyte culture (**a**), on C6 glioma cells (**b**) and on astrocyte-glioma co-culture (**c**). The mRNA relative expression levels as detected by RT-PCR. Two-way ANOVA and post-hoc Tukey were performed. $^{*,**}$Significantly different from cell control ($P<0.05$, and $P<0.001$, respectively)

## 4.3 Capítulo 3

Impact of gallic acid on tumor suppression: Modulation of redox homeostasis and purinergic response in *in vitro* and a preclinical glioblastoma model

Nathalia Stark Pedra[a*], Natália Pontes Bona[b], Mayara Sandrielly Soares de Aguiar[a], Luíza Spohr[a], Fernando Lopez Alves[a], Francieli da Silva dos Santos[b], Juliane Torchelsen Saraiva[b], Francieli Moro Stefanello[b], Elizandra Braganhol[c], Roselia Maria Spanevello[a*]

**Status:** Aceito para publicação no periódico *The Journal of Nutritional Biochemistry*

# Impact of gallic acid on tumor suppression: Modulation of redox homeostasis and purinergic response in *in vitro* and a preclinical glioblastoma model

Nathalia Stark Pedra[a*], Natália Pontes Bona[b], Mayara Sandrielly Soares de Aguiar[a], Luíza Spohr[a], Fernando Lopez Alves[a], Francieli da Silva dos Santos[b], Juliane Torchelsen Saraiva[b], Francieli Moro Stefanello[b], Elizandra Braganhol[c], Roselia Maria Spanevello[a*]

[a] Centro de Ciências Químicas, Farmacêuticas e de Alimentos, Programa de Pós-Graduação em Bioquímica e Bioprospecção - Laboratório de Neuroquímica, Inflamação e Câncer, Universidade Federal de Pelotas, Pelotas, RS, Brazil

[b] Centro de Ciências Químicas, Farmacêuticas e de Alimentos, Programa de Pós-Graduação em Bioquímica e Bioprospecção - Laboratório de Biomarcadores, Universidade Federal de Pelotas, Pelotas, RS, Brazil

[c] Departamento de Ciências Básicas da Saúde, Programa de Pós-Graduação em Biociências – Universidade Federal de Ciências da Saúde de Porto Alegre (UFCSPA), Porto Alegre, RS, Brazil.

* Corresponding authors
Roselia Maria Spanevello and Nathalia Stark Pedra
Centro de Ciências Químicas, Farmacêuticas e de Alimentos/Bioquímica, Prédio 29, Universidade Federal de Pelotas, Campus Capão do Leão, s/n, CEP 9601090, Caixa Postal 354, Pelotas, RS, Brazil
Phone: +55 53 32757355
Email: roselia.spanevello@ufpel.edu.br or nathaliastark@hotmail.com

**Abstract**

Glioblastoma (GBM) is the deadliest primary brain tumor in adults due to the high rate of relapse with current treatment. Therefore, the search for therapeutic alternatives is urgent. Gallic acid (GA), a potent natural antioxidant, has antitumor and modulatory actions on purinergic signaling. In this study, we investigated the cytotoxic effects of GA on the rat GBM (C6) cell line and on astrocyte culture and analyzed its role in regulating oxidative stress and purinergic enzymes involved in GBM proliferation. Cells were exposed to GA from 50 to 400 µM for 24 and/or 48 h. Next, the effect of GA was evaluated in the preclinical model of GBM. *Wistar* rats were treated with 50 or 100 mg/kg of GA for 15 days, and cerebral and systemic redox status and degradation of adenine nucleotides and nucleosides in circulating platelets, lymphocytes, and serum were evaluated. Our results demonstrated that GA has selective anti-glioma activity *in vitro*, without inducing cytotoxicity in astrocyte. Furthermore, GA prevented oxidative stress and changes in the hydrolysis of nucleotides in GBM cells. The anti-glioma effect was also observed *in vivo*, as GA reduced tumor volume by 90%. Interestingly, GA decreased the oxidative damage induced by a tumor in the brain, serum, and platelets, and, also prevented changes in degradation of nucleotides and nucleosides in lymphocytes, platelets, and serum. These results indicate, for the first time, the therapeutic potential of GA in a preclinical model of GBM, whose effects may be related to its role in redox and purinergic modulation.

**Key words:** gallic acid, oxidative stress, purinergic signaling, glioblastoma, brain

## 1. Introduction

Gliomas are the most common brain tumors of the central nervous system (CNS) and can be classified into four groups depending on the degree of malignancy [1]. According to the criteria established by the World Health Organization, grade IV glioma, also called glioblastoma (GBM), is the most aggressive form of primary CNS tumor, as it has complex malignancy mechanisms, including proliferation, invasion, angiogenesis, and necrosis [1, 2]. However, resistance to conventional therapies has become the major obstacle to successfully treating patients with high-grade gliomas [3]. Although advanced multimodal therapeutic strategies include surgical resection and radiotherapy/chemotherapy, patients with GBM have a poor prognosis that shows an average survival of 16 months [4].

The mechanisms involved in the transformation of healthy glial cells into malignant cells constitute a multifactorial process, in which interactions between GBM cells and the tissue microenvironment are essential to provide physiological support for the development of the tumor [5]. In general, the CNS has high metabolic activity and is particularly sensitive to oxidative damage caused by free radicals, especially reactive oxygen species (ROS). It is well known that brain tumorigenesis is related to oxidative stress, which promotes an imbalance between the production of free radicals and antioxidant defense mechanisms, leading to damage to proteins, lipids, and DNA [6]. The increase in oxidative damage in gliomas contributes to the biochemical and molecular changes necessary for tumor development and progression [7].

Furthermore, among the pathological changes that promote the invasion of tumor cells in the surrounding brain tissue, purinergic signaling has emerged as an important cell-cell communication system, which involves mechanisms of extracellular release and metabolism of adenine nucleotides and nucleosides, such as adenosine triphosphate (ATP), adenosine diphosphate (ADP), adenosine monophosphate (AMP), and adenosine [8, 9]. One of the main consequences of necrosis is a large release of ATP, which results in the accumulation of its metabolite adenosine in the tumor microenvironment. These extracellular components participate in various cellular responses, including differentiation, proliferation, migration, and cell death [10]. Furthermore, in addition to oxidative damage, growing evidence suggests the participation of purinergic signaling in the secretion of inflammatory mediators both at the systemic level and in the tumor microenvironment [9, 11].

Given the complexity of the mechanisms involved in tumor progression and adversity in the standard treatment of GBM, the use of natural compounds has emerged as a promising alternative antineoplastic [12]. Gallic acid (GA) or 3,4,5-trihydroxybenzoic acid is a polyphenol found in several natural products, such as grapes and other fruits, gallnuts, tea leaves, and wine [13]. GA is a potent natural antioxidant and has been extensively studied as an anti-inflammatory and anticancer agent [14, 15]. Several studies have reported the cytotoxic activity of GA in human glioma lines; however, its role in regulating the redox state in the tumor microenvironment and peripheral blood is unclear [15, 16, 17]. Furthermore, despite the potential of GA to prevent disorders of purinergic signaling in pathologies that promote changes in the CNS, there is no evidence of the effect of GA on extracellular purine metabolism in GBM [18, 19]. In this context, this study aimed to investigate the effect of GA on the modulation of the redox state and purinergic signaling in *in vitro* and a preclinical model of GBM.

## 2. Materials and Methods

### 2.1 Chemicals

GA, 4-(2-Hydroxyethyl) piperazine-1-ethanesulfonic acid (HEPES), sodium bicarbonate ($NaHCO_3$), dimethylsulphoxide (DMSO), 3(4,5-dimethylthiazole-2-yl)-2,5 diphenyl tetrazolium bromide (MTT), and Sulforhodamine B (SRB) were purchased from Sigma Chemical Co. (St. Louis, MO, USA). Dulbecco's modified Eagle's medium (DMEM), fungizone, penicillin/streptomycin, 0.5% trypsin/ethylene diamine tetraacetic acid (EDTA) solution, and fetal bovine serum (FBS) were obtained from Gibco (Gibco BRL, Carlsbad, CA, USA). Trichloroacetic acid (TCA) and hydrogen peroxide were purchased from Synth® (Brazil). All other chemicals and solvents used were analytical grade.

### 2.2 Animals

*Wistar* rats were obtained from the Central Animal House of Federal University of Pelotas (UFPel, Pelotas, RS, Brazil) and kept at a controlled temperature (22 ± 2 °C) with a 12/12 h light/dark cycle. Six newborn *Wistar* rats (1–2 days old), male or female, were used to prepare primary culture astrocytes. Forty male *Wistar* rats (60 days old; 320–370 g) were used in the preclinical model of glioma. All animal procedures were

approved by the Ethics Committee of Animal Experimentation of the institution (protocol under number 31292). The use of the animals followed the Brazilian Guidelines for the Care and Use of Animals in Scientific Research Activities and with the National Council of Control of Animal Experimentation.

### 2.3 Cytotoxic effect of GA on GBM - *in vitro* assays

#### *2.3.1 GBM cultures*

The rat C6 GBM cell line was purchased from the American Type Culture Collection (ATCC; Rockville, Maryland, USA). Cells were cultured in DMEM containing fungizone (0.1%) and penicillin/streptomycin (100 U/L) and supplemented with 10% (v/v) FBS. The cells were kept in a humidified incubator with 5% $CO_2$.

#### *2.3.2 Rat primary astrocytes cultures*

Astrocyte culture was prepared as previously described by [20]. Briefly, the cortex of newborn *Wistar* rats was removed and mechanically dissociated with calcium and magnesium-free balanced salt buffer (CMF), pH 7.4. The cell suspension was centrifuged at 1000 g for 10 min, and the pellet was resuspended in DMEM supplemented with 10% FBS (pH 7.6). Subsequently, 3 x $10^5$ cells were seeded in 96-well plates pretreated with poli-L-lysine, respectively. Following 4 h of seeding, the DMEM culture medium was changed. Cultures were maintained at 37 °C in a humidified atmosphere with 5% $CO_2$ for 20–25 days and the medium was replaced every 4 days.

#### *2.3.3 GA treatment in GBM cell line and astrocyte culture*

GA was first dissolved in sterile water at a concentration of 10 mM (stock solution), and further diluted in DMEM supplemented with 10% FBS to obtain 50, 100, 200, 300, and 400 µM. In the cytotoxicity assays, the C6 GBM cell line was seeded in 96-well plates at 5 x $10^3$ cells/well and treated with GA concentrations for 24 and 48 h. For oxidative stress and purinergic analysis, C6 cells were seeded in 6-well and 24-well plates at 3 x $10^5$ and 2 x $10^4$ cells/well, respectively, and exposed to GA for 48 h. Primary cultures of astrocytes were prepared as described above. Cell cultures were treated with GA (50–400 µM) for 48 h. Cells maintained only in DMEM supplemented with 10% FBS served as control.

### *2.3.4 Cell viability assay*

Cell viability was determined with the MTT assay as described by Mosmann [21]. This method assesses the ability of viable cell mitochondria to reduce MTT to blue formazan crystals. Briefly, cells were washed with CMF; 0.5 mg/mL of MTT solution was added and incubated for 90 min at 37 °C in a humidified 5% $CO_2$ atmosphere. MTT was removed, the precipitate was dissolved with DMSO, and the optical density (OD) was measured at 492 nm with a microplate reader (SpectraMax 190, Molecular Devices, San Jose, CA, USA). This value was calculated using Prism 5.0 software (Prism GraphPad Software, San Diego, USA) according to the following formula: cell viability rate (%) = (OD492 of exposed cells to GA/OD492 of control) × 100%.

### *2.3.5 Cell proliferation assay*

Cell proliferation was measured using the SRB assay described by [22], which assesses the ability of the dye to bind to cellular proteins. First, cells were washed and fixed in 50% TCA for 45 min at 4 °C. After this period, five washes were performed with distilled water, 0.4% SRB was added and incubated in the dark at room temperature for 30 min. Finally, cells were washed five times with 1% acetic acid for complete removal of noncomplexed dye with proteins and SRB was eluded with 10 mM Tris. OD was measured at 530 nm using a microplate reader (SpectraMax190), and this value was calculated using Prism 5.0 software (Prism GraphPad Software, San Diego, USA) according to the following formula: cell viability rate (%) = (OD530 of exposed cells to GA/OD530 of control) × 100%.

### *2.3.6 Nucleoside triphosphate diphosphohydrolase (NTPDase) and 5'nucleotidase activity in C6 GBM cells*

NTPDase activity was evaluated using ATP and ADP substrates, and 5'nucleotidase activity using AMP as substrate in C6 GBM cells washed three times with phosphate-free incubation medium in the absence of nucleotides. The enzymatic reaction was started by adding an incubation medium containing 2 mM $MgCl_2$ (2 mM $CaCl_2$ for ATPase and ADPase assays), 120 mM NaCl, 5 mM KCl, 10 mM glucose, 20 mM HEPES (pH 7.4), and 2 mM ATP, ADP, or AMP as substrates. Incubation proceeded for 10 min at 37 °C, and then the reaction was stopped by transferring an aliquot of the incubation medium to a prechilled tube containing TCA (final concentration 5% w/v). The release

of inorganic phosphate (Pi) was evaluated using the malachite green method using $KH_2PO_4$ and a Pi standard [23]. Controls to determine non-enzymatic Pi release were performed by incubating the cells in the absence of the substrate or the substrate in the absence of cells. Finally, the activity was expressed as a percentage of the control.

### *2.3.7 Preparation of lysates for oxidative stress assays*

To obtain cell lysate, the C6 GBM cell line was prepared and exposed to GA as described above. After 48 h of treatment, cells were washed two times with sterile water, and the lysate was prepared manually with the aid of a cell scraper. Subsequently, the supernatant was centrifuged at 1000 rpm for 10 min. The pellet was discarded, and the supernatant was used for oxidative parameters analysis. ROS levels, total sulfhydryl content (SH content), and the activity of antioxidants enzymes, such as superoxide dismutase (SOD), catalase (CAT), and glutathione peroxidase (GPx), were evaluated in C6 GBM cells as described in a previous study [20] from our laboratory and in session 2.5.

## 2.4 Characterization of the effect of GA on a preclinical model of GBM

### *2.4.1 GBM implantation*

After reaching 90% confluency, a total of $1 \cdot 10^6$ C6 GBM cells were resuspended in 3 µL of DMEM/FBS-free medium and injected into the right striatum (coordinates relative to bregma: 0.5 mm later, 3.0 mm lateral, and 6.0 mm depth) of *Wistar* rats pre-anesthetized with intraperitoneal (i.p.) administration of ketamine and xylazine as described by [24].

### *2.4.2 Treatment of animals with GA*

Five days after GBM implantation, *Wistar* rats were randomly divided into four groups: (1) Control (water-treated); (2) GBM (water-treated); (3) GBM + GA 50 (50 mg/kg body weight) [25]; (4) GBM + GA 100 (100 mg/kg body weight) [26]. GA was dissolved in water and administered intragastrically for 15 days in the animals of groups 3 and 4. The animals in groups 1 and 2 received only water. On day 21 of tumor implantation, the animals were subjected to behavioral tests. Subsequently, the rats were anesthetized with isoflurane and blood was collected by cardiac puncture and used for

biochemical determinations of toxicity serum (alanine aminotransferase [ALT], aspartate aminotransferase [AST], creatinine, and urea) and enzymatic assays in lymphocytes, platelets, and serum. In addition, the brain was removed, sectioned and fixed with 10% paraformaldehyde (pH 7.4) for pathological analysis or frozen at -80 °C for oxidative stress parameters determination.

*2.4.3 Behavioral assay*

The animals were weighed every day and examined for neurological deficits, such as motor deficit and head tilt. In addition, signs of epileptic seizures have also been observed. On day 21 after tumor implantation, the animals were exposed to an open field test. Open field exploration was carried on a 72 x 72 x 33 cm (width × length × height) arena, whose floor is divided into 16 equal squares (18 x 18 cm) as described by [27]. The number of quadrants crossed with all paws (crossing) and rearing (standing on the hind legs without contact with the sides of the arena) for 5 min was used as a measurement to evaluate locomotor activity and exploratory, respectively. The apparatus was cleaned with a 40% ethanol solution and dried after each test session on each animal.

*2.4.4 Pathological determinations and quantification of tumor volume*

After euthanasia, the brain was divided into three slices, fixed and stained with hematoxylin and eosin (HE) (4 μm thick in paraffin blocks). Pathological analysis was conducted by a pathologist in a blinded manner. Images were captured by a digital camera attached to the microscope (×2 magnification; Nikon Eclipse TE300) for tumor quantification. Tumor area ($mm^2$) was quantified using ImageJ software, while the total volume ($mm^3$) of the tumor was calculated by multiplying the slice section and adding the segmented area as described by [27].

*2.4.5 Preparation of hematological samples for ectonucleotidase enzyme activity*

After a cardiac puncture, blood samples were collected in tubes containing EDTA and sodium citrate as an anticoagulant to separate lymphocytes and platelets, respectively. Lymphocytes were separated on Ficoll-Histopaque density gradients according to the method established by Böyum [28]. The preparation of platelet-rich plasma (PRP) from total blood was performed as previously described by [29]. In addition, whole blood was collected in tubes without an anticoagulant system and centrifuged at 3500 rpm for 15

min at 25 °C. The clot was removed, and the serum was preserved and used for biochemical determinations.

*2.4.5.1 NTPDase activity in lymphocytes*

NTPDase activity was measured as previously described by [30]. Cell intact lymphocytes suspended in a saline solution were added to the reaction medium containing 0.5 mM $CaCl_2$, 120 mM NaCl, 5 mM KCl, 6 mM glucose, and 50 mM Tris-HCl buffer (pH 8.0). After 70 min of incubation, the reaction started by adding substrate (ATP or ADP) and stopped with 15% TCA. Then, the released Pi was quantified by the malachite green method using $KH_2PO_4$ and a Pi standard [23]. Controls were performed to determine non-enzymatic Pi release by adding the enzyme preparation after TCA addition to correct for non-enzymatic nucleotide hydrolysis. The activity was expressed as nmol Pi/min/mg of protein.

*2.4.5.2 NTPDase and 5'-nucleotidase assays in platelets*

For the NTPDase enzymatic assay, PRP was preincubated in a reaction medium containing 5 mM $CaCl_2$, 100 mM NaCl, 5 mM KCl, 6 mM glucose, and 50 mM Tris-HCl buffer (pH 7.4), for 10 min at 37 °C as described by [31]. For 5'-nucleotidase activity, 5 mM $CaCl_2$ was replaced with 10 mM $MgCl_2$ in the above-mentioned reaction medium, according to [29]. The reaction was initiated by adding ATP or ADP at a final concentration of 1 mM and AMP at a final concentration of 2 mM. Both enzyme assays were incubated for 60 min, and the reaction was stopped with 10% TCA. The released Pi concentration was assayed by the method established by [23]. Controls to determine non-enzymatic Pi release were performed by adding platelet samples after TCA addition to correct for non-enzymatic nucleotide hydrolysis. Enzymatic specific activities were expressed as nmol Pi released/min/mg of protein.

*2.4.5.3 NTPDase and 5'-nucleotidase activity assays in serum*

The activity of NTPDase and 5'nucleotidase in serum was performed as described by [32]. Serum samples were preincubated at 37 °C for 10 min in a reaction medium containing 112.5 mM Tris-HCl (pH 8.0). To initiate the reaction, substrates (ATP, ADP, or AMP) were added to the mixture at a final concentration of 3 mM. After 40 min of incubation, the reaction was stopped with 10% TCA. The amount of Pi released was

determined following the method developed by [23], and the activity of ectonucleotidase was expressed as nmol Pi released/min/mg of protein.

*2.4.5.4 Adenosine deaminase (ADA) activity in lymphocytes, platelets, and serum*

ADA activity was quantified according to Giusti and Gakis [33], where ammonia reacts with hypochlorite and phenol to produce the blue indophenol. After 60 minutes of incubation at 37 °C, the reaction catalyzed by ADA were interrupted by adding nitroprusside and phenol solution. ADA activity was expressed as U/L.

*2.4.6 Brain oxidative stress assays*

After euthanasia, the brain was collected and divided into the left and right hemispheres. Once glioblastoma cells were injected into the right striatum for tumor implantation, the right hemisphere of the brain was homogenized in sodium phosphate buffer, pH 7.4 containing KCl (1:10, w/v) and centrifuged at 3500 rpm for 10 min at 4 °C. Then, the pellet was discarded, and the supernatant was used for determinations of oxidative stress as described in session 2.5.

**2.5 Oxidative stress assays – C6 cells and preclinical model of GBM**

*2.5.1 ROS production*

ROS generation was assayed by oxidation of DCFH-DA (2',7'-dichlorodihydrofluorescein diacetate) to fluorescent dichlorofluorescein (DCF). After 48 h treatment with GA, C6 glioblastoma cells ROS levels were measured according Pedra et al [20] and results expressed as percentual of control. By other hand, intracellular ROS formation in brain tumor tissue, platelets, and serum samples was determined by Ali et al [34] and reported as μmol DCF per mg of protein. Briefly, samples were incubated with 1 mM DCFH-DA for 30 min, and DCF fluorescence intensity emission was registered at excitation wavelengths of 525 and 488 nm for 30 min, using a microplate reader (SpectraMax190).

*2.5.2 Nitrite levels*

In tumor tissue, platelets, and serum samples, nitrite concentrations were measured using a colorimetric reaction with Griess reagent [35]. Briefly, 50 ⌈L of the sample was incubated with 50 μL of 1% sulfanilamide and 50 μL of 0.3% N-(1-Naphthyl)ethylenediamine dihydrochloride at 25 °C for 10 min. Subsequently, nitrite levels were quantified by a microplate reader (SpectraMax190) at 540 nm using sodium nitrite as the standard. The results were expressed as μM nitrite/mg protein.

*2.5.3 Thiobarbituric acid reactive substances (TBARS) quantification*

Lipid peroxidation was assessed as described by [36]. Tumor tissue samples were mixed with 15% TCA and centrifuged at 2500 g for 5 min. The supernatant was mixed with 0.67% thiobarbituric acid and heated for 30 min at 100 °C. Subsequently, TBARS levels were measured at 535 nm with a microplate reader (SpectraMax190) and expressed as nmol TBARS/mg of protein.

*2.5.4 Total SH content*

The total SH content was measured in glioblastoma cell lysate, brain tumor tissue, platelets and serum samples as described by Aksenov and Markesbery [37]. This assay is based on the reduction of 5,5-dithio-bis-(2-nitrobenzoic acid) (DTNB) by thiols due to oxidation (disulfide) generated an yellow derivative (2-nitro-5-thiobenzoic acid) (TNB). In brief, the samples were added to PBS buffer containing EDTA (pH 7.4). The reaction was started by adding DTNB whose absorption is determined in the microplate reader (SpectraMax190) at 412 nm. Glioblastoma cell results were reported as percentage of control, while tumor tissue, platelets and serum samples results were expressed as nmol TNB/mg of protein.

*2.5.5 SOD activity*

The SOD activity was analyzed in cell lysate, tumor tissue, platelets and serum samples as previously described by Misra and Fridovich [38]. This test is based on the inhibition of adrenaline auto-oxidation, which is scavenged by SOD in a microplate reader (SpectraMax190) at 480 nm. SOD activity in the cell lysate was expressed as

percentage of control, while brain tumor tissue, platelets and serum samples results were reported as units/mg of protein.

*2.5.6 CAT activity*

CAT activity was measured as described by [39]. This assay is based on the decomposition of hydrogen peroxide ($H_2O_2$), which were monitored for 180 s using a microplate reader (SpectraMax190) at 240 nm at 37 ºC. Results in the cell lysate were expressed as percentage of control, while the brain tumor tissue, platelets and serum samples results were reported as units/mg of protein.

*2.5.7 Glutathione peroxidase (GPx) activity*

GPx activity was determined using a commercial kit (RANSEL®; Randox Lab, Atrim, UK) which catalyzes glutathione (GSH) by cumene hydroperoxide. Subsequently, in the presence of glutathione reductase (GR) and NADPH, the oxidized glutathione (GSSG) is converted into the reduced form generating $NADP^+$. The conversion of NADPH to $NADP^+$ was measured at 340 nm using microplate reader (SpectraMax190) and GPx activity was expressed as a percentage of control in lysate glioblastoma cells.

*2.5.8 Glutathione S-transferase (GST) activity*

GST activity was analyzed in brain tumor tissue, platelets and serum samples using 1-chloro-2,4-dinitrobenzene (CDNB) as a substrate, as previously described by [40]. This method mixture contained 1 mM CDNB (in ethanol), 10 mM glutathione, 20 mM potassium phosphate buffer (pH 6.5), and 20 µL of samples. GST activity was expressed as µmol GS-DNB min/mg protein.

**2.5 Protein determination**

Protein levels were quantified according to [41] to assess oxidative stress parameters in the C6 GBM cell lysate and TBARS, SH-content levels, and SOD, CAT, and GST activity of samples of brain tissue, lymphocytes, platelets, and serum. In contrast, the Bradford method [42] was used to measure protein levels to analyze ROS

and nitrite levels in samples of brain tissue, lymphocytes, platelets, and serum and ectonucleotidase activity.

### 2.6 Statistical analysis

Data were expressed as means ± standard error of the means, and the results were analyzed with one-way analysis of variance followed by the Tukey post hoc test using GraphPad Prism version 5.0 Program (Intuitive Software for Science, São Diego, CA). A P-value of less than 0.05 was considered a statistically significant difference.

## 3. Results

### 3.1 GA selectively decreases GBM cell viability and proliferation

Rat C6 GBM cell line exposed to 50–400 ⌈M of GA for 24 and 48 h, exhibiting a cytotoxic effect in a concentration and time-dependent manner (Figure 1A-D). After 48 h of treatment, GA at a concentration of 400 ⌈M inhibited 60% and 70% C6 GBM cell viability and proliferation, respectively, compared to control cells. Interestingly, exposure of primary astrocyte cell culture to GA for 48 h did not alter cell viability or proliferation, suggesting a selective effect on glioblastoma cells (Figure 1D, E).

### 3.2 GA modulates oxidative stress parameters in GBM cells

The results of the oxidative stress parameters of GBM cells exposed to GA for 48 h are described in Figure 2. GA reduced the production of ROS in GBM cells in a concentration-dependent manner by up to 90% after 48 h of treatment (Figure 2A). In contrast, at a concentration of 400 μM GA promoted an increase in levels of SH content of about 600% compared with control cells (Figure 2B). Furthermore, GA caused an increase in the activity of the antioxidant enzymes SOD, CAT, and GPx. Compared with GBM control cells, GA 400 uM significantly increased SOD activity by 400%, CAT activity by 1060%, and GPx activity by 390% after 48 h of treatment (Figure 2C-E).

### 3.3 GA changes the hydrolysis of ATP, ADP, and AMP in GBM cells

As shown in Figure 3, extracellular nucleotide metabolism was decreased in GBM cells exposed to GA. After 48 h of treatment with GA at concentrations of 300 and 400 µM, the hydrolyses were reduced 35% and 40% to ATP (Figure 3A) and 40% and 45% to ADP (Figure 3B), respectively, compared to control cells. In addition, the activity of 5'nucleotidase decreased when GBM cells were incubated with AMP in the presence of 200, 300, and 400 µM GA, respectively, in 25%, 35%, and 40% compared with control cells (Figure 3C).

### 3.4 GA suppresses *in vivo* growth and promotes behavioral improvement in GBM-bearing rats

Given the promising cytotoxic effect of GA, we evaluated the anti-glioma potential of this phenolic compound in a preclinical, experimental model of GBM. According to Figure 4, the animals treated with GA 50 and 100 mg/kg exhibited a significant reduction in tumor volume (84.85 ± 35.93 $mm^3$ and 97.42 ± 20.54 $mm^3$, respectively; n = 5) compared to the animals in the GBM group (829.1 ± 131.9 $mm^3$; n = 5). It is important to note that no animal showed signs of epileptic seizures or tilting its head (data not shown). Furthermore, no changes in renal (creatinine and urea) and liver (ALT and AST) damage markers were observed between the experimental groups evaluated (Table 1).

Before implantation, there were no statistical differences in body weight between the experimental groups. However, the average body weight after implantation was lower in the GBM group (357.9 ± 14.27 g, n = 8) compared to the control group (392.3 ± 7.46 g; n = 8) and GA (GA 50 mg/kg: 373.4 ± 11.0 g; GA 100 mg/kg: 370.8 ± 6.75 g; n = 8) treated groups (Figure 5A). Furthermore, the locomotor activity in the open field revealed that the GBM group exhibited a significant decrease in the total number of crossings and rearings (49.88 ± 6.32 and 14.63 ± 1.94, respectively; n = 8) compared with the control group (90.13 ± 8.40 and 34.75 ± 4.14, respectively; n = 8). In contrast, treatment with GA 50 mg/kg (91.38 ± 5.45 and 34.38 ± 3.6, respectively; n = 8) and GA 100 mg/kg (93.25 ± 6.37 and 34.25 ± 2.98, respectively; n = 8) prevented this reduction (Figure 5B, C).

### 3.5 GA prevents oxidative brain damage in GBM-bearing rats

Since oxidative stress favors cancer progression, the antioxidant effect of GA on the tumor microenvironment of GBM-implanted rats was evaluated. As shown in Table 2, the levels of ROS ($P < 0.0001$; $n = 5$), nitrites ($P < 0.05$; $n = 5$), and TBARS ($P < 0.05$; $n = 5$) were higher in the GBM group than in the control group, respectively. The administration of GA 50 and 100 mg/kg prevented the increase in levels of ROS ($P < 0.0001$; $n = 5$), nitrites ($P < 0.05$; $n = 5$), and TBARS ($P < 0.01$; $n = 5$).

Furthermore, treatment with GA 50 and 100 mg/kg prevented the decrease in SH content ($P < 0.05$; $n = 5$) and activity of the antioxidant enzymes SOD ($P < 0.05$; $n = 5$) and CAT ($P < 0.05$; $n = 5$) promoted by GBM. However, no changes in GST activity were found between the experimental groups.

### 3.6 Effect of GA on oxidative stress parameters in platelets and serum in GBM-bearing rats

It is well established that oxidative stress is involved in the malignancy of brain tumors, the damage of which reflects both brain tissue and peripheral blood [43]. In this context, we evaluated the effect of GA on platelets and serum of rats submitted to the preclinical model of GBM. As shown in Table 3, the administration of GA 50 and 100 mg/kg was able to reduce the levels of ROS ($P < 0.01$; $n = 5$) and nitrite ($P < 0.01$; $n = 5$) in platelets compared to animals in the GBM group ($P < 0.0001$ and $P < 0.01$, respectively; $n = 5$). Furthermore, tumor mice showed a significant reduction in CAT activity in platelets ($P < 0.05$; $n = 5$), while treatment with GA 50 and 100 mg/kg was able to prevent this change ($P < 0.05$; $n = 5$). In all groups evaluated in this study, no changes were observed in total SH content, SOD, and GST activity.

The administration of GA 50 and 100 mg/kg was able to significantly reduce the levels of ROS ($P < 0.0001$; $n = 5$) and nitrite ($P < 0.0001$, respectively; $n = 5$) in the serum of the sick animals, compared to the GBM group ($P < 0.0001$; $n = 5$). Additionally, SOD and CAT activities were higher in the control group than in the GBM group ($P < 0.01$; $n = 5$). Treatment with both doses of GA prevented this damage ($P < 0.05$ and $P < 0.01$ to SOD and CAT, respectively; $n = 5$). No significant changes were observed in the total SH content and activity of the GST enzyme.

### 3.7 GA modulates ectonucleotidase and ADA activities in lymphocytes, platelets, and/or serum from GBM-bearing rats

To assess whether treatment with GA affects the peripheral response, the activity of ectonucleotidase enzymes was evaluated in lymphocytes, platelets, and serum from GBM-implanted rats as described in the Materials and Methods. In lymphocytes, the hydrolysis of ATP (Figure 6A), ADP (Figure 6B), and adenosine (Figure 6C) was significantly increased in the GBM group (174.1 ± 25.5, 34.44 ± 3.60, and 71.66 ± 7.11 nmol Pi/min/mg of protein, respectively; n = 5) compared to the control group (82.46 ± 12.02, 23.30 ± 2.85, and 38.87 ± 3.84 nmol Pi/min/mg of protein, respectively; n = 5). However, treatment with GA 50 (92.27 ± 17.11, 22.07 ± 2.75, 37.11 ± 2.0 nmol Pi/min/mg of protein, respectively; n = 5) and 100 mg/kg (87.04 ± 11.74, 24.32 ± 3.46, 29.93 ± 2.53 nmol Pi/min/mg of protein, respectively; n = 5) prevented an increase in the activity of the enzymes NTPDases and ADA.

The results of the ectonucleotidases activity in platelets are shown in Figure 7. A significant reduction in the hydrolysis of ATP and AMP was observed in the platelets from the GBM group (4.15 ± 0.29 and 2.59 ± 0.90 nmol Pi/min/mg of protein, respectively; n = 5), which was reversed by treatment with GA 50 mg/kg (9.02 ± 0.68 and 7.85 ± 1.01 nmol Pi/min/mg of protein, respectively; n = 5) and and GA 100 mg/kg (9.12 ± 0.90 and 7.64 ± 1.47 nmol Pi/min/mg of protein, respectively; n = 5). In animals treated with GA 50 and 100 mg/kg, a decrease in ADP hydrolysis (7.38 ± 0.35 and 5.59 ± 0.54 nmol Pi/min/mg of protein, respectively; n = 5) and ADA activity (1.29 ± 0.19 and 1.02 ± 0.06 U/L, respectively; n = 5) compared with the GBM group (14.93 ± 1.72 nmol Pi/min/mg of protein and 4.80 ± 0.50 U/L, respectively; n = 5) was observed.

In serum, our results showed a decrease in ATP hydrolysis (Figure 8A) in rats of the GBM group (1.12 ± 0.07 nmol Pi/min/mg of protein; n = 5) compared with the control (2.04 ± 0.22 nmol Pi/min/mg of protein; n = 5), which was reversed by treatment with GA 50 mg/kg (1.81 ± 0.16 nmol Pi/min/mg of protein; n = 5) and GA 100 mg/kg (1.82 ± 0.04 nmol Pi/min/mg of protein; n = 5). In all groups evaluated in this study, no changes were observed in ADP and AMP hydrolysis and ADA activity in serum (Figure 8B, D).

## 4. Discussion

High-grade gliomas are the most malignant brain tumors whose treatment options remain limited. Despite intense efforts to prevent tumor progression, conventional therapies make the remaining GBM cells more aggressive and resistant [2, 44]. In this

way, natural compounds that exhibit multiple bioactivities have emerged as a new alternative to complement conventional treatments [44]. In this context, this study demonstrated the effect of GA, a natural phenolic compound, on reducing the growth of GBM *in vitro* and *in vivo*.

Our results demonstrated that GA significantly reduced the proliferation of the C6 GBM cell line, whose $IC_{50}$ values were 396.5 µM for the cell viability assay and 260.7 µM for the cell proliferation assay, after 48 h of treatment. Despite the high $IC_{50}$ values demonstrated in these studies, no cytotoxicity effects was observed on the primary culture of healthy astrocytes, suggesting a selective cytotoxic action. Previous studies have demonstrated the cytotoxic effect of GA on several tumor cell lines, including human glioma cell lines [15, 16, 17]. Lu et al. [16] revealed that gallic acid induces antiproliferative effects at high concentrations, showing $IC_{50}$ values of 125 µg/mL (734.7 µM) in human glioma cell line U87MG. Paolini et al. [17] report $IC_{50}$ values greater than 100 µg/mL (587.8 µM) in human glioma cell lines T98G. According to Subramanian et al. [45], gallic acid exhibits an $IC_{50}$ of 740 µM after 72 h of treatment in HCT-15 human colon cancer cells.

Additionally, studies have pointed to the variability between the $IC_{50}$ values of temozolomide (TMZ) on glioblastoma cell lines, the standard chemotherapy drug in antiglioma therapy. Azambuja et al. [46] demonstrated that C6 glioblastoma cells exposed to TMZ exhibit an $IC_{50}$ of 993.5 µM after 72 h of treatment. According to Afshari et al. [47], TMZ reduces the viability of human glioblastoma cells (U87MG) at high concentrations, exhibiting $IC_{50}$ values of 141.7 µg/mL (729.8 µM) and 88.42 µg/mL (455.4 µM) after 24 and 48 h of treatment, respectively. Furthermore, Poon et al. [48] highlight that the T98G cell line and patient-derived glioma cells exhibit a median $IC_{50}$ of 438.3 µM and 220 µM, respectively, after 72 h of treatment.

Although a plethora of human-derived cell lines is widely useful for researching new anti-glioma therapies, such tumor lines are inappropriate for studies of the tumor microenvironment [49]. The microenvironment of gliomas consists of a complex network that comprises different cell types, components of the extracellular matrix, cytokines, and growth factors [3, 50]. Therefore, although human-derived lines exhibit morphological and genetic characteristics similar to GBM, they do not mimic the invasive and vascular behavior of the tumor microenvironment. According to Giakoumettis et al. [49], the ideal glioma model must be similar to the human GBM in terms of morphological characteristics and continuous interaction between tumor cells and the surrounding

microenvironment. The C6 cell line is one of the most widely used experimental models in neuro-oncology for studying high-grade gliomas. C6 cells simulate the histological and biological characteristics of human GBM when injected intracerebroventricularly into *Wistar* rats, such as high mitotic index, migration and invasion, interruption of the blood-brain barrier, angiogenesis, foci of necrosis, production and regulation of growth factors, and nuclear polymorphism [49].

Given the potential selective cytotoxic effect of GA on the C6 GBM cell line, a preclinical trial was initiated to assess the effect of phenolic acid on the tumor microenvironment. According to the data obtained, GA reduced 90% of tumor volume compared to the animals in the GBM group. This is the first study to demonstrate the effect of GA in a preclinical model of GBM. Although behavioral assessment is little used to analyze brain tumor growth in a preclinical GBM model, it allows the detection of sensory or motor dysfunctions characteristic of tumor evolution [51]. Our results show that animals with GBM exhibited a significant reduction in locomotor activity and vertical exploratory behavior compared to healthy animals in the open field test. According to Vannini et al. [52], after 14 days of GBM induction, it is possible to observe a deterioration in motor performance due to the growth of the tumor mass in the sensorimotor cortex. In contrast, our data revealed that GA could restore the locomotor activity of rats with GBM. Corroborating with other studies, our findings also demonstrated that the administration of GA did not induce any biochemical changes related to biomarkers of damage to the liver or kidney of animals with intracerebral tumors [53, 54].

One of the mechanisms involved in the *in vitro* anticancer activity of GA is associated with its ability to regulate ROS [15]. In gliomas, cellular redox imbalance is associated with tumor development and progression [55]. In this study, rats with GBM exhibited a significant increase in the levels of reactive species and lipid peroxidation, as well as a reduction in the activity of antioxidant enzymes in the tumor microenvironment compared to the brain tissue of healthy mice. Corroborating with our results, Schiffer et al. [56] emphasized that the tumor microenvironment participates in the process of gliomagenesis by increasing the production of ROS through oxidative stress. In addition to affecting the cell cycle, the generation of ROS by tumor cells has been associated with chemoresistance in GBM; thus, causing cell proliferation, especially due to the increased formation of superoxide anion ($O_2^-$) [57]. Several reactive species can be formed from $O_2^-$, such as $H_2O_2$ and the hydroxyl radical ($^-OH$) [7]. $O_2^-$ can also interact with the nitric

oxide radical ($NO^-$) in the presence of L-arginine and NADPH-oxidase, resulting in the formation of other reactive nitrogen species [58]. High concentrations of these reactive species damage intracellular macromolecules, such as nucleic acids and polyunsaturated fatty acids (PUFAs), triggering lipid peroxidation [7]. In brain tumors, the oxidation of PUFAs by lipid peroxides plays a critical role in the regulation of inflammation and cell death, favoring tumor progression [6, 59].

In this study, GA decreased ROS levels in C6 cells and tumor tissue of rats with GBM and was also able to significantly reduce nitrite concentrations and prevent lipid peroxidation in the tumor microenvironment. In addition, GA promoted a significant increase in the activity of the antioxidant enzymes SOD and CAT in both experimental protocols. SOD acts by catalytically converting $O_2^-$ into $H_2O_2$ and molecular oxygen, while CAT prevents the accumulation of $H_2O_2$, which is toxic, degrading this reactive species into water and molecular oxygen [54]. Together with SOD and CAT, the GPx enzyme participates in the body's first enzymatic antioxidant defense line by suppressing oxidative stress and maintaining redox homeostasis [58]. In addition to being an important brain antioxidant, glutathione acts as a cofactor for GPx in reducing $H_2O_2$ and other peroxides [60]. Studies show that GPx brain activity is reduced in C6 intracerebral implant models, as well as in patients diagnosed with GBM [6, 7, 61]. Given the results found, we suggest that the reduction in the levels of reactive species both *in vitro* and in the tumor microenvironment may be due to the antioxidant effects of GA; thus, reducing the oxidative damage triggered by the tumor.

Growing evidence indicates that systemic inflammation is more severe in GBM than in brain metastases [43, 62]. In general, both glioma neoplastic cells and the tumor microenvironment release biomolecules into the circulation, where serum and platelets represent the main source of circulating tumor DNA [63]. Studies show that increased ROS release by glioma cells promotes an increase in lipid peroxidation and levels of proinflammatory cytokines in the circulation, which vary according to the degree and molecular subtype of the tumor [62, 64]. Barciszewska et al. [43] also reported similar levels of oxidative damage markers in tumor tissue and peripheral blood samples from patients with GBM. In this study, we found high levels of ROS and nitrites in serum and platelet samples from rats with GBM compared to healthy animals. Meanwhile, in addition to avoiding such changes, treatment with GA prevented the reduction of CAT activity in serum and blood platelets of rats with a brain tumor.

Platelets play a central role in tumor angiogenesis and coordination of the tumor microenvironment, releasing a plethora of growth factors, inflammatory mediators, and chemokines, in addition to modulating the immune response [65]. Platelets are activated by various agonists, including ADP secreted by tumor cells [65]. It is well established that adenine nucleotides and nucleosides act as extracellular messengers by modulating the immune and inflammatory response [10]. The ectonucleotidases responsible for controlling these molecules in the extracellular space are expressed on the surface of several cells, including platelets and lymphocytes, where the conversion of ATP and ADP to AMP is catalyzed by the enzyme NTPDase, while 5'-nucleotidase acts by dephosphorylating AMP into adenosine. Subsequently, adenosine is degraded to inosine by the action of ADA [8, 16]. In the present investigation, we demonstrated that adenine metabolism is altered in platelets, lymphocytes, and serum of rats with GBM compared with healthy animals. Indeed, ectonucleotidase activity has been shown to be altered in pathologies associated with oxidative stress since high levels of ROS play a pro-aggregating role, altering platelet function and, consequently, the systemic immune response [65].

When evaluating the metabolism of extracellular adenine nucleotides in circulating platelets of rats with GBM, we observed a reduction in ATP hydrolysis but an increase in ADP hydrolysis, suggesting a depletion in ADP levels compared to healthy controls. The accumulation of evidence supports the findings that the GBM microenvironment is characterized by high levels of ADP, which induces the activation and formation of intratumoral platelet aggregates, stimulating angiogenesis, and promoting a dramatic increase in cell growth and malignancy [65, 66, 67]. However, no studies have elucidated the activity of NTPDase enzymes in the circulation of patients with GBM. In this context, we suggest that the extracellular pool of ADP reflected by increased ADPase activity may be due to the release of ADP from platelets, which can act as an additional source of ADP in GBM [65]. Although ADP plays a crucial role in platelet activation, ATP also consists of an important pro-aggregating molecule [67]. In this study, the reduction in NTPDase activity in relation to ATP in platelets and serum from animals with tumors suggests an increase in this nucleotide in the extracellular environment. Furthermore, we also observed reduced AMP hydrolysis and increased ADA activity in platelets from rats with GBM, suggesting a reduction in extracellular levels of adenosine, a potent inhibitor of platelet aggregation [67].

The platelet-lymphocyte relationship has been associated with cancer stage, reflecting a correlation between the level of systemic inflammatory and the immune response caused by GBM cells [64, 68]. In corroboration with other studies, we observed an increase in the activity of NTPDases and ADA enzymes in lymphocytes from tumor-bearing rats compared to healthy animals [27, 69]. Although increased ADA activity has been reported in serum from cancer patients [69, 70], no change was observed in the activity of this enzyme in serum from rats with GBM. ADA has two isoforms, ADA1—found in all cells but with greater lymphocyte activity—and ADA2—the predominant isoenzyme in serum and with low affinity for the substrate [70]. Studies indicate that ADA activity is not altered in serum from patients with brain tumors, suggesting that ADA1 plays an important role in the pathophysiology of GBM [71, 72]. An increase in the activity of this enzyme indicates a reduction in extracellular levels of adenosine in lymphocytes, an important anti-inflammatory molecule.

In contrast, the administration of GA prevented changes in purinergic enzymes in blood platelets, lymphocytes, and serum in rats with brain tumors and maintained the activity of purinergic enzymes similar to that found in healthy animals. Chang et al. [73] point out that GA can inhibit platelet aggregation and P-selectin expression induced by different stimulants. This antiaggregation effect of GA is in part due to its structural similarity to P-selectin, an adhesive molecule involved in platelet activation that is widely expressed in circulating platelets from patients with GBM [74]. Furthermore, it has been shown that this polyphenol can prevent the formation of platelet-leukocyte aggregates by decreasing the intracellular mobilization of $Ca^{2+}$ and inhibiting the phosphorylation of the PKCα/p38 MAPK and Akt/GSK3β pathways in stimulated platelets; thus, reducing tumor angiogenesis induced by these cells [73]. Da Silva Pereira et al. [19] also reported the ability of GA to prevent complications related to immunological and thrombo-regulatory mechanisms regulating NTPDases and ADA enzymes in lymphocytes. In addition to regulating the activity of purinergic enzymes in peripheral cells of animals with brain tumors, this study also demonstrated, for the first time, the ability of GA to reduce the hydrolysis of adenine nucleotides in C6 GBM cells.

In conclusion, these results change the view of GBM from a brain tumor confined to a systemic disease, in which several cell subpopulations stimulate tumor progression and malignancy through mechanisms orchestrated by different signaling pathways capable of altering redox homeostasis and the purinergic system. Furthermore, our results demonstrate that GA reduced the characteristic malignant parameters of GBM *in vitro*

and *in vivo* and that such effects may be related to its antioxidant properties and modulation of purinergic signaling in the tumor microenvironment and systemic immune response. However, further studies are warranted to explore the effect of GA in standard chemotherapy-resistant GBM models.

## Declaration of competing interests

The authors declare that there are no conflicts of interest.

## Funding

This work was supported by the Brazilian agencies: Conselho Nacional de Desenvolvimento Científico e Tecnológico (CNPq), Coordenação de Aperfeiçoamento de Pessoal de Nível Superior (CAPES) - Finance code 001, and Fundação de Amparo à Pesquisa do Estado do Rio Grande do Sul (FAPERGS).

## CRediT authorship contribution statement

**Nathalia S. Pedra:** Conceptualization, Methodology, Investigation, Validation, Formal analysis, Data curation, Visualization, Writing – original draft, Writing – review & editing. **Natália P. Bona:** Methodology, Investigation, Validation, Formal analysis, Data curation, Writing – review & editing. **Mayara S. P. Soares:** Conceptualization, Methodology, Investigation, Validation, Formal analysis, Data curation, Visualization, Project administration, Writing – review & editing. **Luíza Spohr:** Methodology, Investigation, Validation, Formal analysis, Data curation, Writing – review & editing. **Fernando L. Alves:** Methodology, Investigation, Validation, Data curation, Writing – review & editing. **Francieli S. Santos:** Investigation, Validation, Writing – review & editing. **Juliane T. Saraiva:** Investigation, Validation, Writing – review & editing. **Francieli M. Stefanello:** Conceptualization, Funding acquisition, Supervision, Recourses, Writing – review & editing. **Elizandra Braganhol:** Conceptualization, Supervision, Resources, Writing – review & editing. **Roselia M. Spanevello:** Conceptualization, Validation, Visualization, Funding acquisition, Resources, Project administration, Writing – original draft, Writing – review & editing.

## Acknowledgments

This research was supported by the Conselho Nacional de Desenvolvimento Científico e Tecnológico (CNPq), Coordenação de Aperfeiçoamento de Pessoal de Nível Superior (CAPES), and Fundação de Amparo à Pesquisa do Estado do Rio Grande do Sul (FAPERGS).

**Reference**

[1] Louis DN, Perry A, Reifenberger G, Von Deimling A, Figarella-Branger D, Cavenee WK, et al. The 2016 World Health Organization classification of tumors of the central nervous system: a summary. Acta Neuropathol 2016; 131:803-20. doi:10.1007/s00401-016-1545-1.

[2] Trejo-Solís C, Serrano-Garcia N, Escamilla-Ramírez Á, Castillo-Rodríguez RA, Jimenez-Farfan D, Palencia G, et al. Autophagic and apoptotic pathways as targets for chemotherapy in glioblastoma. Int J Mol Sci 2018; 19:3773-3827. doi:10.3390/ijms19123773.

[3] Da Ros M, De Gregorio V, Iorio AL, Giunti L, Guidi M, De Martino M, et al. Glioblastoma chemoresistance: The double play by microenvironment and blood-brain barrier. Int J Mol Sci 2018; 19:2879-2902. doi:10.3390/ijms19102879.

[4] Ostrom QT, Rubin JB, Lathia JD, Berens ME, Barnholtz-Sloan JS. Females have the survival advantage in glioblastoma. Neuro Oncol 2018; 20:576-7. doi: 10.1093/neuonc/noy002.

[5] Broekman ML, Maas SL, Abels ER, Mempel TR, Krichevsky AM, Breakefield XO. Multidimensional communication in the microenvirons of glioblastoma. Nat Rev Neurol 2018; 14:482-95.doi:10.1038/s41582-018-0025-8.

[6] Illán-Cabeza NA, García-García AR, Martínez-Martos JM, Ramírez-Expósito MJ, Peña-Ruiz T, Moreno-Carretero MN. A potential antitumor agent,(6-amino-1-methyl-5-nitrosouracilato-N3)-triphenylphosphine-gold (I): Structural studies and in vivo biological effects against experimental glioma. Eur J Med Chem 2013; 64:260-72. doi: 10.1016/j.ejmech.2013.03.067.

[7] Ramírez-Expósito MJ, Martínez-Martos JM. The delicate equilibrium between oxidants and antioxidants in brain glioma. Curr Neuropharmacol 2019; 17:342-51.doi: 10.2174/1570159X16666180302120925.

[8] Burnstock, G. Introduction to purinergic signaling. In: Pelegrín P, editor. Purinergic Signaling. Methods in Molecular Biology, New York: Humana; 2020, p. 1-15. doi: 10.1007/978-1-4939-9717-6_1.

[9] Braganhol E, Wink MR, Lenz G, Battastini AMO. Purinergic signaling in glioma progression. In: Barańska J, editor. Glioma signaling. Advances in Experimental Medicine and Biology, Springer: Cham; 2020, p. 87-108. doi: 10.1007/978-3-030-30651-9_5.

[10] Di Virgilio F, Adinolfi E. Extracellular purines, purinergic receptors and tumor growth. Oncogene 2017; 36:293-303.doi: 10.1038/onc.2016.206.

[11] Cekic C, Linden J. Purinergic regulation of the immune system. Nat Rev Immunol 2016; 16:177-92.doi:10.1038/nri.2016.4.

[12] Mitra T, Bhattacharya R. Phytochemicals modulate cancer aggressiveness: A review depicting the anticancer efficacy of dietary polyphenols and their combinations. J Cell Physiol 2020; 235:7696-708. doi: 10.1002/jcp.29703.

[13] Kahkeshani N, Farzaei F, Fotouhi M, Alavi SS, Bahramsoltani R, Naseri R, et al. Pharmacological effects of gallic acid in health and diseases: A mechanistic review. Iran J Basic Med Sci 2019; 22:225-37. doi: 10.22038/ijbms.2019.32806.7897.

[14] Verma S, Singh A, Mishra A. Gallic acid: molecular rival of cancer. Environ Toxicol Pharmacol 2013; 35:473-85. doi: 10.1016/j.etap.2013.02.011.

[15] Hsu SS, Chou CT, Liao WC, Shieh P, Kuo DH, Kuo CC, et al. The effect of gallic acid on cytotoxicity, $Ca^{2+}$ homeostasis and ROS production in DBTRG-05MG human glioblastoma cells and CTX TNA2 rat astrocytes. Chem Biol Interact 2016; *252:*61-73. doi: 10.1016/j.cbi.2016.04.010.

[16] Lu Y, Jiang F, Jiang H, Wu K, Zheng X, Cai Y, et al. Gallic acid suppresses cell viability, proliferation, invasion and angiogenesis in human glioma cells. Eur J Pharmacol 2010; 641:102-7. doi: 10.1016/j.ejphar.2010.05.043.

[17] Paolini A, Curti V, Pasi F, Mazzini G, Nano R, Capelli E. Gallic acid exerts a protective or an anti-proliferative effect on glioma T98G cells via dose-dependent epigenetic regulation mediated by miRNAs. Int J Oncol 2015; 46:1491-7. doi: 10.3892/ijo.2015.2864.

[18] Kade IJ, Rocha JBT. Gallic acid modulates cerebral oxidative stress conditions and activities of enzyme-dependent signaling systems in streptozotocin-treated rats. Neurochem Res 2013; *38:*761-71. doi: 10.1007/s11064-013-0975-6.

[19] Da Silva Pereira A., De Oliveira LS, Lopes TF, Baldissarelli J, Palma TV, Soares MSP, et al. Effect of gallic acid on purinergic signaling in lymphocytes, platelets, and serum of diabetic rats. Biomed Pharmacother 2018; 101:30-6. doi: 10.1016/j.biopha.2018.02.029.

[20] Pedra NS, Galdino, KDCA, Da Silva DS, Ramos PT, Bona NP, Soares MSP, et al. Endophytic Fungus Isolated From *Achyrocline satureioides* Exhibits Selective

Antiglioma Activity—The Role of Sch-642305. Front Oncol 2018; *8:*476-96. doi: 10.3389/fonc.2018.00476.

[21] Mosmann T. Rapid colorimetric assay for cellular growth and survival: application to proliferation and cytotoxicity assays. J Immunol *Methods 1983;* 65:55-63. doi: 10.1016/0022-1759(83)90303-4.

[22] Pauwels B, Korst AE, De Pooter CM, Pattyn GG, Lambrechts HA, Baay MF, et al. Comparison of the sulforhodamine B assay and the clonogenic assay for in vitro chemoradiation studies. Cancer Chemother Pharmacol 2003; 51:221-6. doi:10.1007/s00280-002-0557-9.

[23] Chan KM, Delfert D, Junger KD. A direct colorimetric assay for $Ca^{2+}$-stimulated ATPase activity. Anal Biochem 1986; 157:375-80. doi:10.1016/0003-2697(86)90640-8.

[24] Bona NP, Pedra NS, Azambuja JH, Soares MS, Spohr L, Gelsleichter NE et al. Tannic acid elicits selective antitumoral activity in vitro and inhibits cancer cell growth in a preclinical model of glioblastoma multiforme. Metab Brain Dis 2020; 35:283-93. doi: 10.1007/s11011-019-00519-9.

[25] Aglan HA, Ahmed HH, El-Toumy SA, Mahmoud, NS. Gallic acid against hepatocellular carcinoma: An integrated scheme of the potential mechanisms of action from in vivo study. Tumor Biol 2017; 39:1-10. doi:1 0.1177/1010428317699127.

[26] Senapathy JG, Jayanthi S, Viswanathan P, Umadevi P, Nalini N. Effect of gallic acid on xenobiotic metabolizing enzymes in 1, 2-dimethyl hydrazine induced colon carcinogenesis in Wistar rats–a chemopreventive approach. Food Chem Toxicol 2011; 49:887-92. doi: 10.1016/j.fct.2010.12.012.

[27] Da Silveira EF, Chassot JM, Teixeira FC, Azambuja JH, Debom G, Beira FT, et al. Ketoprofen-loaded polymeric nanocapsules selectively inhibit cancer cell growth in vitro and in preclinical model of glioblastoma multiforme. Invest New Drugs 2013; 31:1424-35. doi: 10.1007/s10637-013-0016-y.

[28] Boyum A. Isolation of mononuclear cells and granulocytes from human blood. Isolation of monuclear cells by one centrifugation, and of granulocytes by combining centrifugation and sedimentation at 1 g. Scand J Clin Lab Invest Suppl 1968; 97:77.

[29] Lunkes GIL, Lunkes DS, Morsch VM, Mazzanti CM, Morsch AL, Miron VR et al. NTPDase and 5′-nucleotidase activities in rats with alloxan-induced diabetes. Diabetes Res Clin Prac 2004; 65:1-6. doi:10.1016/j.diabres.2003.11.016.

[30] Leal DB, Streher CA, Neu TN, Bittencourt FP, Leal CA, Da Silva JE, et al. Characterization of NTPDase (NTPDase1; ecto-apyrase; ecto-diphosphohydrolase; CD39; EC 3.6. 1.5) activity in human lymphocytes. Biochim Biophys Acta Gen Subj 2005; 1721:9-15. doi: 10.1016/j.bbagen.2004.09.006.

[31] Pilla C, Emanuelli T, Frassetto SS, Battastini AMO, Dias RD, Sarkis JJF. ATP diphosphohydrolase activity (apyrase E.C. 3.6.1.5) in human blood platelets. Platelets. 1996; 7:225-30. doi:10.3109/09537109609023582.

[32] Fürstenau CR, Trentin DS, Gossenheimer AN, Ramos DB, Casali EA, Barreto-Chaves MLM et al. Ectonucleotidase activities are altered in serum and platelets of L-NAME-treated rats. Blood Cells Mol Dis 2008; 41:223-9. doi:10.1016/j.bcmd.2008.04.009.

[33] Giusti G, Galanti B. Colorimetric method. Adenosine deaminase. In: Bergmeyer HU, editor. Methods of Enzymatic Analysis. 3rd ed. Weinheim: Verlag Chemie; 1984; 315-3233.

[34] Ali SF, LeBel CP, Bondy SC. Reactive oxygen species formation as a biomarker of methylmercury and trimethyltin neurotoxicity. Neurotoxicol 1992; 13:637-48.

[35] Stuehr DJ, Nathan CF. Nitric oxide. A macrophage product responsible for cytostasis and respiratory inhibition in tumor target cells. J Exp Med 1989; 169:1543-55. doi: 10.1084/jem.169.5.1543.

[36] Esterbauer H, Cheeseman KH. Determination of aldehydic lipid peroxidation products: malonaldehyde and 4-hydroxynonenal. Methods Enzymol 1990; 186:407-21. doi:10.1016/0076-6879(90)86134-H.

[37] Aksenov MY, Markesbery WR. Changes in thiol content and expression of glutathione redox system genes in the hippocampus and cerebellum in Alzheimer's disease. Neurosci Lett 2001; 302:141-5. doi:10.1016/S0304-3940(01)01636-6.

[38] Misra HP, Fridovich I. The role of superoxide anion in the autoxidation of epinephrine and a simple assay for superoxide dismutase. J Biol Chem 1972; 247:3170-5. doi:10.1016/S0021-9258(19)45228-9.

[39] Aebi H. Catalase in vitro. Methods Enzymol 1984; 105:121-6. doi:10.1016/S0076-6879(84)05016-3.

[40] Habig WH, Pabst MJ, Jakoby WB. Glutathione S-transferases: the first enzymatic step in mercapturic acid formation. J Biol Chem 1974; 249:7130-7139. doi:10.1016/S0021-9258(19)42083-8.

[41] Lowry OH, Rosebrough NJ, Farr AL, Randall RJ. Protein measurement with the Folin phenol reagent. J Biol Chem 1951; 193:265-75.

[42] Bradford MM. A rapid and sensitive method for the quantitation of microgram quantities of protein utilizing the principle of protein–dye binding. Anal Biochem 1976; 72:248-254. doi:10.1016/0003-2697(76)90527-3.

[43] Barciszewska AM, Giel-Pietraszuk M, Perrigue PM, Naskręt-Barciszewska M. Total DNA methylation changes reflect random oxidative DNA damage in gliomas. Cells 2019; 8:1065-79. doi:10.3390/cells8091065.

[44] Erices JI, Torres Á, Niechi I, Bernales I, Quezada C. Current natural therapies in the treatment against glioblastoma. Phytother Res 2018; 32:2191-2201. doi:10.1002/ptr.6170.

[45] Subramanian AP, Jaganathan SK, Mandal M, Supriyanto E, Muhamad II. Gallic acid induced apoptotic events in HCT-15 colon cancer cells. World J Gastroenterol 2016; 22:3952. doi: 10.3748/wjg.v22.i15.3952.

[46] Azambuja JH, Gelsleichter NE, Beckenkamp LR, Iser IC, Fernandes MC, Figueiró F, et al. CD73 downregulation decreases *in vitro* and *in vivo* glioblastoma growth. Mol Neurobiol 2019; 56:3260-79. doi: 10.1007/s12035-018-1240-4.

[47] Afshari AR, Roshan MK, Soukhtanloo M, Ghorbani A, Rahmani F, Jalili-Nik M, et al. Cytotoxic effects of auraptene against a human malignant glioblastoma cell line. Avicenna J Phytomedicine 2019; 9:334-46.

[48] Poon MTC, Bruce M, Simpson JE, Hannan CJ, Brennan PM. Temozolomide sensitivity of malignant glioma cell lines – a systematic review assessing consistencies between in vitro studies. BMC Cancer 2021; 21:1240-9. doi:10.1186/s12885-021-08972-5.

[49] Giakoumettis D, Kritis A, Foroglou N. C6 cell line: the gold standard in glioma research. Hippokratia 2018; 22:105-12.

[50] Manini I, Caponnetto F, Bartolini A, Ius T, Mariuzzi L, Di Loreto C, et al. Role of microenvironment in glioma invasion: what we learned from in vitro models. Int J Mol Sci 2018; 19:147-79. doi: 10.3390/ijms19010147.

[51] Souza TKF, Nucci MP, Mamani JB, Da Silva HR, Fantacini DMC, De Souza LEB, et al. Image and motor behavior for monitoring tumor growth in C6 glioma model. PLoS One 2018; 13:e0201453. doi:10.1371/journal.pone.0201453.

[52] Vannini E, Maltese F, Olimpico F, Fabbri A, Costa M, Caleo M, et al. Progression of motor deficits in glioma-bearing mice: Impact of CNF1 therapy at symptomatic stages. Oncotarget 2017; 8:23539-50. doi:10.18632/oncotarget.15328.

[53] Variya BC, Bakrania AK, Madan P, Patel SS. Acute and 28-days repeated dose sub-acute toxicity study of gallic acid in albino mice. Regul Toxicol Pharmacol 2019; 101:71-8. doi: 10.1016/j.yrtph.2018.11.010.

[54] Bai J, Zhang Y, Tang C, Hou Y, Ai X, Chen X, et al. Gallic acid: Pharmacological activities and molecular mechanisms involved in inflammation-related diseases. Biomed Pharmacother 2021; 133:1-14. doi:10.1016/j.biopha.2020.110985.

[55] Zhou Y, Wang L, Wang C, Wu Y, Chen D, Lee TH. Potential implications of hydrogen peroxide in the pathogenesis and therapeutic strategies of gliomas. Arch Pharm Res 2020; 43:187-203. doi:10.1007/s12272-020-01205-6.

[56] Schiffer D, Annovazzi L, Casalone C, Corona C, Mellai M. (2019). Glioblastoma: microenvironment and niche concept. Cancers 2021; 11:5-22. doi:10.3390/cancers11010005.

[57] Olivier C, Oliver L, Lalier L, Vallette FM. Drug resistance in glioblastoma: The two faces of oxidative stress. Front Mol Biosci 2021; 7:468-84. doi: 10.3389/fmolb.2020.620677.

[58] Ighodaro OM, Akinloye OA. First line defence antioxidants-superoxide dismutase (SOD), catalase (CAT) and glutathione peroxidase (GPx): Their fundamental role in the entire antioxidant defence grid. Alexandria J Med 2018; 54:287-93. doi: 10.1016/j.ajme.2017.09.001.

[59] Hayes JD, Dinkova-Kostova AT, Tew KD. Oxidative stress in cancer. Cancer cell 2020; 38:167-97. doi:10.1016/j.ccell.2020.06.001.

[60] Backos DS, Franklin CC, Reigan P. The role of glutathione in brain tumor drug resistance. Biochem Pharmaco 2012; 83:1005-12. doi:10.1016/j.bcp.2011.11.016.

[61] Tanriverdi T, Hanimoglu H, Kacira T, Sanus GZ, Kemerdere R, Atukeren P, et al. Glutathione peroxidase, glutathione reductase and protein oxidation in patients with glioblastoma multiforme and transitional meningioma. J Cancer Res Clin Oncol 2007; 133:627-33. doi:10.1007/s00432-007-0212-2.

[62] Cirak B, Inci S, Palaoglu S, Bertan V. Lipid peroxidation in cerebral tumors. Clin Chim Acta 2003; 327:103-7. doi:10.1016/S0009-8981(02)00334-0.

[63] Best MG, Sol N, Zijl S, Reijneveld JC, Wesseling P, Wurdinger T. Liquid biopsies in patients with diffuse glioma. Acta Neuropathol 2015; 129:849-65. doi:10.1007/s00401-015-1399-y.

[64] Wang PF, Meng Z, Song HW, Yao K, Duan ZJ, Yu CJ, et al. Preoperative changes in hematological markers and predictors of glioma grade and survival. Front Pharmacol 2018; 9:886-93. 10.3389/fphar.2018.00886.

[65] Marx S, Xiao Y, Baschin M, Splittstöhser M, Altmann R, Moritz E, et al. The role of platelets in cancer pathophysiology: focus on malignant glioma. Cancers 2019; 11:569-81. doi:10.3390/cancers11040569.

[66] Wink MR, Lenz G, Braganhol E, Tamajusuku AS, Schwartsmann G, Sarkis JJ, et al. Altered extracellular ATP, ADP and AMP catabolism in glioma cell lines. Cancer Lett 2003; 198: 211-8. doi:10.1016/S0304-3835(03)00308-2.

[67] Cattaneo M. The platelet P2 receptors. In: Michelson AD, editor. Platelets. Academic Press: Elsevier Inc; 2019, p. 259-77. doi:10.1016/B978-0-12-813456-6.00014-X.

[68] Baran O, Kemerdere R, Korkmaz TS, Kayhan A, Tanriverdi T. Can preoperative neutrophil to lymphocyte, lymphocyte to monocyte, or platelet to lymphocyte ratios differentiate glioblastoma from brain metastasis? Medicine 2019; 98:e18306. doi:10.1097/MD.0000000000018306.

[69] Zanini D, Schmatz R, Pelinson LP, Pimentel VC, Da Costa P, Cardoso AM, et al. Ectoenzymes and cholinesterase activity and biomarkers of oxidative stress in patients with lung cancer. Mol Cell Biochem 2013; 374:137-48. doi:10.1007/s11010-012-1513-6.

[70] Urunsak IF, Gulec UK, Paydas S, Seydaoglu G, Guzel AB, Vardar MA. Adenosine deaminase activity in patients with ovarian neoplasms. Arch Gynecol Obstet 2012; 286:155-9. doi:10.1007/s00404-012-2279-5.

[71] Manjula S, Raja A, Rao SN, Aroor AR, Rao A. Serum adenosine deaminase activity in brain tumours. Acta neurochir 1993; 121:149-151. doi:10.1007/BF01809267.

[72] Yegutkin, GG. Nucleotide-and nucleoside-converting ectoenzymes: important modulators of purinergic signalling cascade. *Biochim Biophys Acta Mol Cell* Res 2008; 1783:673-94. doi:10.1016/j.bbamcr.2008.01.024.

[73] Chang SS, Lee VS, Tseng YL, Chang KC, Chen KB, Chen YL, et al. Gallic acid attenuates platelet activation and platelet-leukocyte aggregation: Involving pathways of Akt and GSK3β. Evid *Based* Complementary Altern Med 2012; 2012:1-9. doi:10.1155/2012/683872.

[74] Campanella R, Guarnaccia L, Cordiglieri C, Trombetta E, Caroli M, Carrabba G, et al. Tumor-educated platelets and angiogenesis in glioblastoma: another brick in the wall

for novel prognostic and targetable biomarkers, changing the vision from a localized tumor to a systemic pathology. Cells 2020; 9:294-309. doi:10.3390/cells9020294.

**Table 1.** Serum markers of tissue damage in control animals and *Wistar* rats with GBM-implant or treated with GA

| | Control | GBM | GA 50 | GA 100 |
|---|---|---|---|---|
| Glucose (mg/dL) | 112.0 ± 3.3 | 83.0 ± 5.0 | 97.4 ± 7.5 | 99.4 ± 3.9 |
| Creatinine (mg/dL) | 0.43 ± 0.03 | 0.45 ± 0.02 | 0.42 ± 0.01 | 0.37 ± 0.01 |
| Urea (mg/dL) | 47.2 ± 3.0 | 47.4 ± 2.6 | 47.2 ± 2.6 | 48.6 ± 2.3 |
| ALT (U/L) | 49.0 ± 2.5 | 48.0 ± 2.1 | 41.6 ± 4.6 | 41.0 ± 1.1 |
| AST (U/L) | 203.2 ± 19.5 | 247.2 ± 3.9 | 218.2 ± 9.7 | 206.0 ± 11.5 |

Control and GBM (water-treated), GA 50 (50 mg/kg/day), or GA 100 (100 mg/kg/day) were administered for 15 days. Data are analyzed with one-way analysis of variance followed by the Tukey post hoc test and expressed as mean ± standard error.

**Table 2.** ROS, TBARS, nitrite, and SH levels and SOD, CAT, and GST activities in the brain of *Wistar* rats with GBM-implant or treated with GA

| | Control | GBM | GA 50 | GA 100 |
|---|---|---|---|---|
| ROS | 34.3 ± 2.2 | 75.4 ± 3.5$^{###}$ | 40.81 ± 4.2$^{***}$ | 37.5 ± 2.5$^{***}$ |
| TBARS | 7.8 ± 1.1 | 13.2 ± 1.5$^{#}$ | 7.6 ± 0.4$^{**}$ | 8.7 ± 0.5$^{**}$ |
| Nitrite | 9.3 ± 0.7 | 13.7 ± 0.9$^{#}$ | 9.4 ± 1.2$^{*}$ | 9.3 ± 0.9$^{*}$ |
| SH | 102.4 ± 4.1 | 68.5 ± 4.5$^{#}$ | 104.4 ± 10.5$^{*}$ | 103.9 ± 9.7$^{*}$ |
| SOD | 13.9 ± 0.5 | 7.6 ± 2.6$^{###}$ | 11.0 ± 0.6$^{*}$ | 11.2 ± 0.6$^{*}$ |
| CAT | 2.1 ± 0.2 | 0.9 ± 0.2$^{##}$ | 1.8 ± 0.1$^{*}$ | 1.7 ± 0.1$^{*}$ |
| GST | 497.8 ± 29.0 | 476.3 ± 39.6 | 472.5 ± 46.4 | 520.3 ± 77.2 |

Abbreviations: GA 50, (50 mg/kg/day treated); GA 100, (100 mg/kg/day treated); GBM, glioblastoma; ROS, reactive oxygen species; SH, sulfhydryl content; SOD, superoxide dismutase; CAT, catalase; GST, glutathione S-transferase.

ROS levels are expressed as ⌈mol DCF/mg protein, nitrite levels as ⌈M nitrite/mg protein, thiol content as nmol TNB/mg protein, SOD and CAT activities as U/mg protein, and GST as ⌈mol GS-DNB min/mg protein. Data are analyzed with one-way analysis of variance followed by the Tukey post hoc test and expressed as mean ± standard error. $^{#, ##, ###}$Significant difference compared with the control group ($P < 0.05$, $P < 0.01$, and $P < 0.0001$, respectively). $^{*, **, ***}$Significant difference compared with the GBM group ($P < 0.05$, $P < 0.01$, and $P < 0.0001$, respectively).

**Table 3.** ROS, TBARS, nitrite, and SH levels and SOD, CAT, and GST activities in serum and platelets of *Wistar* rats with GBM implant or treated with GA

| | Control | GBM | GA 50 | GA 100 |
|---|---|---|---|---|
| **Serum** | | | | |
| ROS | 47.7 ± 4.9 | 200.1 ± 28.8$^{###}$ | 38.4 ± 2.5$^{***}$ | 32.4 ± 5.5$^{***}$ |
| Nitrite | 6.8 ± 0.6 | 21.6 ± 3.0$^{###}$ | 5.6 ± 1.1$^{***}$ | 5.3 ± 1.6$^{***}$ |
| SH | 51.9 ± 9.8 | 46.9 ± 2.6 | 31.6 ± 4.9 | 51.2 ± 1.8 |
| SOD | 10.2 ± 1.4 | 3.4 ± 1.3$^{##}$ | 9.4 ± 0.7$^{*}$ | 9.3 ± 0.8$^{*}$ |
| CAT | 0.3 ± 0.04 | 0.8 ± 0.01$^{##}$ | 0.2 ± 0.05$^{**}$ | 0.3 ± 0.03$^{**}$ |
| GST | 1613.0 ± 303.6 | 1647.0 ± 192.5 | 1728.0 ± 294.0 | 1331.0 ± 160.7 |
| **Platelets** | | | | |
| ROS | 63.1 ± 8.4 | 146.0 ± 15.5$^{###}$ | 87.5 ± 8.7$^{**}$ | 57.7 ± 8.8$^{**}$ |
| Nitrite | 5.3 ± 0.9 | 12.0 ± 1.7$^{##}$ | 7.2 ± 1.2 | 4.8 ± 0.9$^{**}$ |
| SH | 190.7 ± 41.4 | 257.3 ± 31.0 | 261.9 ± 25.6 | 200.0 ± 13.5 |
| SOD | 450.3 ± 90.9 | 469.8 ± 71.8 | 565 ± 49.4 | 423.7 ± 12.9 |
| CAT | 30.6 ± 4.6 | 14.8 ± 1.7$^{#}$ | 30.8 ± 2.0$^{*}$ | 29.6 ± 3.2$^{*}$ |
| GST | 1329.0 ± 260.3 | 1451.0 ± 173.9 | 1572.0 ± 58.2 | 1047.0 ± 39.4 |

Abbreviations: GA 50, (50 mg/kg/day treated); GA 100, (100 mg/kg/day treated); GBM, glioblastoma; ROS, reactive oxygen species; SH, total sulfhydryl content; SOD, superoxide dismutase; CAT, catalase; GST, glutathione S-transferase.

ROS levels are expressed as ⌈mol DCF/mg protein, nitrite levels as ⌈M nitrite/mg protein, thiol content as nmol TNB/mg protein, SOD and CAT activities as U/mg protein, and GST as ⌈mol GS-DNB min/mg protein. Data are analyzed with one-way analysis of variance followed by the Tukey post hoc test and expressed as mean ± standard error. $^{#, ##, ###}$Significant difference compared with the control group ($P < 0.05$, $P < 0.01$, and $P < 0.0001$, respectively). $^{*, **, ***}$Significant difference compared with the GBM group ($P < 0.05$, $P < 0.01$, and $P < 0.0001$, respectively).

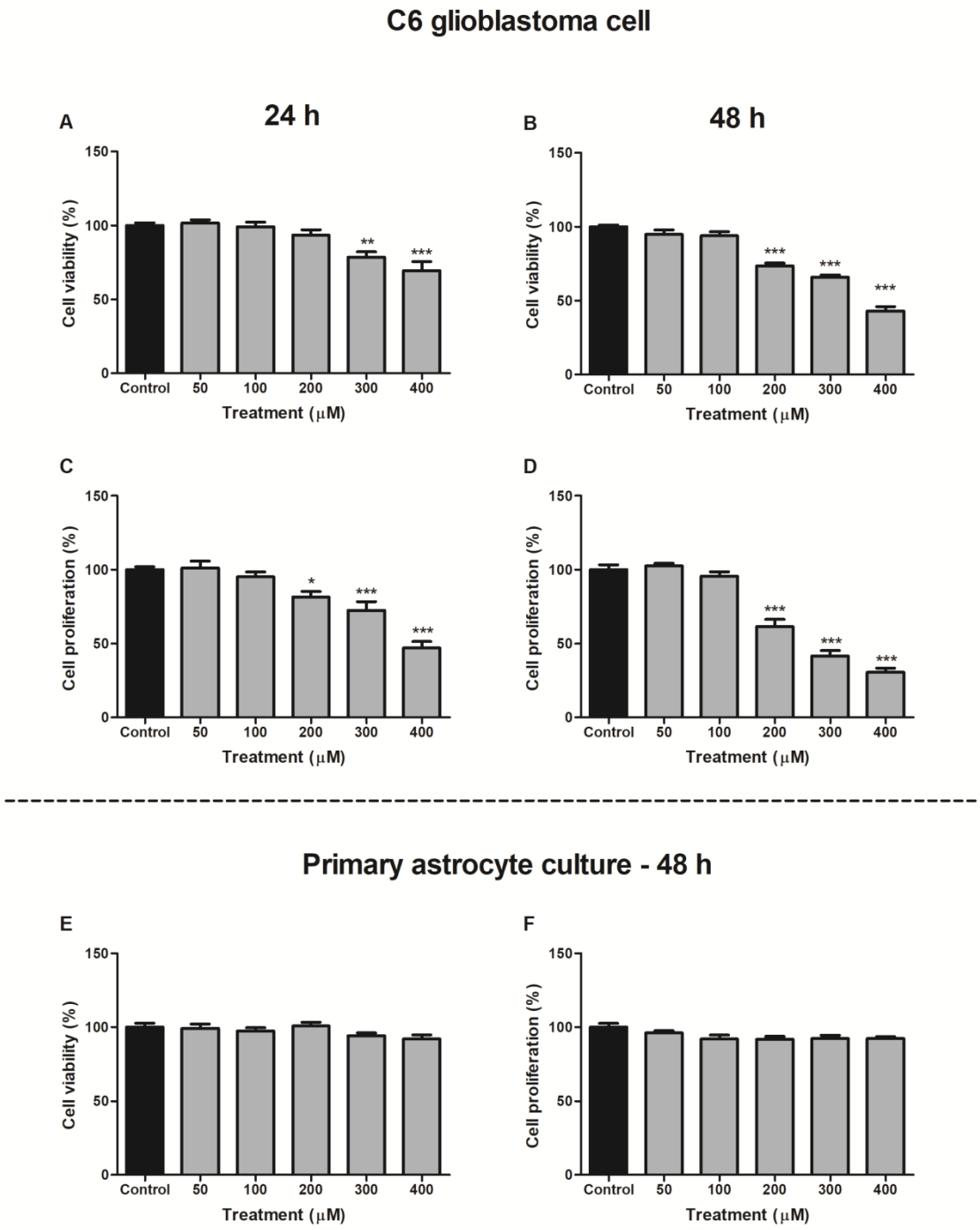


**Figure 1.** Effect of GA on viability (**A** and **B**) and cell proliferation (**C** and **D**) of the C6 GBM cell line after 24 (**A** and **C**) and 48 h (**B** and **D**) of treatment. Analysis of viability (**E**) and proliferation (**F**) of primary astrocyte cultures exposed to GA are also observed after 48 h of treatment. Data are analyzed with one-way analysis of variance followed by the Tukey post hoc test and expressed as mean ± standard error. *, **, ***Significant difference compared to control cells ($P < 0.05$, $P < 0.01$, and $P < 0.0001$, respectively).

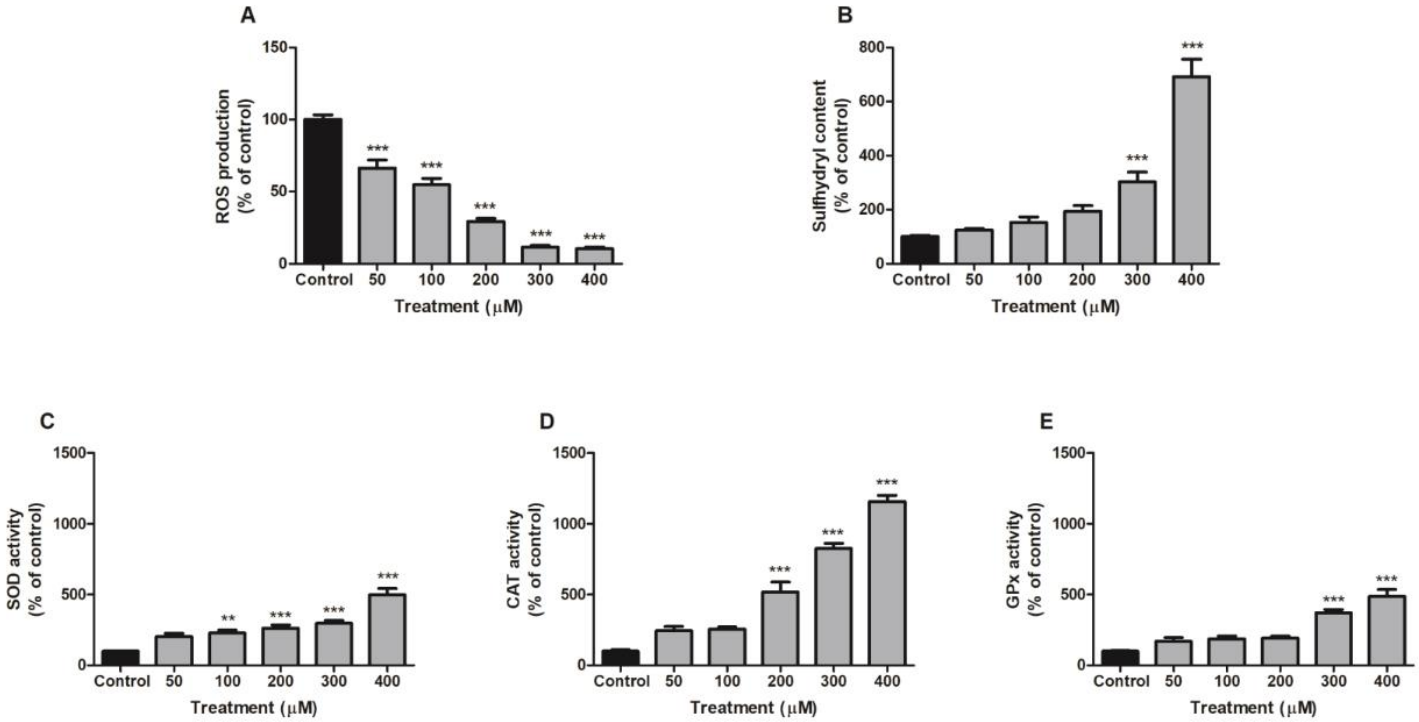


**Figure 2.** Parameters of oxidative stress in C6 GBM cells exposed to GA for 48 h. (**A**) Production of reactive oxygen species (ROS); (**B**) total sulfhydryl content (SH content); (**C**) superoxide dismutase (SOD) activity; (**D**) catalase (CAT) activity and (**E**) glutathione peroxidase (GPx). Results are expressed as a percentage of control (control value ROS, 1200.25 mol DCF/mg protein; control value SH, 87.41 nmol TNB/mg of protein; control value SOD, 371.56 units/mg of protein; control value CAT, 6.18 units/mg of protein; control value GPx, 68.66 units/mg of protein). Data are analyzed with one-way analysis of variance followed by the Tukey post hoc test and expressed as mean ± standard error. $^{**}$, $^{***}$Significant difference compared to control cells ($P < 0.01$ and $P < 0.0001$, respectively).

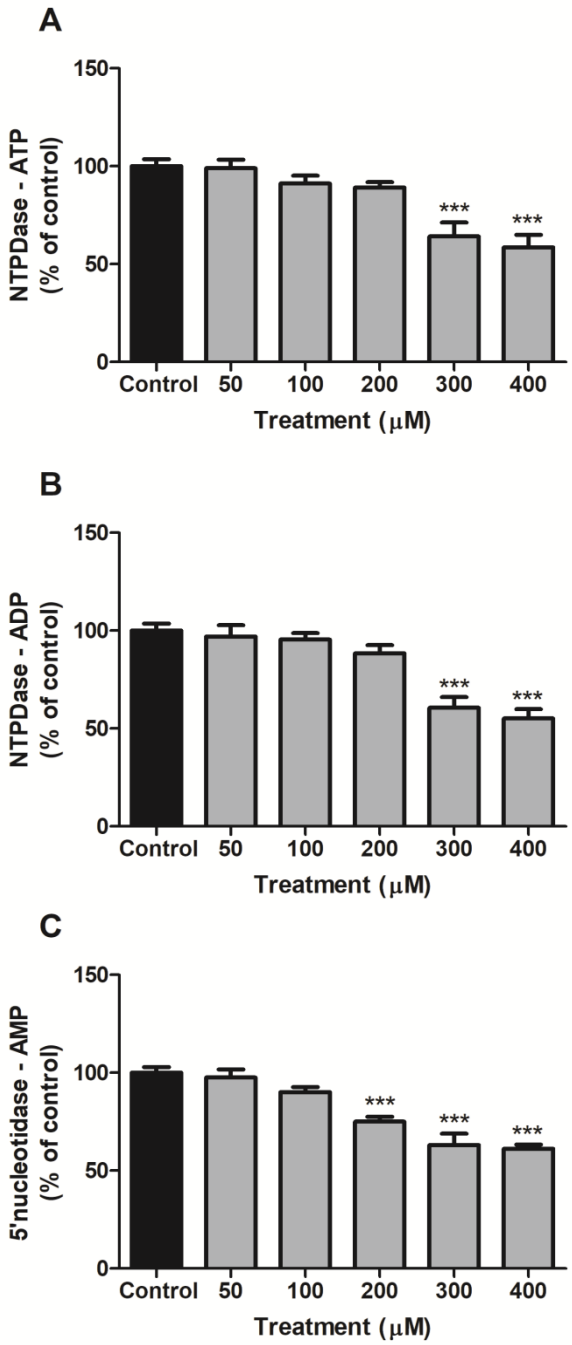


**Figure 3.** Nucleotide hydrolysis in C6 GBM cells exposed for 48 h to GA. (**A**) NTPDase activity using ATP as substrate; (**B**) NTPDase activity using ADP as substrate and (**C**) 5'nucleotidase activity using AMP as substrate. Results are expressed as a percentage of control (control value ATP hydrolysis, 8.20 nmol Pi released/min/mg of protein; control value ADP hydrolysis, 6.73 Pi released/min/mg of protein; control value AMP hydrolysis, 32.29 Pi released/min/mg of protein). Data are analyzed with one-way analysis of variance followed by the Tukey post hoc test and expressed as mean ± standard error. $^{***}$Significant difference compared to control cells ($P < 0.0001$).

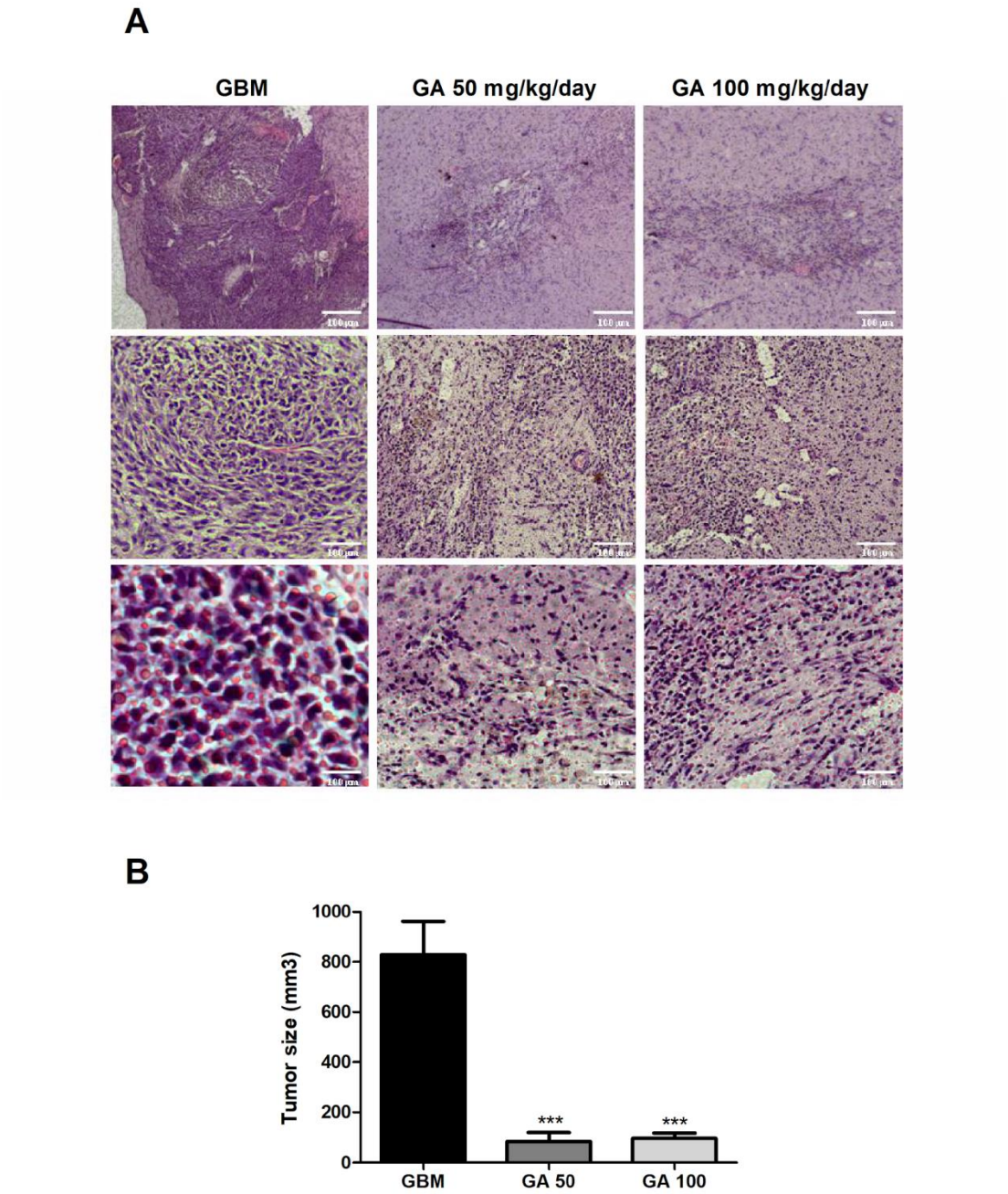


**Figure 4.** Histological characteristics (**A**) and tumor size quantification (**B**) of *Wistar* rats with GBM implant or treated with GA. For tumor size quantification, images are captured from HE slices of the implanted GBM using a digital camera connected to a microscope and the total volume ($mm^3$) is determined using ImageJ Software. Magnification 4, 20, and 40 for top, central, and bottom panels, respectively. Data are analyzed with one-way analysis of variance followed by the Tukey post hoc test and expressed as mean ± standard error. $^{***}$Significant difference compared to the GBM group ($P < 0.0001$).

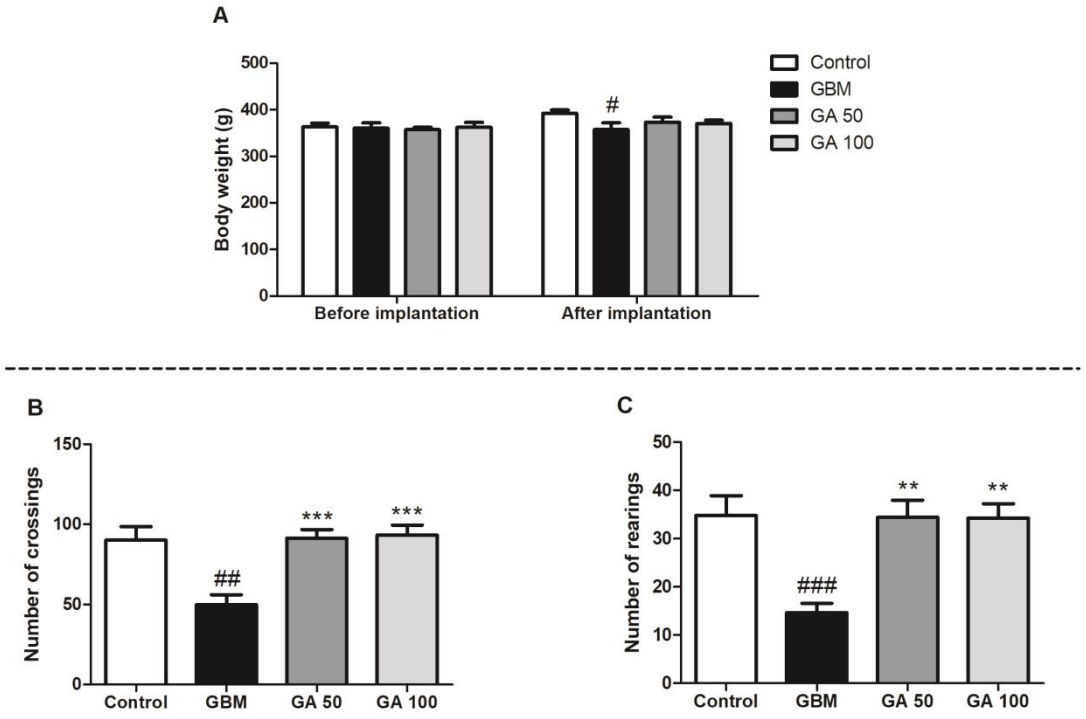


**Figure 5.** Analysis of body weight and behavioral changes in *Wistar* rats with GBM implants or treated with GA. Body weight (**A**) is analyzed every 3 days. Locomotor activity was evaluated through the number of crossings (**B**) and rearings (**C**). Data are analyzed with one-way analysis of variance followed by the Tukey post hoc test and expressed as mean ± standard error. $^{\#, \#\#, \#\#\#}$Significant difference compared to the control group ($P < 0.05$, $P < 0.01$, and $P < 0.0001$, respectively). $^{**, ***}$Significant difference compared to the GBM group ($P < 0.01$ and $P < 0.0001$, respectively).

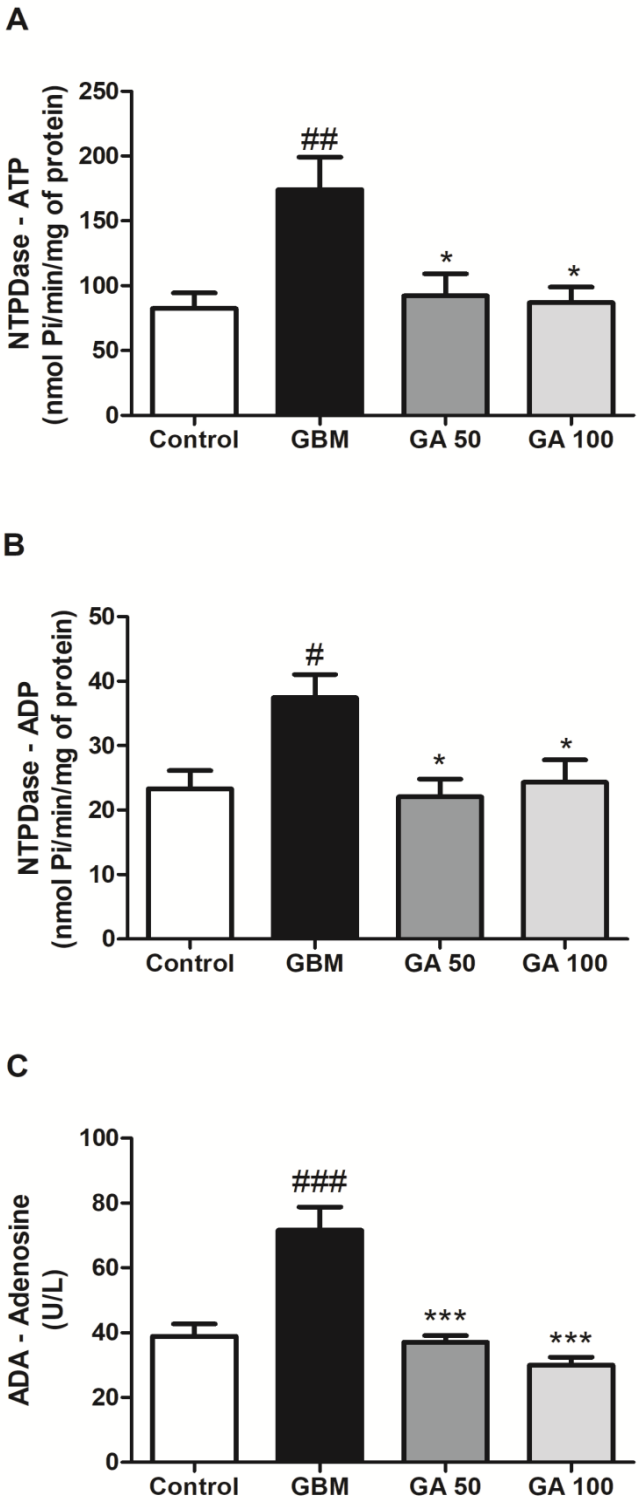


**Figure 6.** Nucleotide hydrolysis in lymphocytes of *Wistar* rats with GBM implant or treated with GA. (**A**) NTPDase activity using ATP as substrate; (**B**) NTPDase activity using ADP as substrate and (**C**) adenosine deaminase (ADA) activity using adenosine as substrate. Data are analyzed with one-way analysis of variance followed by the Tukey post hoc test and expressed as mean ± standard error. $^{\#, \#\#, \#\#\#}$Significant difference compared to the control group ($P < 0.05$, $P < 0.01$, and $P < 0.0001$, respectively). $^{*, ***}$Significant difference compared to the GBM group ($P < 0.05$ and $P < 0.0001$, respectively).

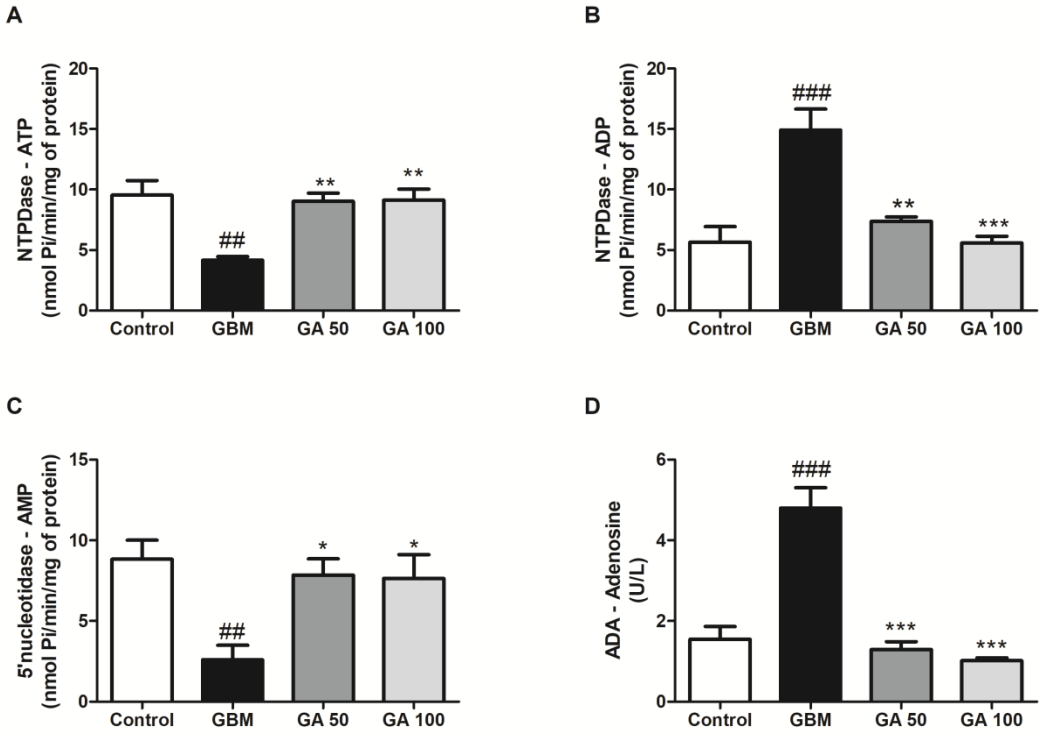


**Figure 7.** Nucleotide hydrolysis in platelets of *Wistar* rats with GBM implant or treated with GA. (**A**) NTPDase activity using ATP as substrate; (**B**) NTPDase activity using ADP as substrate; (**C**) 5'nucleotidase activity using AMP as substrate and (**D**) adenosine deaminase (ADA) activity using adenosine as substrate. Data are analyzed with one-way analysis of variance followed by the Tukey post hoc test and expressed as mean ± standard error. $^{\#\#,\#\#\#}$Significant difference compared to the control group ($P < 0.01$ and $P < 0.0001$, respectively). $^{*,**,***}$Significant difference compared to the GBM group ($P < 0.05$, $P < 0.01$, and $P < 0.0001$, respectively).

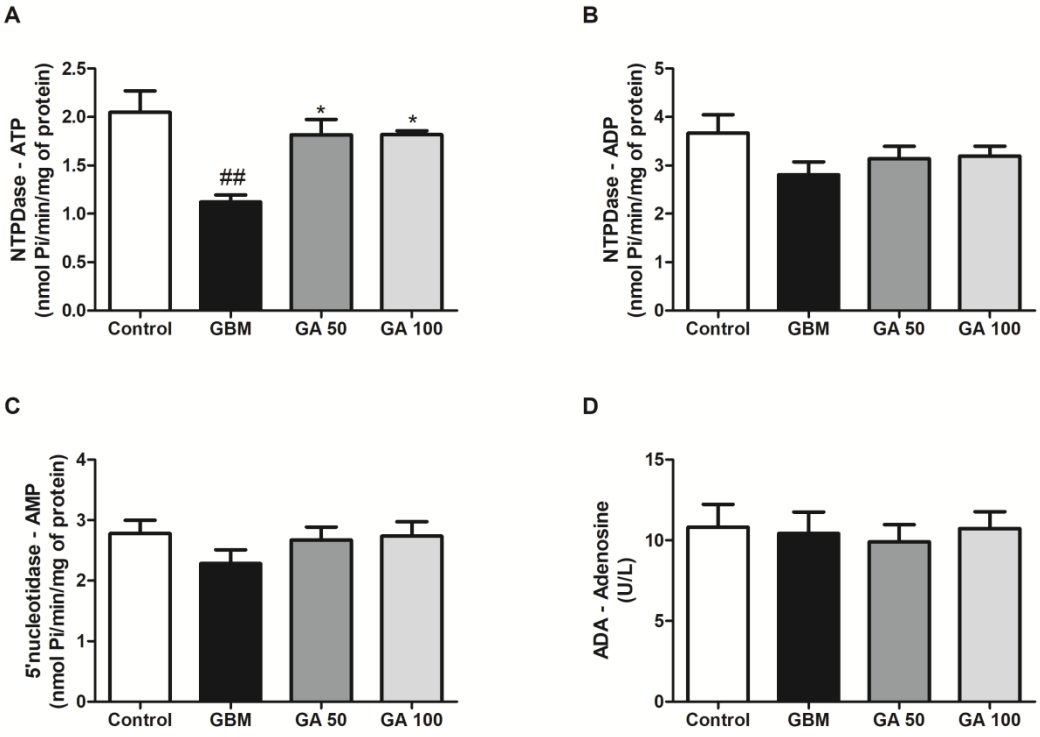


**Figure 8.** Nucleotide hydrolysis in serum of *Wistar* rats with GBM implant or treated with GA. (**A**) NTPDase activity using ATP as substrate; (**B**) NTPDase activity using ADP as substrate; (**C**) 5'nucleotidase activity using AMP as substrate and (**D**) adenosine deaminase (ADA) activity using adenosine as substrate. Data are analyzed with one-way analysis of variance followed by the Tukey post hoc test and expressed as mean ± standard error. $^{\#\#}$Significant difference compared to the control group ($P < 0.01$). $^{*}$Significant difference compared to the GBM group ($P < 0.05$).

## 5. DISCUSSÃO INTEGRADA

O câncer é considerado o principal problema de saúde pública mundial (SIEGEL *et al*., 2021). De acordo com o Observatório Global do Câncer (GLOBOCAN, do inglês "*Global Cancer Observatory*"), aproximadamente 10 milhões de pessoas morrem a cada ano. Além disso, a taxa de incidência e mortalidade tem aumentado rapidamente em todo o mundo (SUNG *et al*., 2021). Atualmente, a terapia anticâncer padrão inclui ressecção cirúrgica, quimioterapia e/ou radioterapia.

A quimioterapia consiste no tratamento padrão para a maioria dos pacientes com neoplasias malignas, especialmente quando a remoção cirúrgica total não é possível (ZHANG *et al*., 2020). A principal desvantagem da quimioterapia consiste na não seletividade dos agentes quimioterápicos. De acordo com Yarana e Clair (2017), cerca de 50% dos agentes antineoplásicos aprovados pelo FDA estão associados com a produção de ERO. Apesar de ser bem estabelecida a importância da formação de ERO na morte celular programada das células tumorais, os tecidos saudáveis também tornam-se alvos de danos oxidativos aumentando o risco de recorrência e metástases (AKTER *et al*., 2021).

Diante dos efeitos adversos e resistência terapêutica desencadeada por uma variedade de agentes antitumorais aplicados na clínica, diversos pesquisadores têm focado no uso de produtos naturais como coadjuvantes no tratamento do câncer (AKTER *et al*., 2021; ZHANG *et al*., 2018). Plantas, fungos, insetos e organismos marinhos desempenham um importante papel na produção de compostos naturais de interesse farmacológico (ZHANG *et al*., 2018).

De maneira geral, os fungos são conhecidos por sua atividade patogênica, podendo desencadear doenças em plantas, animais e humanos mediante a produção de micotoxinas (TYAGI *et al*., 2021). No entanto, os fungos endofíticos, um nicho que tem se destacado no meio científico, são microrganismos que habitam os tecidos saudáveis compartilhando uma relação endossimbiótica com a planta hospedeira. Assim, os fungos endofíticos produzem metabólitos secundários que promovem o crescimento e protegem a planta de patógenos, além de aumentar a capacidade da planta de tolerar o estresse biótico e abiótico. Em troca, a planta hospedeira fornece nutrientes para a sobrevivência desses endófitos (STROBEL; DAISY, 2003).

Há uma grande diversidade biológica de microrganismos endofíticos distribuídos naturalmente no Ártico, na Antártida, em regiões temperadas e florestas tropicais (YU *et al*., 2014; JIA *et al*., 2016). Evidências sugerem ainda que as plantas medicinais podem hospedar um ou mais fungos endofíticos (STROBEL; DAISY, 2003; KUSARI, HERTWECK; SPITELLER, 2012).

Famosa por suas propriedades anti-inflamatórias e eficácia no tratamento de distúrbios gastrointestinais, a *A. satureioides* (família Astereaceae) foi instituída como “Planta Medicinal Símbolo do Estado do Rio Grande do Sul” sob a Lei nº 11.858, de 5 de dezembro de 2002 (BRASIL, 2002). Além disso, de acordo com a lista de plantas de interesse do SUS, a *A. satureioides* ocupa a primeira posição na Relação Estatual de Plantas Medicinais Nativas mais utilizadas pela população do Rio Grande do Sul (BRASIL, 2017). Diante das atribuições farmacológicas e da falta de estudos avaliando a composição endofítica desta planta medicinal, recentemente estudos prévios do nosso grupo de pesquisa demonstraram o isolamento de um fungo endofítico a partir de *A. satureioides*, cuja micoteca foi armazenada no acervo do Laboratório de Neuroquímica, Inflamação e Câncer sob o código MF31b11 (PEDRA *et al*., 2018). No entanto, dificuldades na caracterização das estruturas reprodutivas do fungo isolado prejudicaram a identificação morfológica deste microrganismo.

Neste contexto, inicialmente, o capítulo 1 da presente tese visou elucidar a taxonomia do endófito de *A. satureioides*. Para isso, a região ITS foi amplificada e as sequências obtidas foram comparadas com sequências de nucleotídeos existentes no repositório do GenBank. De acordo com a análise molecular, o fungo endofítico foi identificado como *Biscogniauxia* sp. (ON257911). Evidências apontam que espécies de *B. repanda* (CALLAN, 1986) e *B. petrensis* (DAS *et al*., 2020; SAHOO; SUBBAN; CHELLIAH, 2021) liberam gotículas avermelhadas após 10 a 14 dias de crescimento em meio de cultivo de batata-dextrose-ágar a 25 ºC. Esta característica também foi observada na superfície do micélio de *Biscogniauxia* sp. isolado de *A. satureioides*, a partir de 14 dias de inoculação nas mesmas condições de cultivo.

A ocorrência de *Biscogniauxia* tem sido relatada em espécies de líquen *Usnea mutabilis* Stirt. (ZHAO *et al*., 2021), e algas marinhas como *Halimeda macroloba*, *Enteromorpha flexuosa* e *Champia parvula* (SAHOO; SUBBAN; CHELLIAH, 2021). Esses microrganismos também habitam os tecidos saudáveis

de plantas medicinais do gênero *Cinnamomum* sp. (CHENG *et al*., 2012), *Echinacea* sp. (CARVALHO *et al*., 2016) e *Dendrobium* sp. (MA *et al*., 2020). Além disso, cabe ressaltar que este microrganismo tem sido frequentemente encontrado em espécies de plantas e algas distribuídas em países da América do Norte, Ásia, Europa e África (CARVALHO *et al*., 2016; BUBKAMP; LANGER; LANGER, 2020; MA *et al*., 2020; SAHOO; SUBBAN; CHELLIAH, 2021; YANGUI *et al*., 2021), no entanto, os dados do presente estudo consistem no primeiro relato evidenciando a ocorrência de *Biscogniauxia* no Brasil.

Embora cepas de *Biscogniauxia* apresentem comportamento endofítico, estes microrganismos podem atuar como patógenos oportunistas em plantas suscetíveis ao estresse hídrico prolongado, induzindo descoloração dos tecidos lenhosos, morte e câncer de caules e galhos (EVIDENTE *et al*., 2005; ZHAO *et al*., 2021). Dada a utilização de caules sadios, sem sintomas de doença, e a eficiência no processo de desinfestação superficial (PEDRA *et al*., 2018), esta tese descreve pela primeira vez a identificação taxonômica de um fungo endofítico isolado a partir de plantas do gênero *Achyrocline* spp., bem como a habilidade de espécies de *A. satureioides* em hospedar o endófito *Biscogniauxia* sp.

De modo geral, microrganismos endofíticos que habitam os tecidos de plantas medicinais são caracterizados por produzirem compostos com estruturas únicas e inúmeras propriedades farmacológicas, atuando como um interessante reservatório de substâncias bioativas, especialmente na terapia anticâncer (HRIDOY *et al*., 2022). Desde o primeiro estudo sobre os componentes químicos produzidos por *Biscogniauxia* sp. (EVIDENTE *et al*., 2005), vários metabólitos secundários foram relatados, incluindo as azafilonas, isocumarinas, meroterpenóides e sesquiterpenos (EVIDENTE *et al*., 2005; CHENG *et al*., 2012; AMAND *et al*., 2012; ZHAO *et al*., 2017; ZHAO *et al*., 2021; SRITHARAN *et al*., 2019).

No presente estudo, 17 compostos foram identificados na fração purificada ($F_{DCM}$) do endofítico de *A. satureioides*. A identificação putativa foi determinada de acordo com dados disponíveis na literatura, como padrão analítico autêntico, massa molecular exata, fórmula molecular, padrões de fragmentação iônica (MS/MS) e/ou biossíntese desses metabólitos a partir da família Xylariaceae, a qual o *Biscogniauxia* pertence. Por outro lado, 11

compostos não puderam ser identificados (compostos desconhecidos A-J), pois seus componentes cromatográficos ou espectrais não coincidem com relatos científicos para espécies desta família. É importante salientar que o termo “composto desconhecido” não torna estas substâncias inéditas, apenas que estes metabólitos não exibem características químicas de substâncias produzidas pela família Xylariaceae podendo assim, ser sintetizados a partir outras famílias endofíticas.

De acordo com a caracterização química do extrato fracionado $F_{DCM}$, apenas os meroterpenóides (biscogniácido A [**13**], biscognina A [**15**] e biscognina B [**10**]) e as meleínas (8-metoxi-5-metilmeleína [**14**] e 5-metoxicarbonilmeleína [**18**]) têm sido descritos como compostos bioativos produzidos por fungos do gênero *Biscogniauxia*. (AMAND *et al*., 2012; RAJA *et al*., 2015; RUBALCABA; FERNÁNDEZ, 2017; ZHAO *et al*., 2017). Neste sentido, o presente estudo descreve pela primeira vez a habilidade desta cepa endofítica em sintetizar interessantes metabólitos secundários como: a isocumarina orthosporina [**7**]; os sesquiterpenos nigriterpeno A [**8**] e 10-xilariterpenoide [**12**]; as citocalasinas curtacalasina A [**23**], citocalasina E [**24**] e epoxicitocalasinas Z8 [**26**], Z8 isômero [**27**] e Z17 [**28**]; assim como outros derivados de policetídeos como a daldinina C [**4**], 7'dicloro-5'-hidroxigriseofulvina [**6**] e daldinona D [**17**].

Adicionalmente, a síntese da lactona macrocíclica Sch-642305 [**22**] pelo *Biscogniauxia* de *A. satureioides* também foi observada. A Sch-642305 é comumente produzida por fungos do gênero *Phomopsis* (família Diaporthaceae) (ADELIN *et al*., 2011) e *Penicillium* (família Aspergillaceae) (CHU *et al*., 2003; NICOLLETI *et al*., 2007), no entanto a biossíntese desta lactona por endofíticos da família Xylariaceae não é mencionada na literatura. Embora não pertençam à ordem Xylariales, estes microrganismos são frequentemente isolados a partir de plantas da família Astereaceae (CARUSO *et al*., 2020). Neste sentido, a produção de Sch-642305 por um membro da família Xylariaceae é inédita.

É bem estabelecido que a distância espacial entre plantas presentes em um determinado ecossistema pode alterar a composição endofítica das mesmas. Assim, análises filogenéticas de herbáceas nativas da família Asteraceae, sugerem que a presença de comunidades microbianas divergentes reflete as condições ambientais locais, resultando assim, na produção de metabólitos secundários inéditos inclusive de fungos endofíticos conhecidos (WHITAKER *et*

*al*., 2020). Neste contexto, uma vez que os compostos gerados a partir de um único fungo endofítico podem ser influenciados tanto pelas interações entre estes microrganismos quanto pelos componentes químicos da planta hospedeira (YAN *et al*., 2019), a síntese de Sch-642305 pelo *Biscogniauxia* sp. pode ser resultado da comunicação com endófitos coexistentes e associações simbióticas com a *A. satureioides*.

Diversas propriedades farmacológicas têm sido relacionadas aos metabólitos bioativos produzidos por cepas endofíticas de *Biscogniauxia*, como atividades antimicrobiana (CHENG *et al*., 2012; LIU *et al*., 2019), anti-inflamatória (JANTAHARN *et al*., 2021; ZHAO *et al*., 2021); antioxidante (SRITHARAN *et al*., 2019) e anticolinesterásica (WU *et al*., 2016; LIU *et al*., 2019). Além disso, terpenóides, meleínas e derivados de policetídeos sintetizados por espécies de *Biscogniauxia* induzem citotoxicidade em linhagens de câncer de cólon humano (HCT-15, HT-29, HCT-116 e SW480), adenocarcinoma cervical humano (HeLa), adenocarcinoma de mama humano (MCF-7), adenocarcinoma de pulmão humano (A549), leucemia mielogênica humana (K562) e câncer hepático humano (HepG2) (FIGUEROA *et al*., 2015; ZHAO *et al*., 2017; MA *et al*., 2020; JANTAHARN *et al*., 2021; SAHOO; SUBBAN; CHELLIAH, 2021).

Diante dos efeitos antitumorais promovidos pelo metabolismo secundário de *Biscogniauxia*, inicialmente avaliamos a atividade citotóxica da fração purificada $F_{DCM}$ sobre a linhagem celular de melanoma humano (A375). A A375 é uma linhagem celular altamente invasiva obtida a partir de melanoma metastático sólido (JURKOWSCA *et al*., 2010). Estudos apontam que a taxa de resposta de pacientes com melanoma metastático ao quimioterápico dacarbazina é relativamente baixa (SOLAK *et al*., 2021; LAUX *et al*., 2022). De acordo com Laux e colaboradores (2022), após 72 h de tratamento, este agente alquilante exibe $IC_{50}$ de 29,27 µg/mL sobre células de melanoma humano (A375) e provoca danos às células saudáveis.

Na presente investigação, o $F_{DCM}$ reduziu significativamente a viabilidade e proliferação das células de melanoma humano (A375). Após 72 h de tratamento, o extrato fracionado exibiu valores de $IC_{50}$ inferiores à 11 µg/mL, induzindo morte e parada no ciclo celular em G2/M. Similarmente, conforme demonstrado por Pedra e colaboradores (2018), os efeitos antiproliferativos da lactona Sch-642305 foram acompanhados por parada na fase G2/M do ciclo

celular de células de glioma de rato (C6). Tais resultados sugerem promissora atividade terapêutica do metabolismo secundário de *Biscogniauxia* sp. isolado de *A. satureioides*, encorajando mais pesquisas neste campo.

O melanoma metastático e os gliomas de alto grau são tumores malignos de origem neuroectodérmica, caracterizados por elevadas taxas de proliferação tumoral e baixo prognóstico (ENDICOTT; TAYLOR; WALSH, 2016). Comparado com outros tumores sólidos, em estágios avançados o melanoma cutâneo frequentemente induz metástases cerebrais, as quais consistem na segunda principal causa de óbitos relacionados ao melanoma metastático (SUNDARARAJAN *et al*., 2022).

Embora pacientes com glioma raramente desenvolvam metástases, a natureza infiltrativa destas neoplasias malignas torna os glioma de alto grau os tumores cerebrais primários mais agressivos do SNC (ZHANG *et al*., 2021). A quimiorresistência induzida pelo TMZ, consiste em um dos principais desafios na terapia antiglioma (FAN *et al*., 2013). Uma possível explicação para a resposta refratária dos pacientes ao tratamento é que a quimioterapia padrão não leva em consideração a participação do microambiente na progressão tumoral.

A progressão dos gliomas resulta da comunicação cruzada entre as células malignas e células normais circundantes (GAGLIANO *et al*., 2009). De fato, o GBM é caracterizado por uma população heterogênea de células, composta por astrócitos, células-tronco de GBM, células endoteliais, fibroblastos, pericitos, macrófagos e microglia, os quais facilitam o recrutamento de fatores imunes e inflamatórios, bem como, o desenvolvimento de novos vasos, além de alterar a permeabilidade da barreira hematoencefálica (SCHIFFER *et al*., 2019).

Entre os diferentes tipos celulares presentes no microambiente neoplásico, os astrócitos constituem classe de células gliais mais abundantes no microambiente do GBM, cuja interação com as células de glioma estimula a proliferação tumoral, favorece a invasão do tumor no parênquima cerebral circundante e reduzem a eficácia terapêutica mediante a secreção de fatores de crescimento e citocinas inflamatórias (BRANDÃO *et al*., 2018; TAMAI *et al*., 2022). Assim, uma vez que a presença de um microambiente heterogêneo, rico em mediadores inflamatórios é essencial para a progressão dos gliomas, torna-

se altamente relevante analisar o efeito do metabolismo secundário do fungo endofítico *Biscogniauxia* sp. sobre o sítio tumoral.

Neste contexto, no capítulo 2 da presente tese, em uma tentativa de reproduzir *in vitro* as comunicações celulares existentes no microambiente dos gliomas, avaliamos o papel do $F_{DCM}$ sobre a linhagem celular de glioma de rato C6, cultura primária de astrócitos corticais de ratos neonatos e em um modelo experimental de interação glioma-astrócito. Para a realização desta metodologia, a cultura primária de astrócitos foi cocultivada com a linhagem de glioma. Amplamente utilizada em pesquisas neuro-oncológicas, células de glioma C6 são caracterizadas por simular a alta taxa de crescimento e caráter infiltrativo do GBM (GIAKOUMETTIS; KRITIS; FOROGLOU, 2018).

Estudos apontam que astrócitos associados ao tumor desenvolvem fenótipo reativo através do processo de astrogliose (CHEKHONIN *et al*., 2018; TAMAI *et al*., 2022). Este fenômeno atenua a atividade antiproliferativa e apoptose induzida por agentes quimioterápicos como o TMZ, a doxorrubicina e a vincristina (YANG *et al*., 2014; CHEN *et al*., 2015). Contudo, neste estudo observamos que, além de reduzir significativamente a atividade metabólica das células de glioma, os efeitos citotóxicos promovidos pelo extrato fracionado de *Biscogniauxia* sp. não foram alterados pela comunicação astrócito-glioma.

Entre os mecanismos envolvidos com a resistência terapêutica induzida pela interação cruzada entre astrócitos e glioma, o estresse oxidativo desempenha um importante papel na carcinogênese e recorrência neoplásica (SCHIFFER *et al*., 2019; OLIVIER *et al*., 2021). Além de estimular a astrogliose reativa em condições patológicas, os radicais livres gerados no microambiente tumoral alteram vias relacionadas à inflamação, como a sinalização purinérgica (CHEN *et al*., 2020; SAVIO *et al*., 2021).

Evidências sugerem uma estreita relação entre o estresse oxidativo e o sistema purinérgico. Enquanto os danos oxidativos reduzem a atividade de ectoenzimas responsáveis pela hidrólise de ATP, ADP e AMP extracelulares, a ativação de determinados purinoreceptores por estes nucleotídeos estimula a produção de radicais livres (SAVIO *et al*., 2021; HUANG; TANG; SPERLAGH, 2022), resultando no aumento da proliferação, angiogênese, migração e invasão do GBM (BRAGANHOL *et al*., 2020; OSTROWSKI; PUCKO, 2022).

Corroborando com achados prévios (WINK *et al*., 2003), comparado à cultura primária de astrócitos, as células de glioma C6 isoladas e em condições de cocultivo exibiram uma redução significativa da hidrólise de ATP e um aumento na hidrólise de AMP. O catabolismo alterado dos nucleotídeos de adenina foi acompanhado por um aumento significativo nos níveis de ERO e redução expressiva do conteúdo tiólico total e atividade das enzimas antioxidantes SOD, CAT e GST em linhagem de glioma C6 e no cocultivo de astrócito-glioma, quando comparado aos astrócitos corticais saudáveis.

Diferenças importantes também foram observadas entre os modelos experimentais de glioma. A comunicação cruzada entre astrócito e glioma desencadeou um aumento na atividade ATPase e ADPase, mas uma redução na hidrólise de AMP quando comparado às culturas de glioma C6 isoladas. Não há estudos avaliando o efeito da comunicação astrócito-glioma na modulação da sinalização purinérgica mediante técnica de cocultivo. No entanto, segundo Braganhol e colaboradores (2009), a linhagem celular C6 e o modelo de células de glioma C6 *ex vivo* exibem padrões semelhantes no metabolismo de nucleotídeos extracelulares. Neste sentido, embora a interação astrócito-glioma altere vias relacionadas com a proliferação do tumor, pode-se inferir que a presença de outros componentes celulares é crucial para a modulação da resposta purinérgica no microambiente tumoral.

Com relação aos parâmetros de estresse oxidativo, o modelo de cocultivo exibiu um aumento na atividade das enzimas antioxidantes SOD e CAT, mas uma redução na atividade da enzima GST e no conteúdo sulfidril total quando comparados à linhagem celular de glioma C6. Tais alterações foram acompanhadas por modificações na liberação de citocina pró-inflamatória IL-6, no entanto, não foram observadas alterações na produção de ERO entre os protocolos experimentais.

De fato, achados prévios sugerem que os astrócitos são capazes de se adaptar ao estresse oxidativo elevando a sua capacidade antioxidante mediante o aumento dos níveis de mRNA das enzimas SOD e CAT (RÖHRDANZ *et al*., 2001; BATHIA *et al*., 2019). Além disso, entre as células dos SNC, os astrócitos são as células gliais com os níveis mais elevados de glutationa (MCBEAN, 2017), um tripeptídeo rico em grupos sulfidrilas que atua como *scavenger* de ERO e como substrato na detoxificação de subprodutos carcinogênicos pela enzima

GST (HAYES; FLANAGAN; JOWSEY, 2005; DRINGEN *et al*., 2014). No entanto, a alta taxa de secreção da citocina pró-inflamatória IL-6 por astrócitos associados ao tumor provocam alterações no metabolismo tiólico destas células gliais, reduzindo a atividade de enzimas antioxidantes, como a GST, e consequentemente reduzindo a capacidade *scavenger* de espécies reativas (STEELE *et al*., 2013).

Ao avaliar o efeito dos componentes químicos do *Biscogniauxia* sp. na modulação de tais alterações, observamos que o $F_{DCM}$ aumentou a hidrólise de ATP, ADP e AMP em ambas as culturas tumorais, mas não na cultura primária de astrócitos. Uma vez que a reduzida atividade ATPase e ADPase das células de glioma sugere um acúmulo de nucleotídeos no meio extracelular (WINK *et al*., 2003; BRAGANHOL *et al*., 2020), o aumento do catabolismo promovido pelo $F_{DCM}$ poderia ser um mecanismo compensatório a fim de impedir os efeitos pró-tumorais mediados pela ativação de purinoreceptores.

No entanto, a elevada taxa de hidrólise de AMP indica um aumento dos níveis de ADO. Embora a ADO esteja envolvida com a progressão e agressividade dos gliomas (AZAMBUJA *et al*., 2019), o extrato de *Biscogniauxia* sp. reduziu a proliferação celular. Além disso, o bloqueio dos receptores de adenosina não interferiu na atividade antiglioma exercida pelo $F_{DCM}$, sugerindo que os compostos produzidos pelo fungo endofítico não atuam via ativação de receptor P1.

Neste sentido, a ADO pode estar sendo catalisada a inosina pela enzima ADA (VIJAYAN; SMYTH; TENG, 2018) ou ainda captada para o interior da célula por meio de transportados de nucleosídeos extracelulares (ZHULAI *et al*., 2022). Uma vez no interior da célula, a ADO pode ser convertida em AMP pela enzima adenosina quinase (ZHULAI *et al*., 2022). Evidências apontam que concentrações elevadas de AMP intracelular são tóxicos para células de glioma C6 (OHKUBO; NAGATA; NAKAHATA, 2007). No entanto, estudos adicionais são necessários a fim de elucidar o efeito do $F_{DCM}$ na via adenosinérgica.

O ambiente imunossupressor desencadeado por níveis elevados de ADO em neoplasias malignas, promove danos celulares através da geração de ERO por células inflamatórias e tumorais (LUNKES *et al*., 2022). Contudo, o metabolismo secundário de *Biscogniauxia* sp. reduziu eficientemente a produção intracelular de ERO nos modelos experimentais de glioma em níveis similares

aqueles encontrados na cultura primária de astrócitos saudáveis. Esta redução foi acompanhada por um aumento na atividade das enzimas antioxidantes e do conteúdo tiólico total. Adicionalmente, o extrato reduziu a liberação de IL-6 e elevou os níveis de IL-10 na linhagem celular C6 e no cocultivo de astrócito-glioma.

O perfil antioxidante exibido pelos metabólitos bioativos do fungo endofítico de *A. satureioides* está de acordo com achados prévios. Pedra e colaboradores (2018) encontraram resultados similares ao avaliar o efeito de frações purificadas e de Sch-642305 na regulação da homeostase redox de células de glioma C6. Além disso, Sritharan e colaboradores (2019) relataram interessante atividade *scavenger* de isocumarinas produzidas por espécies de *Biscogniauxia*.

Interessantemente, a modulação enzimática redox exercida pelo $F_{DCM}$ diferiu entre os modelos experimentais de glioma presentes neste estudo. Enquanto os componentes bioativos de *Biscogniauxia* sp. aumentaram a atividade das enzimas antioxidantes SOD, CAT e GST na linhagem de glioma C6, nenhuma alteração foi observada na atividade da SOD em condições de cocultivo. Ademais, também foram encontradas modificações entre os níveis de expressão relativa de mRNA de marcadores inflamatórios e pró-tumorais entre as culturas experimentais expostas ao $F_{DCM}$.

A SOD atua na linha de frente na defesa contra danos oxidativos desencadeados por ERO, catalisando a dismutação do $O_2^{\bullet -}$ em $H_2O_2$. (IGHODARO; AKINLOYE, 2018). Evidências crescentes têm demonstrado que a ativação da quinase regulada por sinal extracelular (ERK) por agentes antineoplásicos, pode aumentar a expressão e atividade da SOD, reduzindo assim, os níveis de ERO (NAVARRO *et al*., 2006; GOMEZ-SAROSI; STRASBERG-RIEBER; RIEBER, 2009; PARK *et al*., 2021). Além disso, estudos têm demonstrado que a redução de ERO está diretamente relacionada à redução da enzima pró-inflamatória ciclooxigenase-2 (COX-2), visto que a produção destas espécies reativas pode depender da função peroxidase da COX (PALOZZA *et al*., 2005; DESAI; PRICKRIL; RASOOLY, 2018).

Além de aumentar a atividade da SOD, o $F_{DCM}$ induziu um aumento da expressão de ERK1/2 e reduziu seletivamente a expressão de COX-2 em células de glioma C6. No entanto, nenhuma alteração foi observada na expressão

desses genes na interação astrócito-glioma ou na cultura primária de astrócitos expostos ao extrato fracionado de *Biscogniauxia* sp. A redução seletiva de COX-2 associada à redução dos níveis de ERO sugere que a citotoxicidade induzida pelos componentes bioativos de *Biscogniauxia* sp. pode ser mediada, pelo menos em parte, pelo seu potencial antioxidante e anti-inflamatório.

Além disso, embora a ativação constitutiva de ERK1/2 geralmente promova a proliferação celular, diversos compostos antitumorais induzem seus efeitos antiproliferativos, regulam a progressão do ciclo celular e provocam morte celular programada através da ativação desta via de sinalização (SUGIURA; SATOH; TAKASAKI, 2021). De fato, os metabólitos do *Biscogniauxia* sp parecem fazer parte deste vasto repertório de compostos, uma vez que o $F_{DCM}$ induz parada no ciclo celular e apoptose em células de glioma C6 (**Anexo A**).

Ademais, outro tipo de morte celular programada desencadeada pela ativação de ERK1/2 é a piroptose dependente de caspase-1 (Casp-1) (ZHOU *et al*., 2019; RUAN; WANG; WANG, 2020). Uma vez ativada, a caspase-1 induz condensação da cromatina de maneira semelhante à apoptose, promove a abertura de poros na membrana plasmática, inchaço celular e ruptura da membrana levando à liberação de fatores pró-inflamatórios como IL-6 e, principalmente, a IL-1β (RUAN; WANG; WANG, 2020). Esta, por sua vez, é amplamente expressa em gliomas de alto grau, estando associada à proliferação, migração e invasão celular (LITMANOVICH; KHAZIM; COHEN, 2018).

Curiosamente, os componentes bioativos do fungo endofítico aumentaram os níveis de expressão relativa de mRNA da casp-1 na linhagem de glioma C6, sugestivo de piroptose, mas não em condições de cocultivo. Embora a superexpressão de casp-1 promova a liberação e a clivagem de pro-IL-1β na sua forma ativa (IL-1β) (PETRASEK *et al*., 2012), o $F_{DCM}$ reduziu significativamente a expressão desta citocina pró-inflamatória nas culturas de glioma. Neste contexto, diante do potencial do *Biscogniauxia* sp. em reduzir significativamente parâmetros inflamatórios, estes resultados sugerem que o metabolismo secundário do fungo endofítico pode alterar vias relacionadas à maturação de IL-1β.

De maneira geral, a proteção fornecida por astrócitos reativos às células tumorais depende do contato direto destas células gliais com as células de

glioma (CHEN *et al*., 2015). Embora a expressão de marcadores de astrogliose reativa, como a proteína ácida fibrilar glial (GFAP, do inglês *Glial Fibrillary Acid Protein*), não tenha sido avaliada, alterações na homeostase redox, no metabolismo de purinas e na secreção de citocinas sugere que o modelo experimental de cocultivo estimula a liberação de mediadores inflamatórios e danos oxidativos relacionados com o desenvolvimento e progressão dos gliomas.

Apesar de poucos estudos explorarem os mecanismos envolvidos com as atividades biológicas de espécies de *Biscogniauxia*, a capacidade antioxidante do $F_{DCM}$ em modular vias inflamatórias relacionadas à progressão neoplásica, tanto na linhagem de glioma C6 quanto na comunicação cruzada entre astrócito e glioma, torna este microrganismo endofítico um promissor reservatório de metabólitos de interesse farmacológico. Todavia, a análise do metabolismo secundário de *Biscogniauxia* sp. sobre modelo experimental pré-clínico de GBM é essencial para elucidar o efeito antiglioma desses metabólitos no microambiente tumoral.

Além de investigar a atividade antiglioma de compostos biossintetizados por fungos endofíticos, o nosso grupo de pesquisa tem avaliado o efeito de outros produtos naturais sobre protocolos experimentais *in vitro* e *in vivo* de GBM (BONA *et al*., 2020; DA SILVEIRA *et al*., 2022; BONA *et al*., 2022). De modo geral, os compostos fenólicos são reconhecidos por suas propriedades antioxidantes e anti-inflamatórias, exibindo interessantes efeitos antineoplásicos sobre tumores primários do SNC e neoplasias malignas do sistema nervoso periférico (PERRONE; SAMPAOLO; MELONE, 2020). Entre os polifenóis, o AG consiste em um ácido tri-hidrobenzoico amplamente difundido por todo o reino vegetal (GAO *et al*., 2019) e abundantemente encontrado em nozes, uvas, vinho, folhas de chá e em espécies de plantas, incluindo a *A. satureioides* (HATAMI *et al*., 2012; KAHKESHANI *et al*., 2019).

Diversos estudos têm demonstrado os efeitos citotóxicos do AG em linhagens tumorais de GBM humano e o seu papel neuroprotetor contra danos oxidativos e desordens na sinalização purinérgica em patologias do SNC (LU *et al*., 2010; KADE; ROCHA, 2013; PAOLINI *et al*., 2015; HSU *et al*., 2016; PEREIRA *et al*., 2018). No entanto, não há relatos acerca do seu papel na regulação do estado redox e do metabolismo extracelular de purinas em modelos

experimentais de glioma. Neste contexto, no capítulo 3 da presente tese investigamos o impacto do polifenol AG *in vitro* e em modelo pré-clínico de GBM.

O AG exibiu citotoxicidade seletiva, visto que reduziu a proliferação e atividade metabólica das células de glioma C6 em até 70%, mas não alterou a viabilidade celular da cultura primária de astrócitos. Interessantemente, o composto fenólico foi capaz de reduzir 90% do crescimento tumoral no modelo pré-clínico de GBM, prevenindo a deterioração locomotora e exploratória observada em ratos com o tumor cerebral. Além disso, ao avaliar biomarcadores de toxicidade, observamos que o tratamento com o AG não induziu danos sistêmicos.

Neste estudo, os efeitos antiproliferativos *in vitro* e *in vivo* do AG foram acompanhados por alterações na modulação purinérgica e na homeostase redox. Em ambas as condições experimentais, o tratamento com o polifenol reduziu os níveis de ERO e aumentou o conteúdo tiólico total e a atividade das enzimas antioxidantes SOD e CAT. Adicionalmente, a administração intragástrica de AG preveniu a peroxidação lipídica e o aumento dos níveis de nitritos presentes no microambiente tumoral de animais com GBM. Ainda, o tratamento com AG promoveu um aumento na atividade da enzima antioxidante GPx em células de glioma C6, mas não alterou a atividade da GST no modelo experimental *in vivo*.

Curiosamente, vale ressaltar, que embora no capítulo 2 desta tese tenha sido demonstrado diferenças significativas na atividade enzimática da GST entre a cultura primária de astrócitos saudáveis e as condições de cocultivo astrócito-glioma, nenhuma alteração foi observada na atividade desta enzima entre os animais do grupo saudável e com o tumor cerebral. Este achado está de acordo com resultados prévios que também não observaram modificações na atividade desta enzima antioxidante em animais submetidos ao implante intracerobroventricular de células de glioma C6, sugerindo que no modelo pré-clínico de GBM a atividade da GST não está relacionada à malignidade e crescimento do tumor (BONA et al., 2022).

Apesar do microambiente tumoral desempenhar um papel decisivo na agressividade dos gliomas, a inflamação sistêmica pode ser mais severa que as metástases cerebrais (CIRAK *et al*., 2003; BARCISZEWSKA *et al*., 2019). Tanto as células de glioma quanto os componentes do microambiente tumoral liberam

biomoléculas na circulação, como espécies reativas, resultando no aumento da peroxidação lipídica e secreção de mediadores inflamatórios (WANG *et al*., 2018; BARCISZENSKA *et al*., 2019). Assim, o sangue consiste em uma amostra biológica promissora para adquirir informações sobre características e danos sistêmicos induzidos pelo tumor (BETTEGOWDA *et al*., 2014).

De maneira similar ao microambiente cerebral, o soro de ratos com GBM apresentaram níveis elevados de ERO e nitritos, mas uma redução na atividade da SOD, comparados aos animais saudáveis. Por outro lado, observamos uma redução da atividade da CAT em amostras de soro de ratos com o tumor cerebral. De fato, Ylmaz e colaboradores (2006) relataram um aumento na atividade desta enzima em amostras de soro de pacientes diagnosticados com glioma. Em contrapartida, o tratamento com o AG preveniu os danos oxidativos induzidos pelo tumor, sugerindo que este composto fenólico é capaz de modular a resposta local e sistêmica promovida pela carcinogênese.

Plaquetas circulantes também podem liberar uma variedade de fatores de crescimentos e inflamatórios que podem, direta ou indiretamente, modificar a atividade das células de glioma, o crescimento e a angiogênese tumoral (MARX *et al*., 2019). Além disso, uma vez que pacientes com GBM apresentam risco aumentado para eventos cardiovasculares sistêmicos, a modulação de vias que estimulam a ativação plaquetária, é essencial (MARX *et al*., 2019).

No presente estudo, a injeção intracerebroventricular de células de glioma C6 desencadeou um aumento na produção de ERO e nitritos, e uma redução na atividade antioxidante da CAT nas plaquetas sanguíneas. A CAT consiste na principal enzima reguladora do metabolismo de $H_2O_2$. Assim, a atividade reduzida desta enzima resulta em um acúmulo de $H_2O_2$, cujas concentrações elevadas estimulam a ativação plaquetária (GÓTH; RASS; PÁY, 2004; FARIA *et al*., 2020). Contudo, o tratamento com a dose de 100 mg/kg/dia de AG reverteu os danos oxidativos de maneira eficiente através do aumento da atividade antioxidante da CAT, consequentemente evitando o acúmulo de $H_2O_2$.

Além da ativação mediada por espécies reativas, as plaquetas podem ser ativadas por nucleotídeos de adenina secretados pelas células tumorais (MARX *et al*., 2019). O ATP, o ADP e a ADO atuam como moléculas sinalizadoras modulando a resposta imune e trombo regulatória em diferentes neoplasias (DO CARMO *et al*., 2005; SÉVIGNY; MARTÍN-SAUÉ; PINTOR, 2015; MANICA *et al*.,

2018). Neste contexto, diante da importância do controle do metabolismo purinérgico na resposta sistêmica, avaliamos a atividade das NTPDases, 5´nucleotidase e/ou ADA no soro e células sanguíneas de ratos submetidos ao modelo pré-clínico de GBM.

Assim como o ADP, o ATP também exerce um importante papel na ativação plaquetária e formação de agregados celulares (CATTANEO, 2019). Neste estudo observamos uma redução significativa da atividade ATPásica em soro e plaquetas de animais com tumor cerebral comparado aos animais saudáveis, sugerindo um aumento dos níveis de ATP no meio extracelular e uma redução da concentração extracelular de ADP. Confrontando este resultado, verificamos um aumento da atividade ADPase em plaquetas de ratos com glioma.

No GBM, o ADP é responsável por induzir a ativação e agregação plaquetária no microambiente tumoral (CATTANEO, 2019; MARX *et al*., 2019). A adesão e ativação inicial é seguida pelo recrutamento de plaquetas circulantes adicionais, cuja ativação e agregação é mediada pela produção de tromboxanos A2. Estes por sua vez, liberam ADP a partir de seus grânulos a fim de ativar as plaquetas recém recrutadas (KOUPENOVA *et al*., 2018). Assim, dada a importância do ADP como principal agonista envolvido na ativação plaquetária, o pool deste nucleotídeo extracelular sugerido pelo aumento da atividade NTPDase, pode ser devido a liberação do ADP a partir das plaquetas circulantes.

Além disso, também observamos uma redução na hidrólise de AMP e aumento da atividade da ADA em plaquetas de animais com glioma. Estes resultados indicam uma redução dos níveis extracelular de ADO, um importante inibidor da agregação plaquetária (CATTANEO, 2019). Diante do exposto, as plaquetas circulantes parecem exercer um papel crucial na malignidade do GBM em resposta às alterações presentes no tecido neoplásico.

Interessantemente, o AG impediu as alterações purinérgicas promovidas pelo GBM. Estudos prévios já relataram o potencial do AG na inibição da agregação plaquetária em modelos experimentais *in vitro* e *in vivo* (CHANG *et al*., 2012; PEREIRA *et al*., 2018; ZHANG *et al*., 2022). Tais efeitos têm sido atribuídos à capacidade do AG em inibir a expressão de P-selectina, uma molécula envolvida na ativação plaquetária e amplamente expressa em

plaquetas sanguíneas de pacientes diagnosticados com gliomas de alto grau (CAMPANELLA *et al*., 2020).

Assim como as plaquetas, os linfócitos são importantes indicadores inflamatórios, cujos níveis no sangue periférico estão fortemente associados à extensão da inflamação crônica característica do microambiente dos gliomas (YANG *et al*., 2020). Ao investigar o catabolismo purinérgico de ratos submetidos ao implante do tumor, verificamos um aumento na atividade das NTPDases e da ADA, reduzindo as concentrações extracelulares de ADO.

Enquanto no microambiente tumoral níveis elevados de ADO estão associados à progressão do GBM (AZAMBUJA *et al*., 2019), este nucleosídeo demonstra papel protetor contra danos teciduais em determinadas células, exibindo efeitos imunorregulatórios e anti-inflamatórios (PASQUINI *et al*., 2021). Desta forma, as enzimas NTPDases e ADA atuam como reguladores da resposta inflamatória. Corroborando com achados prévios (ZANINI *et al*., 2012; DA SILVEIRA *et al*., 2013), os linfócitos dos animais com GBM apresentaram um aumento na atividade das enzimas purinérgicas, sugerindo uma depleção de ADO no meio extracelular e assim, um aumento da resposta inflamatória sistêmica.

Notavelmente, o tratamento com o AG reverteu de maneira eficiente as alterações linfocitárias no metabolismo das purinas, desencadeadas pelo tumor cerebral, alcançando níveis de atividade enzimática similares aos controles saudáveis. Além disso, o composto fenólico reduziu a atividade das enzimas NTPDases e 5´nucleotidase em células de glioma C6, evitando a proliferação celular desencadeada pelo acúmulo de ADO. Diante do exposto, torna-se imperativo ressaltar o elevado potencial antiglioma do AG na modulação de alterações locais e sistêmicas induzidas pelo GBM.

## 6. CONCLUSÕES

A partir do presente estudo foi possível elucidar a taxonomia do fungo endofítico isolado a partir de *A. satureioides*, sendo este, o primeiro relato acerca da identificação molecular de um microrganismo endofítico obtido a partir de plantas medicinais do gênero *Achyrocline*. Com base na caracterização dos componentes químicos presentes na fração purificada do fungo endofítico *Biscogniauxia* sp., observamos a capacidade deste microrganismo em produzir metabólitos conhecidos, porém inéditos quando comparado aos compostos comumente sintetizados por este gênero. Além disso, apesar do vasto repertório de substâncias geradas por espécies endofíticas da família Xylariaceae, descrevemos pela primeira vez a produção da lactona Sch-642305 por um microrganismo desta família.

O extrato fracionado $F_{DCM}$ exibiu propriedades antiproliferativas que culminaram na morte celular e em alterações do ciclo celular das linhagens celulares de melanoma (A375) e glioma (C6). No entanto, não alterou a atividade metabólica de astrócitos corticais saudáveis. Interessantemente, a citotoxicidade induzida pelo $F_{DCM}$ não foi afetada pela presença de astrócitos associados às células tumorais. Com base nos resultados obtidos, pode-se observar que o efeito antiglioma promovido pelo metabolismo secundário de *Biscogniauxia* sp. parece estar relacionado às suas propriedades antioxidante e anti-inflamatória, permitindo a modulação de vias envolvidas no crescimento e malignidade do tumor. Estes achados revelam o *Biscogniauxia* sp como um exímio produtor de metabólitos de interesse farmacológico, encorajando o isolamento dos compostos bioativos a fim de elucidar os mecanismos associados ao seu potencial antiglioma em modelos experimentais *in vitro* e *in vivo*.

Além da promissora atividade terapêutica do fungo endofítico isolado, com base nos resultados encontrados na presente investigação, pode-se observar importante efeito antiglioma *in vitro* e *in vivo* promovido pelo polifenol AG. O composto fenólico reduziu significativamente a proliferação celular da linhagem de glioma C6 e o volume tumoral de ratos submetidos ao modelo pré-clínico de GBM, inibindo os danos oxidativos presentes no microambiente tumoral. Adicionalmente, as alterações no metabolismo de purinas no soro, plaquetas e linfócitos de ratos com GBM, foram prevenidas pela administração com AG. O composto fenólico também regulou de maneira eficiente o *status*

redox no soro e plaquetas sanguíneas de animais com o tumor cerebral, reduzindo os níveis de espécies reativas mediante o aumento da resposta antioxidante. Essas descobertas são extremamente relevantes não apenas para elucidar as atividades biológicas do AG frente ao modelo pré-clínico do GBM, mas também para o entendimento das alterações fisiopatológicas induzidas por esta neoplasia maligna na resposta local e sistêmica.

Diante do exposto, é notável a relevância terapêutica promovida pelos produtos naturais. Importantemente, este estudo destaca o elevado potencial dos fungos endofíticos na produção de metabólitos únicos, cujas estruturas bioativas exibem promissoras propriedades farmacológicas. Neste contexto, estes microrganismos constituem uma fonte inesgotável de compostos, podendo ser utilizados como uma importante ferramenta para a busca de novos agentes antineoplásicos. Assim, a síntese de metabólitos de origem endofítica e seus análagos poderiam aprimorar a atividade antitumoral possibilitando a translação para futuros experimentos clínicos.

## 7. REFERÊNCIAS

ADELIN, E. et al. Isolation, structure elucidation and biological activity of metabolites from Sch-642305-producing endophytic fungus Phomopsis sp. CMU-LMA. Phytochemistry, v. 72, n. 18, p. 2406-2412, 2011.

AKTER, R. et al. Potential role of natural products to combat radiotherapy and their future perspectives. Molecules, v. 26, n. 19, p. 5997, 2021.

AMAND, S. et al. Guaiane sesquiterpenes from Biscogniauxia nummularia featuring potent antigerminative activity. Journal of Natural Products, v. 75, n. 4, p. 798-801, 2012.

ARNOLD, M. et al. Global burden of cutaneous melanoma in 2020 and projections to 2040. JAMA dermatology, v. 158, n. 5, p. 495-503, 2022.

AZAMBUJA, J. H. et al. CD73 downregulation decreases in vitro and in vivo glioblastoma growth. Molecular Neurobiology, v. 56, n. 5, p. 3260-3279, 2019.

AZEVEDO, J. L. Microrganismos endofíticos. Ecologia Microbiana, v. 1, n. 1, p. 117- 137, 1998.

BARCISZEWSKA, A. M. et al. Total DNA methylation changes reflect random oxidative DNA damage in gliomas. Cells, v. 8, n. 9, p. 1065, 2019.

BHATIA, T. N. et al. Astrocytes do not forfeit their neuroprotective roles after surviving intense oxidative stress. Frontiers in molecular neuroscience, v. 12, p. 87, 2019.

BETTEGOWDA, C. et al. Detection of circulating tumor DNA in early-and late-stage human malignancies. Science translational medicine, v. 6, n. 224, p. 224ra24-224ra24, 2014.

BIANCHI, S. E. et al. Achyrocline satureioides compounds, achyrobichalcone and 3-O-methylquercetin, induce mitochondrial dysfunction and apoptosis in human breast cancer cell lines. IUBMB life, v. 72, n. 10, p. 2133-2145, 2020.

BOHJANEN, K. Estrutura e funções da pele. Dermatologia Clínica. Seção I Bases para diagnóstico e tratamento, v.1, n.1, p. 1-5, 2017.

BONA, N. P. et al. Tannic acid elicits selective antitumoral activity in vitro and inhibits cancer cell growth in a preclinical model of glioblastoma multiforme. Metabolic Brain Disease, v. 35, n. 2, p. 283-293, 2020.

BONA, N. P. et al. Tannic Acid Attenuates Peripheral and Brain Changes in a Preclinical Rat Model of Glioblastoma by Modulating Oxidative Stress and Purinergic Signaling. Neurochemical Research, v. 47, n. 6, p. 1541-1552, 2022.

BRAGANHOL, E. et al. A comparative study of ectonucleotidase and P2 receptor mRNA profiles in C6 cell line cultures and C6 ex vivo glioma model. Cell and Tissue Research, v. 335, n. 2, p. 331-340, 2009.

BRAGANHOL, E. et al. Purinergic signaling in glioma progression. In: Baranska J (eds.) Glioma Signaling. Advances in Experimental Medicine and Biology, Springer, Dordrecht, v. 986, p. 81-102, 2013.

BRAGANHOL, E. et al. Purinergic signaling in glioma progression. In: In: Barańska, J. (eds). Glioma signaling. Advances in Experimental Medicine and Biology, Springer, Cham, vol 1202, p. 87-108, 2020.

BRANDAO, M. et al. Astrocytes, the rising stars of the glioblastoma microenvironment. Glia, v. 67, n. 5, p. 779-790, 2019.

BRASIL. Lei nº 11.858, de 5 de dezembro de 2002. Institui a Marcela Planta Medicinal Símbolo do Estado do Rio Grande do Sul e dá outras providências. Palácio Piratini, Porto Alegre, 2002. Disponível em: <http://www.al.rs.gov.br/filerepository/repLegis/arquivos/11.858.pdf> Acesso em: 27 de Junho de 2022.

BRASIL. GOVERNO DO ESTADO RIO GRANDE DO SUL SECRETARIA DA SAÚDE. Portaria SES/RS 588/2017: Institui a Relação Estadual de Plantas Medicinais de interesse do Sistema Único de Saúde no Rio Grande do Sul e listas complementares, 2017, RS.
Disponível em: <https://saude.rs.gov.br/upload/arquivos/carga20171201/22110143-portaria-replame-rio-grande-do-sul.pdf#:~:text=Portaria%20SES%2FRS%20588%2F2017%20Institui%20a%20Rela%C3%A7%C3%A3o%20Estadual%20de,DA%20SA%C3%9ADE%20no%20uso%20de%20suas%20atribui%C3%A7%C3%B5es%20e%2C> Acesso em: 27 de Junho de 2022.

BUßKAMP, J.; LANGER, G. J.; LANGER, E. J. Sphaeropsis sapinea and fungal endophyte diversity in twigs of Scots pine (Pinus sylvestris) in Germany. Mycological Progress, v. 19, n. 9, p. 985-999, 2020.

BURNSTOCK, G. Pathophysiology and therapeutic potential of purinergic signaling. Pharmacological Reviews, v. 58, n. 1, p. 58-86, 2006.

BURNSTOCK, G.; DI VIRGILIO, F. Purinergic signalling and cancer. Purinergic Signalling, v. 9, n. 4, p. 491-540, 2013.

CALLAN, B. E.; ROGERS, J. D. Cultural characters and anamorphs of *Biscogniauxia* (= Nummularia) *marginata*, *B. dennisii*, and *B. repanda*. Canadian journal of botany, v. 64, n. 4, p. 842-847, 1986.

CAMPANELLA, R. et al. Tumor-educated platelets and angiogenesis in glioblastoma: another brick in the wall for novel prognostic and targetable

biomarkers, changing the vision from a localized tumor to a systemic pathology. Cells, v. 9, n. 2, p. 294, 2020.

CARUSO, G. et al. Linking endophytic fungi to medicinal plants therapeutic activity. A case study on Asteraceae. Agriculture, v. 10, n. 7, p. 286, 2020.

CARVALHO, C. R. et al. Molecular phylogeny, diversity, and bioprospecting of endophytic fungi associated with wild ethnomedicinal North American plant *Echinacea purpurea* (Asteraceae). Chemistry & Biodiversity, v. 13, n. 7, p. 918-930, 2016.

CATTANEO, M. The platelet P2 receptors. In: Platelets. Academic press, 2019. p. 259-277.

CHAMBERLIN, S. R. et al. Natural product target network reveals potential for cancer combination therapies. Frontiers in pharmacology, v. 10, n. 1, p. 557, 2019.

CHANG, S. S. et al. Gallic acid attenuates platelet activation and platelet-leukocyte aggregation: Involving pathways of Akt and GSK3β. Evidence-Based Complementary and Alternative Medicine, v. 2012, n. 1, p. 1-9, 2012.

CHEKHONIN, I. V. et al. Glioma Cell and Astrocyte Co-cultures As a Model to Study Tumor–Tissue Interactions: A Review of Methods. Cellular and molecular neurobiology, v. 38, n. 6, p. 1179-1195, 2018.

CHEN, L. et al. Endophytic fungi with antitumor activities: Their occurrence andanticancer compounds. Critical Reviews in Microbiology, v. 42, n. 3, p. 454-473, 2016.

CHEN, W. et al. Glioma cells escaped from cytotoxicity of temozolomide and vincristine by communicating with human astrocytes. Medical oncology, v. 32, n. 3, p. 1-13, 2015.

CHEN, Y. et al. The role of astrocytes in oxidative stress of central nervous system: A mixed blessing. Cell proliferation, v. 53, n. 3, p. e12781, 2020.

CHENG, M. J. et al. Secondary metabolites from the endophytic fungus *Biscogniauxia formosana* and their antimycobacterial activity. Phytochemistry Letters, v. 5, n. 3, p. 467-472, 2012.

CHU, M. et al. Isolation and Structure Elucidation of Sch 642305, a Novel Bacterial DNA Primase Inhibitor Produced by *Penicillium verrucosum*. Journal of natural products, v. 66, n. 12, p. 1527-1530, 2003.

CIRAK, B. et al. Lipid peroxidation in cerebral tumors. Clinica chimica acta, v. 327, n. 1-2, p. 103-107, 2003.

CONITEC. Relatório para sociedade - informações sobre recomendações de incorporação de medicamentos e outras tecnologias no SUS. 2020a.

Disponível em: <https://www.gov.br/conitec/pt-br/midias/consultas/relatorios/2019/sociedade/resoc189_terapiaalvo_imunoterapia_melanoma.pdf>
Acesso em: 20 de Julho de 2022.

CONITEC. Diretrizes diagnósticas e terapêuticas de tumor cerebral adulto. 2020b
Disponível em: <20201218_pcdt_tumor_cerebral_em_adulto_isbn.pdf (www.gov.br)>
Acesso em: 20 de Julho de 2022.

DA SILVEIRA, E. F. et al. Ketoprofen-loaded polymeric nanocapsules selectively inhibit cancer cell growth *in vitro* and in preclinical model of glioblastoma multiforme. Investigational new drugs, v. 31, n. 6, p. 1424-1435, 2013.

DA SILVEIRA, L. M. et al. Selective in vitro anticancer effect of blueberry extract (*Vaccinium virgatum*) against C6 rat glioma: Exploring their redox status. Metabolic Brain Disease, v. 37, n. 2, p. 439-449, 2022.

DAS, K. et al. A new report of *Biscogniauxia petrensis* isolated from mosquitoes in Korea. The Korean Journal of Mycology, v. 48, n. 2, p. 87-93, 2020.

DE SOUZA, P. O. et al. Anticancer activity of flavonoids isolated from *Achyrocline satureioides* in gliomas cell lines. Toxicology In Vitro, v. 51, n. 1, p. 23-33, 2018.

DESAI, S. J.; PRICKRIL, B.; RASOOLY, A. Mechanisms of phytonutrient modulation of cyclooxygenase-2 (COX-2) and inflammation related to cancer. Nutrition and cancer, v. 70, n. 3, p. 350-375, 2018.

DI MEO, S.; VENDITTI, P. Evolution of the knowledge of free radicals and other oxidants. Oxidative Medicine and Cellular Longevity, v. 2020, n. 1, p. 1-32, 2020.

DO CARMO ARAÚJO, M. et al. Enzymes that hydrolyze adenine nucleotides in platelets from breast cancer patients. Biochimica et Biophysica Acta (BBA)-Molecular Basis of Disease, v. 1740, n. 3, p. 421-426, 2005.

DONEDA, E. et al. 3-O-Methylquercetin from Achyrocline satureioides—cytotoxic activity against A375-derived human melanoma cell lines and its incorporation into cyclodextrins-hydrogels for topical administration. Drug Delivery and Translational Research, v. 11, n. 5, p. 2151-2168, 2021.

DRINGEN, R. et al. Glutathione-dependent detoxification processes in astrocytes. Neurochemical research, v. 40, n. 12, p. 2570-2582, 2015.

ELDER, D. E. et al. The 2018 World Health Organization classification of cutaneous, mucosal, and uveal melanoma: detailed analysis of 9 distinct

subtypes defined by their evolutionary pathway. Archives of pathology & laboratory medicine, v. 144, n. 4, p. 500-522, 2020.

ENDICOTT, A. A.; TAYLOR, J. W.; WALSH, K. M. Telomere length connects melanoma and glioma predispositions. Aging (Albany NY), v. 8, n. 3, p. 423, 2016.

ERICES, J. I. et al. Current natural therapies in the treatment against glioblastoma. Phytotherapy Research, v. 32, n. 11, p. 2191-2201, 2018.

EVIDENTE, A. et al. Biscopyran, a phytotoxic hexasubstituted pyranopyran produced by *Biscogniauxia mediterranea*, a fungus pathogen of cork oak. Journal of natural products, v. 68, n. 4, p. 568-571, 2005.

FAN, C. H. et al. $O_6$-methylguanine DNA methyltransferase as a promising target for the treatment of temozolomide-resistant gliomas. Cell Death & Disease, v. 4, n. 10, p. e876- e876, 2013.

FARIA, A. V. S. et al. Platelets in aging and cancer—"double-edged sword". Cancer and Metastasis Reviews, v. 39, n. 4, p. 1205-1221, 2020.

FERNÁNDEZ-FERNÁNDEZ, A. M. et al. Antioxidant, Antidiabetic, and Antiobesity Properties, TC7-Cell Cytotoxicity and Uptake of *Achyrocline satureioides* (Marcela) Conventional and High Pressure-Assisted Extracts. Foods, v. 10, n. 4, p. 893, 2021.

FIGUEROA, M. et al. Fluorescent azaphilonoidal pigments from the endophytic fungus *Biscogniauxia* sp. Planta Medica, v. 81, n. 11, p. PT41, 2015.

FRANKE, H. et al. Pathophysiology of astroglial purinergic signalling. Purinergic Signalling, v. 8, n. 3, p. 629-657, 2012.

GAGLIANO, N. et al. Glioma-astrocyte interaction modifies the astrocyte phenotype in a co-culture experimental model. Oncology reports, v. 22, n. 6, p. 1349-1356, 2009.

GALDINO, K. C. A. Fungos endofíticos isolados a partir de Mikania hastato-cordata: obtenção dos extratos e avaliação da atividade antiglioma. 71 f. 2016. Dissertação (Mestrado em Bioquímica e Bioprospecção) – Programa de Pós-Graduação em Bioquímica e Bioprospecção, Universidade Federal de Pelotas, Pelotas. 2016.

GAO, J. et al. A role of gallic acid in oxidative damage diseases: A comprehensive review. Natural Product Communications, v. 14, n. 8, p. 1934578X19874174, 2019.

GEHRING, M. P. et al. P2X7 receptor as predictor gene for glioma radiosensitivity and median survival. The International Journal of Biochemistry & Cell Biology, v. 68, n. 1, p. 92-100, 2015.

GIAKOUMETTIS, D.; KRITIS, A.; FOROGLOU, N. C6 cell line: The gold standard in glioma research. Hippokratia, v. 22, n. 3, p. 105, 2018.

GIULIANI, A. L.; SARTI, A. C.; DI VIRGILIO, F. Extracellular nucleotides and nucleosides as signalling molecules. Immunology Letters, v. 205, n. 1, p. 16-24, 2019.

GOMEZ–SAROSI, L. A.; STRASBERG–RIEBER, M.; RIEBER, M. ERK activation increases nitroprusside induced apoptosis in human melanoma cells irrespective of p53 status: role of superoxide dismutases. Cancer biology & therapy, v. 8, n. 12, p. 1173-1182, 2009.

GONÇALVES, G. G.; FERREIRA, M. I.; MING, L. C. Achyrocline satureioides (Lam.) DC. In: Medicinal and Aromatic Plants of South America. Springer, Dordrecht, 2018. p. 81-88.

GÓTH, L.; RASS, P.; PÁY, A. Catalase enzyme mutations and their association with diseases. Molecular Diagnosis, v. 8, n. 3, p. 141-149, 2004.

GUO, W.; WANG, H.; LI, C. Signal pathways of melanoma and targeted therapy. Signal Transduction and Targeted Therapy, v. 6, n. 1, p. 1-39, 2021.

HANAHAN, D. Hallmarks of cancer: new dimensions. Cancer discovery, v. 12, n. 1, p. 31-46, 2022.

Hanahan, D; Weinberg, RA. Hallmarks of cancer: the next generation. Cell, v. 144, n. 5, p. 646-674, 2011.

HATAMI, T. et al. Supercritical fluid extraction of bioactive compounds from Macela (*Achyrocline satureioides*) flowers: kinetic, experiments and modeling. The Journal of Supercritical Fluids, v. 65, n. 1, p. 71-77, 2012.

HAYES, J. D. et al. Glutathione transferases. Annual review of pharmacology and toxicology, v. 45, n. 1, p. 51-88, 2005.

HIDA, T. et al. Elucidation of melanogenesis cascade for identifying pathophysiology and therapeutic approach of pigmentary disorders and melanoma. International Journal of Molecular Sciences, v. 21, n. 17, p. 6129, 2020.

HOWELL, A. E. et al. Testing for causality between systematically identified risk factors and glioma: a Mendelian randomization study. Bmc Cancer, v. 20, n. 1, p. 1-11, 2020.

HRIDOY, M. et al. Putative Anticancer Compounds from Plant-Derived Endophytic Fungi: A Review. Molecules, v. 27, n. 1, p. 296, 2022

HSU, S. et al. The effect of gallic acid on cytotoxicity, Ca2+ homeostasis and ROS production in DBTRG05MG human glioblastoma cells and CTX TNA2 rat astrocytes. Chemico-Biological Interactions, v. 252, n. 1, p. 61-73, 2016.

HUANG, L.; TANG, Y.; SPERLAGH, B. Glial Purinergic Signaling-Mediated Oxidative Stress (GPOS) in Neuropsychiatric Disorders. Oxidative Medicine and Cellular Longevity, v. 2022, n. 1, p. 1-12, 2022.

HUBER, F. et al. Fast diagnostics of BRAF mutations in biopsies from malignant melanoma. Nano letters, v. 16, n. 9, p. 5373-5377, 2016.

IGHODARO, O. M.; AKINLOYE, O. A. First line defence antioxidants superoxide dismutase (SOD), catalase (CAT) and glutathione peroxidase (GPX): Their fundamental role in the entire antioxidant defence grid. Alexandria Journal of Medicine, v. 54, n. 4, p. 287-293, 2018.

ILLÁN-CABEZA, N. A et al. A potential antitumor agent,(6-amino-1-methyl-5-nitrosouracilato-N3)- triphenylphosphine-gold (I): Structural studies and in vivo biological effects against experimental glioma. European Journal of Medicinal Chemistry, v. 64, n. 1, p. 260-272, 2013.

INCA. Estimativa 2020: incidência de câncer no Brasil. Rio de Janeiro, p. 26, 2020.
Disponível em:
<https://www.inca.gov.br/sites/ufu.sti.inca.local/files//media/document//estimativa-2020-incidencia-de-cancer-no-brasil.pdf>
Acesso em: 02 de janeiro de 2021.

JACKETT, L. A.; SCOLYER, R. A. A review of key biological and molecular events underpinning transformation of melanocytes to primary and metastatic melanoma. Cancers, v. 11, n. 12, p. 2041, 2019.

JANTAHARN, P. et al. Anti-inflammatory and anti-proliferative activities of chemical constituents from fungus Biscogniauxia whalleyi SWUF13-085. Phytochemistry, v. 191, n. 1, p. 112908, 2021.

JI, B. C. et al. Gallic acid induces apoptosis via caspase-3 and mitochondrion-dependent pathways in vitro and suppresses lung xenograft tumor growth in vivo. Journal of Agricultural and Food Chemistry, v. 57, n. 16, p. 7596-7604, 2009.

JI, Z. et al. Involvement of P2X7 receptor in proliferation and migration of human glioma cells. BioMed Research International, v. 2018, n. 1, p. 1-12, 2018.

JIA, M. et al. Friendly relationship between endophytic fungi and medicinal plants: a systematic review. Frontiers in Microbiology, v. 7, n. 1, p. 1-14, 2016.

JIANG, G. et al. A novel approach to overcome temozolomide resistance in glioma and melanoma: Inactivation of MGMT by gene therapy. Biochemical and Biophysical Research Communications, v. 406, n. 3, p. 311-314, 2011.

JIANG, Y. et al. Gallic Acid: A Potential Anti-Cancer Agent. Chinese journal of integrative medicine, v. 1, n. 1, p. 1-11, 2021.

JURKOWSKA, H. et al. The expression and activity of cystathionine-γ-lyase and 3-mercaptopyruvate sulfurtransferase in human neoplastic cell lines. Amino acids, v. 41, n. 1, p. 151-158, 2011.

KADE, I. J.; ROCHA, J. B. T. Gallic acid modulates cerebral oxidative stress conditions and activities of enzyme-dependent signaling systems in streptozotocin-treated rats. Neurochemical research, v. 38, n. 4, p. 761-771, 2013.

KAHKESHANI, N. et al. Pharmacological effects of gallic acid in health and diseases: A mechanistic review. Iranian Journal of Basic Medical Sciences, v. 22, n. 3, p. 225, 2019.

KLAUNIG, J. E. Oxidative stress and cancer. Current Pharmaceutical Design, v. 24, n. 40, p. 4771-4778, 2018.

KOUPENOVA, M. et al. Circulating platelets as mediators of immunity, inflammation, and thrombosis. Circulation research, v. 122, n. 2, p. 337-351, 2018.

Kreeger, P. K.; Lauffenburger, D. A. Cancer systems biology: a network modeling perspective. Carcinogenesis, v. 31, n. 1, p. 2-8, 2010.

KUDUGUNTI, S. K. et al. Efficacy of caffeic acid phenethyl ester (CAPE) in skin B16-F0 melanoma tumor bearing C57BL/6 mice. Investigational new drugs, v. 29, n. 1, p. 52-62, 2011.

KUO, H. C. et al. Inhibitory effect of caffeic acid phenethyl ester on the growth of C6 glioma cells in vitro and in vivo. Cancer letters, v. 234, n. 2, p. 199-208, 2006.

KUSARI, S.; HERTWECK, C.; SPITELLER, M. Chemical ecology of endophytic fungi: origins of secondary metabolites. Chemistry & biology, v. 19, n. 7, p. 792-798, 2012.

LACAVA, P. T.; ANDREOTE, F. D.; AZEVEDO, J. L. Metabólitos secundários produzidos por micro-organismos endofíticos. In: Marcia do Vale Barreto Figueiredo; Helio Almeida Burity; Newton Pereira Stamford; Caroline Etienne de Rosália e Santos. (Org.). Micro-organismos e Agrobiodiversidade: o novo desafio para agricultura. 1 ed. Guaíba: AgroLivros, 2008, v. 1, p. 209-228.

LAUX, A. et al. In vitro evaluation of the anti-melanoma effects (A375 cell line) of the gel and whole leaf extracts from selected aloe species. Journal of Herbal Medicine, v. 31, n. 1, p. 100539, 2022.

LEE, S. Y. Temozolomide resistance in glioblastoma multiforme. Genes & Diseases, v. 3, n. 3, p. 198-210, 2016.

LITMANOVICH, A.; KHAZIM, K.; COHEN, I. The role of interleukin-1 in the pathogenesis of cancer and its potential as a therapeutic target in clinical practice. Oncology and therapy, v. 6, n. 2, p. 109-127, 2018.

LIU, Y. Y. et al. New phthalide derivatives from the Biscogniauxia sp. and their activities. Fitoterapia, v. 137, n. 1, p. 104184, 2019.

LO, C. et al. Gallic acid induces apoptosis in A375. S2 human melanoma cells through caspase-dependent and-independent pathways. International journal of oncology, v. 37, n. 2, p. 377-385, 2010.

LO, C. et al. Gallic acid inhibits the migration and invasion of A375. S2 human melanoma cells through the inhibition of matrix metalloproteinase-2 and Ras. Melanoma research, v. 21, n. 4, p. 267-273, 2011.

LOUIS, D. N. et al. The 2016 World Health Organization Classification of Tumors of the Central Nervous System: a summary. Acta Neurophatologica, v. 131, n. 6, p. 803-820, 2016.

LOUIS, D. N. et al. The 2021 WHO classification of tumors of the central nervous system: a summary. Neuro-oncology, v. 23, n. 8, p. 1231-1251, 2021.

LU, Y. et al. Gallic acid suppresses cell viability, proliferation, invasion and angiogenesis in human glioma cells. European journal of pharmacology, v. 641, n. 2-3, p. 102-107, 2010.

LUNKES, V. L. et al. Curcumin and Vinblastine Disturb Ectonucleotides Enzymes Activity and Promote ROS Production in Human Cutaneous Melanoma Cells. Brazilian Archives of Biology and Technology, v. 65, n. 1, p. 1-9, 2022.

MA, X. Y. et al. *Biscogniauxia dendrobii* sp. nov. and *B. petrensis* from *Dendrobium orchids* and the first report of cytotoxicity (towards A549 and K562) of *B. petrensis* (MFLUCC 14-0151*) in vitro*. South African Journal of Botany, v. 134, n. 1, p. 382-393, 2020.

MANICA, A. et al. High levels of extracellular ATP lead to chronic inflammatory response in melanoma patients. Journal of Cellular Biochemistry, v. 119, n. 5, p. 3980-3988, 2018.

MANINI, I. et al. Role of microenvironment in glioma invasion: what we learned from in vitro models. International Journal of Molecular Sciences, v. 19, n. 1, p. 147, 2018

MARX, S. et al. The role of platelets in cancer pathophysiology: focus on malignant glioma. Cancers, v. 11, n. 4, p. 569, 2019.

MCBEAN, G. J. Cysteine, glutathione, and thiol redox balance in astrocytes. Antioxidants, v. 6, n. 3, p. 62, 2017.

MORRONE, F. B. et al. Extracellular nucleotides and nucleosides induce proliferation and increase nucleoside transport in human glioma cell lines. Journal of Neuro-Oncology, v. 64, n. 3, p. 211-218, 2003.

NAVARRO, R. et al. Superoxide anions are involved in doxorubicin-induced ERK activation in hepatocyte cultures. Annals of the New York Academy of Sciences, v. 1090, n. 1, p. 419-428, 2006.

NICOLETTI, R. et al. Production and fungitoxic activity of Sch 642305, a secondary metabolite of *Penicillium canescens*. Mycopathologia, v. 163, n. 5, p. 295-301, 2007.

NISA, H. et al. Fungal endophytes as prolific source of phytochemicals and otherbioactive natural products: A review. Microbial Pathogenesis, v. 82, n. 1, p. 50-59, 2015.

OHKUBO, S.; NAGATA, K.; NAKAHATA, N. Adenosine uptake-dependent C6 cell growth inhibition. European journal of pharmacology, v. 577, n. 1-3, p. 35-43, 2007.

OLIVIER, C. et al. Drug resistance in glioblastoma: the two faces of oxidative stress. Frontiers in Molecular Biosciences, v. 7, n. 1, p. 620677, 2021.

ORGANIZAÇÃO PAN-AMERICADA DA SAÚDE. Câncer (Folha informativa atualizada em outubro de 2020). 2020.
Disponível em: <Câncer - OPAS/OMS | Organização Pan-Americana da Saúde (paho.org)>
Acesso em: 23 de Julho de 2022.

OSTROM, Q. T. et al. Progress in Neurological Surgery. Vol. 30, New York, 2016. p. 1-11.

OSTROM, Q. T. et al. Epidemiology of intracranial gliomas. Intracranial Gliomas Part I-Surgery, v. 30, n. 1, p. 1-11, 2018.

OSTROWSKI, R. P.; PUCKO, E. B. Harnessing oxidative stress for anti-glioma therapy. Neurochemistry International, v. 1, n. 1, p. 105281, 2022.

PALOZZA, P. et al. β-Carotene Downregulates the Steady-State and Heregulin-α–Induced COX-2 Pathways in Colon Cancer Cells. The Journal of nutrition, v. 135, n. 1, p. 129-136, 2005.

PAOLINI, A. et al. Gallic acid exerts a protective or an anti-proliferative effect on glioma T98G cells via dose-dependent epigenetic regulation mediated by miRNAs. International Journal of Oncology, v. 46, n. 4, p. 1491-1497, 2015.

PAPP, O. et al. Organ specific copy number variations in visceral metastases of human melanoma. Cancers, v. 13, n. 23, p. 5984, 2021.

PARK, J. Y. et al. Heregulin-β1 Activates NF-E2-related Factor 2 and Induces Manganese Superoxide Dismutase Expression in Human Breast Cancer Cells via Protein Kinase B and Extracellular Signal-regulated Protein Kinase Signaling Pathways. Journal of cancer prevention, v. 26, n. 1, p. 54, 2021.

PASQUINI, S. et al. Adenosine and inflammation: here, there and everywhere. International journal of molecular sciences, v. 22, n. 14, p. 7685, 2021.

PEDRA, N. S. et al. Endophytic fungus isolated from Achyrocline satureioides exhibits selective antiglioma activity - The role of Sch642305. Frontiers in Oncology, v. 8, n. 1, p. 476, 2018.

PELLERINO, A. et al. Epidemiology, risk factors, and prognostic factors of gliomas. Clinical and Translational Imaging, v. 1, n. 1, p. 1-9, 2022.

PEREIRA, A. et al. Effect of gallic acid on purinergic signaling in lymphocytes, platelets, and serum of diabetic rats. Biomedicine & Pharmacotherapy, v. 101, n. 1, p. 30-36, 2018.

PÉREX-HERRERO, E; FERNÁNDEZ-MEDARDE, A. Advanced targeted therapies in cancer: drug nanocarriers, the future of chemotherapy. European journal of pharmaceutics and biopharmaceutics, v. 93, n. 1, p. 52-79, 2015.

PERRONE, L.; SAMPAOLO, S.; MELONE, M. A. B. Bioactive phenolic compounds in the modulation of central and peripheral nervous system cancers: Facts and misdeeds. Cancers, v. 12, n. 2, p. 454, 2020.

PETRASEK, J. et al. IL-1 receptor antagonist ameliorates inflammasome-dependent alcoholic steatohepatitis in mice. The Journal of clinical investigation, v. 122, n. 10, p. 3476-3489, 2012.

PILLERON, S. et al. Estimated global cancer incidence in the oldest adults in 2018 and projections to 2050. International journal of cancer, v. 148, n. 3, p. 601-608, 2021.

RAJA, H. A. et al. Phylogenetic and chemical diversity of fungal endophytes isolated from *Silybum marianum* (L) Gaertn. (milk thistle). Mycology, v. 6, n. 1, p. 8-27, 2015.

RAMÍREZ-EXPÓSITO, M. J.; MARTÍNEZ-MARTOS, J. M. The Delicate equilibrium between oxidants and antioxidants in brain glioma. Current Neuropharmacology, v. 17, n. 4, p. 342-351, 2019.

RETTA, D. et al. Marcela, a promising medicinal and aromatic plant from Latin America: Areview. Industrial Crops and Products, v. 38, n. 1, p. 27–38, 2012.

RÖHRDANZ, E. et al. The influence of oxidative stress on catalase and MnSOD gene transcription in astrocytes. Brain research, v. 900, n. 1, p. 128-136, 2001.

RUAN, J.; WANG, S.; WANG, J.. Mechanism and regulation of pyroptosis-mediated in cancer cell death. Chemico-biological interactions, v. 323, n. 1, p. 109052, 2020.

RUBALCAVA, M. L.; FERNÁNDEZ, R. E. Secondary metabolites of endophytic Xylaria species with potential applications in medicine and agriculture. World Journal of Microbiology and Biotechnology, v. 33, n. 1, p. 1-22, 2017.

RUFFA, M. J. et al. Cytotoxic effect of Argentine medicinal plant extracts on human hepatocellular carcinoma cell line. Journal of Ethnopharmacology, v.79, n. 3, p. 335–339, 2002.

SACKS, P.; RAHMAN, M. Epidemiology of brain metastases. Neurosurgery Clinics, v. 31, n. 4, p. 481-488, 2020.

SAHOO, S.; SUBBAN, K.; CHELLIAH, J. Diversity of marine macro-algicolous endophytic fungi and cytotoxic potential of Biscogniauxia petrensis metabolites against cancer cell lines. Frontiers in Microbiology, v. 12, n. 1, p. 650177, 2021.

SALAZAR-RAMIRO, A. et al. Role of redox status in development of glioblastoma. Frontiers in Immunology, v. 7, n. 1, p. 1-15, 2016.

SAVIO, L. E. B. et al. Purinergic signaling in the modulation of redox biology. Redox Biology, v. 47, n. 1, p. 102137, 2021.

SCARBROUGH, P. M. et al. Exploring the association between melanoma and glioma risks. Annals of epidemiology, v. 24, n. 6, p. 469-474, 2014.

SCHIFFER, D. et al. Glioblastoma: microenvironment and niche concept. Cancers, v. 11, n. 1, p. 5, 2019

SÉVIGNY, J.; MARTÍN-SATUÉ, M.; PINTOR, J. Purinergic signalling in immune system regulation in health and disease. Mediators of inflammation, v. 2015, n. 1, p. 1-3, 2015.

SIEGEL, R. L. et al. Cancer statistics, 2021. A Cancer Journal of Clinicians, v. 71, n. 1, p. 7-33, 2021.

SOERJOMATARAM, I.; BRAY, F. Planning for tomorrow: Global cancer incidence and the role of prevention 2020–2070. Nature reviews Clinical oncology, v. 18, n. 10, p. 663-672, 2021.

SOLAK, M.; KILICKAP, S.; CELIK, I. Retrospective evaluation of malignant melanoma patients: A single-center experience. Family Practice and Palliative Care, v. 6, n. 2, p. 98-104, 2021.

SRITHARAN, T. et al. Isocoumarins and dihydroisocoumarins from the endophytic fungus Biscogniauxia capnodes isolated from the fruits of Averrhoa carambola. Natural Product Communications, v. 14, n. 5, p. 1934578X19851969, 2019.

STEELE, M. L. et al. Chronic inflammation alters production and release of glutathione and related thiols in human U373 astroglial cells. Cellular and molecular neurobiology, v. 33, n. 1, p. 19-30, 2013.

STEWART, J. et al. Pattern of Recurrence of Glioblastoma Versus Grade 4 IDH-Mutant Astrocytoma Following Chemoradiation: A Retrospective Matched-Cohort Analysis. Technology in Cancer Research & Treatment, v. 21, n. 1, p. 15330338221109650, 2022.

STIERLE, A.; STROBEL, G. STIERLE, D. Taxol and taxane production by *Taxomyces andreanae* an endophytic fungus on Pacific yew. Science, v. 260, n. 5105, p. 214-216, 1993

STRASHILOV, S.; YORDANOV, A. Aetiology and pathogenesis of cutaneous melanoma: Current concepts and advances. International journal of molecular sciences, v. 22, n. 12, p. 6395, 2021.

STROBEL, G.; DAISY, B. Bioprospecting for microbial endophytes and theirnatural products. Microbiology and Molecular Biology Reviews, v. 67, n. 4, p.491-502, 2003.

STROBEL, G. A.; LONG, D.M. Endophytic microbes embody pharmaceuticalpotential. ASM News, v. 64, n. 5, p. 263-268, 1998.

SU, T. R. et al. Inhibition of melanogenesis by gallic acid: Possible involvement of the PI3K/Akt, MEK/ERK and Wnt/β-catenin signaling pathways in B16F10 cells. International journal of molecular sciences, v. 14, n. 10, p. 20443-20458, 2013.

SUBRAMANIAN, V. et al. Topical application of Gallic acid suppresses the 7, 12-DMBA/Croton oil induced two-step skin carcinogenesis by modulating anti-oxidants and MMP-2/MMP-9 in Swiss albino mice. Food and chemical toxicology, v. 66, n. 1, p. 44-55, 2014.

SUGIURA, R.; SATOH, R.; TAKASAKI, T.. ERK: A double-edged sword in cancer. ERK-dependent apoptosis as a potential therapeutic Strategy for cancer. Cells, v. 10, n. 10, p. 2509, 2021.

SUNDARARAJAN, S.; THIDA, A. M.; BADRI, T. Metastatic Melanoma. In: StatPearls [Internet]. StatPearls Publishing, 2021. Disponível em: <https://www.ncbi.nlm.nih.gov/books/NBK470358/> Acesso em: 20 de Julho de 2022.

SUNG, H. et al. Global cancer statistics 2020: GLOBOCAN estimates of incidence and mortality worldwide for 36 cancers in 185 countries. CA: a cancer journal for clinicians, v. 71, n. 3, p. 209-249, 2021.

TAMAI, S. et al. Tumor Microenvironment in Glioma Invasion. Brain Sciences, v. 12, n. 4, p. 505, 2022.

TAWBI, H. A. et al. Inhibition of DNA repair with MGMT pseudosubstrates: phase I study of lomeguatrib in combination with dacarbazine in patients with advanced melanoma and other solid tumours. British journal of cancer, v. 105, n. 6, p. 773-777, 2011.

TYAGI, G. et al. Cure lies in nature: medicinal plants and endophytic fungi in curbing cancer. 3 Biotech, v. 11, n. 6, p. 1-24, 2021

VERMA, S.; SINGH, A.; MISHRA, A. Gallic acid: molecular rival of cancer. Environmental toxicology and pharmacology, v. 35, n. 3, p. 473-485, 2013.

VIJAYAN, D.; SMYTH, M. J.; TENG, M. W. L. Purinergic receptors: novel targets for cancer immunotherapy. In: Oncoimmunology. Springer, Cham, 2018. p. 115-141.

WALKER, J. The study of the effect of two flavone isomers derived from *Gnaphalium elegans* and *Achyrocline bogotensis* in breast cancer. 29 f. 2013. Undergraduate Honors Theses, East Tennessee State University, Tennessee. 2013.

WANG, J.; COX, D. G.; DING, W.; HUANG, G.; LIN, Y.; LI, C. Three new Resveratrol derivatives from the mangrove endophytic fungus *Alternaria* sp. Marine Drugs, v. 12, n. 5, p. 2840-2850, 2014.

WANG, P. F. et al. Preoperative changes in hematological markers and predictors of glioma grade and survival. Frontiers in Pharmacology, v. 9, n. 1, p. 886, 2018.

WANG, B. et al. The role of extracellular-5′-nucleotidase/CD73 in glioma peritumoural brain edema. Neurological Sciences, v. 37, n. 4, p. 603-611, 2016.

WELSH, T. G.; KUCENAS, S. Purinergic signaling in oligodendrocyte development and function. Journal of Neurochemistry, v. 145, n. 1, p. 6-18, 2018.

WHITAKER, B. K. et al. Foliar fungal endophyte community structure is independent of phylogenetic relatedness in an Asteraceae common garden. Ecology and Evolution, v. 10, n. 24, p. 13895-13912, 2020.

WHITE, N.; BURNSTOCK, G. P2 receptors and cancer. Trends in Pharmacological Sciences, v. 27, n. 4, p. 211-217, 2006.

WHITFIELD, B. T.; HUSE, J. T. Classification of adult-type diffuse gliomas: Impact of the World Health Organization 2021 update. Brain Pathology, v. 1, n. 1, p. e13062, 2022.

WINK, M. R. et al. Altered extracellular ATP, ADP and AMP catabolism in glioma cell lines. Cancer letters, v. 198, n. 2, p. 211-218, 2003.

WORLD HEALTH ORGANIZATION. WHO report in cancer: setting priorities, investing wisely and providing care for all. Geneva. 2020. Disponível em: <https://www.who.int/health-topics/cancer#tab=tab_1> Acesso em: 23 de Julho.

WU, B. et al. *Biscogniauxone*, a new isopyrrolonaphthoquinone compound from the fungus *Biscogniauxia mediterranea* isolated from deep-sea sediments. Marine drugs, v. 14, n. 11, p. 204, 2016.

WU, K. et al. LncRNA POU3F3 contributes to dacarbazine resistance of human melanoma through the MiR-650/MGMT axis. Frontiers in oncology, v. 11, n. 1, p. 643613, 2021.

XU, S. et al. Synergy between the ectoenzymes CD39 and CD73 contributes to adenosinergic immunosuppression in human malignant gliomas. Neuro-Oncology, v. 15, n. 9, p. 1160-1172, 2013.

YAN, L. et al. Beneficial effects of endophytic fungi colonization on plants. Applied microbiology and biotechnology, v. 103, n. 8, p. 3327-3340, 2019.

YANG, C. et al. Systemic inflammatory indicators as prognosticators in glioblastoma patients: a comprehensive meta-analysis. Frontiers in neurology, v. 11, n. 1, p. 580101, 2020.

YANG, J. T. et al. Gallic Acid Enhances the Anti-Cancer Effect of Temozolomide in Human Glioma Cell Line via Inhibition of Akt and p38-MAPK Pathway. Processes, v. 10, n. 3, p. 448, 2022.

YANG, S. H. et al. Andrographolide induces apoptosis of C6 glioma cells via the ERK-p53-caspase 7-PARP pathway. BioMed research international, v. 2014, n. 1, p. 1-15, 2014.

YANGUI, I. et al. Occurrence of *Biscogniauxia mediterranea* in cork oak stands in Tunisia. Phytoparasitica, v. 49, n. 1, p. 131-141, 2021.

YARANA, C.; ST. CLAIR, D. K. Chemotherapy-induced tissue injury: an insight into the role of extracellular vesicles-mediated oxidative stress responses. Antioxidants, v. 6, n. 4, p. 75, 2017.

YE, J. et al. Targeted delivery of chlorogenic acid by mannosylated liposomes to effectively promote the polarization of TAMs for the treatment of glioblastoma. Bioactive materials, v. 5, n. 3, p. 694-708, 2020.

YILMAZ, N. et al. Lipid peroxidation in patients with brain tumor. International journal of neuroscience, v. 116, n. 8, p. 937-943, 2006.

YU, N. H. et al. Diversity of endophytic fungi associated with bryophyte in the maritime Antarctic (King George Island). Polar Biology, v. 37, n. 1, p. 27-36, 2014.

YUAN, F.; W., Y.; MA, C. Current WHO Guidelines and the Critical Role of Genetic Parameters in the Classification of Glioma: Opportunities for Immunotherapy. Current Treatment Options in Oncology, v. 1, n. 1, p. 1-11, 2022.

ZHAN, Y. et al. Chlorogenic acid inhibits esophageal squamous cell carcinoma growth in vitro and in vivo by downregulating the expression of BMI1 and SOX2. Biomedicine & Pharmacotherapy, v. 121, n. 1, p. 109602, 2020.

ZHANG, H. et al. Circulating tumor cells for glioma. Frontiers in oncology, v. 11, n. 1, p. 607150, 2021.

ZHANG, Q. Y et al. Natural product interventions for chemotherapy and radiotherapy-induced side effects. Frontiers in pharmacology, v. 9, n. 1, p. 1253, 2018.

ZHANG, X. et al. Role of non-coding RNAs and RNA modifiers in cancer therapy resistance. Molecular cancer, v. 19, n. 1, p. 1-26, 2020.

ZHANG, Y. et al. Functional and binding studies of gallic acid showing platelet aggregation inhibitory effect as a thrombin inhibitor. Chinese Herbal Medicines, v. 14, n. 2, p. 303-309, 2022.

ZANINI, D. et al. Ectoenzymes and cholinesterase activity and biomarkers of oxidative stress in patients with lung cancer. Molecular and cellular biochemistry, v. 374, n. 1, p. 137-148, 2013.

ZHAO, H. et al. Dimericbiscognienyne A: A meroterpenoid dimer from *Biscogniauxia* sp. with new skeleton and its activity. Organic letters, v. 19, n. 1, p. 38-41, 2017.

ZHAO, H. et al. Two New Diterpenoids from *Biscogniauxia* sp. and Their Activities. Frontiers in chemistry, v. 9, n. 1, p. 1-7, 2021.

ZHOU, R. et al. Recombinant CC16 inhibits NLRP3/caspase-1-induced pyroptosis through p38 MAPK and ERK signaling pathways in the brain of a neonatal rat model with sepsis. Journal of Neuroinflammation, v. 16, n. 1, p. 1-13, 2019.

ZHULAI, G. et al. Adenosine-Metabolizing Enzymes, Adenosine Kinase and Adenosine Deaminase, in Cancer. Biomolecules, v. 12, n. 3, p. 418, 2022.

ZIMMERMANN, H. Ectonucleotidases in the nervous system. In: Purinergic signalling in neuron–glia interactions: Novartis Foundation Symposium 276. Chichester, UK: John Wiley& Sons, Ltd, 2006. p. 113-130.

# ANEXOS

# ANEXO – RESULTADOS ADICIONAIS

# ANEXO A

## Análise de morte e ciclo celular de células de glioma C6 expostas ao $F_{DCM}$

Para melhor compreender o efeito antiptoliferativo mediado pelo metabolismo secundário do *Biscogniauxia* sp., análises de ciclo celular e morte celular foram realizadas em células de glioma C6 após 72 h de tratamento, utilizando metodologias previamente descritas no manuscrito 1.

A análise da distribuição do ciclo celular evidenciou que o $F_{DCM}$ (10 µg/mL) promoveu um acúmulo de células na fase S do ciclo celular e redução da população de células em G1 (**Figura 1**). Adicionalmente, um aumento nas taxas de apoptose inicial (~115%) e apoptose tardia/necrose (~105%) foi observada nestas células após coloração com anexina V-Pi (**Figura 2**).

Tais resultados refletem o potencial antiglioma do $F_{DCM}$ em induzir morte celular programada e bloqueio da proliferação tumoral. Diante do exposto, como perspectivas futuras, é altamente relevante investigar o impacto do $F_{DCM}$ sobre o ciclo e morte celular em condições de cocultivo astrócito-glioma.

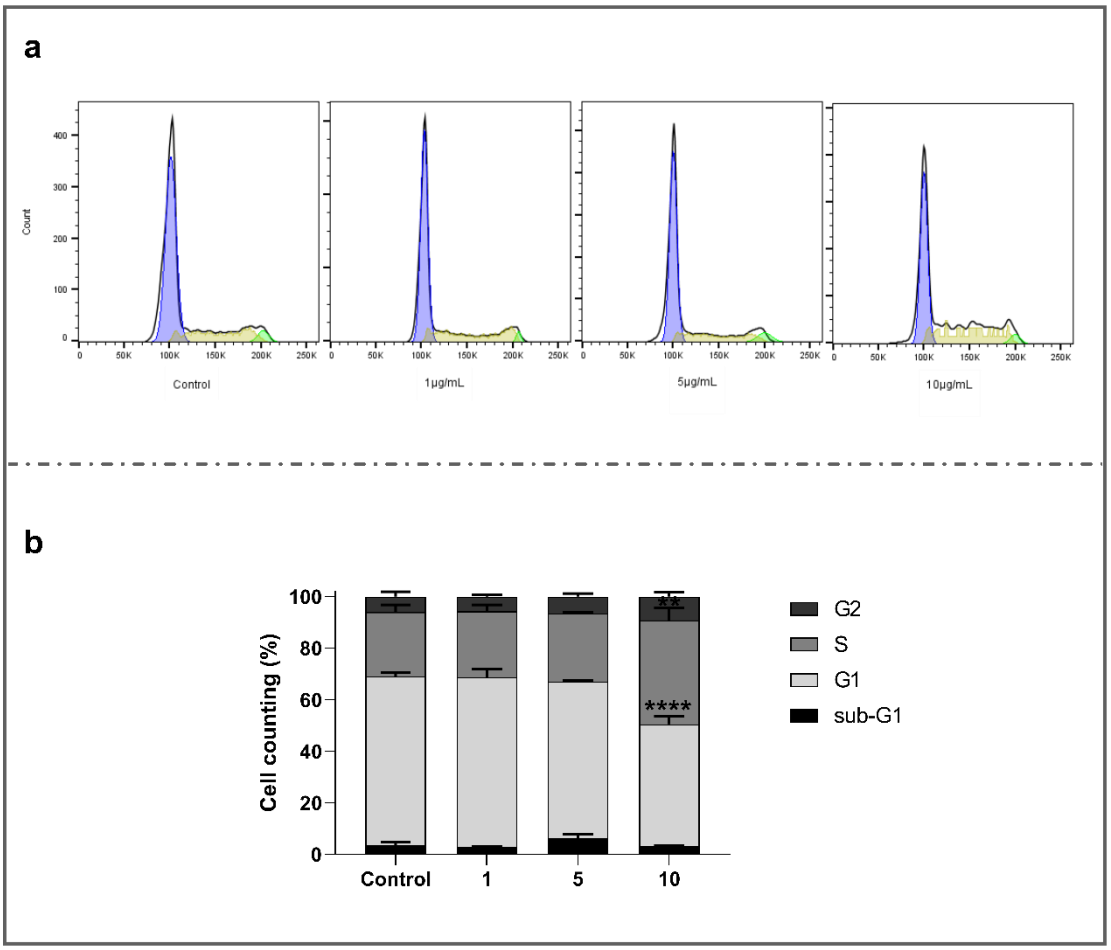


**Figura 1.** Efeito do metabolismo secundário de *Biscogniauxia* sp. na distribuição de células de glioma de rato em diferentes fases do ciclo celular. As células C6 foram tratadas com 1, 5 e 10 µg/ml de $F_{DCM}$ por 72 h. (**a**) Gráficos de citometria de fluxo representativos de células de glioma expostas ao $F_{DCM}$. (**b**) O efeito de $F_{DCM}$ nas porcentagens de células C6 nas fases Sub-G1, G1, S e G2/M. **,**** Significativamente diferente das células de controle (*P*<0,01 e *P*<0,0001, respectivamente).

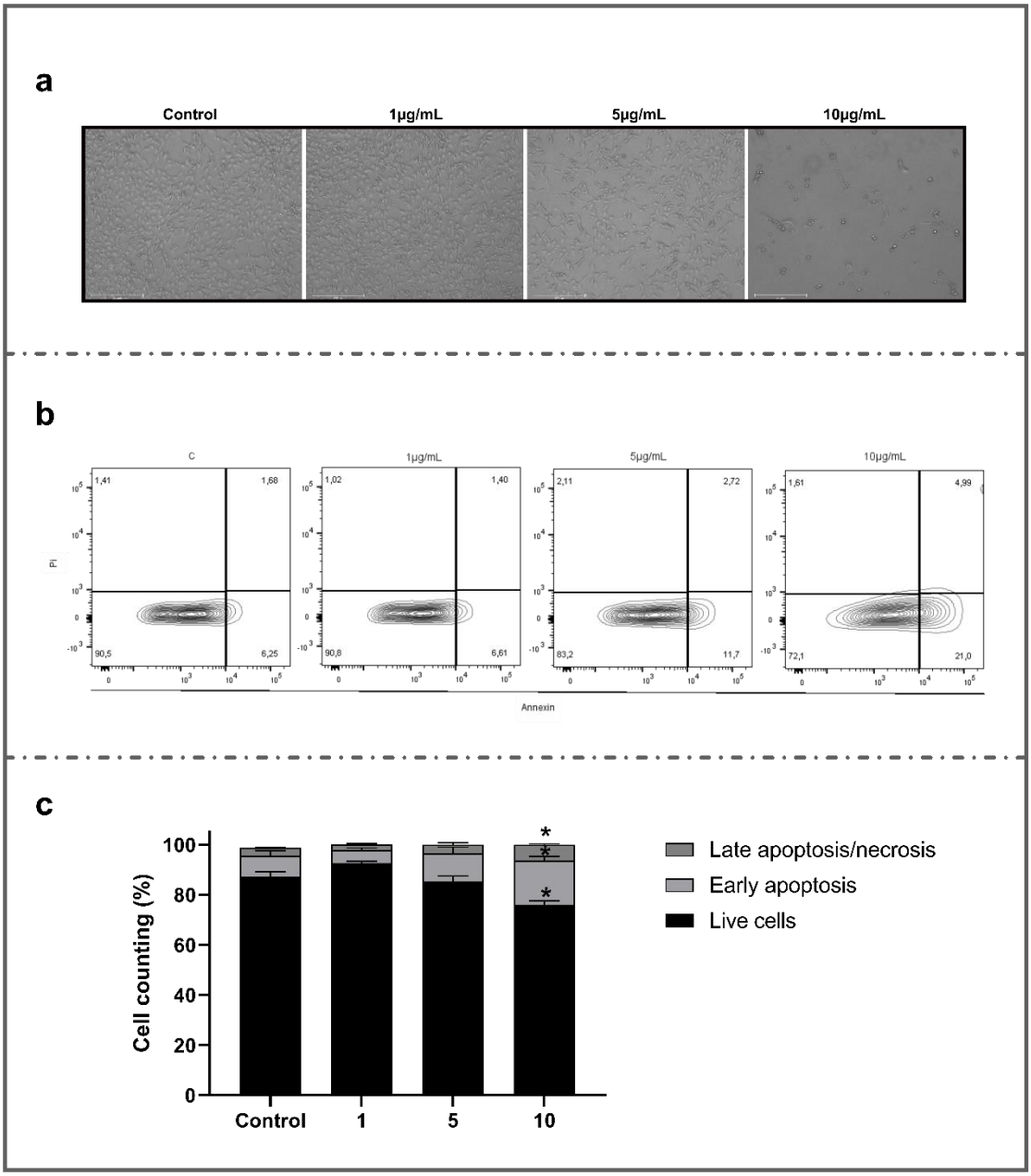


**Figura 2**. Efeito do metabolismo secundário de *Biscogniauxia* sp. na morte celular de células de glioma de rato. As células C6 foram tratadas com 1, 5 e 10 µg/ml de $F_{DCM}$ por 72 h. (**a**) Microfotografias representativas (ampliação de 10x) e (**b**) gráficos de citometria de fluxo representativos de células de glioma expostas ao $F_{DCM}$. (**c**) O efeito de $F_{DCM}$ nas percentagens de células vivas, células apoptóticas iniciais e células apoptóticas/necróticas tardias. *Significativamente diferente das células de controle ($P$<0,05).

# ANEXOS – APROVAÇÃO NO COMITÊ DE ÉTICA EM EXPERIMENTAÇÃO ANIMAL DA UFPel

# ANEXO B

## Carta de aprovação do comitê de ética – modelo experimental *in vitro*

UFPel

Pelotas, 04 de agosto de 2016

Certificado

Certificamos que a proposta intitulada "**Caracterização e avaliação das atividades antitumoral e antioxidante de extratos de fungo endofítico isolado a partir de *Achyrocline satureoides***", registrada com o nº23110.004755/2016-15, sob a responsabilidade de **Roselia Maria Spanevello**- que envolve a produção, manutenção ou utilização de animais pertencentes ao filo Chordata, subfilo Vertebrata (exceto humanos), para fins de pesquisa científica (ou ensino) – encontra-se de acordo com os preceitos da Lei nº 11.794, de 8 de outubro de 2008, do Decreto nº 6.899, de 15 de julho de 2009, e com as normas editadas pelo Conselho Nacional de Controle de Experimentação Animal (CONCEA), e recebeu parecer **FAVORÁVEL** a sua execução pela Comissão de Ética em Experimentação Animal, em reunião de 04/07/2016.

| Finalidade | ( X ) Pesquisa ( ) Ensino |
|---|---|
| Vigência da autorização | 15/08/2016 a 15/08/2018 |
| Espécie/linhagem/raça | *Rattus norvegicus*/ Wistar |
| N° de animais | 12 |
| Idade | 1-3 dias |
| Sexo | Machos e Fêmeas |
| Origem | Biotério Central - UFPel |

**Solicitamos, após tomar ciência do parecer, reenviar o processo à *CEEA*.**

Salientamos também a necessidade deste projeto ser cadastrado junto ao *COBALTO* para posterior registro no *COCEPE* (código para cadastro nº **CEEA 4755-2016**).

**M.V. Dra. Anelize de Oliveira Campello Felix**

*Presidente da CEEA*

Ciente em: 03 / 10 /2016

Assinatura do Professor Responsável: Roselia Maria Spanevello

# ANEXO C

## Carta de aprovação do comitê de ética – modelo experimental *in vitro* e *in vivo*

UNIVERSIDADE FEDERAL DE PELOTAS

**PARECER Nº** **104/2018/CEEA/REITORIA**
PROCESSO Nº 23110.031292/2018-18

Certificado

Certificamos que a proposta intitulada **"Avaliação das atividades antitumoral e antioxidante de produtos naturais em modelo pré - clínico de glioblastoma multiforme"** processo número 23110.031292/2018-18, de responsabilidade de Francieli Moro Stefanello- que envolve a produção, manutenção ou utilização de animais pertencentes ao filo Chordata, subfilo Vertebrata (exceto humanos), para fins de pesquisa científica (ou ensino) – encontra-se de acordo com os preceitos da Lei nº 11.794, de 8 de outubro de 2008, do Decreto nº 6.899, de 15 de julho de 2009, e com as normas editadas pelo Conselho Nacional de Controle de Experimentação Animal (CONCEA), e recebeu parecer **FAVORÁVEL** a sua complementação pela Comissão de Ética em Experimentação Animal, em reunião de 10/09/2018.

| Finalidade | ( X ) Pesquisa ( ) Ensino | |
|---|---|---|
| Vigência da autorização | 15/09/2018 a 01/07/2020 | |
| Espécie/linhagem/raça | *Rattus norvegicus*/Wistar | |
| Nº de animais | 296 | |
| Idade | 80 RN | 216 com 60 dias |
| Sexo | Machos e Fêmeas | Machos |
| Origem | Biotério Central - UFPel | |

Código para cadastro **CEEA 31292-2018**

SEI/UFPel - 0278125 - Parecer

**M.V. Dra. Anelize de Oliveira Campello Felix**

*Presidente do CEEA*

Documento assinado eletronicamente por **ANELIZE DE OLIVEIRA CAMPELLO FELIX, Médico Veterinário**, em 14/09/2018, às 11:36, conforme horário oficial de Brasília, com fundamento no art. 6º, § 1º, do Decreto nº 8.539, de 8 de outubro de 2015.

A autenticidade deste documento pode ser conferida no site http://sei.ufpel.edu.br/sei/controlador_externo.php?acao=documento_conferir&id_orgao_acesso_externo=0, informando o código verificador **0278125** e o código CRC **5A02D3A7**.

**Referência:** Processo nº 23110.031292/2018-18 SEI nº 0278125

# ANEXOS – ACEITE E SUBMISSÃO DE MANUSCRITOS EM PERIÓDICOS INDEXADOS

**ANEXO D**

**Aceite do manuscrito 3 (capítulo 3) para publicação no periódico *The Journal of Nutritional Biochesmistry***


Manuscript Number: JNB-D-21-01008R1

Impact of gallic acid on tumor suppression: Modulation of redox homeostasis and purinergic response in in vitro and a preclinical glioblastoma model

Dear Dr Spanevello,

Thank you for submitting your manuscript to The Journal of Nutritional Biochemistry.

We are pleased to inform you that your manuscript has been accepted for publication.

Your accepted manuscript will now be transferred to our production department. We will create a proof which you will be asked to check, and you will also be asked to complete a number of online forms required for publication. If we need additional information from you during the production process, we will contact you directly.

# ANEXO E

## Carta de submissão do manuscrito 1 (capítulo 1) no periódico *Applied Biochemistry and Biotechnology*

---------- Forwarded message ---------
De: **Applied Biochemistry and Biotechnology** <em@editorialmanager.com>
Date: sáb., 3 de set. de 2022 às 09:29
Subject: ABAB-D-22-01321 - Acknowledgement of Receipt
To: Roselia Spanevello <rspanevello@gmail.com>

Dear Dr Spanevello:

Thank you for submitting your manuscript, "Endophytic fungus of Achyrocline satureioides: molecular identification, chemical characterization and cytotoxic evaluation of its metabolites on human melanoma cell line", to Applied Biochemistry and Biotechnology.

The submission id is: ABAB-D-22-01321
Please refer to this number in any future correspondence.

During the review process, you can keep track of the status of your manuscript by accessing the following web site.

Your username is: rspanevello@gmail.com
If you forgot your password, you can click the 'Send Login Details' link on the EM Login page at https://www.editorialmanager.com/abab/.

With kind regards,

The Editorial Office
Applied Biochemistry and Biotechnology